Conformational Analysis and Application in Diagnostic of Glycosylphosphatidylinositols glycan Derivatives

Inaugural-Dissertation

to obtain the academic degree

Doctor rerum naturalium (Dr. rer. nat.)

Submitted to the Department of Biology, Chemistry and Pharmacy

of Freie Universität Berlin

by

MONIKA GARG

From Larha, Himachal Pradesh (INDIA)

July, 2017

The work in this doctoral thesis was performed between September 2013 and February 2017 under the guidance of Dr. Daniel Varón Silva in the GPI and Glycoproteins Group, Department of Biomolecular Systems, Max Planck Institute of Colloids and Interfaces and Institute of Chemistry and Biochemistry, Freie Universität Berlin.

1st Reviewer: Dr. Daniel Varón Silva

2nd Reviewer: Prof. Dr. Rainer Haag

Date of oral defense: 25 Oct. 2017

Declaration

This is to certify that the entire work in this thesis has been carried out by Mrs. Monika Garg. The assistance and help received during the course of investigation have been fully acknowledged.

---------- ----------

(Date, Place) (Signature)

Acknowledgement

At first, I would like to express my gratitude to my supervisor Dr. Daniel Varon Silva, Group Leader, GPI and Glycoproteins, Department of Biomolecular Systems, Max Planck Institute of Colloids and interfaces for his invaluable guidance, motivation and encouragement throughout this work. His continuous support and suggestion have provided me an insight in to the intricacies of experimentation involved in this work.

I consider myself privileged and would like to thank Prof. Dr. Peter H. Seeberger for giving me this opportunity to carry out my PhD thesis at the Department of Biomolecular Systems, Max Planck Institute of Colloids and interfaces, Golm, Potsdam, Germany.

Besides, I am grateful to Prof. Dr. Frank Seeber, Robert Koch Institute (RKI), Berlin, Germany for hosting me in his laboratory to perform the biological experiments and also for useful discussions.

Also I would like to thank my thesis committee advisor Prof. Dr. Rainer Haag, Institute of Chemistry and Biochemistry, Freie Universität, Berlin, Germany.

I am thankful to my collaborator: Dr. Mark Santer and Dr. Marko Wehle, Department of Theory and Bio-Systems, Max Planck Institute of Colloids and Interfaces for molecular dynamic study.

I am thankful to the Executive board and Steering committee members of International Max Planck Research School (IMPRS) on Multiscale Bio-Systems, Max Planck Institute of Colloids and Interfaces, especially to Dr. Angelo Valleriani. Financial Support from IMPRS is highly appreciated.

I thank all the former and current members of my group for their support and co-operation.

I would like to thank Eva Settels and Olaf Niemeyer for keeping technical stuff running in the department and Dorothee Böhme for the organizational support.

I am grateful to Renee Roller for the German translation of summary and Dr. Maria Bräutigam for proof reading of the summary.

I would also like to thank my friends (especially for Friday night's dinner) and colleagues in the BMS department Dr. Bo-Young Lee, Priya Bharate, Feifei Xu, Zhou Ye, Dr. Kathirvel Alagesan, Dr. Dana Michael, Dr. Bopanna P. Monnanda, Dr. Sharavathi G. Parameswarappa, Dr. Claney L. Pariera, Dr. Marilda P. Lisboa, Dr. Madhu Emmadi, Dr. Maria Antonietta Carillo, Dr. Maurice Grube, Renee Roller, Silvia Varela, Matthew Plutschack, Pietro Dallabernardina, Andrew Kononov, Dr. Martina Delbianco, Antonella Rella, Hyunil Oh.

Last but not least, I would like to thank my parents and almighty God. The love and unconditional support provided by my parents have always been a constant inspiration to reach any goal in my life. It is my great pleasure to acknowledge my husband (Sanjay) and my brothers (Vipan, Deepak, Rishab) for their love, support and encouragement.

Dedicated to my beloved parents

List of Publications

A) **Scientific Publications and Book Chapters**

1. M. Garg, P. H. Seeberger, and D. Varon Silva, Glycosylphosphatidylinositols: Occurrence, Synthesis, and Properties, *In Reference Module in Chemistry, Molecular Sciences and Chemical Engineering*, Elsevier, 2016, ISBN 9780124095472. https://doi.org/10.1016/B978-0-12-409547-2.11657-9

B) **Scientific Conferences and Symposium**

1. International Carbohydrate Symposium **(ICS2016)**, New Orleans, Louisiana, USA, July17-21, 2016: "Synthesis of GPIs and their Analog to study their Structural aspects and Biological Relevance" **(Oral presentation)**

2. European Carbohydrate Symposium **(EUROCARB)**, Moscow, Russia, August 2-6, 2015: "Conformational analysis of Glycosylphosphatidyl-Inositol (GPIs) using Paramagnetic-NMR Techniques" **(Oral presentation)**

3. RIKEN-Max Planck Joint Symposium, Berlin, Germany, April17-19, 2016: "Synthesis of GPIs to study Structural and Biological Aspects" **(Poster)**

4. RIKEN-Max Planck Joint Symposium, Kobe, Osaka, Japan, May11-14, 2015: "Synthesis of Paramagnetic Linker Tagged GPIs to study Conformation and Dynamics" **(Poster)**

5. Warren Workshop, Galway, Ireland, August 6-9, 2014: "Glycosylphosphatidylinositols (GPIs) of Trypanosoma gondii and Trypanosoma congolense VSG for Conformational Analysis Using Paramagnetic-NMR Techniques" **(Poster)**

Table of Contents

List of Abbreviations

$(NH_4)_2CO_3$	Ammonium carbonate
$[Ir(Cod)(PPh_2Me)_2]PF_6$	(1,5-Cyclooctadiene)bis(methyldiphenylphosphine)iridium(I) Hexafluorophosphate
AAG	1-alkyl-2-acylglycerol
Ac	Acetyl
Ac_2O	Acetic anhydride
AcCl	Acylchloride
AcOH	Acetic acid
AgOTf	Silver triflate
AllBr	Allyl Bromide
Asn	Asparagine
$BF_3.Et_2O$	Boron trifluoride diethyl etherate
Bn	Benzyl
BnBr	Benzylbromide
Boc	*tert*-Butoxycarbonyl
Bu_2SnO	Dibutyltinoxide
Bz	Benzoyl
CAN	Ceric ammonium nitrate
CCl_3CN	Trichloroacetonitrile
$CHCl_3$	Chloroform
CSA	Camphor sulfonic acid
DAG	Diacylglycerol
DAF	Decay accelerating factor
DBDIPPA	Dibenzyl diisopropyl phosphoramidite
DBU	1,8-diazabicycloundec-7-ene
DCC	*N*,*N'*-Dicyclohexylcarbodiimide
DCM	Dichloromethane
DDQ	2,3-Dichloro-5,6-dicyano-1,4-benzoquinone
DIPEA	N,N-Diisopropylethyl amine
DMAP	4-Dimethylaminopyridine
DMC	2-chloro-1,3-dimethylinidazolinium chloride

DMF	Dimethylformamide
DMSO	Dimethyl Sulfoxide
ER	Endoplasmic Reticulum
Et_2O	Diethyl ether
Et_3N	Triethylamine
EtNP	Phosphoethanolamine
EtOH	Ethanol
FI	Fluorescence Intensity
Fmoc	9-Fluorenylmethoxycarbonyl
FRET	Fluorescence resonance energy transfer
GAG	Glycosaminoglycan
GIPL	Glycoinositol phospholipids
GlcNAc	N-acetylglucosamine
GPI-APs	Glycosylphosphatidylinositols Anchored Proteins
GPIs	Glycosylphosphatidylinositols
GTP	Guanosine-5'-triphosphate
HCOOH	Formic acid
HF-Pyridine	Hydrogen fluoride in pyridine
$Hg(OAc)_2$	Mercury(II) acetate
I_2	Iodine
IL	Interleukin
Ino	Inositol
K_2CO_3	Potassium Carbonate
Lev	Levulinoyl
LPGs	Lipophosphoglycans
Man	Mannose
MeCN/ACN	Acetonitrile
MeOH	Methanol
MFI	Mean Fluorescence Intensity
Na	Sodium
NaH	Sodium hydride
NaOAc	Sodium Acetate
NaOMe	Sodium Methoxide

NaN_3	Sodium Azide
NapBr	2-Naphthylmethyl bromide
NCAM	Neural Cell adhesion molecules
NIS	N-iodosuccinimide
NMR	Nuclear Magnetic Resonance
NOE	Nuclear Overhauser Effect
PBS	Phosphate Buffer Saline
PCS	Pseudo Contact Shift
$Pd(OH)_2/C$	Palladium hydroxide on activated charcoal
Pd/C	Palladium on activated charcoal
$PdCl_2$	Palladium(II) Chloride
$PdCl_2$(dppf)	1,1′-Bis(diphenylphosphino)ferrocene]dichloropalladium(II)
PGAP	Post GPI attachment to protein
Ph_3P	Triphenylphosphine
$PhCH(OMe)_2$	Benzaldehyde dimethyl acetal
PhMe	Toluene
PhSH	Thiophenol
PI	Phosphatidylinositol
PIG	Phosphatidylinositol Glycan
PIMs	Phosphatidylinositol mannosides
PI-PLC	Phosphoinositide phospholipase C
PivCl	Pivaloyl chloride
PNH	Paroxysmal Nocturnal Hemoglobinuria
Py	Pyridine
$Sc(OTf)_3$	Scandium(III) triflate
TBDMSCl	*tert*-Butyldimethylsilyl chloride
TBDPSCl	*tert*-Butyldiphenylsilyl chloride
TCA	Trichloroacetonitrile
Tf_2O	Trfluoromethansulfonic acid anhydride, Triflic anhydride
TFA	Trifluoroacetic acid
THF	Tetrahydrofuran
TLC	Thin Layer Chromatography
TLRs	Toll like receptors

TMSOTf	Trimethylsilyltrifluoromethanesulfonate
TNF-α	Tumor necrosis factor-alpha
VSGs	Variant Surface Glycoproteins
$Yb(OTf)_3$	Yetterbium triflate
Zn	Zinc

Summary

Glycosylphosphatidylinositols (GPIs) are the most complex class of glycolipids present on the membrane of eukaryotic cells. GPIs share the common core structure: Manα(1→2)Manα(1→6)Manα(1→4)GlcNα(1→6)-*myo*-Inositol-1-PO_4-lipid, which is generally modified in a tissue and cell-dependent manner by additional phosphorylations, carbohydrate side chains and the presence of additional fatty acid chains. GPIs can be found as free glycolipids or attached to the *C*-terminus of the proteins using a phosphoethanolamine unit on the Man-III residue of the glycan core forming the so-called GPI-anchored proteins (GPI-APs). These GPI-anchored proteins are known to play an important role in various biological processes and have gained the interest of synthetic chemists and biologists.

Diverse synthetic strategies have been developed to obtain the complex GPI anchors as well as their derivatives to get insight into the structure-activity relationship of these molecules. Immunization experiments in animal models and studies using microarrays have showed the potential of these molecules as valuable antigens for anti-parasitical vaccines or as diagnostic markers in diseased patients.

In a recent report, our group has shown that the glycan part of a GPI of *T. gondii* can be used as a diagnostic marker for toxoplasmosis and to distinguish between latent and acute infection based on the detection of the anti-GPI IgG and IgM antibodies levels in patient sera using microarrays.

In order to expand the diagnostic potential of the GPI of *T. gondii* for a sero-epidemiological study, in the first part of this work, the phosphoglycan part of GPIs from *T. gondii* was synthesized and used in the development of a diagnostic test for toxoplasmosis using a bead-based assay. It was demonstrated that the selected GPI glycan can be used to distinguish between infected and healthy cases using a Luminex-based sero-diagnostic assay. Different conditions were optimized, including: coupling of the antigen to the magnetic beads, antigen concentration, secondary antibody conjugation type and concentration, serum sample dilution and buffer composition. Under optimized conditions, 180 human serum samples were analyzed identifying the positive cases with 95 % specificity and 76 % sensitivity. Furthermore, these results were compared with the results from ELISA showing less than 10 % false negative rate. The high specificity and

sensitivity along with less false negative results using GPI molecule indicated that GPI based Luminex assay can be used as a valuable tool for the diagnosis of toxoplasmosis in clinical settings.

To obtain a better understanding of the GPI structures and biological functions of these glycolipids, in the second part of this work a paramagnetic NMR technique was employed along with the MD simulations to study the conformation and dynamics of the glycan part of the core of GPI anchors. In order to use paramagnetic ions (Lanthanides) assisted NMR spectroscopy, the disaccharides Manα1→2Man and Manα1→6Man, and the trisaccharide Manα1→2Manα1→6Man fragments of the GPI-core tagged with a metal chelating unit were successfully synthesized. First, a linker containing a tagging unit was synthesized from 1,2-diamino benzene in a four step process. Then, this linker was coupled to the GPI fragment having an amine at the reducing end. ^{1}H and ^{1}H-^{13}C HSQC spectra of the synthesized tagged-GPI fragments were acquired in the presence of diamagnetic reference (La^{3+}) and paramagnetic metal ions (Dy^{3+}, Yb^{3+}, Eu^{3+}). To obtain structural information of the glycans, the pseudocontact shift (PCS) values were determined for each proton and carbon as the difference of ^{1}H and ^{13}C chemical shift values between the carbohydrate complex with paramagnetic metal ion and diamagnetic reference in all the three fragments.

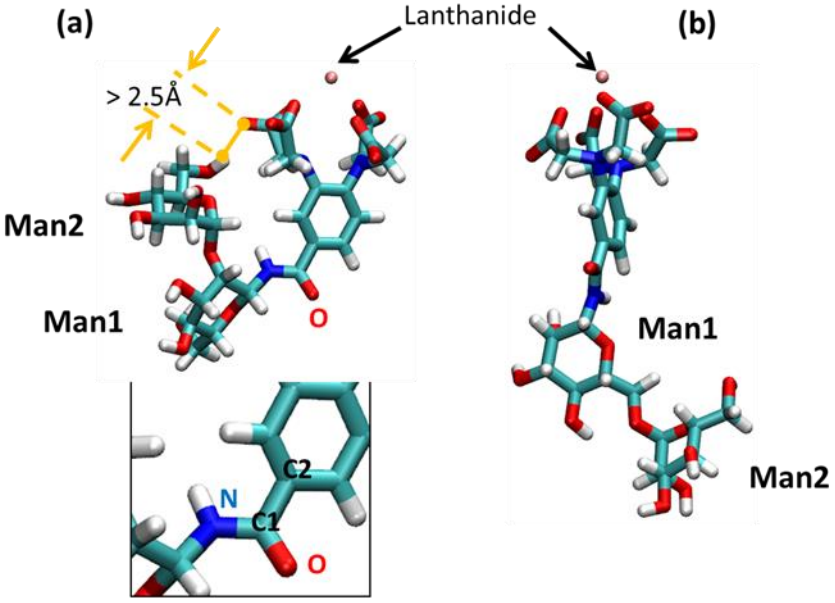

Figure 1: (a) Man α1→2Man, with linker attached as a β-anomer. (b) Same for Manα1→6Man.

The PCS values obtained experimentally were compared with the data obtained from the computational analysis. The experimental PCS values showed a good agreement with the back calculated PCS (Q) values. In the case of Manα1→2Man disaccharide, the better agreement was obtained when europium (Eu^{3+}) and ytterbium (Yb^{3+}) were used. Europium as paramagnetic ion showed a narrow distribution around 0.05, ytterbium (Yb) produced the lowest Q-values on the selected single frames even lower than 0.01 suggesting that both metal ions are equally good. The characteristic molecular geometries of the disaccharide Manα1→2Man and Manα1→6Man resulted from the NMR experiments and molecular dynamics study showed that in case of disaccharide Manα1→2Man, the non-reducing mannose Man2 is always in close proximity to the metal ion, indicating the most probable conformation as shown in the Figure 1a. In case of Manα1→6Man, the most visited conformation was the extended conformation showed in Figure 1b. These results confirmed previous observations assigning the flexibility of the GPI core to the α1→6 linkage, which has an additional rotation around the glycosidic linkage. Furthermore, this study demonstrated the high flexibility of the glycans and the need of using a larger and rigid linker in paramagnetic NMR experiments.

The third part of this work focused on the synthesis of GPI building blocks for the semi-synthesis of GPI-anchored proteins from protozoan and mammalian cells. For this process, the synthetic GPIs were obtained containing a cysteine residue attached to the phosphoethanolamine unit. The cysteine can undergo a chemoselective reaction with a *C*-terminal protein thioester via a trans-thioesterification and rearrangement processes to give GPI anchored proteins. The synthesis of the GPIs **76** and **77** were completed following a convergent synthetic strategy (Figure 2). The glycan part was assembled using three building blocks and a [2+1+2] glycosylation strategy. To obtain a model GPI from protozoa, the glycan moiety was phosphorylated using H-phosphonate of bilipid **A** and cysteine modified phosphoethanolamine H-phosphonate **D**. The mammalian GPI model was obtained using H-phosphonate of monolipid **B**, the phosphoethanolamine unit **C** and the cysteine-modified building block **D** for the installation of the phosphorylations. These two GPIs are currently being used for the development of semi-synthetic methods to obtain homogeneous GPI-anchored proteins to reveal the significance of glypiation in the structure and activity of these proteins.

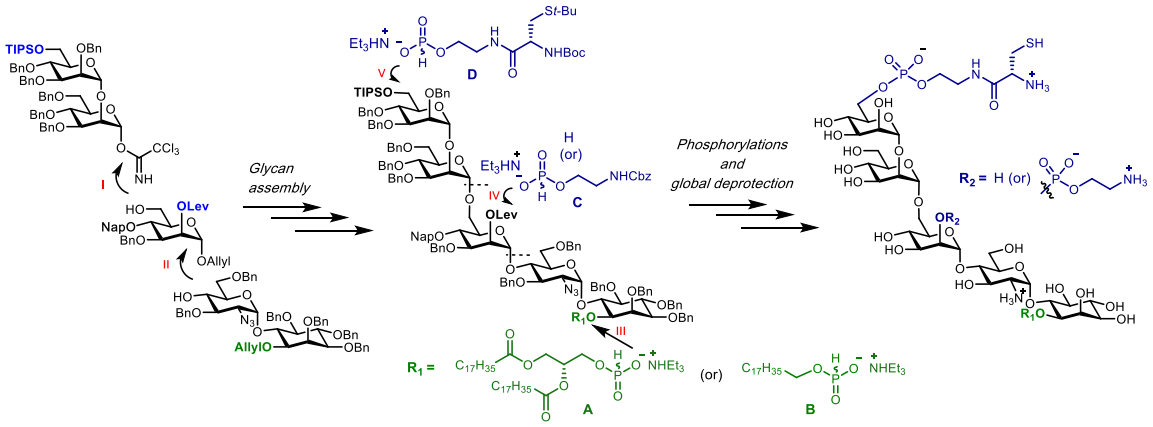

Figure 2: Convergent synthetic strategy used for the synthesis of GPI anchors.

Additional part of this work was the synthesis of agarose beads-attached phosphorylated trimannose of the GPI glycan core for the affinity purification of the carbohydrate binding proteins. The synthesis was carried out following the same strategy as shown in Figure 2. A thiol linker was introduced at the anomeric position, which was used for the immobilization of trimannose on iodoacetyl modified agarose beads. Currently, affinity purification and characterization of carbohydrate binding proteins using mass spectrometry is under investigation at Max Planck Institute of colloids and interfaces.

Zusammenfassung

Glykosylphosphatidylinositole (GPIs) bilden die komplexeste Klasse der auf eukaryotischen Zellmembranen vorkommenden Glykolipide. GPIs haben folgende gemeinsame Kernstruktur: Manα(1→2)Manα(1→6)Manα(1→4)GlcNα(1→6)-*myo*-Inositol-1-PO_4-Lipid, die im Allgemeinen auf gewebe- und zellspezifische Art durch zusätzliche Phosphorylierungen, Kohlenhydratseitenketten und das Vorkommen weiterer Fettsäureketten modifiziert ist. GPIs können als freie Glykolipide vorkommen, oder sind mit Hilfe einer Phosphoethanolamin-Einheit am Man-III-Rest des Glykankerns am C-Terminus von Proteinen verankert. Die so gebildeten Moleküle werden GPI-verankerte Proteine (GPI-AP) genannt. Diese GPI-verankerten Proteine spielen eine wichtige Rolle in unterschiedlichen biologischen Prozessen und haben das Interesse vieler synthetischer Chemiker und Biologen geweckt.

Diverse synthetische Strategien wurden entwickelt, um GPI-Anker und deren Derivative herstellen zu können und so Einblicke in die Struktur-Aktivität-Beziehungen dieser Moleküle zu erlangen. Immunisierungsexperimente in Tiermodellen sowie Mikroarray-Studien haben das Potential dieser Moleküle als wertvolle Antigene in anti-parasitären Impfstoffen oder auch als diagnostische Marker in erkrankten Personen gezeigt.

In einer kürzlich veröffentlichten Studie konnte unsere Gruppe zeigen, dass der Kohlenhydratanteil des GPIs von *T. gondii* als diagnostischer Marker für Toxoplasmose eingesetzt werden kann, und sogar eine Unterscheidung zwischen einer latenten und einer akuten Infektion auf der Basis der Detektion von anti-GPI IgG und IgM Antikörper-Titern in den Seren von Patienten mittels Mikroarray-Technologie möglich ist.

Um das diagnostische Potential des GPIs von *T. gondii* für eine sero-epidemiologische Studie zu erweitern, wurde im ersten Teil dieser Arbeit der Phosphoglykan-Anteil des GPIs von *T. gondii* als Marker synthetisiert und für die Entwicklung eines diagnostischen Tests für Toxoplasmose in einem Bead-basierten Testverfahren angewendet. Es wurde gezeigt, dass das ausgewählte GPI-Glykan eingesetzt werden kann, um zwischen infizierten und gesunden Personen mittels eines Luminex-basierten sero-diagnostischen Verfahrens zu unterscheiden. Verschiedene Bedingungen wurden optimiert, darunter Antigen-Konzentration, Konjugationstyp des sekundären Antikörpers sowie dessen

Konzentration, Verdünnung der Serum-Probe, und die Pufferzusammensetzung. Unter den optimierten Bedingungen wurden dann 180 humane Serum-Proben analysiert, wobei die positiven Proben mit 95 % Spezifizität und 76 % Sensitivität identifiziert werden konnten. Weiterhin wurden diese Ergebnisse mit denen aus einem ELISA-Test verglichen, was eine Rate von falsch-negativen Ergebnissen von unter 10 % zeigte. Die hohe Spezifizität zusammen mit wenigen falsch-negativen Ergebnissen bei Anwendung des GPI-Moleküls zeigen, dass dieses GPI-basierte Luminex-Verfahren als wertvolles Werkzeug für die Diagnose von Toxoplasmose im klinischen Umfeld eingesetzt werden kann.

Um ein besseres Verständnis der GPI-Strukturen und der biologischen Funktionen dieser Glykolipide zu erlangen, wurde im zweiten Teil dieser Arbeit eine paramagnetische NMR-Methode zusammen mit MD (Molekulardynamik)-Simulationen angewendet, um die Konformation und Dynamiken des Glykananteils des GPI-Kerns zu untersuchen. Um paramagnetische-Ionen (Lanthanoide)-unterstützte NMR-Spektroskopie nutzen zu können, wurden die Disaccharidfragmente Manα1→2Man und Manα1→6Man, sowie das Trisaccharidfragment Manα1→2Manα1→6Man des GPI-Kerns mit einer chelatbildenden Verbindung erfolgreich synthetisiert. Zuerst wurde ausgehend von 1,2-diamino-Benzen ein Linker mit einer Tag-Einheit in vier Schritten synthetisiert. Daraufhin wurde dieser Linker an das GPI-Fragment, welches ein Amin am reduzierenden Ende trägt, angehängt. ^{1}H und ^{1}H-^{13}C HSQC Spektren der synthetisierten getaggten GPI-Fragmente wurden in Gegenwart des diamagnetischen Referenz-Ions (La^{3+}), sowie in Gegenwart der paramagnetischen Metallionen (Dy^{3+}, Yb^{3+}, Eu^{3+}) aufgenommen und analysiert. Um strukturelle Informationen über die Glykane zu erlangen, wurden die PCS-Werte (Pseudo-Kontakt-Verschiebung) als die Differenz der chemischen Verschiebungen von ^{1}H und ^{13}C zwischen dem Kohlenhydratkomplex mit paramagnetischem Ion und der diamagnetischen Referenz in allen drei Fragmenten für jedes Proton und jedes Kohlenstoffatom berechnet.

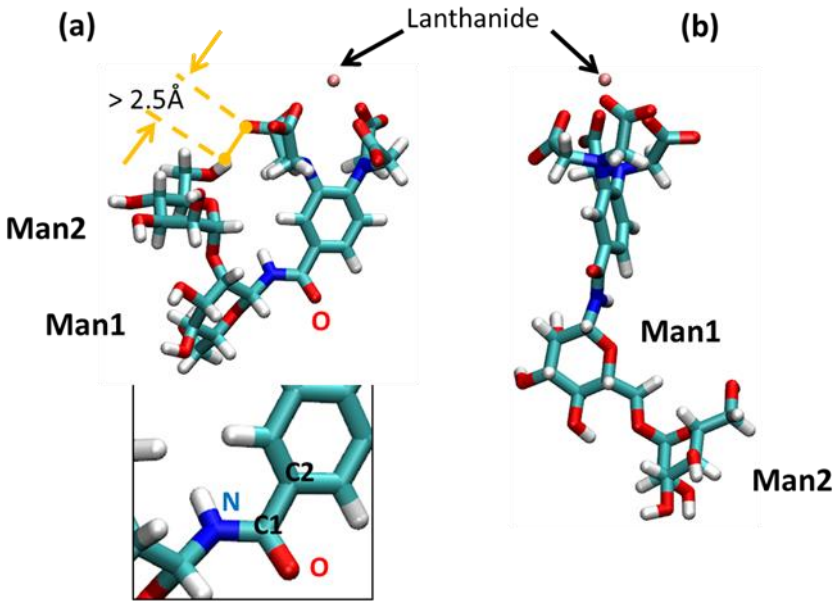

Abbildung 1: (a) Man α1→2Man, mit Linker, verknüpft als β-Anomer. (b) wie a, für Manα1→6Man.

Die experimentell erhaltenen PCS-Werte wurden schließlich mit den Daten aus der rechnergestützten Analyse verglichen. Die experimentellen PCS-Werte zeigen eine gute Übereinstimmung mit den zurückgerechneten PCS (Q)-Werten. Im Falle des Disaccharid-Fragmentes Manα1→2Man wurde die höchste Übereinstimmung erreicht, wenn Europium (Eu^{3+}) und Ytterbium (Yb^{3+}) genutzt wurden. Europium als paramagnetisches Ion zeigte eine enge Verteilung um 0.05, Ytterbium generierte die niedrigsten Q-Werte für die ausgewählten Einzelbilder, sogar unter 0.01, was darauf hinweist, dass beide Metallionen gleichwertig einsetzbar sind. Die charaktieristischen molekularen Geometrien der Disaccharid-Fragmente Manα1→2Man und Manα1→6Man ergaben sich aus den NMR-Experimenten und die Molekulardynamik-Modellierung zeigte, dass im Falle des Disaccharids Manα1→2Man die nichtreduzierende Mannose Man2 stets in direkter Nachbarschaft zu dem Metallion ist, was die in Abbildung 1a gezeigte Konformation als die wahrscheinlichste Konformation nahelegt. Im Falle von Manα1→6Man ist die häufigste Konformation die gestreckte Konformation, die in Abbildung 1b dargestellt ist. Diese Ergebnisse bestätigen vorherige Beobachtungen, welche die Flexibilität des GPI-Kerns der α1→6-Bindung zuordneten, die eine zusätzliche Rotation um die glykosidische Bindung hat. Außerdem demonstriert diese Studie die hohe Flexibilität der Glykane und den Bedarf eines größeren und starreren Linkers in paramagnetischen NMR-Experimenten.

Der dritte Teil dieser Arbeit behandelt schwerpunktmäßig die Synthese von GPI-Bausteinen für die Semi-Synthese von GPI-verankerten Proteinen von Protozoen sowie Säugerzellen. Dafür wurden die synthetischen GPIs mit einem Cystein-Rest an der Phosphoethanolamin-Einheit generiert. Dieser Cystein-Rest kann eine chemoselektive Reaktion mit einem C-terminalen Protein-Thioester über eine Trans-Thioesterifizierung und Umlagerungsreaktionen eingehen, um schließlich GPI-verankerte Proteine zu ergeben. Die Synthese der GPIs **76** und **77** wurde entsprechend einer konvergenten Synthese-Strategie abgeschlossen (Abbildung 2). Der Glykan-Anteil wurde aus drei Bausteinen in einer [2+1+2]-Glykosylierungsstrategie zusammengesetzt. Um ein Modell-GPI aus Protozoen zu erhalten, wurde die Glykan-Einheit mit dem H-Phosphonat des Bilipids **A** sowie dem Cystein-modifizierten Phosphoethanolamin-H-Phosphonat phosphoryliert **D**. Das Säuger-Modell-GPI wurde mit Hilfe des H-Phosphonats des Monolipids **B**, der Phosphoethanolamin-Einheit **C** und dem Cystein-modifizierten Baustein **D** erhalten. Diese beiden Modell-GPIs werden zurzeit für die Entwicklung semisynthetischer Methoden für die Herstellung homogener GPI-verankerter Proteine genutzt, um den Stellenwert der GPI-Verankerung in der Struktur und Aktivität dieser Proteine deutlich zu machen.

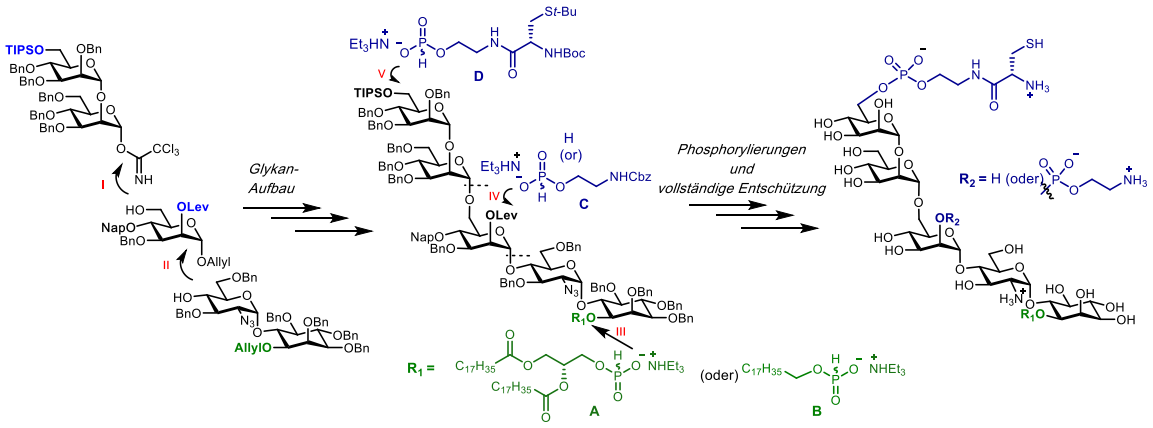

Abbildung 2: Konvergente Synthesestrategie für die Synthese von GPI-Ankern.

Ein weiterer Teil dieser Arbeit war die Synthese von an Agarose-Beads gekoppelter phosphorylierter Trimannose des GPI-Glykankerns für die Affinitätsaufreinigung kohlenhydratbindender Proteine. Die Synthese wurde mit Hilfe derselben Strategie durchgeführt, wie in Abbildung 2 dargestellt. Ein Thiol-Linker wurde an der anomeren Position eingeführt, welcher für die Immobilisierung von Trimannose auf Iodoacetyl-modifizierten Agarose-Beads genutzt wurde. Affinitätsaufreinigung und

Charakterisieung von kohlenhydratbindenden Proteinen mittels Massenspektrometrie wird derzeit am Max Planck Institut für Kolloid- und Grenzflächenforschung untersucht.

Chapter 1

Introduction

This chapter has been adapted in parts from the following article:

M. Garg, P. H. Seeberger, and D. Varon Silva, Glycosylphosphatidylinositols: Occurrence, Synthesis, and Properties, *In Reference Module in Chemistry, Molecular Sciences and Chemical Engineering*, Elsevier, 2016, ISBN 9780124095472. https://doi.org/10.1016/B978-0-12-409547-2.11657-9

License Number: 4152490474659

1.1 General Introduction to the Glycome

Four main classes of biomolecules are responsible for the majority of processes in the cell: lipids (fatty acids), proteins (amino acids), carbohydrates (monosaccharides), and nucleic acids (nucleotides). Among these biomolecules, carbohydrates are the most complex class of biomolecules in composition and type of linkages. In contrast to DNA, RNA (with 5 nucleotides), and proteins (with 20 amino acids), which are polymers linked in a linear form, the complexity of carbohydrates originates from single monosaccharides having α- or β-linkages to complex oligomers and polymers connected in different forms and stereochemistry. The entire repertoire of glycans is known as the "Glycome".[1]

Carbohydrates cover the surface of all type of cells from prokaryotes to eukaryotes forming a complex and dense layer known as the glycocalyx.[2] (Figure 1.1) The carbohydrates or glycans present in the glycocalyx include various structures that are often present in combination with other biomolecules such as glycolipids, glycoproteins (*O*- and *N*-glycan), proteoglycans, glycosaminoglycans (GAGs), and glycosylphosphatidylinositol (GPI) anchors. This combination suggests an important role of glycans in a large number of biological processes (Figure 1.2).[1]

Glycans are mainly distinguished by the type of linkages to the corresponding proteins or lipids. A glycoprotein is a glycoconjugate in which the peptide backbone of a protein is decorated with one or many glycans via *N*-, *P*-, *C*- and *O*- linkages. In *N*-linked glycoproteins, the carbohydrate chains are covalently linked to an asparagine (Asn) residue of a polypeptide chain, usually involving a GlcNAc residue and the consensus

peptide sequence: Asn-Xxx-Ser/Thr (Xxx = not proline). All *N*-Glycans share a common pentasaccharide core structure that is further decorated with other units to form oligomannose (or high-mannose) type, complex-type, and hybrid-type glycans.[3] In *O*-glycans, the carbohydrate chains are linked to the polypeptide mainly via an *N*-acetylgalactosamine (GalNAc) to a hydroxyl group (-OH) of a serine/threonine residue. Among all other glycoproteins, mucins are the heavily *O*-glycosylated glycoprotein found in mucous secretion.[4]

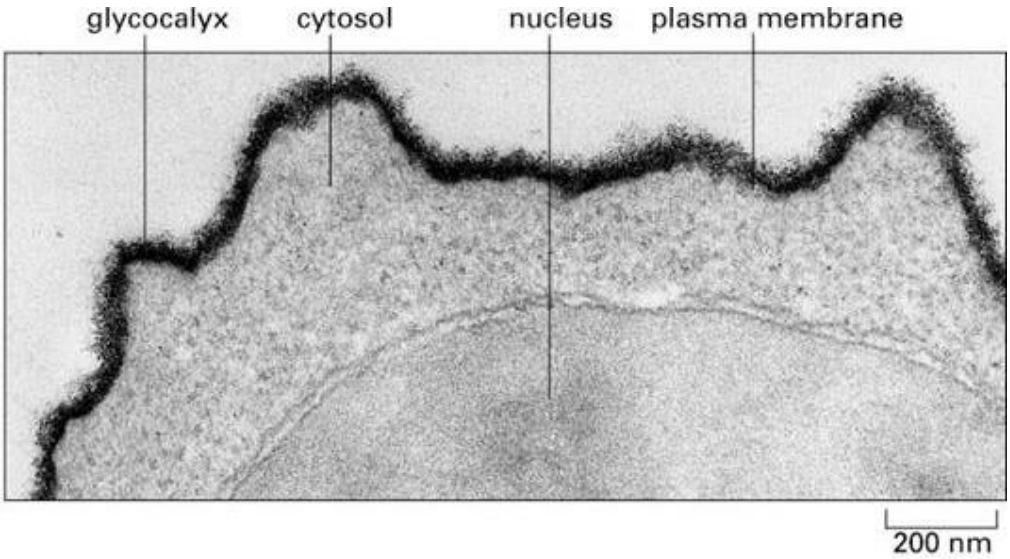

Figure 1.1: Electron micrograph of the cell from "Alberts B, Johnson A, Lewis J, et al. Molecular Biology of the Cell. 4th edition. New York: Garland Science; 2002".[2] https://www.ncbi.nlm.nih.gov/books/NBK21054/

Proteoglycans are proteins heavily glycosylated and contain a basic unit that consists of a core protein with one or more covalently attached glycosaminoglycan (GAG) chains. These GAGs (dermatan sulfate, chondroitin sulfate, heparin sulfate, and keratan sulfate) are attached to serine (Ser) residue of polypeptide chain through a tetrasaccharide core.[5]

Glycosphingolipids are glycolipids that contain a glycan structure attached to a ceramide lipid moiety via a glucose or galactose residue. There are three different types of glycosphingolipids depending on the glycan structures: cerebrosides, gangliosides, and globosides.[6] The glycosylphosphatidylinositol (GPI) anchors are glycolipids that are attached to the C-terminus of proteins through a phosphoethanolamine bridge, which connects a pseudopentasaccharide glycan core to the protein. These glycolipids attach the proteins to the cell membrane using lipid chains on the phosphatidylinositol group and are modified in a tissue and cell-dependent manner.[7] The detailed structure and modifications of GPI anchors will be discussed later in this chapter.

As an active part of the surface of cells, all the classes of glycans mentioned above play an important role in cellular interactions and communication. Indeed there are many cases reported involving the biological interactions through these glycans. These interactions include antibody recognition, cell adhesion, cell-cell interactions, and cell signaling among others.[8] Apart from roles in conjunction with other molecules like proteins and lipids, glycans are the antigenic determinant of ABO blood group type,[9] mediate the binding of human sperm to oocyte through the Sialyl Lewis^x epitope, and are part of the receptor of influenza virus involved in the infection process.[10, 11]

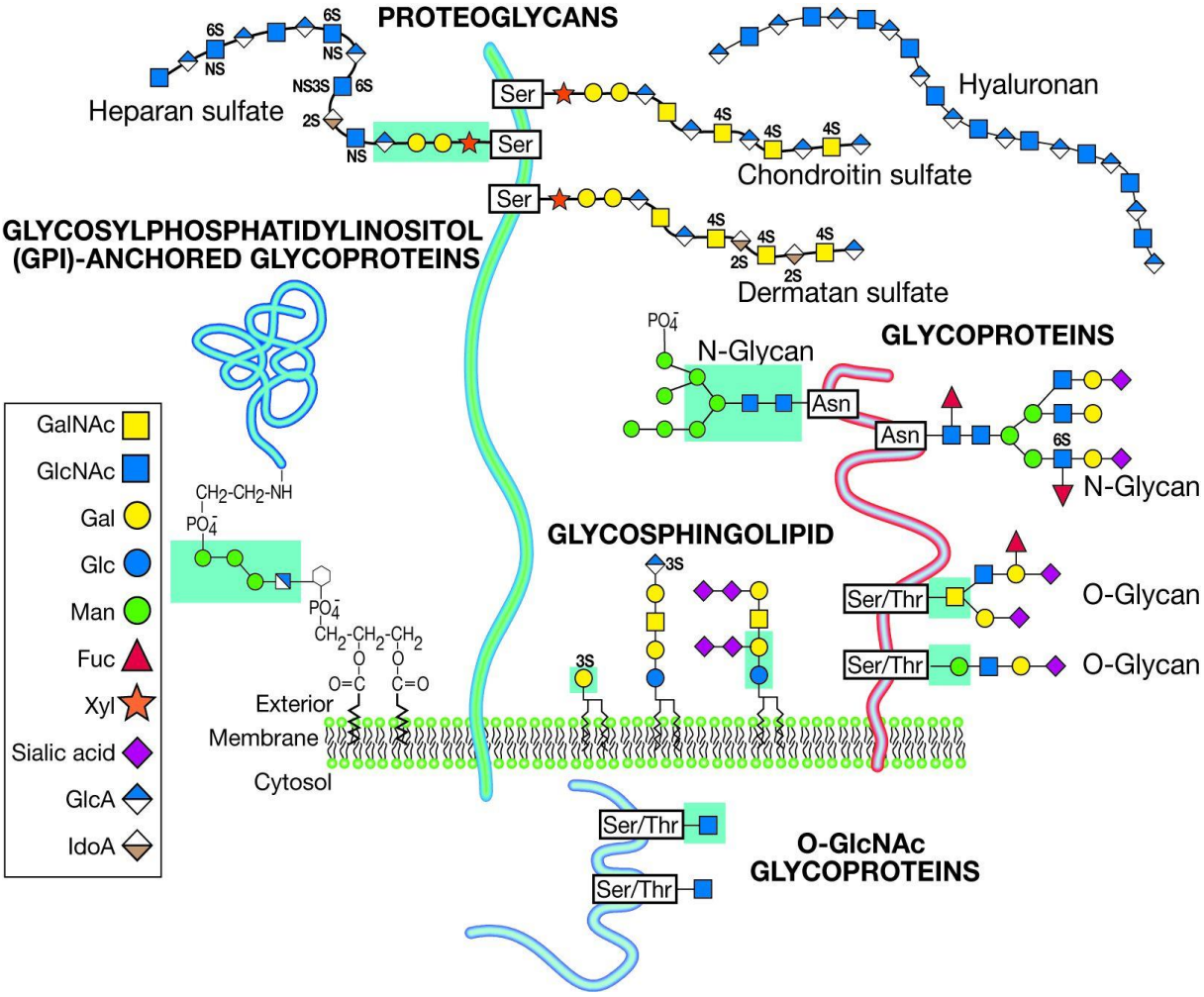

Figure 1.2: Classes of glycans present on the surface of the cell.[1]
https://www.ncbi.nlm.nih.gov/books/NBK1931/

1.2 Introduction to the Glycosylphosphatidylinositol (GPI) anchor

Glycosylphosphatidylinositols (GPIs) are ubiquitous complex glycolipids on the membrane of eukaryotic cells, especially abundant in protozoa. GPIs share the common core structure: Manα(1→2)Manα(1→6) Manα(1→4)GlcNα(1→6)-*myo*-Inositol-1-PO_4-lipid (Figure 1.3), and are naturally found in three forms: they anchor proteins or glycoproteins to the membrane forming GPI-anchored proteins (GPI-APs);[12] they attach extracellular glycoconjugates onto the cell surfaces, mostly glycoinositolphospholipids (GIPL) and lipophosphoglycans (LPGs);[13, 14] or they are present as free glycolipids on the cell membrane, so-called free GPIs. The GPIs' core structure is generally modified in a tissue and cell-dependent manner by additional phosphoethanolamine, carbohydrate side chains, or the presence of additional fatty acid chains. GPIs are attached to the C-terminus of proteins using a phosphoethanolamine unit on the Man-III residue of the glycan core, and are inserted into the cell membrane by the lipid chains (Figure 1.3).

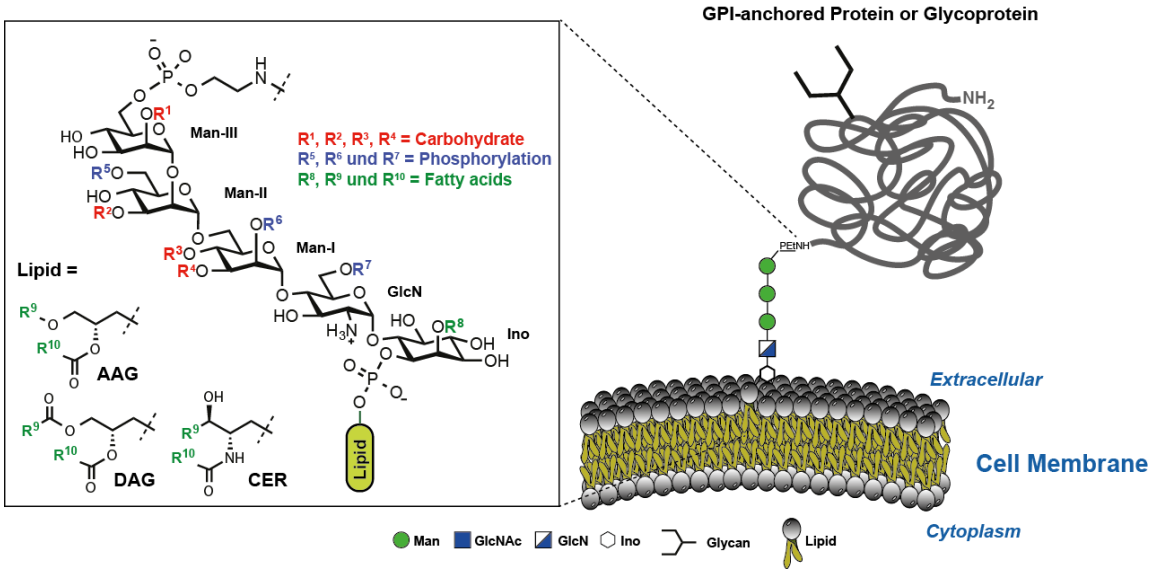

Figure 1.3: Structure and possible modification of glycosylphosphatidylinositols anchored to proteins.

The first elucidation of a GPI structure was reported by Ferguson and co-workers in 1988. They characterized the GPI of the *Trypanosoma brucei's* variant surface glycoproteins (VSGs).[15] Since this report, several total syntheses of GPI anchors have been published. Murakata and Ogawa described the first total synthesis of the GPI from VSGs using a combination of stereoselective glycosylations and highly efficient phosphorylations involving H-phosphonates.[16-20] Other syntheses of this and others GPIs

have been described by different groups, using different chemical strategies.[21-29] Additionally, various GPIs' substructures and mimetics have been prepared to evaluate new methods and strategies to synthesize them, for studies aimed to determine their biological activity and application as a vaccine candidate,[27, 30, 31] or for the diagnosis of parasitic diseases.[32]

GPI-APs play an important role in various biological processes such as cellular communication, signal transduction, cell adhesion, protein trafficking, and prion disease pathogenesis.[12, 33, 34] Naturally, the biosynthesis of the mature GPI attached to a given protein is very similar to the attachment of other posttranslational modifications like *N*- and *O*-glycosylation. The biosynthesis of GPIs starts in the endoplasmic reticulum (ER) and specific enzymes are dedicated to forming the final GPI structure which is transfered to the protein. These steps are discussed in detail in the following section.

1.3 Biosynthesis of GPI-Anchors and their attachment to proteins

The attachment of GPIs to proteins, glypiation, is determined by the presence of a signal sequence at the C-terminus of newly synthesized proteins. This signal peptide is replaced for a preassembled GPI structure by a GPI-transferase present in the lumen of the endoplasmic reticulum (ER). After further modifications of the GPI glycan and lipids in the ER and Golgi, the GPI-AP is expressed on the cell membrane.

The core structure of GPI anchors suggests a conserved biosynthetic pathway. Defects of the GPI biosynthesis in humans, either due to secretion or by GPI degradation in the ER, lead to paroxysmal nocturnal hemoglobinuria (PNH), an acquired hematopoietic stem cell disorder.[35] In parasites, such as *Toxoplasma gondii*, the biosynthesis of GPI-APs is essential for their viability. However, it is still not clear if the lethal effect on Toxoplasma is due to the deficiency of GPI-APs or of free GPIs, which are also common on its membrane.[36]

Over 200 mammalian proteins are anchored to the plasma membrane using GPIs and a total of 26 genes are known to participate in the biosynthesis of GPI-APs. Among these genes, twenty-two are the phosphatidylinositolglycan (PIG) genes, which participate in the GPI pre-assembly and following attachment to the protein. The other four described

genes participate in the modification of GPIs and they are called post GPI attachment to protein (PGAP) genes.[37]

1.3.1 Biosynthetic assembly of the GPI glycan core

The GPI biosynthesis involves at least seven to eight steps for the synthesis of a GPI glycan precursor before it is ready for the attachment to the protein. The process starts on the cytoplasmic side of the ER membrane with the transfer of N-acetyl glucosamine (GlcNAc) to Phosphatidylinositol (PI) using UDP-GlcNAc. The enzyme involved in this step, GPI-GlcNAc transferase (GPI-GnT), consists of seven components (PIG-A, PIG-C, PIG-H, PIG-P, PIG-Q, PIG-Y and DPM2). The PIG-A gene is located on the X-chromosomes and its somatic mutation leads to PNH disease.[38] In the second step, the glucosaminylphosphatidylinositol (GlcN-PI) is obtained by deacetylation of GlcNAc-PI through the action of the PIG-L protein. Although the deacetylase activity of this protein has not been validated yet, disruption of FLAG-PIG-L with proteinase K and hydrolysis of GlcNAc-PI and GlcN-PI with phosphatidylinositol specific phospholipase C (PI-PLC) from intact microsomes suggest the orientation of GlcNAc-PI, GlcN-PI and the enzyme (PIG-L) towards the cytoplasm.[39,40]

In the third step, a flip of GlcN-PI to the lumen side of the ER take place by an unknown mechanism and the GlcN-PI is acylated at the 2-*O* position of inositol to deliver GlcN-AcylPI. This acylation is a prerequisite for the further mannosylation in yeast and mammalian cells but is not necessary in trypanosomes.[41] In the next steps, a mannose is transferred to GlcN-AcylPI by an α1-4 mannosyltransferase forming Manα(1→4)GlcN-AcylPI and the second and third mannoses are added to form Manα(1→6)Manα(1→4)GlcN-AcylPI Manα(1→2) and Manα(1→6)Manα(1→4)-GlcN-AcylPI respectively (Figure 1.4). All three mannoses are transferred from dolicholphosphatemannose (Dol-P-Man) as a substrate donor. The seventh step of the assembly involves the addition of the phosphoethanolamine (EtNP) unit to the glycan generating the mature GPI-anchor precursor EtNP-Manα(1→2) Manα(1→6)Manα(1→4)GlcN-AcylPI. In the eighth step, Man-IV is transferred to the second position of Man-III, which is present in *Plasmodium falciparum*, *Saccharomyces cerevisiae* and some mammalian GPIs.[8]

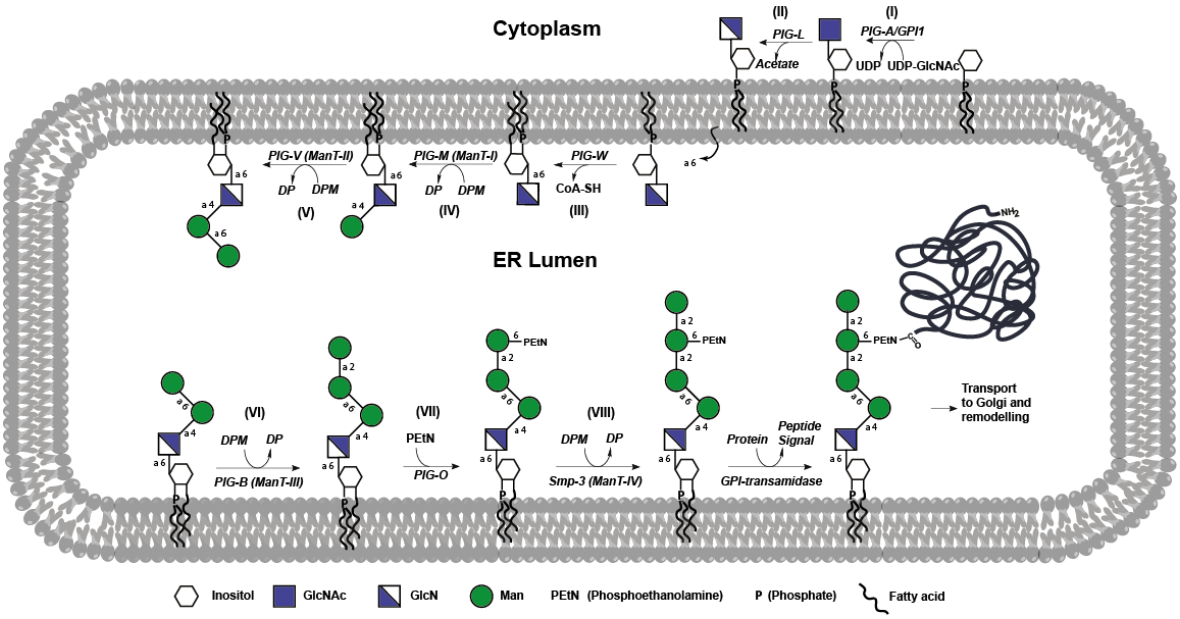

Figure 1.4: Biosynthesis of GPI-anchored proteins.

1.3.2 Attachment of GPIs to Proteins

The GPI-transamidase complex is responsible for the attachment of the GPI precursor and the protein. This complex recognizes the signal peptide at the C-terminus of the protein and, in a simultaneous process, removes the signal peptide from the protein and transfers the GPI precursor. The peptide signal does not have a consensus sequence among eukaryotes but they are transferable through species and present common characteristic features related to the position and polarity of the amino acids in the sequence.[8]

1.3.3 Remodeling of GPIs after the attachment to proteins

Upon attachment of the GPI to the protein, the GPI-glycan and lipid are modified in the ER and Golgi bodies. Little is known about the remodeling of the GPI glycan, but it depends on the glycosylation machinery of the cell type and the protein. The lipid remodeling starts with the removal of the acyl chain at the 2-O position of inositol that is mediated by PGAP1 in mammalians and is a critical step for the transport of GPI-APs from the ER to Golgi. The inositol deacylation is also required for the efficient degradation of misfolded GPI-APs via ER-associated degradation pathway.[42] During the GPI assembly, PIG-G and PIG-F can attach an EtNP unit to the Man-II residue of the GPI precursor, PGAP5 catalyze the removal of this side group.[43] Further remodeling of

the lipid part takes place in the Golgi and it may be essential for the raft association of GPI-APs.[44]

1.4 Diversity in GPI anchor structures

The structure of the GPI anchors in GPI-APs is highly diverse and it arises mainly from the functional groups attached to the glycan core, the variations in the side branches, and the lipid chains attached to inositol (Figure 1.3). There are structural properties in GPIs which are characteristic for each species and cell type, see Table 1.1. GPIs from mammalian proteins are characterized by two modifications at the Man-I residue of the core: an extra EtNP moiety at the 2-O position and an *N*-acetylgalactosamine at the 4-O position. GPIs from parasites lack these modifications.

Table 1.1: Structural modifications of some selected GPI-anchors.[(a)]

Entry	Origin	R^1	R^2	R^3	R^4	R^5	R^6	R^7	R^8	Lipid
1	*T. brucei* VSG 221[45]	±Galα	±Galβ	H	$Gal_{2-4}α$	H	H	H	H	DAG
2	*T. congolense* VSG[46]	H	H	Gal-GlcNAcβ	H	H	H	H	H	DAG
3	*T. cruzi* epimastigote[47]	Manα	H	H	$Gal_{2-4}α$	H	H	AEP	H	AAG
4	*A. fumigatus*[48]	$Man_{1-2}α$	H	H	H	H	H	H	H	Ceramide
5	*L. major* PSP[49]	H	H	H	H	H	H	H	H	AAG
6	*P. falciparum*[50-52]	±Manα	H	H	H	H	H	H	Acyl	DAG
7	*T. gondii*[53]	H	H	±Glc-GalNAcβ	H	H	H	H	H	DAG
8	*S. cerevisiae*[54]	$Man_{1-3}α$	H	H	H	H	H	H	H	Ceramide
9	*P. communis* AGP[55]	H	H	±Galβ	H	H	H	H	H	Ceramide
10	Rat brain Thy-1[56]	±Manα	H	GalNAcβ	H	H	PEtN	H	H	n.d.
11	Hamster brain PrP^{Sc}[57]	±Manα	H	±Sia-±Gal-GalNAcβ	H	H	PEtN	H	H	n.d.
12	Mouse muscle NCAM[58]	±Manα	H	±GalNAcβ	H	H	PEtN	H	H	n.d.
13	Human kidney MDP[59]	±Manα	H	±Gal±GalNAcβ	H	n.d.	PEtN	H	H	n.d.
14	Porcine kidney MDP[59]	H	H	±Gal/Sia-±GalNAcβ	H	±PEtN	PEtN	H	H	DAG
15	Torpedo AChE[60]	Glcα	H	±GalNAcβ	H	±PEtN	PEtN	H	H	DAG
16	Human erythrocyte AChE[61]	H	H	H	H	±PEtN	PEtN	H	Palmitoyl	AAG
17	Human CD52[62]	±Manα	H	H	H	H	PEtN	H	±Palmitoyl	DAG
18	Human erythrocyte CD59[63]	H	H	±GalNAcβ	H	PEtN	PEtN	H	Palmitoyl	AAG
19	Human placental AP[64]	H	H	H	H	GlcNAcβ-P	PEtN	H	H	AAG

[(a)] The positions of the residues R^1 to R^8 correspond with the positions for GPI modifications described in Figure 1.3: AAG = 1-Alkyl-2-acylglycerol; AEP = Aminoethyl phosphonate; AG = 1-Alkyl-2-*lyso*glycerol; DAG = Diacylglycerol; Gal = Galactose; GalNAc = *N*-Acetylgalactosamine; Glc = Glucose; Man = Mannose; n.d. = not determined; Sia = Sialic acid; PEtN: Phosphatidyl ethanolamine.

As mentioned above, the GPI structure-function relationship is poorly understood but many research groups have shown that the GPI anchor plays an important role in biological function besides acting as a protein anchor.[65]

1.5 Importance of the GPI anchor and GPI-anchored proteins

1.5.1 Functions of GPI-anchored proteins

In spite of the poor understanding of the GPI structure-function relationship, the function of GPI-APs has been demonstrated in diverse biological processes. Some of the GPI-APs have an enzymatic activity i.e. alkaline phosphatase (APase), an enzyme that catalyzes the removal of phosphate groups from other biological molecules.[66] Other GPI-APs act as a protecting coat for the cell, i.e. the variant surface glycoprotein (VSG) from *T. brucei*, that form a dense protective coat around the parasite.[12] Also, some GPI-APs are involved in cell-cell interactions such as neural cell adhesion molecules (NCAM) and CD 58.[66]

1.5.2 Functions of the GPI anchor

More than 250 GPI-APs have been characterized so far but not all of them have an assigned function. One definite function of GPIs is to act as a stable anchor for the attachment of the modified protein to the membrane.[67] Considering the fact that there are other ways in which a protein can be attached to the membrane, GPIs are rather complicated structures with quite diverse and specific modifications depending on the organism. So, it is expected that the GPIs have some additional biological activities beside their role as an anchoring unit.

The GPI anchors are suggested to influence the conformation and structure of the attached protein. For instance, antibodies that recognize the GPI-anchored Thy-1 protein does not bind to the protein after its treatment with Phosphoinositide phospholipase C (PI-PLC). Furthermore, circular dichroism (CD) spectra of GPI-anchored human Thy-1 differ from that of soluble human Thy-1 suggesting that the GPI anchor may affect the conformation of the attached protein.[68] A computational study of the conformation of the

GPI anchor of variant surface glycoprotein (VSG) showed that these molecules exist in an extended conformation that lies horizontally to the plasma membrane and helps to maintain the integrity of the VSG coat.[69]

Although the GPI anchor does not cross the cell membrane, it is still hypothesized that they may participate in signal transduction by associating with signal transduction partners like protein tyrosine kinases, integrins, and Guanosine-5'-triphosphate (GTP) binding proteins.[70] GPI anchored proteins are also involved in cell-cell communication such as the decay accelerating factor (DAF) and Thy-1 proteins, and they are part of the immune system. The GPI anchored proteins are not structurally constrained, rather they are more mobile, and the diffusion coefficient of anchored protein is relatively higher than other membrane proteins. This high mobility and lateral redistribution of protein might support their role in cell-cell interactions or communication.[33]

1.5.3 GPI anchor structure-mediated properties of the GPI-anchored proteins

The lipid chains of the glycolipid provides a stable association of the GPI-anchored proteins with the lipid bilayer and have been associated with the presence of GPI-APs within the lipid rafts.[71] Lipid rafts are microdomains in the cell membrane that are enriched in glycosphingolipids, cholesterol, and other lipidated proteins that perform a variety of cellular functions.[71, 72] (Figure 1.5). The GPI-APs are closely packed in lipid rafts along with other signaling proteins like protein tyrosine kinases, integrins, and Guanosine-5'-triphosphate (GTP) binding proteins, and may interact through the interaction of the GPI anchor.[73] Homo and hetero- Förster resonance energy transfer (FRET) experiments show the presence of GPI-APs in membrane domains,[74] however, the existence of lipid rafts and the enrichment of GPI-APs in these domains is still controversial. Therefore, it is still necessary to develop new methods or tools to explore the association of GPI-APs with lipid rafts.

GPI anchored proteins are not completely embedded in the cell membrane and can be used to modify the cell surface by exogenously incorporating them onto the cell membrane.[75] Even before the structure of GPI anchor was known, the GPI-anchored decay accelerating factor (DAF) protein was exogenously inserted into sheep

erythrocytes preserving their character and function.[75] Some studies also indicated that GPI-APs can be transferred from one cell to another *in vivo*.[75]

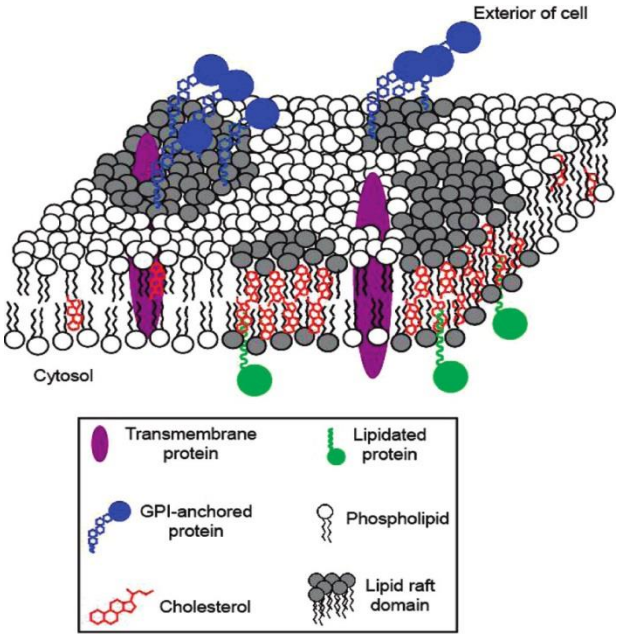

Figure 1.5: Cell membrane containing lipid raft domains. GPI-anchored proteins and other biomolecules are associated with lipid rafts.[76]

1.6 Chemical Synthesis of the GPI anchor

Considering the complexity of GPIs and their importance in several biological processes, they have gained the interest of synthetic chemists and biologists. Since the first structural report, different synthetic methodologies have been disclosed and used to obtain these complex glycolipids.[17, 21, 22, 25, 77]

Depending on the desired modifications to be included, several aspects should be considered for the chemical synthesis of GPIs: an effective combination of permanent and orthogonal protecting groups, the synthesis of optically pure inositol, stereo- and chemo-selective reactions, and the proper selection of activation method for carbohydrates and phosphates. Most of these aspects can be controlled from the design and synthesis of monosaccharides, *myo*-inositol, phospholipids, and phosphoethanolamine building blocks; however, others require special attention to the reaction conditions during the GPI assembly.

A determining factor for the design of the building blocks is the selection of the permanent protecting groups, which are removed at the last step of the synthesis. Benzyl

ethers have been the most commonly used protecting groups for this purpose; but, the need for reductive conditions for their removal has limited their application to obtain GPIs containing unsaturated lipids and other reduction sensitive functional groups. Benzoyl esters and PMB ethers were evaluated as optional permanent protecting groups in GPI synthesis;[78-80] though, the saponification of the lipid esters in GPIs during the removal of benzoyl esters, and the PMB's low stability under the acidic conditions during glycosylation reactions has limited their extensive application. The use of 2-naphtyl-methyl ethers has been recently explored for the synthesis of GPI molecules.[81] However, further studies are still required to probe their applicability to obtain complex GPIs.

1.6.1 Total synthesis of GPIs

Different linear and convergent strategies, depending on the complexity of the final GPI anchor, have been reported to synthesize these glycolipids. These strategies focus typically on obtaining the alpha linkages present in the core and generally follow the routes presented in the retrosynthetic analysis in Figure 1.6 and 1.7, which is useful in designing the individual building block with the appropriate temporary and permanent protecting groups.

Most of the synthetic approaches for the assembly of the GPI's glycan comprise convergent methods and involve a disconnection of the pseudopentasaccharide **A** into a trimannoside **B** and the pseudodisaccharide **C**. The linear assembly generally starts with the *myo*-inositol and involves the stepwise elongation of the glycan chain with monosaccharide building blocks.

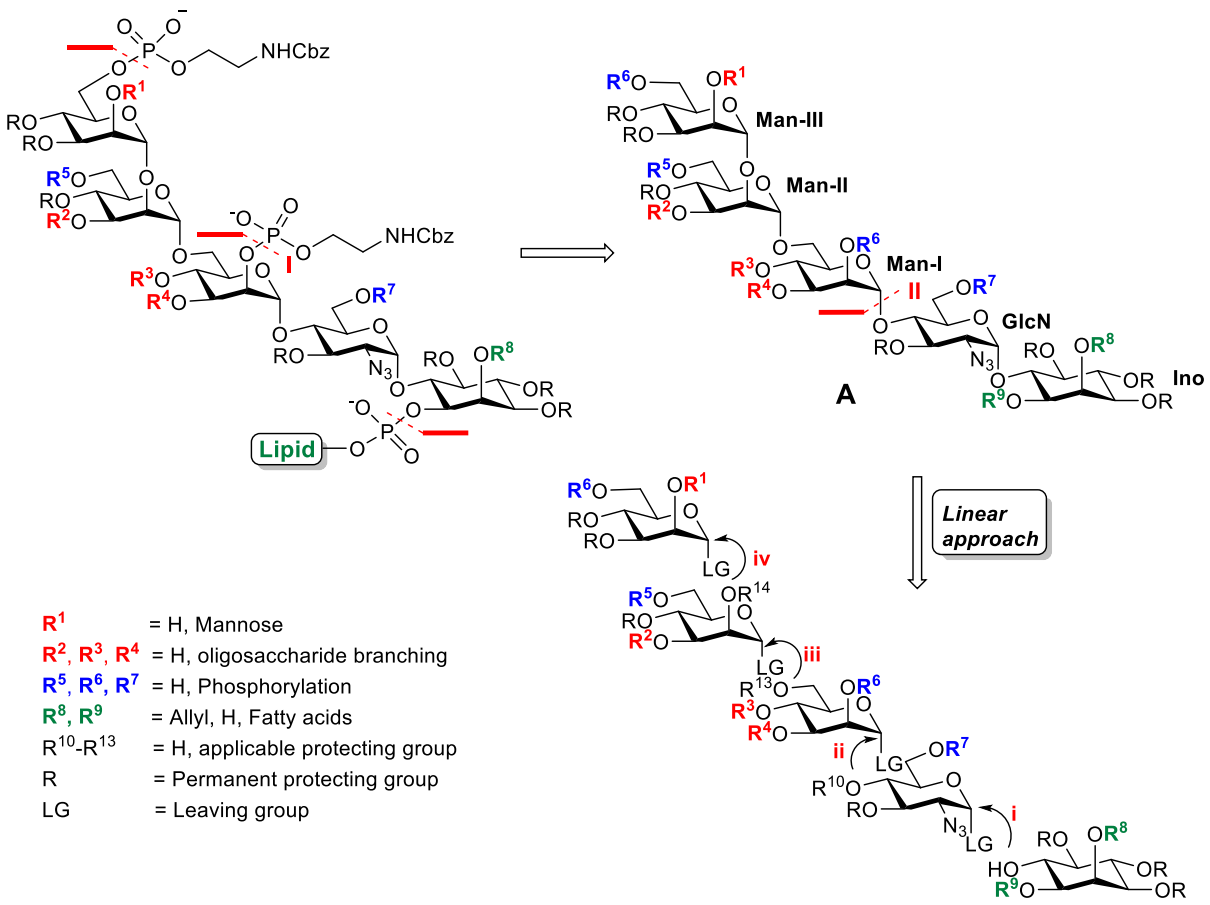

Figure 1.6: General Retrosynthetic approach for the linear synthesis of GPIs.

1.6.2 Synthesis of GPIs using a Linear Strategy

The first linear assembly of a GPI was reported by the Oscarson's group in 2002, and it described the synthesis of the phosphorylated derivative of the GPI glycan core.[82] In this synthesis, the pseudodisaccharide was sequentially elongated with three differentially protected ethyl-thiomannosides.[83]

The same glycosylation sequence was also used by Martin-Lomas to perform a solid phase supported assembly of GPI-backbone structure using trichloroacetamidate donors.[84] In this strategy, the glycan was obtained by attaching the pseudodisaccharide acceptor through the C1 position of *myo*-inositol to the solid support and its further elongation involving stepwise glycosylations with orthogonally protected mannosyl imidates. Fraser-Reid and his group also used a linear assembly to obtain the GPI of the parasite *Plasmodium falciparum*.[28]

1.6.3 Synthesis of GPIs using a Convergent Strategy

Different convergent strategies have been applied to obtain linear and branched GPIs. To assemble the GPI glycan core that lacks the carbohydrate side chain at Man-I, the general approach has been the use of trimannoside or tetramannoside donors to glycosylate the *pseudo*-disaccharide inositol, as shown in figure 1.7. To install branches to the glycan core, most of the strategies involve the installation of the side branching at Man-I before a glycosylation with a mannose donor or its use as a donor to glycosylate the pseudodisaccharide unit. These strategies have been used successfully for the synthesis of the GPI-anchor from the yeast *Saccharomyces cerevisiae*,[85, 86] synthesis of the fully lipidated malarial GPI[29] and other GPIs. Ogawa's and Ley's group have also synthesized the GPI anchor of *Trypanosoma brucei* VSG.[17, 21]

More recently, in our group a generalized strategy has been introduced to obtain diverse branched GPI structures including the two GPIs of *T. gondi*,[87, 88] (Figure 2.2, chapter 2), the core of mammalian GPIs, the GPI from VSG of *Trypanosoma congolense*, and the GPI-anchor of the *Trypanosoma brucei* VSG 117.[87]

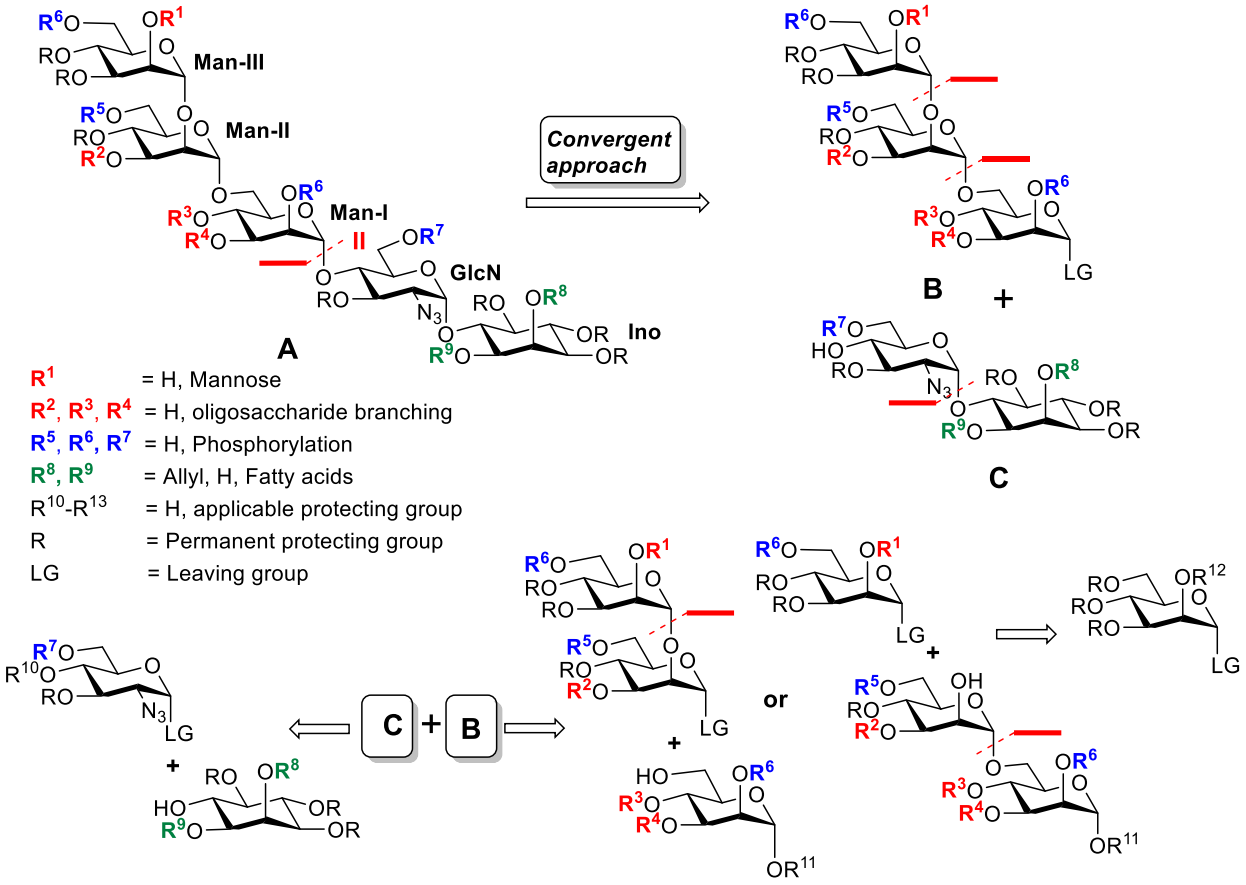

Figure 1.7: General Retrosynthetic approach for the convergent synthesis of GPIs.

1.7 GPI anchor mediated immunological response

GPIs can trigger an immune response by acting as a ligand for natural killer T-cells and by inducing the TNF-α production in macrophages.[89] In the case of malaria, the GPI of *Plasmodium falciparum* acts as a toxin that has been associated with the pathology of this disease. Mice injected with isolated GPIs showed the same symptoms as acute malaria infection including pyrexia, hypoglycemia, and death.[30] Similarly, isolated and synthetic GPIs of the parasite *Toxoplasma gondii* lacking the lipids induce the release of TNF-α in macrophages. The activation of macrophages with lipidated GPI molecules takes place through toll-like receptors and the transcription of factor NF-κB.[65, 90, 91]

From these studies, it is clear that GPIs are biologically relevant, but it is difficult to investigate their structure-activity relationship. The main limitation to study the biological activity of GPIs is the lack of homogeneous material. Generally, isolated GPIs are limited by the amount, purity, and heterogeneity which can lead to contradictory results in functional studies. Therefore, our group has focused on the development of strategies to synthesize these molecules and their deletion sequences, as well as evaluate the biological activity of specific structures to determine the minimal and specific binding epitope for the development of vaccines or diagnostic tools for parasitic infections.

An important emerging tool to investigate glycan-protein interactions is glycan microarrays. Isolated glycan structures from natural sources, libraries generated from natural glycans, and fully synthetic glycans are typically investigated in their recognition by proteins, antibodies, viruses, bacteria, and mammalian cells. The immobilization of these compounds is performed on microtiter plates, functionalized glass slides, nitrocellulose coated slides, gold slides, and others. Depending on the structures used and the target being investigated, a different mechanism of immobilization is applied. Besides affinity adsorption which predominantly uses electrostatic interactions and non-covalent immobilization, a self-assembled alkylthiolate monolayer to immobilize lipidated structures *via* covalent immobilization is widely used. Site-specific covalent immobilization methods are mostly based on the reaction between thiol or amine functionalized structures and the maleimide or epoxy groups on the slides. Other non-specific methods to covalently attach glycans to the surface are condensation, amide coupling, Diels-Alder reactions and radical coupling.

Once the compounds are bound to the slide, the interaction partner, *e.g.* sera, proteins, cells, is left for incubation. The most common type for detection methods of carbohydrate arrays relies on fluorescence. This is typically achieved by employing proteins equipped with a fluorescence tag directly or by indirect detection using fluorescence-tagged antibodies. The evaluation of binding is executed using a fluorescent microarray scanner. Although recent improvements such as live-cell imaging, autofocusing, faster image analysis, and coupling with mass spectrometry are emerging, fluorescence read out is still the predominantly used method.

Glycan-microarray screening has been performed in our group to evaluate the potential of synthetic GPI glycans and their fragments as diagnostic markers for the detection of toxoplasmosis, which is a disease generated by *Toxoplasma gondii*.[32] The results of this study showed the applicability of a *T. gondii* GPI as a diagnostic antigen for the detection of the infection and for the distinction of the acute and latent states of the disease (Figure 1.8). In addition to the detection of Toxoplasmosis, the role of the GPI modifications in the specificity of the immune response was demonstrated by the absence of cross-reactivity of the anti-GPIs antibodies to GPI structures from mammalian cells, Trypanosomes, *Plasmodium falciparum,* (18) and *Chryptosporidium parvum* (19). High-mannan structures (21) from pathogenic yeast, employed as a positive control, showed interaction with the sera.

The pseudodisaccharide (20), a conserved motif of all GPIs, showed no interaction with the tested sera, while smaller fragments of the *Toxoplasma gondii* GPI, containing the specific structural features of the GPI, showed weaker binding. These results clearly suggest that the immune system of the host can distinguish foreign GPIs from their own GPI structures by the presence of the phosphoethanolamine moiety on Man-I, which is a GPI-specific modification of mammalian GPIs. The GPI structure 3 was recognized predominantly, so the serum antibody level against this structure was determined and analyzed in detail.

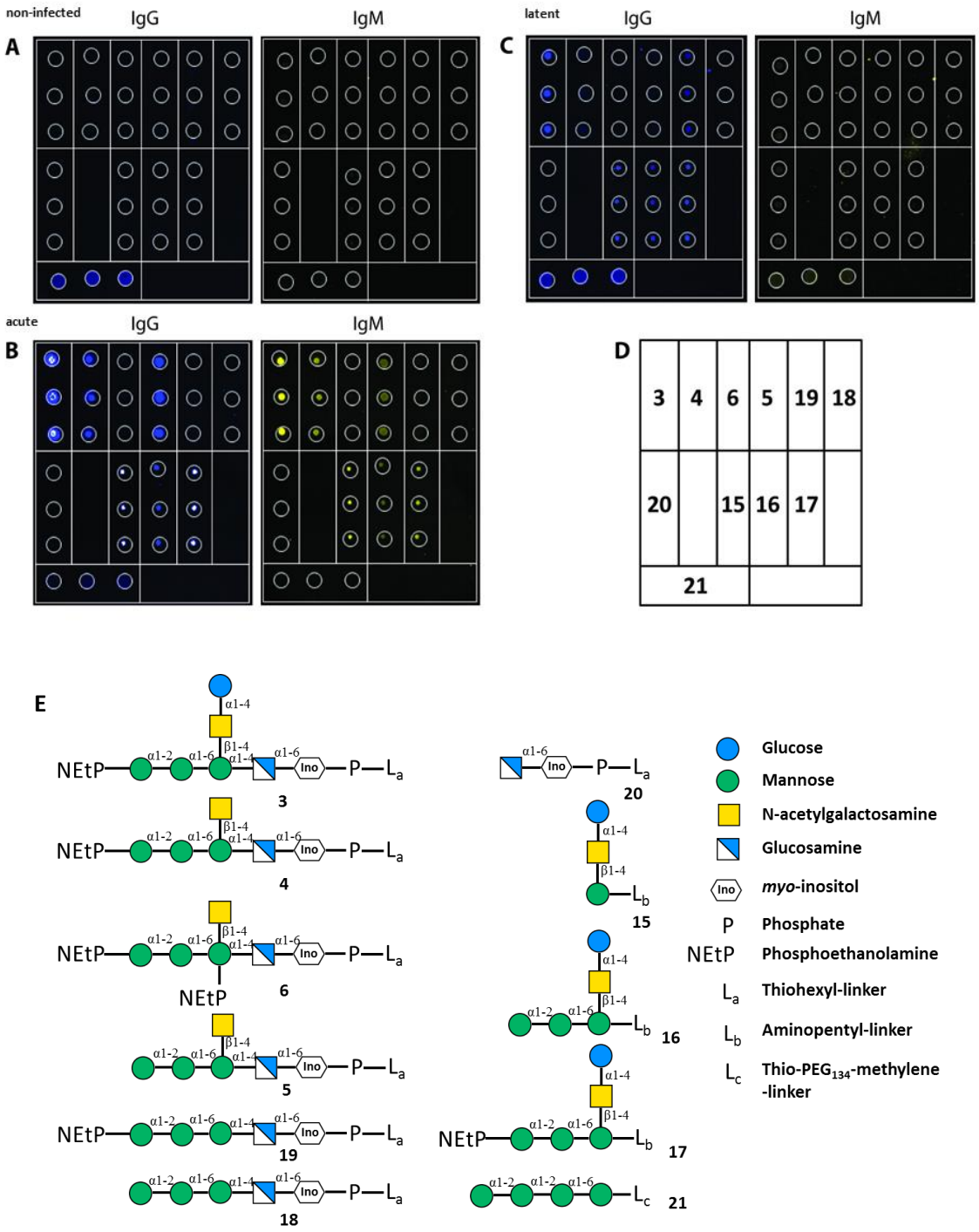

Figure 1.8: Glycan microarray of synthetic GPI and its deletion sequences of *T. gondii*. (**A**) non infected patients (**B**) latent infection (**C**) acute infection (**D**) position of the compounds on the plate (**E**) Printed synthetic structures of *T. gondii* (3-5), minimal structure of mammalian GPI (6), *P. falciparum* GPI (18) and *C. parvum* GPI (19), deletion sequences of *T. gondii* GPI (15-17, 20) and a control compound (21)[32]

The results showed that IgG and IgM levels against structure 3 are significantly increased during the acute phase of infection and after the acute infection, IgM level drops drastically indicating that the GPI structure 3 may be a suitable diagnostic marker to distinguish between acute and latent infection (Figure 1.9).[32]

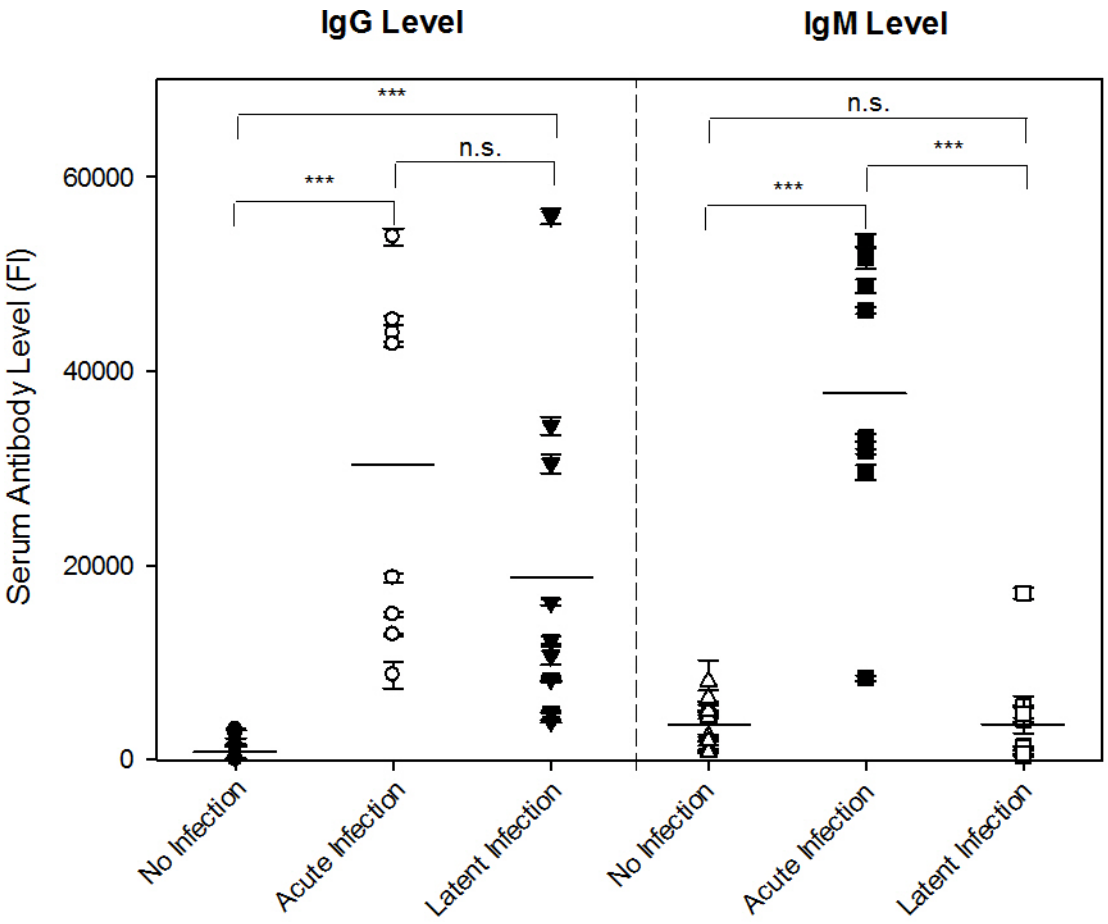

Figure 1.9: Glycan microarray of a synthetic GPI and its deletion sequences of *T. gondii*. IgG and IgM level against antigen **3** in sera samples from different toxoplasmosis cohorts including standard deviation for every data point. Description of cohorts: No Infection (n = 10); Acute Infection (n = 8); Latent Infection (n = 10). Black bars represent mean IgG/IgM levels *(n= number of samples)*

1.8 Analysis of the Conformation and Dynamics of Carbohydrates

1.8.1 Conformation of Monosaccharides (Only Pyranose ring)

The conformation of any given molecule is defined or determined by the spatial arrangement of its atoms and by the rotational degree of freedom around single bonds. When two atoms without further substituents link together, a rotation around the connecting bond does not change the spatial arrangement in the molecule, i.e. molecules of hydrogen (A), chlorine (B), and water (C) (Figure 1.10).

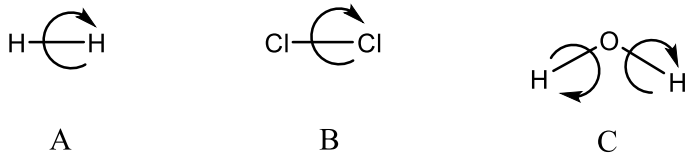

Figure 1.10: Examples showing that rotation in a molecule leading to no conformational change if there is no substituent attached.

However, when atoms of a molecule carry a substitution, the spatial arrangement of the atoms differ because of the free rotation, called the conformation of the molecule. For example hydrogen peroxides. (Figure 1.11)

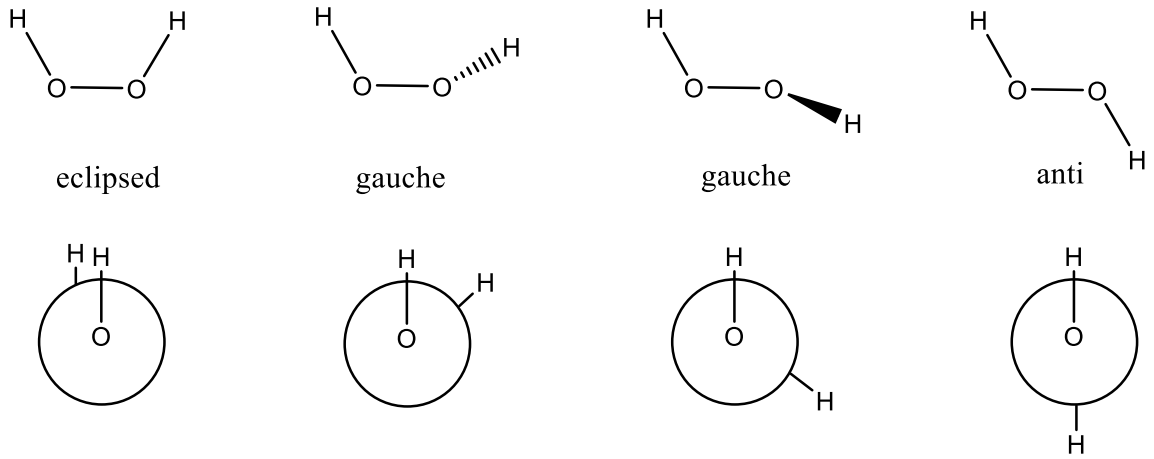

Figure 1.11: Examples showing that rotation in a molecule leading to a conformational change.

Compared to these molecules, the conformation of carbohydrates is much more complicated. In the case of carbohydrates forming pyranose rings, the conformation is very similar to the cyclohexane ring, which exists mainly in two isomeric chair (C) conformations shown in figure 1.12 (A). The conformational shape of a pyranose is mainly governed by the relative stability of the two possible chair conformations which are both free of torsional strain, but one of which, in most cases, is clearly energetically unfavored because of van der Waals interactions of the ring substituents. These conformations can be observed by NMR spectroscopy.[92]

Other principal conformations of pyranoses are half–chair (H), boat (B), and skew (S) conformations, which are named as designated in Figure 1.12B, C, and D. The chair is by far the most stable conformation for hexoses and only the skew conformation has an energy minimum (maximum stability) in a similar range.

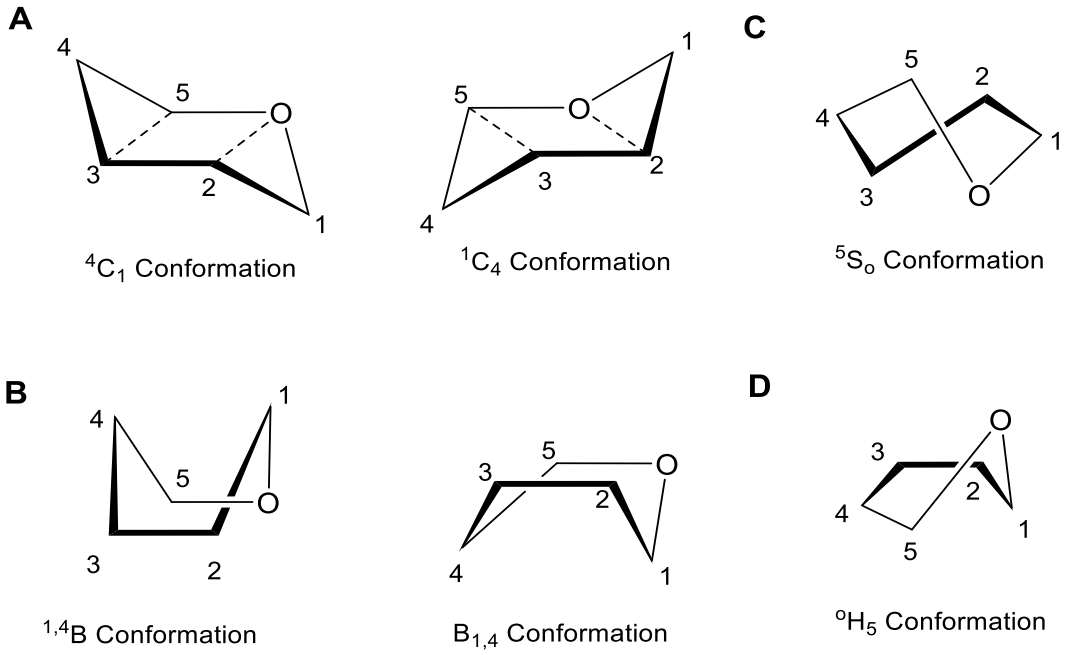

Figure 1.12: A. Isomeric chair (C), **B.** Boat (B), **C.** Skew (S) and **D.** half-chair (H) conformations of pyranose ring.

1.8.2 Conformation of Disaccharide or oligosaccharides

Disaccharides are the simplest glycan unit presenting all the rotational degrees of freedom that determine the conformation and flexibility of more complex oligo- and polysaccharides. For this reason, the investigation of the conformational preferences of disaccharides is not only interesting on its own but also it is an important milestone

toward the understanding of the conformation and dynamics of polysaccharides. From a computational point of view, disaccharides also represent the simplest test systems to validate the methods, i.e. force fields, that ultimately aim at the analysis and simulation of complex oligo- and polysaccharides.

The conformations of disaccharides are defined in terms of torsional angle across the glycosidic linkage. The angle φ (phi) in a glycosidic bond is the torsional angle between H1-C1-O1-Ci(i=4'), where i is the number of the carbon atom on another sugar moiety. The second torsional angle ψ (psi) is the angle between C1-O1-Ci-Hi(i=4'), i being the same as above (figure 1.13-A). In a glycosidic bond that does not involve a carbon atom located in the ring, but an exocyclic carbon, an additional angle (ω) has to be considered and it is defined by the O1-C6'-C5'-H5' bonds (Figure 1.13-B).

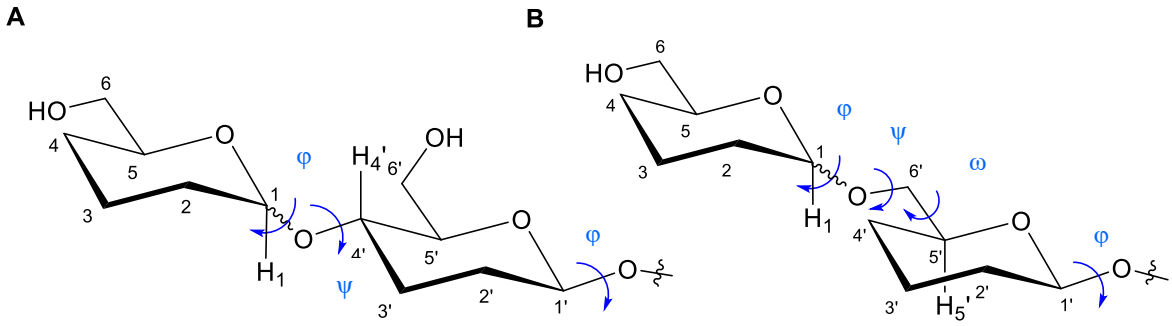

Figure 1.13: Torsional angles φ (phi), ψ (psi) and ω (omega) in the case of carbohydrates.

There are many rather sophisticated methods that are used for the analysis of carbohydrates. These methods include X-ray crystallography, NMR spectroscopy, circular dichroism and optical rotatory dispersion, and molecular modeling.[92] The crystal structure of a large cohort of carbohydrates has been solved using X-ray crystallography.[93] The crystal structure provides the data on bond angles, torsional angles, bond length, and intramolecular distances. However, due to the difficulties to crystallize carbohydrates, this technique can be applied only to a few cases.

NMR spectroscopy is an important tool for the analysis of conformation of sugars in solution. Different groups have developed NMR techniques and combined them with molecular modeling to study the conformation of carbohydrates.[94-98] Generally, the experimental NMR data can be validated using molecular modeling approximations or

used to validate the MD simulations. This combination is especially important to analyze the NMR data for complex molecules.

The use of computational methods such force fields for the molecular modeling of carbohydrates have advanced rapidly in the last years.[99-101] These NMR and molecular modeling techniques have been employed for the structural analysis of carbohydrates as well, and will be discussed in the following section as well as in Chapter 3.

1.8.3 Conformational analysis of GPIs

The conformational characterization of GPIs or any other oligosaccharides has always been a challenging task due to the flexible properties of the glycosidic linkages. Over the past decades, the geometry and conformational flexibility of these carbohydrates have been assessed by a range of computational,[102, 103] crystallographic,[104] NMR spectroscopic, and a combination of theoretical and spectroscopic techniques.[105]

The first study of the conformation of glycosylphosphatidylinositol (GPI) anchor of *Trypanosoma brucei* variant surface glycoprotein (VSG) in solution by using a combination of two-dimensional NMR methods and molecular dynamic simulation was reported by Rademacher *et al.* in 1989. They demonstrated that the GPI glycan exists as an extended configuration along the plane of the membrane and also acts as a space filling model to maintain the integrity of the VSG coat as shown in figure 1.14.[69] This study also showed the difficulties to study the structure of GPI in solution due to the low number of NOE constraints as compared to number of degrees of freedom in the torsional angle of the glycosidic linkages.

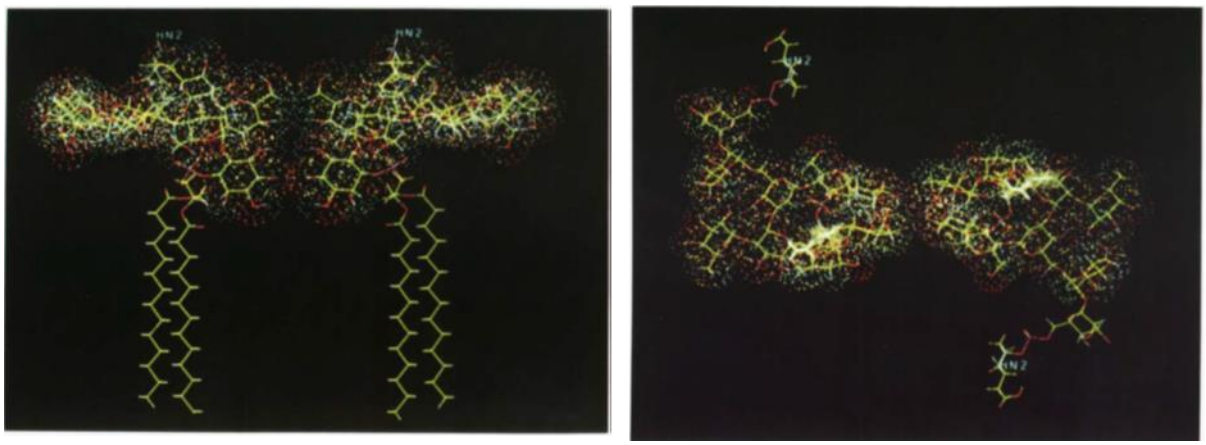

Figure 1.14: (left) Diagramatic representation of the structure with fatty acyl chain, viewed along the plane of the membrane. **(right)** perpendicular view from the top.[69]

In a similar study, Nieto and coworkers reported an analysis of the GPI glycan core along with the inositol moiety describing the glycan as an extended structure with substantial flexibility.[106] Considering the primary role of GPI anchors, this flexibility could be connected to their contribution to controlling the orientation of the attached protein with respect to the membrane. In a recent study, the core structure of GPI was studied and showed as a molecule that is mechanically compressible, which conformational properties are determined by the individual glycosidic linkages (Figure 1.15).[102]

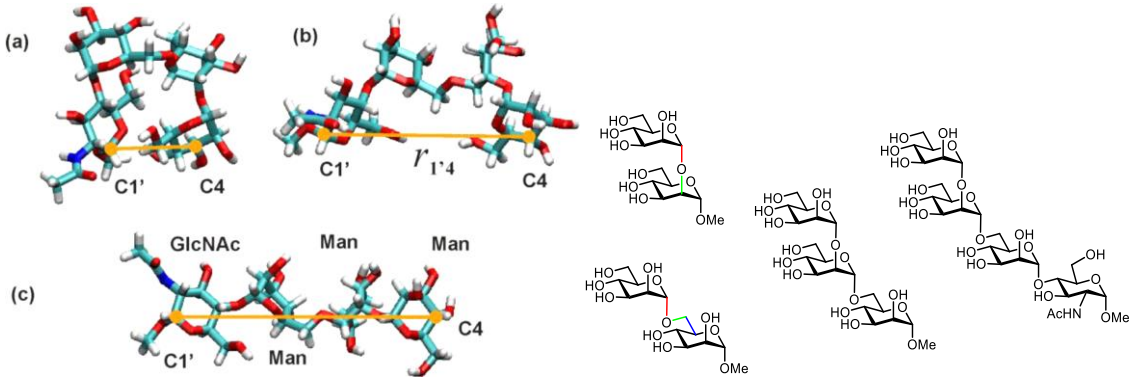

Figure 1.15: (right view) Methyl glycoside fragments of GPI defining the three torsional or dihedral angles φ, ψ and ω as explained previously in figure 1.11. **(left view)** Three configurations of the tetrasaccharide backbone, the frequently visited conformations are similar to the C-like shape in (b), for which each glycosidic dihedral angle pair is close to its global minimum within the corresponding disaccharide fragment. In this snapshot, the distance r1′4 equals 12.7 Å. During a typical 200 ns long trajectory, one observes substantial excursions from this conformation, as shown in (a) and (c). The distance r1′4 between carbon atoms C4 and C1′ (signified by the solid orange lines, all parallel to the plane of the paper) can be as short as 5 Å in (a) and as long as 16 Å in (c).[102]

NMR spectroscopy is a useful technique for the conformational analysis of carbohydrates in solution. However, it is not feasible to determine the dynamic conformation of carbohydrates solely on the basis of local conformational restraints derived from nuclear Overhauser effects (NOEs) and scalar couplings. Recently, paramagnetic NMR techniques have been applied to a variety of biomolecules using a sophisticated immobilization method to attach paramagnetic probes such as lanthanides using chelating groups at a specific site of the molecules of interest (this technique will be discussed in detail in chapter 3). Yamaguchi and Kato demonstrated that this method can be applied to synthetic glycans and natural glycans, glycolipids, or glycoproteins.[107, 108]

Paramagnetic probes are generally attached at a fixed position, mostly at the reducing end of oligosaccharide. These probes can cause paramagnetic relaxation enhancement

(PRE) and pseudocontact shift (PCS), which provides long distance information for the characterization of carbohydrates' conformations at the atomic level. These techniques have been successfully applied to the conformational analysis of disaccharides such as *N*, *N'*-diacetylchitobiose,[107] lactose,[109] and also terminal glycosidic linkages of multi-antennary complex *N*-Glycans[110].

1.9 Aim of the thesis

The main focus of our group at Max Planck Institute of Colloids and Interfaces is to synthesize the glycosylphosphatidylinositol (GPI) anchors of different parasites e.g. *Toxoplasma gondii*, *Trypanosoma brucei*, *Plasmodium falciparum*, *Trypanosoma congolense*, *Trypanosoma cruzi* and also GPI-anchored proteins, to get insight into the structure-activity relationship of these molecules.[77, 81, 88, 111, 112] General synthetic strategies have been developed to get pure material to perform the immunization experiments and microarrays. The results showed the potential of these molecules as valuable antigens for anti-parasitical vaccines or as diagnostic markers in diseased patients.[32, 113-116]

The objective of this work was to contribute to the better understanding of the conformation and dynamics of these molecules and to evaluate the diagnostic potential of the GPI of *T. gondii* for a sero-epidemiological study. In addition to this, we wanted to develop methods for ligating these GPI molecules to the *C*-terminus of proteins to gain insight into the biological functions and activity of the GPI-anchored proteins of interest.

Recently, our group has shown that the GPI of *T. gondii* can be used as a diagnostic marker for toxoplasmosis, and the detected IgG and IgM levels showed that free forms of GPIs can be used to distinguish between latent and acute infections in patients. The selected phosphoglycan of the GPI from the previous study was further investigated by developing a Luminex based assay, which could be useful for the sero-epidemiological surveillance of toxoplasmosis. (Chapter 2)

To study the conformation and flexibility of GPI molecules, the linear glycan core fragments of the GPI molecules were synthesized and attached to the paramagnetic chelating tag at the end of the synthesis and studied by using paramagnetic NMR experiment. (Figure 1.16)

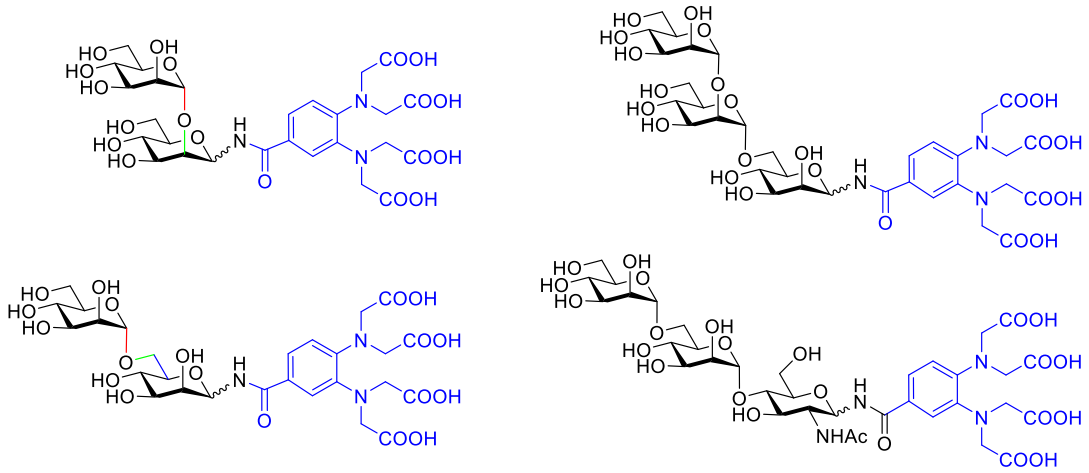

Figure 1.16: GPI fragments attached to the linker for paramagnetic metal ions to be studied by using paramagnetic nuclear magnetic resonance (PNMR).

The experimental data obtained from the NMR experiments were compared with the molecular simulation data which was used to deduce the preferred conformation of these molecules in solution (Chapter 3).

Additionally, to establish a method for the ligation of GPIs to the *C*-terminal part of the protein of interest, model GPIs of parasitic and mammalian systems were synthesized (Chapter 4). Also, the fragments of the glycan part of GPI core structure were synthesized to investigate their role in the activation of macrophages and to evaluate the interactions with anti-GPI antibodies in human serum samples using a glycan microarray (Appendix A).

Chapter 2

Synthetic GPIs for the Diagnosis of Toxoplasmosis Using Multiplex Bead Assay

2.1 Introduction

Toxoplasmosis is a disease caused by the apicomplexan parasite *Toxoplasma gondii,* which is one of the globally distributed parasites that can infect all warm-blooded animals.[117] An infection generally occurs by the ingestion of raw meat or oocysts shed by the cats.[118] However, in some cases, the infection can be acquired by organ transplantation or blood transfusion from an infected patient.[119] About 25 % of world population is infected by *T. gondii* and they exhibit no, or very mild flu-like symptoms of the disease in healthy individuals. Nevertheless, an immunocompromised individual could develop very serious complications like cerebral meningitis, ocular and cerebral toxoplasmosis.[65] A primary infection with *T. gondii* during pregnancy can lead to the transmission of parasite from mother to child and causes physical or mental retardation or even abortion.[120]

Studies performed to investigate the structure of the glycosylphosphatidylinositols in *T. gondii* showed the presence of two main GPI structures (GPI **1** and GPI **2**) on the surface of the parasite. While GPI **1** is a pseudoheptasaccharide present on the cell surface in the free form (without attached protein), GPI **2** is a pseudohexasaccharide anchoring protein antigens to the cell surface (Figure 2.1).[121] Immunological studies revealed that GPI **1** induces the production of the inflammatory cytokine TNF-α in macrophages through the activation of the transcription factor NF-$_k$B and an early IgM response in humans after infection with *T. gondii.*[90,122]

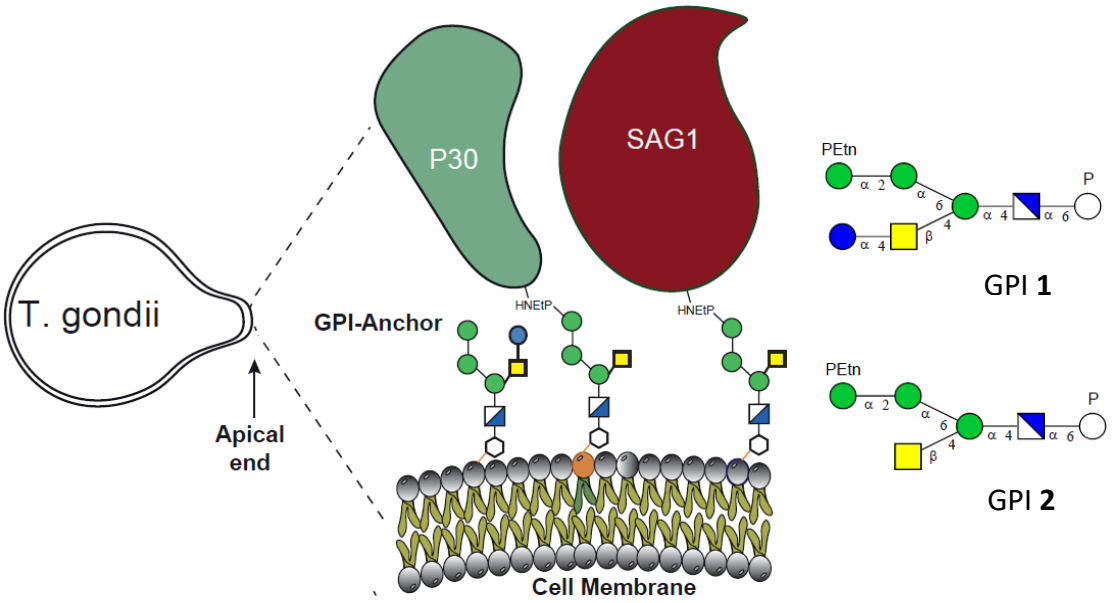

Figure 2.1: Representation of the apical end of *T. gondii parasites* showing the structure of GPIs. GPI **1** also known as the low molecular weight antigen and GPI **2,** which anchors other surface antigens to the membrane.[121, 123]

An early diagnosis of toxoplasmosis is highly important and desirable to stop the infection by chemotherapy. Currently, the diagnosis of toxoplasmosis mainly relies on serological tests such as dye test (DT), enzyme-linked immunosorbent assays (ELISA), indirect fluorescent antibody tests (IFAT), immunosorbent agglutination assays (ISAGA), modified agglutination tests (MAT), and indirect hemagglutination assays (IHA). All these tests have been developed to detect different antigens and different classes of antibodies, mainly IgG, IgM, and in some cases IgA and IgE.[124] Apart from the serological detection, there are some imaging techniques available for the diagnosis of toxoplasmosis. However, they involve the handling of live parasites during testing and have to be performed in reference laboratories.

Although these methods are currently used in the clinical setting, the main limitation of these available methods is that clinicians have to perform more than one test to confirm the infection and this requires ample amount of the sample. Additionally, these tests cannot determine the stage of the infection and the commercially available Platelia Toxo IgM Test, which is performed in the non-reference laboratories, generates a high number of false positives.[125] Therefore, it is essential to characterize or identify suitable antigens from *T. gondii* for developing reliable diagnostic tools.

Recent studies from our group have shown the potential of synthetic GPIs for the diagnosis of toxoplasmosis.[32] By using a microarray analysis, the presence and level of anti-GPI IgG and IgM antibodies in serum samples clearly differentiated the infected patients from the healthy individuals and allowed a differentiation between an acute and latent infection.[32] Although this analysis showed the potential of GPIs, further experiments and a translation to other detection systems (such as immunochromatography, Luminex, etc.) are still required.

In this work, we explored the diagnostic value of GPI **1** as an antigen in a multiplex serological assay that is commonly used for sero-epidemiological surveillance. These sero-epidemiological surveys are important in assessing the disease burden and evaluating the efficacy of interventions. The multiplex serological assay enables the evaluation of multiple antigens for a particular disease and also the simultaneous detection of multiple diseases.[126]

2.2 Multiplex bead assay (Luminex Technology)

In recent years, the Luminex technology based Multiplex bead assay has become an important tool in sero-diagnostic protocols. This assay is based on the availability of internally color coded MagPlex® microspheres/beads (carboxylated magnetic or nonmagnetic polystyrene microparticles) with a precise concentration of multiple fluorescent dyes. Each concentration of multiple fluorescent dyes corresponds to one bead set also called as "bead region". Presently, more than 100 Luminex bead sets or bead regions are available with each bead region being color-coded with varying intensities of red and infra-red fluorophores. This internal dye mixture gives an exclusive identity to each bead region and is referred to as its 'spectral signature'.

The Luminex analyzer has a built-in laser component that identifies the spectral signature, and thereby the uniqueness of each bead region. The built-in laser uses a 532 nm green laser (assay laser) to excite the phycoerythrin dye of the detection antibody (streptavidin-phycoerythrin). The 635 nm red laser (classification laser) is used to excite the dye inside the beads to determine the bead region. The availability of more than 100 unique bead regions allows us to perform a multiplex assay, where several antigens or analytes can be evaluated from a single sample-well simultaneously. So far, this assay has been successfully developed to the measure the plasma IgG level against different

antigens like C-IgL (*Entamoeba histolytica*), KRP42 (*Leishmania donovani*), SAG1 (*Toxoplasma gondii*), SXP1 (*Wuchereria bancrofti*), gag, gp120 and gp41 (HIV), cholera toxin (*Vibrio cholerae*),[126] FCaBP, ISG64, and ISG65 (*T. b. gambiense),*[127] and for the simultaneous detection of antibodies against *C. oncophora*, *D. viviparus* and *F. hepatica* in cattle serum samples.[128]

To explore the applicability of a Luminex based-assay to measure the IgG levels of antibodies against the glycan part of GPI **1** from *T. gondii* in serum samples, the glycan moiety of GPI **1** was synthesized using five building blocks and two H-phosphonates (Figure 2.2).

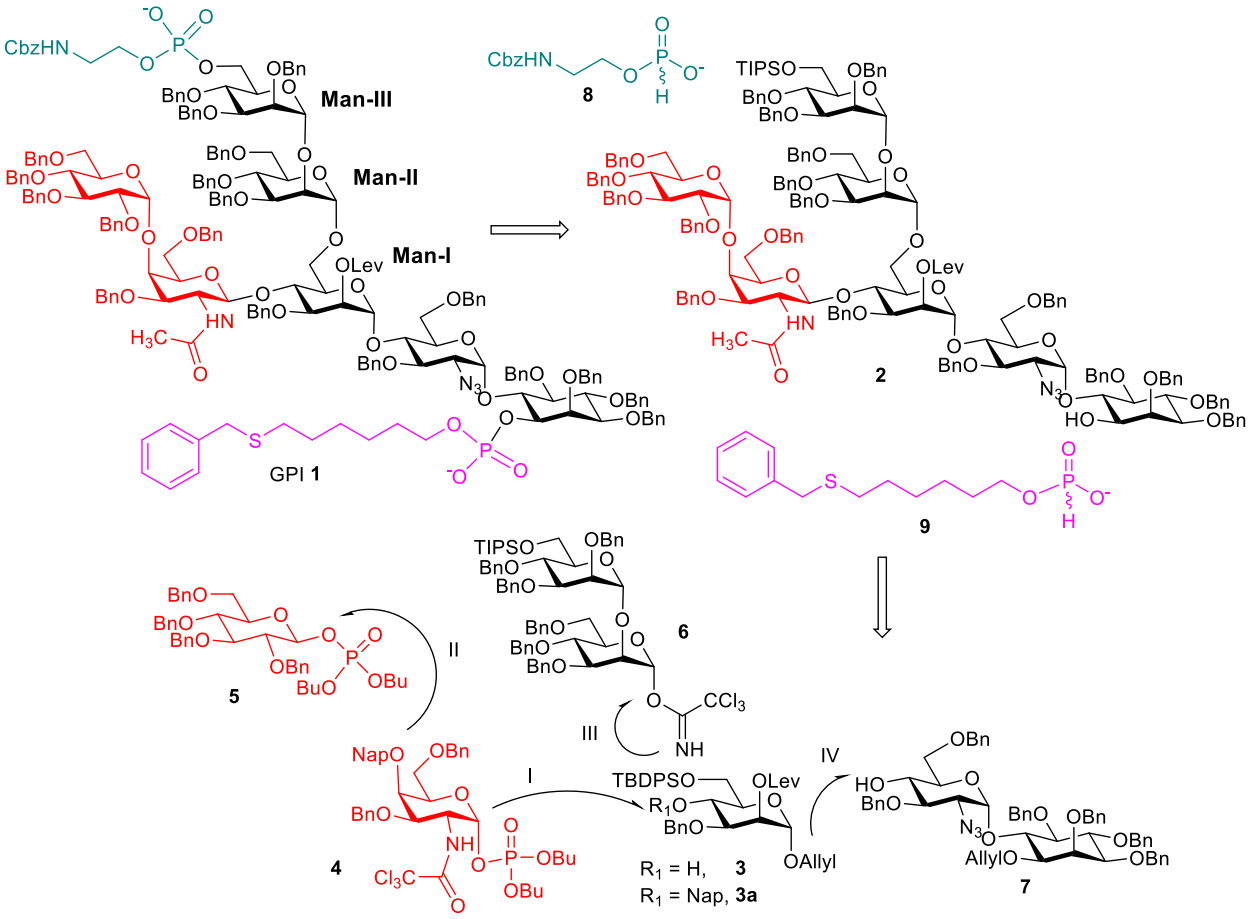

Figure 2.2: Retrosynthetic analysis of GPI 1, the low molecular weight antigen of *T. gondii.*[88]

2.3 Synthesis of GPI 1 of *Toxoplasma gondii*

The desired building blocks (shown in Figure 2.2) were synthesized according to the established protocol in our laboratory.[87, 88] The orthogonally protected building block **3** was provided by Dr. Ivan Vilotijević.

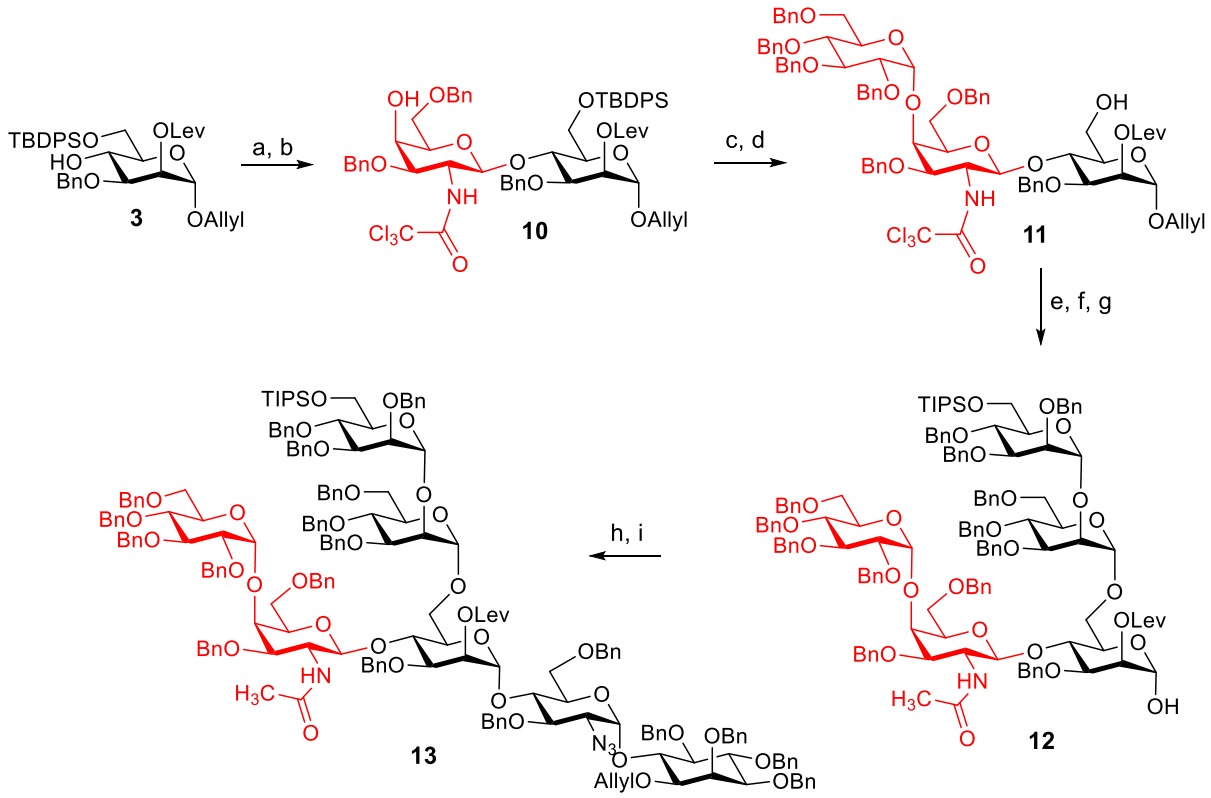

Scheme 2.1: Synthesis of the *T. gondii* glycan part of GPI 1. a) **4**, TMSOTf, anhyd. DCM, -40 °C, 95 %; b) PBS, DDQ, 85 %; c) **5**, TBSOTf, thiophene/toluene (2:1), 0 °C, 82 % (α:β=6:1); d) HF-pyridine, THF, 82%; e) **6**, TBSOTf, thiophene/toluene (2:1), 0 °C, 80 % (Only α); f) Zn, AcOH, 55 °C, 80 %; g) $[Ir(cod)(PPh_2Me)_2]PF_6$,H_2, THF, then $HgCl_2$, HgO, H_2O, acetone; h) Cl_3CCN, DBU, DCM, 65% over two steps; i) **7**, TMSOTf, toluene, -40 °C, 71%.

The assembly of the glycan part of GPI **1** started with the galactosylation of the mannoside **3** (Man-I) using phosphate **4,** followed by the removal of 2-naphthyl-methyl ether (Nap) to obtain the disaccharide **10** in very good yield (85 %). The generated acceptor **10** was glycosylated with glucosyl phosphate **5** to get the trisaccharide as an α/β mixture of the Glc 1→4 GalN linkage of the product, which was separated after the removal of the TBDPS group from the 6-*O* position of Man-I to get the trisaccharide **11**. A glycosylation of **11** with dimannose trichloroacetamidate **6** delivered a pentasaccharide, which was directly submitted to the reduction of trichloroacetamido

group with zinc in acetic acid at elevated temperature, followed by the removal of the allyl group to deliver the hemiacetal **12**. Then the pentasaccharide **12** was converted into a trichloroacetamidate donor and used in a 5+2 glycosylation reaction with pseudodisaccharide acceptor **7** to deliver the fully orthogonally protected heptasaccharide **13** (Scheme 2.1).

A removal of allyl group from the inositol of GPI-glycan **13** provided an alcohol for the installation of a phosphoryl group containing a thiol-alkyl linker. This modification was installed by phosphitylation with H-phosphonate **9** using pivaloyl chloride, followed by oxidation with iodine in wet pyridine to give compound **14** (Scheme 2.2).

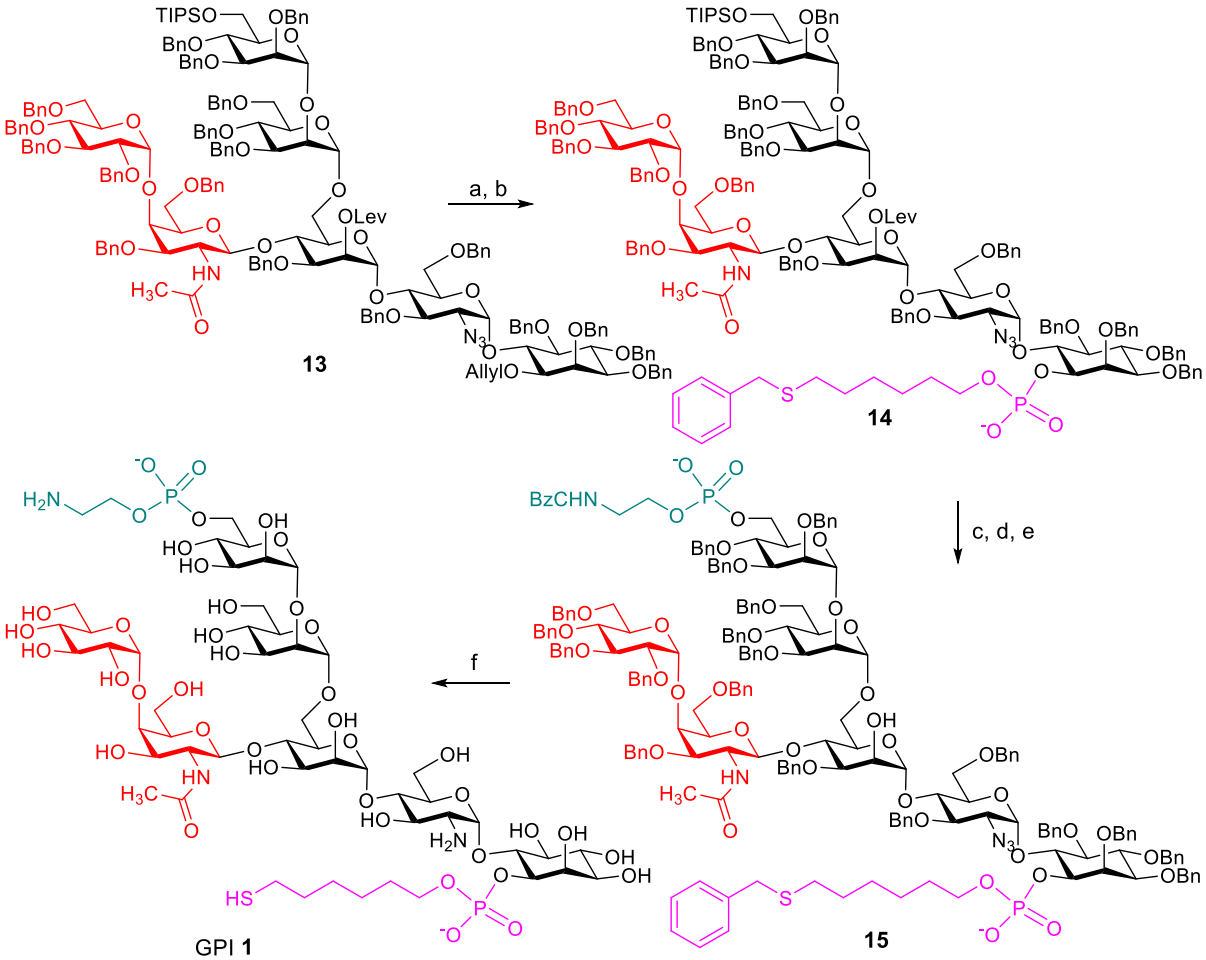

Scheme 2.2: Synthesis of *T. gondii* GPI 1. a) i. $[Ir(Cod)(PPh_2Me)_2]PF_6$, H_2, THF ii. $HgCl_2$, HgO, water, acetone, 80 %; b) **9**, PivCl, Pyridine then, I_2, water, 87 %; c)amberlite Na^+ resin exchange, $Sc(OTf)_3$, ACN, $CHCl_3$, 64 %; d) **8**, PivCl, Pyridine then, I_2, water; e) Hydrazine, pyridine, DCM, acetic acid, rt, 51 %; f) Na, NH_3, -80 °C, THF, MeOH, 50 %.

The triethylammonium cation in the compound **14** was exchanged with sodium (Na^+) using a cation-exchange column, and the triisopropyl silyl (TIPS) group was removed from the Man-III residue under acidic conditions using scandium triflate. The resulting primary alcohol was phosphitylated with the H-phosphonate **8** and the resulting phosphorus III diester was further oxidized with iodine to obtain **15**. The obtained phosphoglycan **15** was deprotected using a Birch reduction to give the GPI **1** as a mixture of free thiol and disulfide product (Scheme 2.2).

The surface of the beads used for Luminex-based multiplex assay is typically functionalized with carboxyl groups, which is commonly used to attach the antigens via activation, followed by reaction with the amine groups present in the antigens. This is typically a good strategy for the attachment of proteins, however, due to the high relevance of the two amine groups in the activity of the GPI-antigen, the conjugation of the GPI **1** to the beads was carried out using the thiol group present in the linker attached to the phosphate moiety at the 1-*O* position of *myo*-inositol unit. Similarly, a trimannoside (Man1→6man1→6Man-thiol linker) **23** (synthesized by Bridget Stokes at MPIKG) was attached to the beads and used as negative control in the study.

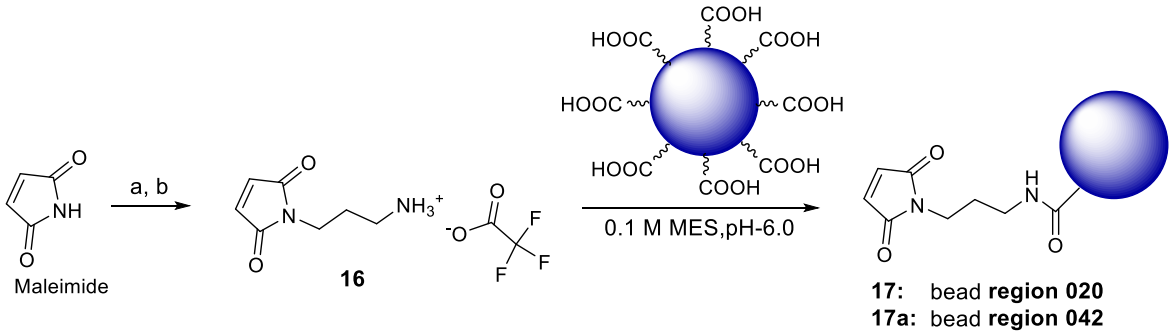

Scheme 2.3: Synthesis of the thiol reactive linker and coupling to the beads. a) Triphenylphosphine (PPh_3), $BocHN(CH_2)_3OH$, diisopropyl azodicarboxylate (DIAD), THF, rt, 48 h; b) TFA, DCM, water, rt, 5 h, 80 % (over two steps).

In order to attach the GPI glycan using the thiol functionality of the linker in GPI **1** and **23**, the MagPlex® (carboxylated magnetic polystyrene microparticles) bead **region 020** (for GPI **1**) and **region 042** (for compound **23**) were modified with the maleimide linker **16.**[129] In order to obtain compound **16**, maleimide was reacted with N-(*tert*-butoxycarbonyl)propanolamine under Mitsunobu reaction conditions using triphenylphosphine and DIAD in THF, followed by the deprotection of the amine group

using trifluoroacetic acid (TFA) to get maleimide linker **16** in very good yield, 80 %. (Scheme 2.3) The coupling of the maleimide linker to the bead regions **020** and **042** was carried out using a EDC coupling reaction in which EDC activated carboxylate groups on the beads react with the amino group on maleimide linker **16** to give maleimide modified bead regions **020** and **042**. (for details, please refer to experimental section 5.2.3).

To evaluate the level of modification of the beads with the maleimide group, Mannose **20** was conjugated to the beads as a model compound. Compound **20** was synthesized by the glycosylation of (6-*S*-acetyl)-1-hexanol with the mannose trichloroacetamidate **18** (Scheme 4). The attachment of the mannose to the beads was detected with FITC-conjugated Concanavalin-A (FITC-ConA), which is a lectin with high specificity for mannoses. The analysis of the lectin-carbohydrate interaction on the beads was performed by flow cytometry.

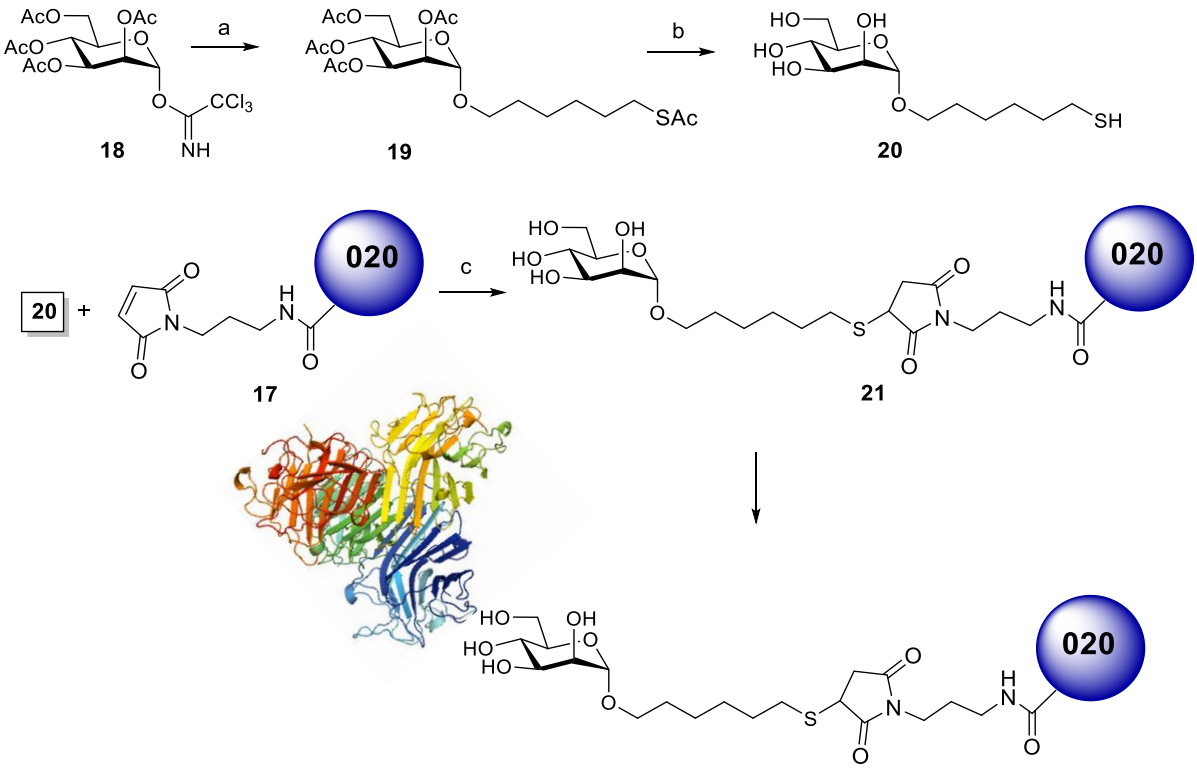

Scheme 2.4: Synthesis of a Bead-Mannose conjugate for evaluation of the modification efficiency. a) $HO(CH_2)_6SAc$, TMSOTf, -20 °C, 60 %; b) NaOMe (freshly prepared), MeOH, 90 %; c) resin bound TCEP, 0.1 M sodium phosphate, 50 mM NaCl, pH 7.0.

To determine the effect of antigen concentration to the level of maleimide modification, the surface of 500,000 beads (region **020** only) was modified with different amounts of maleimide linker (10, 25, 50 and 100 ug/mL) and incubated with equal amounts of the

mannose **20** (which is first reduced to free thiol using resin bound Tris-(2-carboxyethyl)-phosphin (TCEP)) in 0.1 M sodium phosphate buffer with 50 mM sodium chloride at pH 7.0. To check the conjugation efficiency of mannose with the maleimide modified bead, FITC-ConA was used for the analysis which binds to the mannose on the surface of the beads. The obtained results showed the increase in the fluorescence intensity with the increase in the concentration of maleimide linker which indicates that the tested concentrations were not sufficient to modify the bead surface with 100 % efficiency.(Figure 2.3) In order to get the maximum efficiency of the maleimide modification of carboxylate surface, 2 mg/mL of maleimide linker was used for 5 million beads, which is also recommended in the Luminex cookbook.

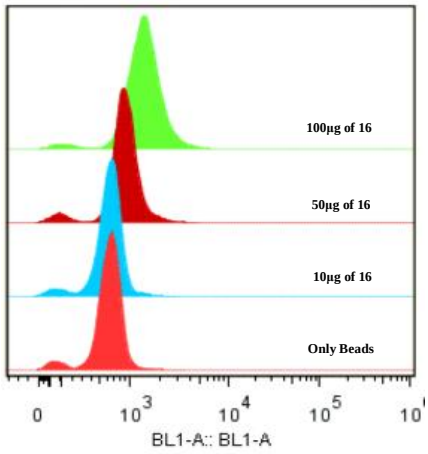

Figure 2.3: FACS analysis showing the increase in binding with the different concentration of maleimide linker **16**.

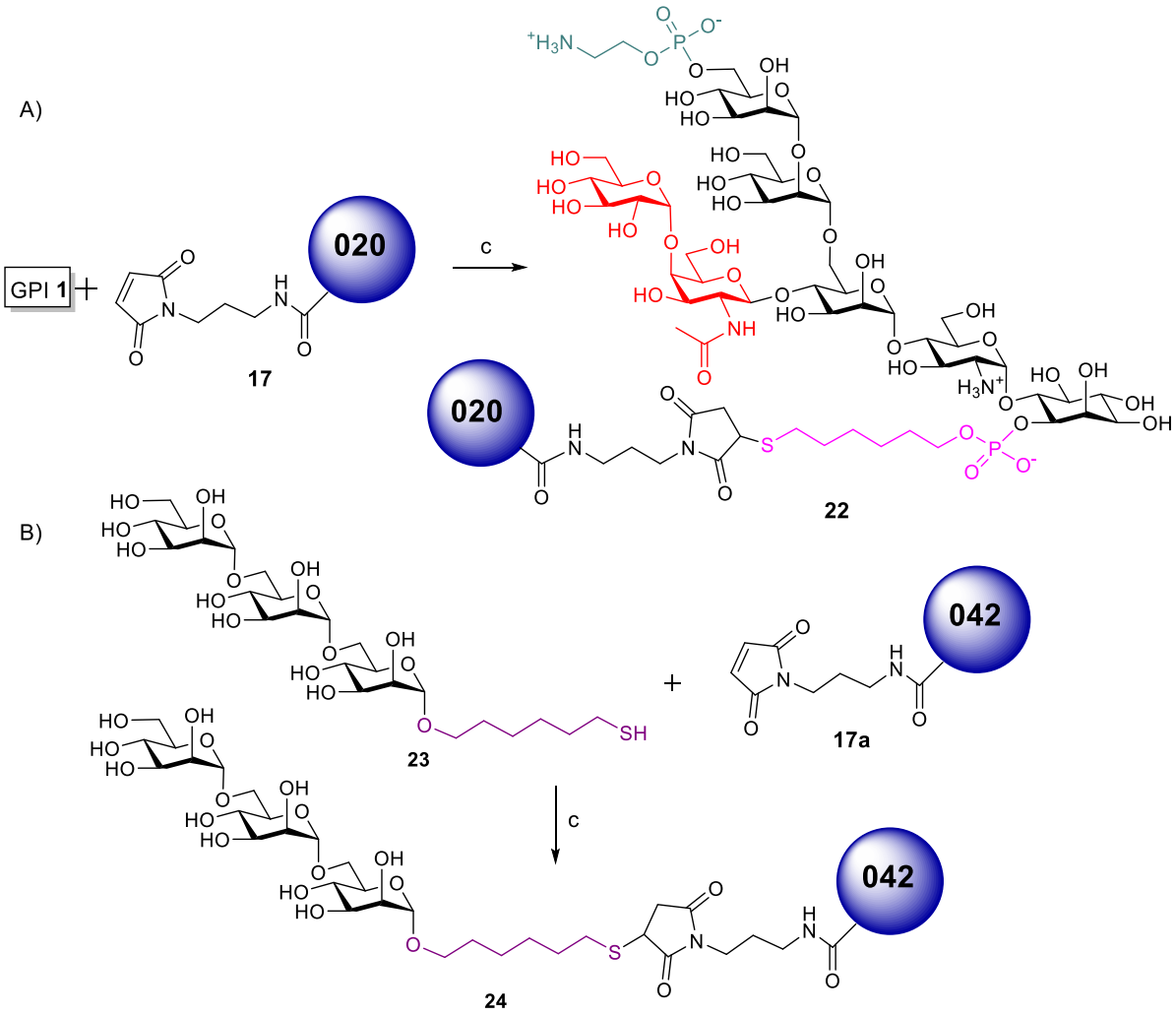

Scheme 2.5: Coupling of the GPI 1 to the bead **region 020** and Trimannose **23** (negative control) to the bead **region 042;** c) resin bound TCEP, 0.1 M sodium phosphate, 50 mM NaCl, pH 7.0.

After modifying the beads surface with the maleimide group to obtain **17** and **17a**, the reduced form of GPI **1** and trimannose **23** were coupled to the beads **17** and **17a,** respectively (Scheme 2.5), using 0.1 M sodium phosphate with 50 mM NaCl at pH 6.0 for 1 h at room temperature with constant vortexing. In addition to the glycan-beads conjugates, affinity pure Goat Anti-human IgG was conjugated to the carboxylated beads of the **region 015** and was used as positive control. Human serum albumin (HSA) was conjugated to carboxylated beads of the **region 007** and was used as a negative control. The coupling of the IgG and HSA proteins were carried out using sulfo-NHS and EDC coupling for the activation of the carboxylate groups on the beads, which reacted with the amino group on the lysine and arginine side chains in the proteins.

2.4 Luminex-based Multiplex Assay Optimization

In order to develop a Luminex-based serological assay for the diagnostic or epidemiological surveillance of toxoplasmosis using glycosylphosphatidylinositol (GPI), a cohort of samples containing ELISA-based positive or negative sera for toxoplasmosis was used to optimize the assay. Various factors were considered for the development and optimization of the assay including:

- Type of conjugation of the secondary antibody
- Concentration of the secondary antibody
- Serum sample dilutions
- Buffer used for the assay
- among others

Each of these optimization factors will be discussed separately in the following sections.

2.4.1 Optimization of the Antigen (GPI 1) concentration and of the secondary antibody

The glycan antigen GPI **1** was coupled to **region 020** Luminex beads using thiol-maleimide chemistry in two different concentrations: 50 µg and 25 µg/2.5 million beads. The detection of antibodies from the serum samples (either positive or negative) recognizing the GPI **1** on the beads was accomplished using a two- or three-step protocol involving two types of secondary antibodies (Figure 2.4). In the three-step protocol, the GPI-conjugated beads were incubated with the sera samples, then incubated with a biotinylated Affinity Pure Goat anti-human IgG(H+L) antibodies and following the detection of biotin with phycoerythrin-tagged streptavidin. In the two-step protocol, the GPI-beads were incubated with the sera samples and the detection was performed by using R-Phycoerythrin conjugated Affinity Pure Goat antihuman IgG.

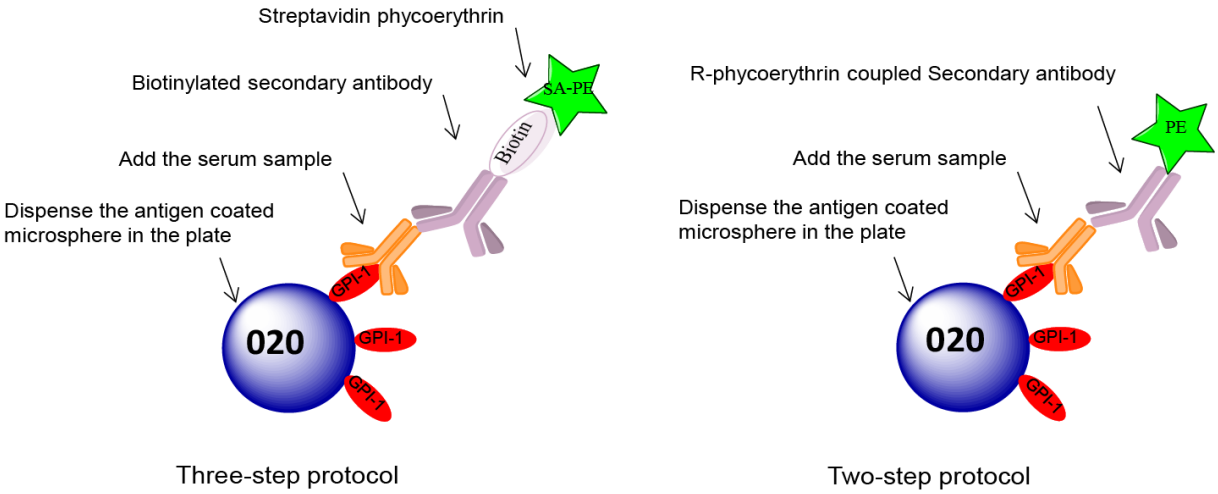

Figure 2.4: Detection of the recognition of GPI-1-Beads conjugated by Anti-GPI antibodies using a three-step or a two-step protocol.

The results with the biotinylated secondary antibody clearly shows higher mean fluorescence intensity (MFI) signals in the positive samples when compared to the negative samples when 50 µg of GPI **1** were used. On the contrary, by using 25 µg of GPI **1** there was no statistical difference between the positive and negative samples. It is worth noting here that the background was quite high in the negative samples (Figure 2.5). Two concentrations of the secondary antibody were evaluated for the detection of the GPI-antibody conjugate.

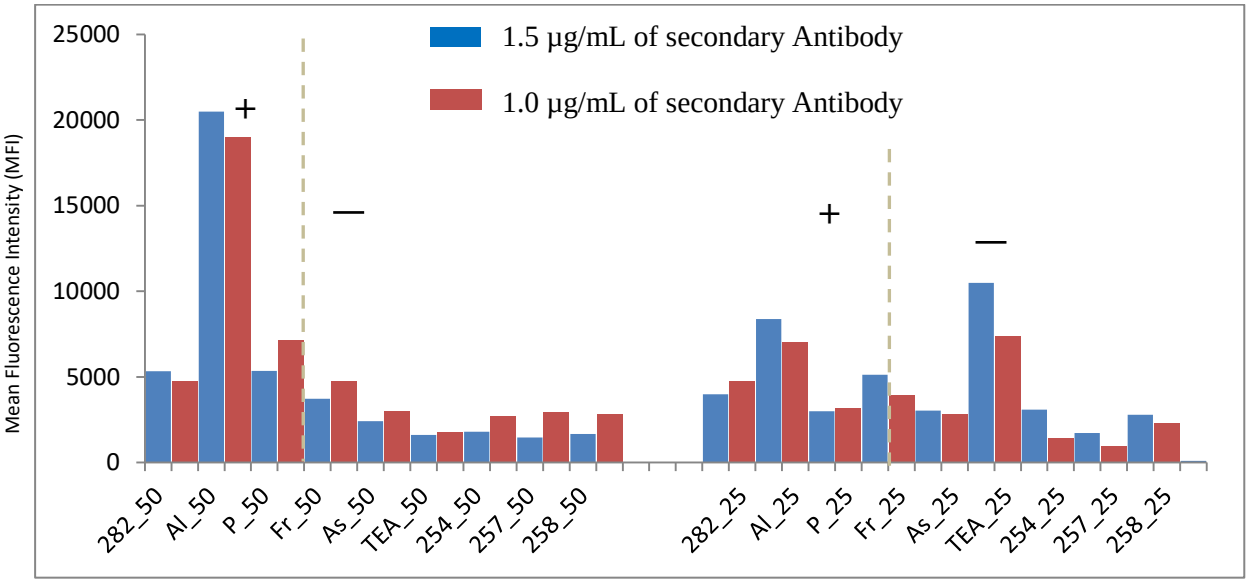

Figure 2.5: Testing two different concentrations of the antigen with the biotinylated secondary antibody: Luminex beads were coupled with two different concentrations of GPI 1 (50 and 25 µg). 1.5 µg/mL (blue bar) or 1 µg/mL (red bar) of biotinylated secondary antibody with 3 µg/mL of detection

antibody (Streptavidin-phycoerythrin) was used. The left panel shows the results with 50 µg of GPI 1 and the right panel shows the resulting MFI with 25 µg of GPI 1. 1:100 dilutions of serum samples were used.

By using a phycoerythrin-conjugated secondary antibody for the direct detection of the anti GPI-antibodies and GPI interactions (Figure 2.6), the signal to noise ratio was lower when compared to the signal to noise ratio in the three-steps protocol for most of the negative samples. Except in a few cases, which could be attributed to the nature of the individual serum, considering the fact that the MFI values for positive samples were also compromised. These results clearly showed that 50 µg per 2.5 million beads delivered a better conjugation of the GPI **1** to the beads for the assay; this conjugate was therefore considered for the next optimization steps. Furthermore, the clearer detection of the anti-GPI antibodies and better signal to noise ratio using Phycoerythrin-conjugated secondary antibody was selected as the better method of detection.

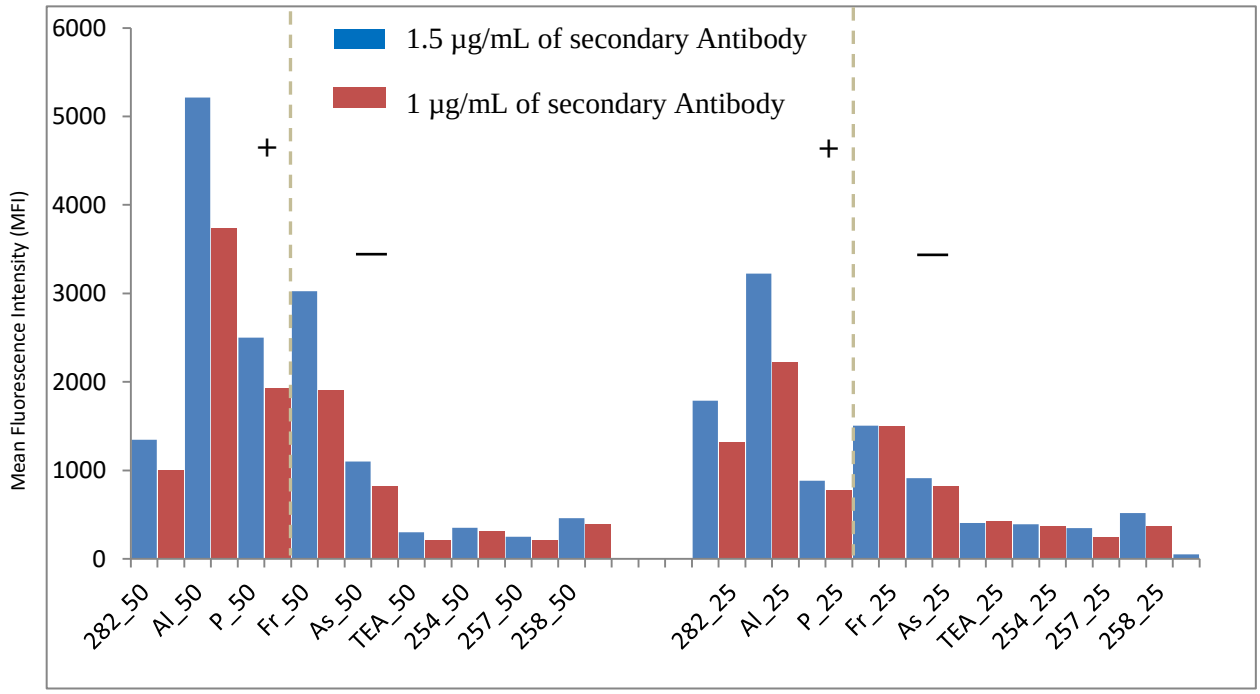

Figure 2.6: Testing two different concentrations of the antigen with the directly coupled secondary antibody: Luminex beads were coupled with two different concentrations of GPI 1 (50 and 25 µg). 1.5 µg/mL (blue bar) or 1 µg/mL (red bar) of phycoerythrin-coupled secondary antibody was used. The left panel shows the results with 50 µg of GPI 1 and the right panel shows the resulting MFI with 25 µg of GPI 1. 1:100 dilutions of serum samples were used.

2.4.2 Optimization of the secondary antibody concentration

Different concentrations of the secondary antibody were tested to determine the optimal concentration for the detection of the GPI-antibodies' interactions and a possible reduction of the background signal. The results clearly indicate that the used concentration of 1.5 µg/mL was the optimal concentration for the assay giving clear high MFI values for the positive samples and low MFI values for the negative samples (Figure 2.7).

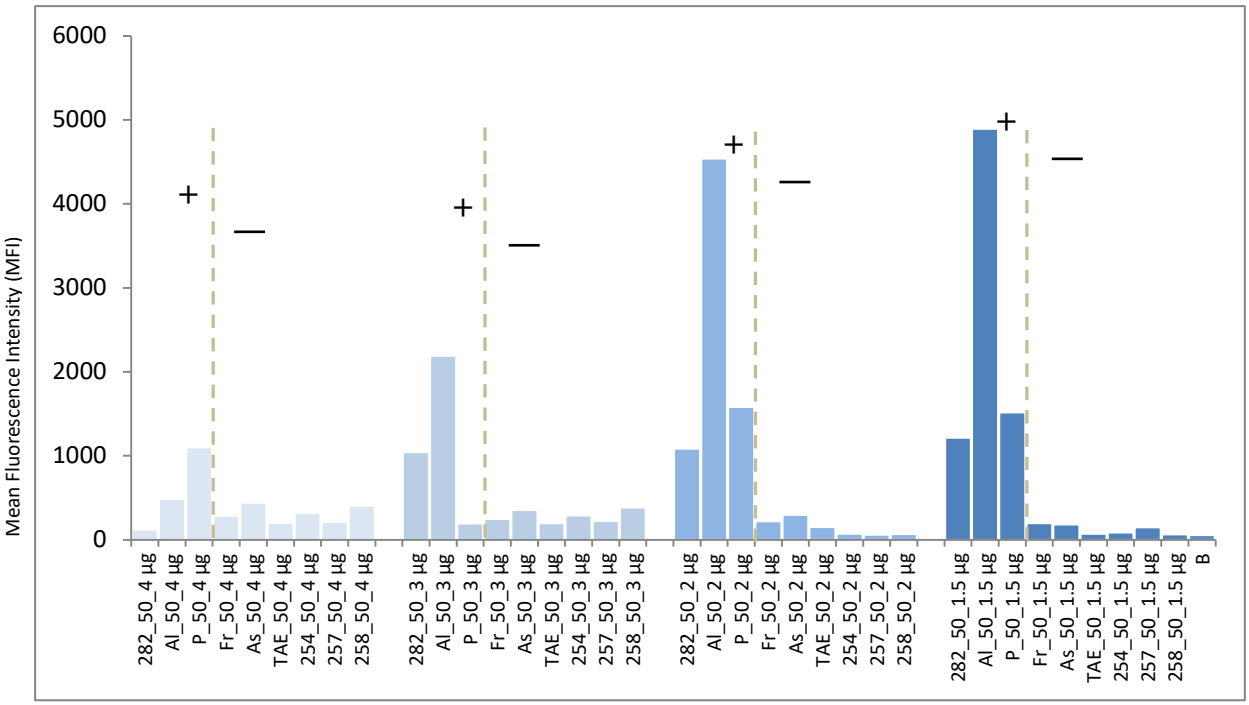

Figure 2.7: Antibody concentration optimization: different concentrations of the directly coupled secondary antibody was tested. Results show that the 1.5 µg/mL concentration is optimal. 1:100 dilutions of serum samples were used.

2.4.3 Serum sample dilution

Even though the Luminex-based assay was in agreement with the ELISA results, a high signal to noise ratio was still obtained in the negative samples. Therefore, the role of the sera sample dilution on the background signal and its effect in the detection of the positive samples was evaluated. Sera dilutions between 1:100 and 1:1000 were tested.

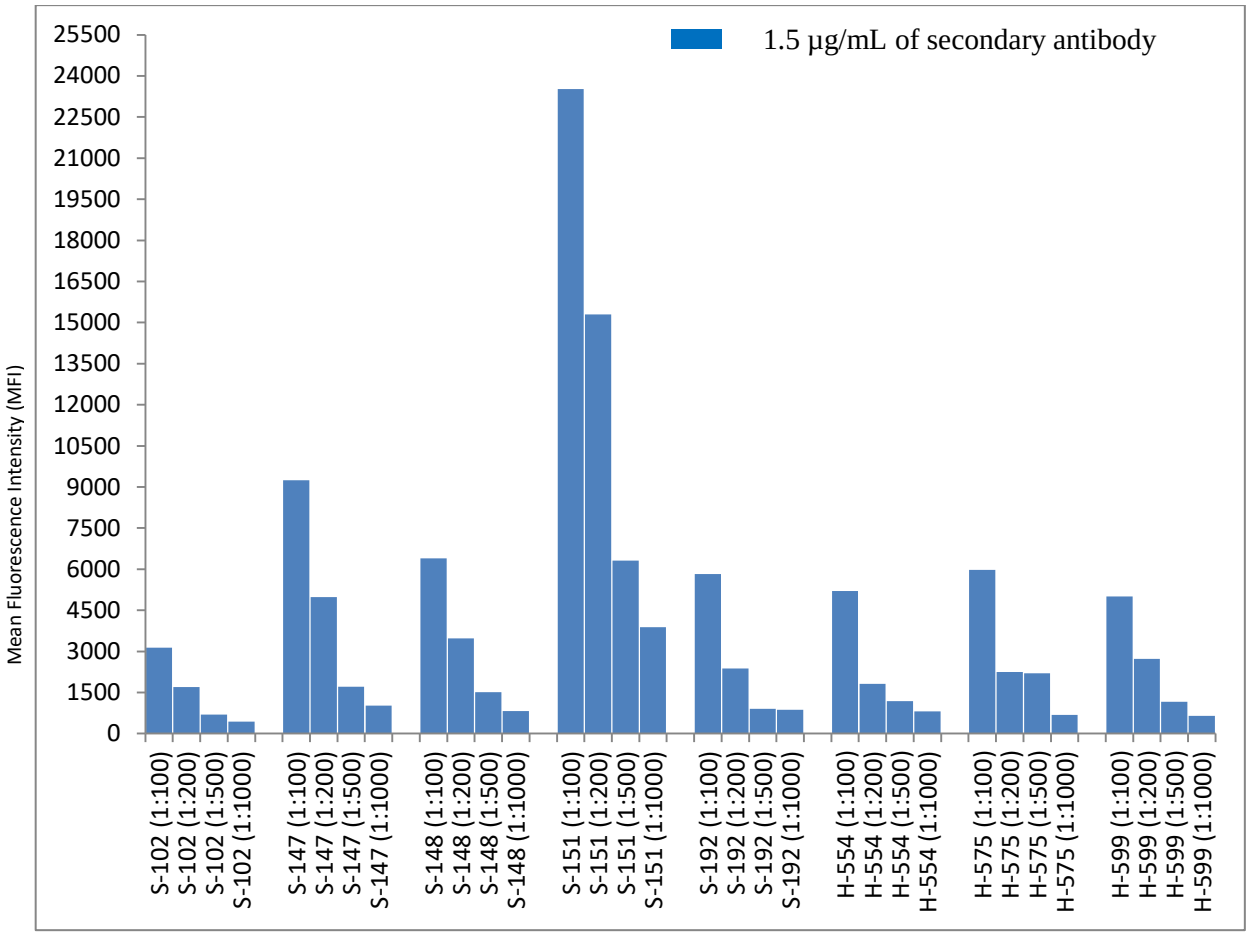

Figure 2.8: serum sample dilution: different serum sample dilutions were tested: 1:100, 1:200, 1:500, 1:1000. Results show the decrease in the signal with higher dilution.

The analysis of eight positive sera samples at 1:100, 1:200, 1:500 and 1:1000 dilution showed that the dilution of 1:100 delivered the best signals that allow a differentiation of positive sera from the background.. By increasing the sera dilution from 1:100 to 1:1000, the MFI values detected decreases exponentially in all the tested serum samples. (Figure 2.8)

The background signal in the analysis was still high even with the optimization of the antigen and secondary antibody concentration, sample dilution, and the detection method used in the assay. Looking for other factors that may generate this high signal, the types of buffers used in the analysis and possible unspecific interactions of other anti-glycan antibodies present in the sera were further evaluated.

According to the Luminex protocol cookbook, the recommended buffer used for the serological assay was “assay buffer” with a composition of 1 % BSA in PBS at a neutral pH which is commonly used for antigenic proteins. For glycan antigens, the

recommended buffer might not be a good option, so a different buffer with high salt concentration and added detergent was used to see the effect on the signal to noise ratio in the serum samples. Currently, to reduce the interference in the immunoassay, "low cross buffer" has been used to improve the quality of detection and to reduce the nonspecific interactions. The composition of this buffer is PBS with 300 mM NaCl, 0.25 % triton-100, and 5 % ethylene glycol (EG). Because of the cost-effectiveness of low cross buffer, in-house low cross buffer was used for the assay with and without ethylene glycol as the importance of ethylene glycol was unclear. The results showed the increase in the MFI values for positive serum samples and reduction in MFI values for negative serum samples (not in all the cases) with higher concentration of salt in the assay buffer and by the addition of a detergent. The addition of ethylene glycol was not helpful in this assay. (Figure 2.9)

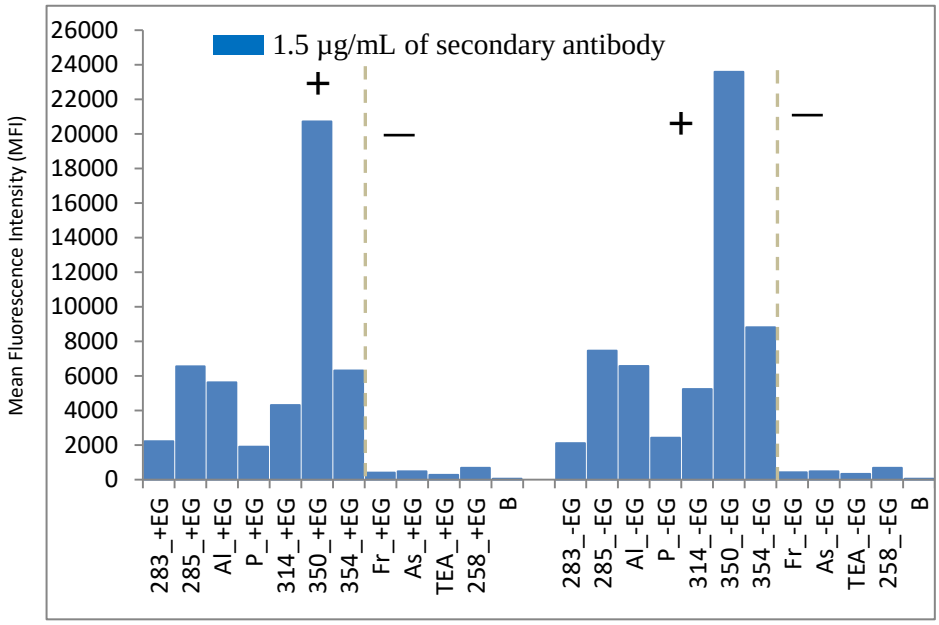

Figure 2.9: Assay buffer: a different buffer was tested to see the effect on the signal to noise ratio. **Left panel**: PBS+ 300 mM NaCl+0.25 % triton X100, 5 % ethylene glycol (EG). **Right panel**: PBS+ 300 mM NaCl+0.25 % triton X100. Results show the improvement in the MFI values of positive serum samples and the reduction (not substantial though) in the negative serum samples when there is no ethylene glycol.

The epitope mapping of the GPI-**1** showed that the specific binding of antibodies to the side branch part (Glc-GalNAc moiety) of the GPI is required for the diagnosis of toxoplasmosis. An analysis of possible parts in GPI-**1** that may be responsible for unspecific interactions enhancing the background signal clearly suggests the oligomannoses as possible epitopes. Oligomannoses having α-1-2 and α-1-6-linkages are

frequently found in nature and are part of the carbohydrate antigens of different pathogens.[130]

In order to evaluate the level of unspecific binding coming from the mannoses, the binding of sera to beads containing the trimannose **23** was evaluated. On the basis of the data obtained with these beads (Figure 2.10), it was clear that high MFI values can be obtained for negative and positive samples as a result of unspecific binding to this sugar moiety.[32] It is worth noting that the nature of this signal can also be a specific interaction of anti-mannose antibodies present in the sera with the mannoses present in GPI's structure. However, as demonstrated in the previous work of our group, these interactions have a lower potential in the diagnosis of toxoplasmosis.

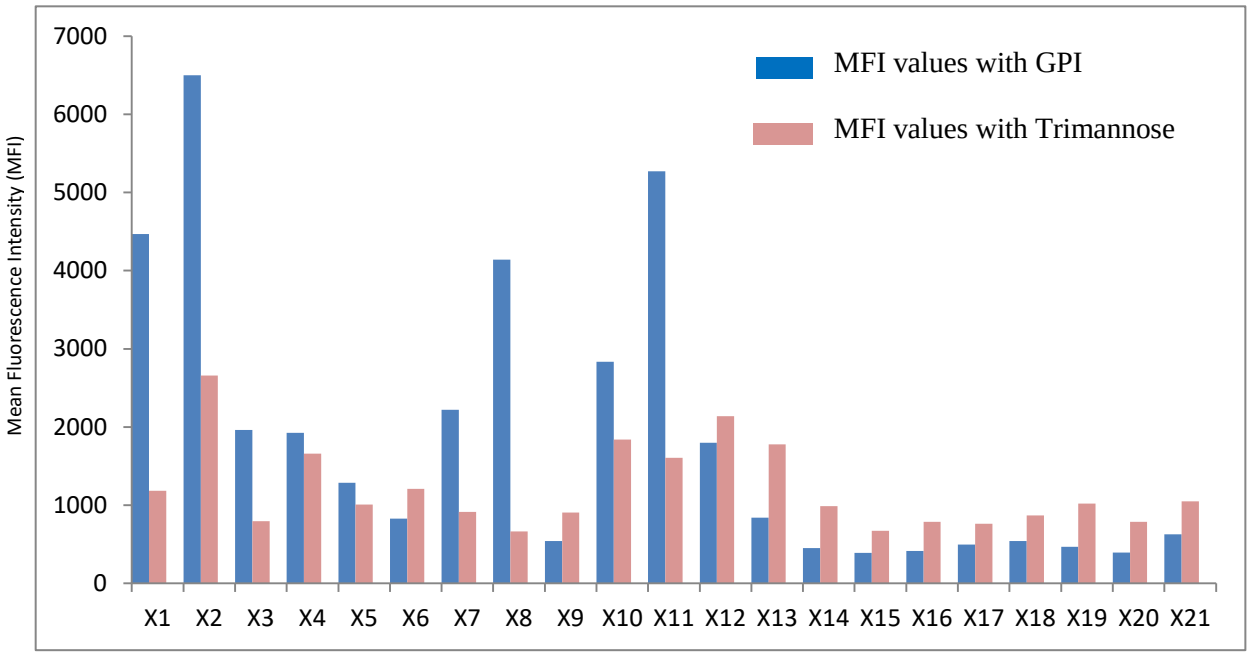

Figure 2.10: Comparison of GPI 1 (blue bar) and trimannose 23 (red bar) binding in the same sample set: Results show that there is some unspecific binding with trimannose 23 which might explain the unspecific binding with GPI 1 as well. (X1 to X21 is the number of samples tested)

After standardizing the conditions, the assay was carried out in PBS with 300 mM NaCl and 0.25 % triton X100. By using these standardized conditions, 185 samples were tested and statistically analyzed. ROC analysis was performed to test the specificity (false positive rate) and sensitivity (true positive rate) of the assay (Figure 2.11 and 2.12).

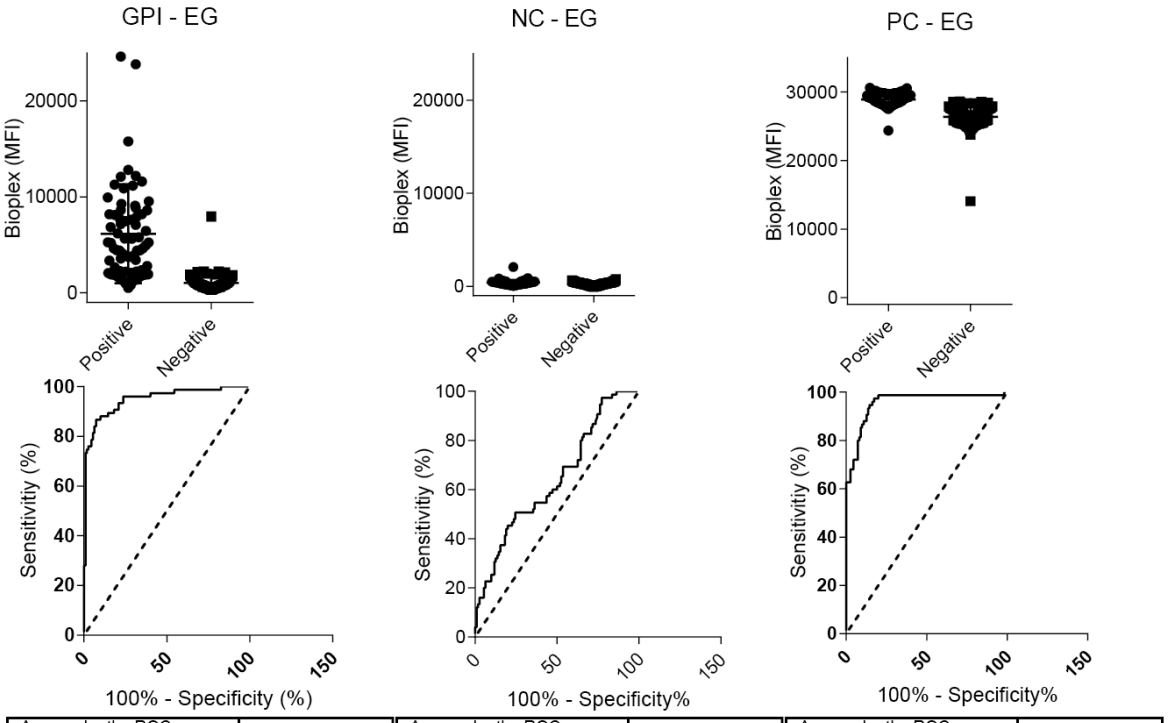

Area under the ROC curve	
Area	0.9478
Std. Error	0.01706
95% confidence interval	0.9143 to 0.9812
P value	<0.0001

Area under the ROC curve	
Area	0.6427
Std. Error	0.04124
95% confidence interval	0.5619 to 0.7236
P value	0.0010

Area under the ROC curve	
Area	0.9542
Std. Error	0.01621
95% confidence interval	0.9224 to 0.986
P value	<0.0001

Figure 2.11: ROC analysis of the data using Prism to show the accuracy of the assay in terms of specificity and sensitivity to test the diagnostic potential of the test. The area under the ROC curve is used to compare the diagnostic performance of the two diagnostic tests. In our case, discrimination between diseased cases (Toxoplasmosis **positive**) and normal cases (Toxoplasmosis **negative**) was done using an ELISA assay and the same samples were analyzed using the multiplex system. The results showed a 95 % confidence level for sensitivity and specificity. **GPI-EG**: Panel with the GPI coated beads; **NC-EG**: panel with the negative control (Human serum albumin) coated beads; **PC-EG**; panel with the positive control (Anti-human IgG) coated beads

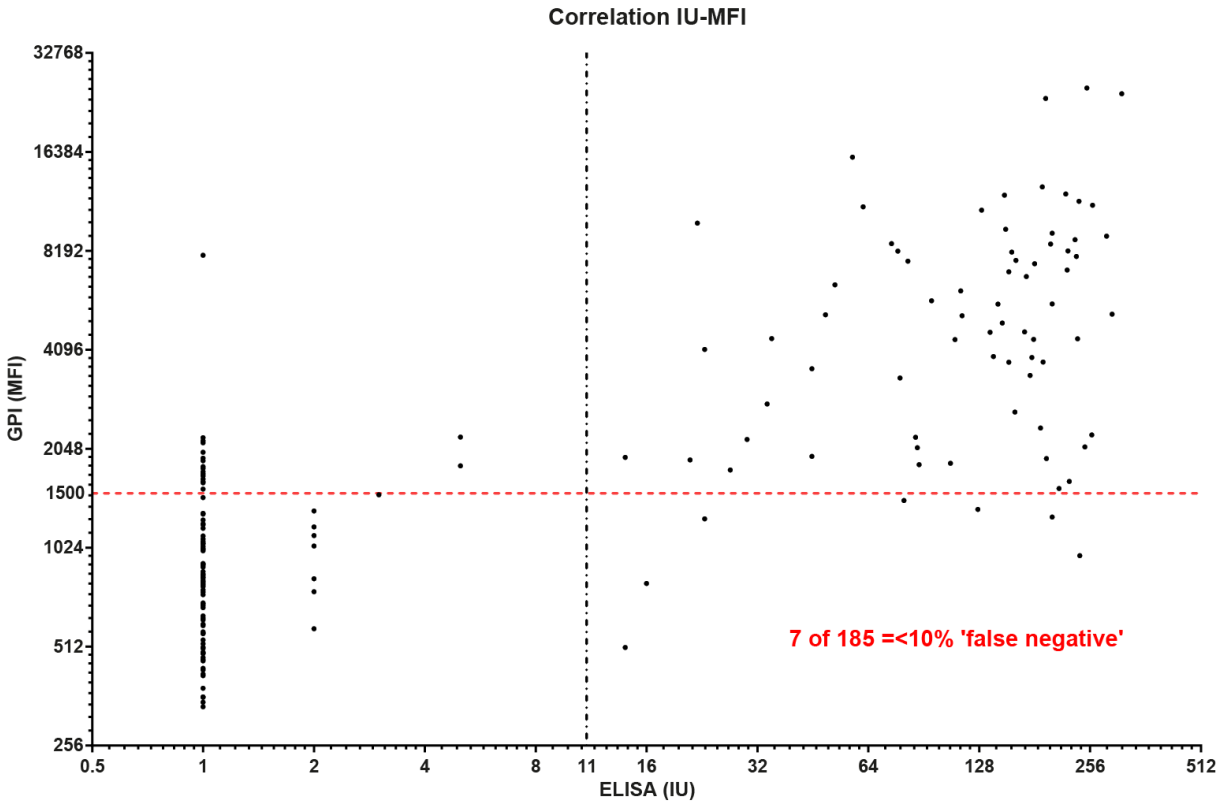

Figure 2.12: Correlation between MFI values from the Luminex assay and ELISA titer values. The results show a 10 % false negative rate.

2.5 Conclusion and Perspective

The selected structure GPI **1**, which corresponds to the glycan part of the GPIs found free on the surface of *T. gondii*, is a good antigen to detect the immune response to the parasitic GPIs induced in humans. Microarray studies showed the potential of using this molecule to discriminate between toxoplasmosis infected and non-infected patients, and to discriminate the type of infection, latent or acute.[32] Here, it was demonstrated that GPI **1** can be used to distinguish between infected and healthy cases using a Luminex-based sero-diagnostic assay. The conditions including antigen concentration, antibody type and concentration, serum sample dilution, and buffer composition for the assay were optimized. The optimized assay was used to screen 180 human serum samples. The positive cases were identified with 95 % specificity and 76 % sensitivity and also compared with the results obtained using commonly used protocols such as ELISA (Figure 2.12).

Further analysis and a larger serum cohort have to be screened to determine the performance of this assay in large sample screening. However, on the basis of the obtained results, it was demonstrated here the potential of the Luminex-based assay using GPI **1** as a diagnostic marker in the sero-epidemiology surveillance of toxoplasmosis. Furthermore, the results of this work suggest that Luminex-based assays are a good methodology to study the diagnostic potential of immunogenic glycan antigens, which can find applications in the diagnosis of other diseases.

Chapter 3

Synthesis of paramagnetic chelating GPI's fragments to study the conformation and dynamics using Paramagnetic NMR spectroscopy

3.1 Introduction

Glycosylphosphatidylinositol (GPI) anchors are biologically active molecules that have a common core structure. It is very important to understand the factors affecting the conformation and dynamic of this core structure and its interplay in the function of GPI glycolipids. The core of GPI molecules consists of a trimannoside, a glucosamine, and a *myo*-inositol unit that are connected in a linear arrangement. The glycosidic linkages involved in the construction of this pseudopentasaccharide core comprises two types of bonds: bonds involving secondary hydroxyl groups, in which the orientation is defined by the torsional angles φ and ψ, and a bond involving a primary hydroxyl group in which the configuration is defined by the three torsional angles φ, ψ and ω. (Figure 1.13)

It is challenging to characterize the conformational behavior of GPI molecules due to the high degree of internal flexibility that blurs the determination of a defined picture by standard methods such as NMR and X-rays diffraction. Only few studies have been reported describing the conformational flexibility of these molecules.[69, 102, 106] These studies have been performed combining NMR experiments and molecular dynamics and characterizing the core as a space filling model, which is considered to facilitate the multiple spatial orientation of the GPI-anchored protein and enable its interaction with other membrane associated biomolecules.[106]

There are many methods reported in the literature to study the conformation and dynamics of carbohydrates including: X-ray crystallography,[104] NMR techniques[131-133] and molecular dynamic (MD) simulations.[134] Among these, MD simulations is highly interesting approach and important for the interpretation of experimental data that facilitate the studies of carbohydrates and allow the possibility to design and fine-tuning of the systems *in silico.* Although molecular dynamic calculations can be performed in a

sophisticated manner, they still require experimental validation to make sure that the outcome is reliable and relevant.

Nowadays, NMR spectroscopy is an appropriate and extremely valuable tool used for the study of carbohydrates. It allows the investigations of molecular conformations, dynamics and interactions with other molecules in solution phase.[135] Compared to proteins and nucleic acids, the resonance signals of carbohydrates cluster within a small region. The chemical shifts, coupling constants and nuclear overhauser effects (NOEs) observed in NMR spectroscopy have direct relation to the conformational state of carbohydrates.[69] Chemical shifts are a reflection of the electronic and geometric environment of the nucleus and deliver information about the orientation of the substituents on the carbon atoms of a carbohydrate ring, i.e. axially and equatorially oriented protons in pyranoses resonate at different frequencies.[136]

The coupling constant (*J*) of vicinal protons in carbohydrates and its relation with the torsion angle around the H-C-C-H bond connecting the coupled atoms is generally described by a karplus-type equation.[137] This equation describes the higher coupling constant between axially oriented hydrogen atoms with a torsional angle ~180° compared to the equatorially oriented with a torsional angle ~±60° (Figure 3.1).[136]

Karplus Equation:- $^{3}J(\theta) = A\cos 2\theta + B\cos\theta + C$; A, B and C are coupling coefficient.

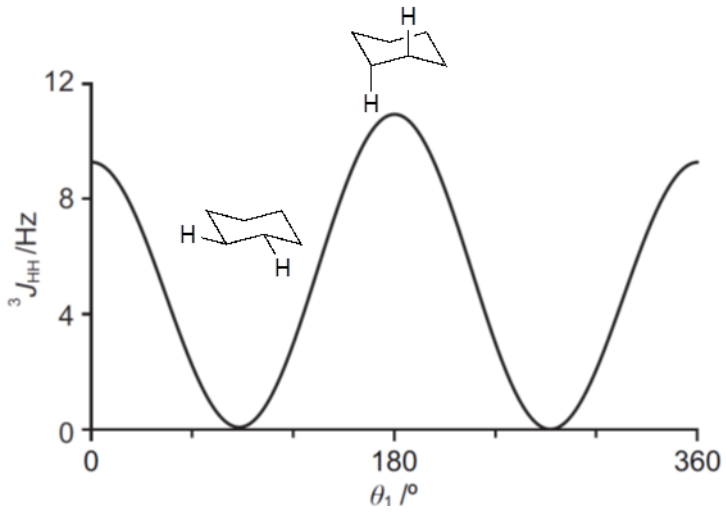

Figure 3.1: The vicinal proton-proton *J* coupling dependence of the intervening torsional angle (*i.e.*, a Karplus relationship); $\theta_1 I°$ is the degree of torsional angle. $^{3}J_{HH}$ indicates ^{1}H coupled to another ^{1}H atom three bonds away, *via* H-C-C-H (vicinal proton).

Apart from chemical shifts and coupling constants, the NOEs observed between hydrogen atoms in the NMR experiment reflect the distance between them. NOEs show inverse sixth power dependence to the interatomic distance and it can be observed between the atoms which are closer than 5 Å in space. By measuring the NOEs between the hydrogen atoms in the glycosidic linkage, the torsional angles can be estimated.[138] The combination of these NMR parameters based on the bond (Chemical shifts and coupling constants) and through space (NOE measurements) can provide information about the 3D structural organization of carbohydrates.[138] Although, the advances in NMR spectroscopy provides glycochemist or biochemist with valuable information, the analysis of carbohydrates by NMR spectroscopy has to deal with overlap of signals due to lack of sufficient resonances appears in the carbohydrate structure. Subsequently, the insufficient number of restraints in the NOE experiments compared to the number of degrees of freedom in the carbohydrate chains makes the characterization of conformational ensemble difficult. To overcome this issue in carbohydrate NMR spectroscopy, new NMR methods have been developed employing the use of paramagnetism.[139]

3.2 Paramagnetic effect – source of long distance information

Paramagnetism-based NMR approaches have been used recently for the structural analysis of biomolecules and for the study of carbohydrate-protein interactions.[140] These paramagnetic NMR approaches involve the introduction of paramagnetic metal chelating tag into the molecules of interest at a certain distance. The effect of the metal in the NMR spectrum provide information about the geometric arrangement of nuclei through dipole-dipole interactions between unpaired electron and the nuclei in a magnetic field. This technique has been used for the structural analysis by determining the differences in the NMR signals of diamagnetic and paramagnetic states of the molecule that are observed as residual dipolar coupling (RDC), pseudocontact shift (PCS) and paramagnetic relaxation enhancement (PRE).

The PCSs are changes in the chemical shift values induced by the dipole-dipole interactions of the different nuclei with a paramagnetic center. This anisotropic effect provides long-distance information and can be measured for nuclei even around 40 Å

from the ion. The PCS values are determined by measuring the difference of ^{1}H and ^{13}C chemical shift values between the carbohydrate complex with paramagnetic metal ion (mostly lanthanides) and diamagnetic reference (mostly La^{3+}).

The paramagnetic chelating tag is usually a rigid structure that is coupled to the reducing end of carbohydrates. The stiffness of the chelating tag is crucial for the accurate quantification of observed PCS values.[108, 109, 139] Using PCS and Monte Carlo molecular dynamics approach, the conformational dynamics of lactose was successfully characterized (Figure 3.2).[109]

Paramagnetic relaxation enhancements (PRE) are the enhanced relaxation of the spins, induced by the presence of paramagnetic center. PREs are increasingly used for providing the long distance information that complements nuclear overhauser effect (NOE). A good example of this application is the attachment of nitroxide spin to the reducing end of a high mannose N-glycan overexpressed in genetically engineered yeast, which was evaluated by NMR using the PREs to reveal the conformation and dynamics of carbohydrate units involve in protein-fate-determination processes in cells.[141]

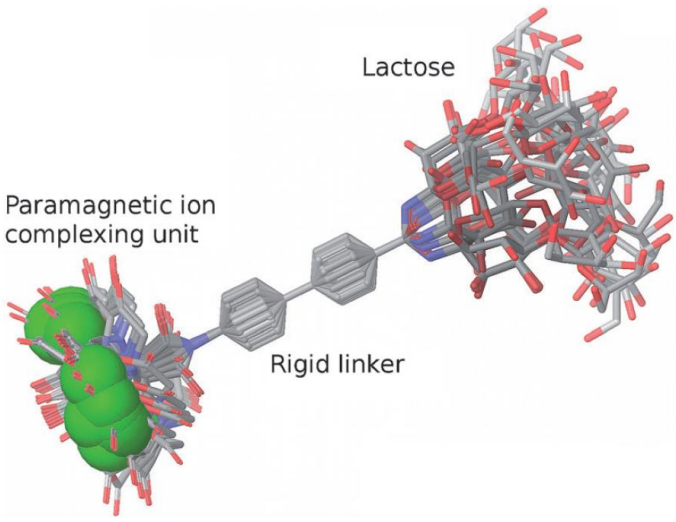

Figure 3.2: Overlaid conformations of lactose connected to a paramagnetic center through a rigid biphenyl–EDTA-type paramagnetic tag. By using a defined distance between the metal and the saccharide the paramagnetic relaxation-induced line broadening is controlled. The structures were generated using a systematic Monte Carlo conformational search with the program MacroModel.[109]

The glycosidic linkages present in complex carbohydrates have significant number of degrees of freedom. Therefore, the NMR data obtained for carbohydrates is always interpreted as an average of the different dynamic conformational ensembles and they are

not assigned to a single conformational state. Theoretical approaches are an important tool for the analysis and interpretation of experimental data and to assign the average values from the dynamic conformational ensembles. There are many theoretical models and methods available that have been coupled with NMR structural analysis to investigate the conformation of carbohydrates, some of them are: Molecular mechanics (MM) and Molecular dynamics (MD), semi-empirical methods, *Ab initio* and density functional modeling, interactions with solvent and hybrid Quantum mechanics (QM)/MM, QM/QM.[142]

The conformational characterization of GPIs has been a challenging task because of the presence of side branching glycans, lipid chains and protein attached to the GPI core structure. Paramagnetism-assisted NMR spectroscopy in combination with theoretical approaches might allow better understanding of the conformational dynamics of these glycolipids.[35, 65, 90] Based on the fact that the flexibility and mechanical compressibility of the GPI core structure have been demonstrated to depend on the individual glycosidic linkages, In this work the conformational properties of the Manα1→2Man and Manα1→6Man, key glycosidic linkages from GPIs were investigated separately and together in the trisaccharide (Manα1→2Manα1→6Man) using paramagnetic NMR and MD simulations.

3.3 Synthesis of paramagnetic chelating fragments of GPI anchor

The disaccharides Manα1→2Man and Manα1→6Man, and the trisaccharide Manα1→2Manα1→6Man that are part of core structure of GPI anchor were synthesized following an established strategy in our group. The glycans were coupled to a chelating tag **(27)** at the last stage of the synthesis. The key step to perform paramagnetic tagging for NMR experiments is to introduce the metal chelating unit into the reducing end of the oligosaccharide. Several chelating units have been developed over the last years, they are based on phenylenediamine- or ethylenediamine tetraacetic acid (EDTA) moieties.[107, 140, 143-145] The most commonly used metal ions in NMR are lanthanides (Dy^{3+}, Tb^{3+}, Tm^{3+}, Er^{3+}, Yb^{3+}, Eu^{3+}), giving this technique the name of Lanthanides-assisted NMR spectroscopy.

For the synthesis of paramagnetic chelating tagged dimannose or trimannose for NMR studies, the chelating tag **27** was selected on the basis of previous reports, in which large rigid structures were used to decrease the effect of the paramagnetic relaxation enhancement (PRE) by separating the metal ion from the glycans.[110] The carbohydrate part (dimannose or trimannose) can be synthesized with an anomeric azide, which can be reduced to obtain a glycosyl amine. A coupling of the amino group on anomeric position of the carbohydrate with a carboxylic group from the chelating tag using a HATU-mediated activation would deliver the formation of an amide linkage and the desired tagged sugars (Figure 3.3).

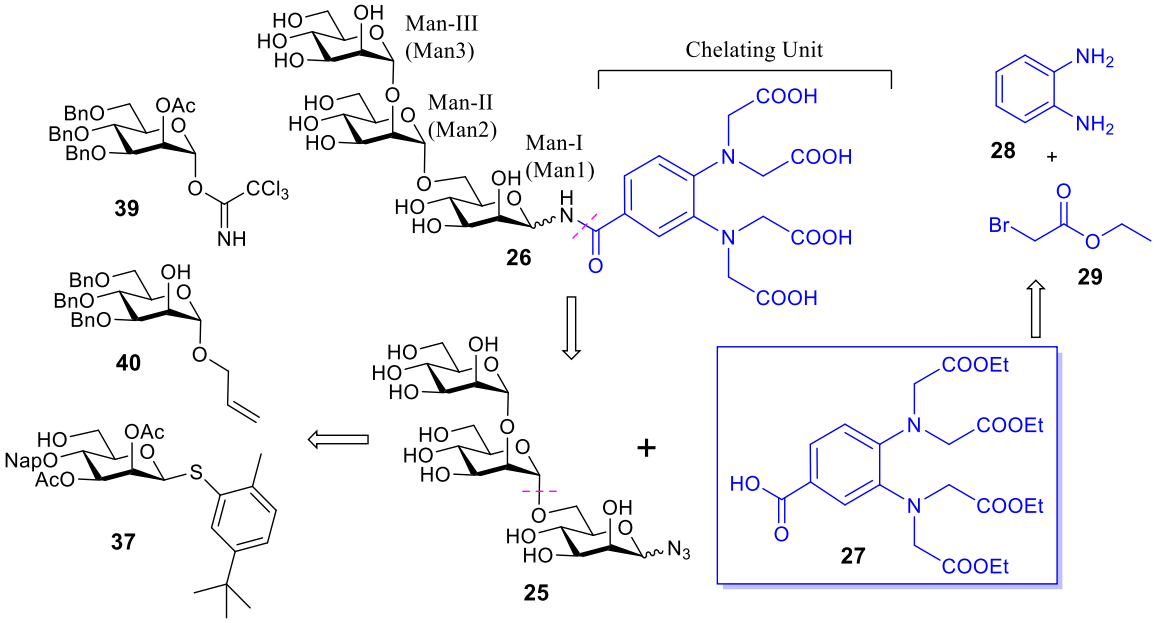

Figure 3.3: Retrosynthesis for paramagnetic chelating linked fragments of GPI.

After synthesizing GPI fragments tagged with the chelating unit, ^{1}H and ^{1}H-^{13}C HSQC spectra were acquired in the presence of one molar equivalent of lanthanide ions. Lanthanum (La^{3+}) was used as a diamagnetic reference and dysprosium (Dy^{3+}), europium (Eu^{3+}) and ytterbium (Yb^{3+}) were used as paramagnetic ions. The ratio of tagged glycan to the lanthanide ion was decided on the basis of previous reports where the sugar to metal ion concentration was titrated in NMR experiment and found out a ratio of 1:1 (carbohydrate: metal) complex gives a stable complex.[107, 143]

The PCS values were measured as the difference in the ^{1}H and ^{13}C chemical shifts of the compound chelated to the paramagnetic ion and those observed with the diamagnetic ion in their ^{1}H and ^{13}C spectra. These PCS shifts arise from the dipolar interactions between

the unpaired electron of a metal ion and the nuclei in the vicinity of the ion. The PCS gives rise to the large changes in the shift that decreases with the distance between the metal ion and nuclear spin with $1/r^3$ dependence. The calculated PCS values were compared with the values obtained from a molecular dynamics study to get the improved understanding of conformational dynamics of GPI core structure.

3.3.1 Synthesis of paramagnetic chelating unit

The synthesis of a protected chelating unit was started from commercially available benzene 1, 2-diamine **28** as shown in the scheme 3.1. Alkylation of the 1, 2-diamine using an excess of ethyl bromoacetate in the presence of *N, N*-diisopropylethylamine (DIPEA) delivered the tetraester **30** in 75 % yield. In the next step, compound **30** was brominated using Oxone and potassium bromide (KBr) in 75 % yield. The resulting bromide was used to perform a $PdCl_2$(dppf) catalyzed carbonylation using Lithium formate to give the acid **27** in 50 % yield. This product was ready for coupling to the carbohydrates of interest.

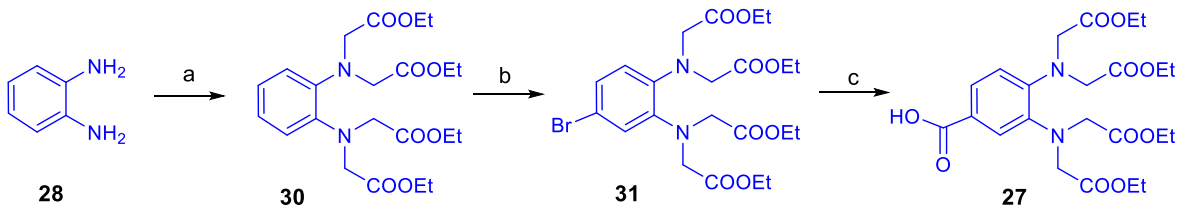

Scheme 3.1: Synthesis of protected chelating fragment. a) Ethyl bromoacetate (**29**), DIPEA, acetonitrile, 60 °C, 4 days, 75 %; b) Oxone, KBr, anhy. MeOH, rt, 75 %; c) Lithium formate, $PdCl_2$, Ac_2O, DIPEA, DCM, 120 °C, 46 h, 50 %.

3.3.2 Synthesis of the tagged Manα1→6Man disaccharide fragment

The synthesis of the dimannose Manα1→6Man started with the synthesis of mannose building block **37** (Scheme-3.2). Peracetylated mannose **32** was converted into the aromatic thioglycoside **33** as a α/β mixture using $SnCl_4$ as Lewis acid activator. This thioglycoside was quantitatively deacetylated using freshly prepared sodium methoxide and was protected without further purification at the 6-*O* position using tertbutyldiphenylsilylchloride (TBDPSCl) and imidazole as base to give the mannosyl

triol **34**. Following, the 2-*O* and 3-*O* positions were blocked by formation of a 2,3-*O*-*iso*-propylidene acetal **35**. The remaining hydroxyl group in **35** was protected by methyl naphthylation of the 4-*O* hydroxyl group to obtain **35a** (Scheme 3.2). Subsequently, the 2,3-*O*-*iso*-propylidene acetal was hydrolyzed using 80 % acetic acid to give the diol **36**, which was acetylated using acetic anhydride and pyridine to give **36a** in 95 % yield. Finally, TBDPS group from compound **36a** was removed using HF-Pyridine to deliver Man-I building block (**37)** as an acceptor for the glycosylation reaction.

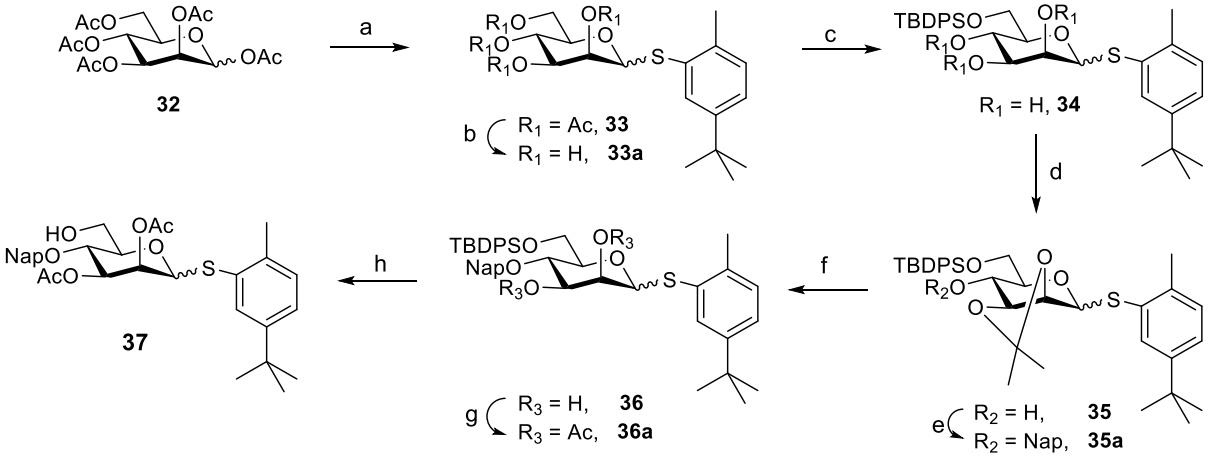

Scheme 3.2: Synthesis of Man-I building block. a) 5-(tert-butyl)-2-methylbenzenethiol, $SnCl_4$, DCM, 0-25 °C, 3h, 75 %; b) NaOMe, MeOH, 30 min, rt, 97 %; c) TBDPSCl, imidazole, DMF, 22-50 °C, 2h, 90 %; d) 2,2-dimethoxypropane, CSA, rt, 1.5 h, 95 %; e) NapBr, NaH, DMF, 0-25 °C, 2 h, 75 %; f) Acetic acid (80 %), $CHCl_3$, 65 °C, 4 h, 70 %; g) Ac_2O, Pyridine, 0-25 °C, 3 h, 96 %; h) HF-Pyridine, THF, rt, 14 h, 94 %.

The glycosyl donor **39** (Man-II) and the glycosyl acceptor **40** were synthesized from the mannose **38**.[146] Mannose **40** was prepared by deacetylation of **38** using freshly prepared NaOMe in 95 % yield. The allyl group from the anomeric position of **38** was removed in a two-step process by isomerization of the allyl ether using an iridium catalyst and a following hydrolysis using mercury salt. The released hemiacetal was treated with trichloroacetonitrile (TCA) and DBU to give the trichloroacetimidate donor **39** (Scheme 3.3).

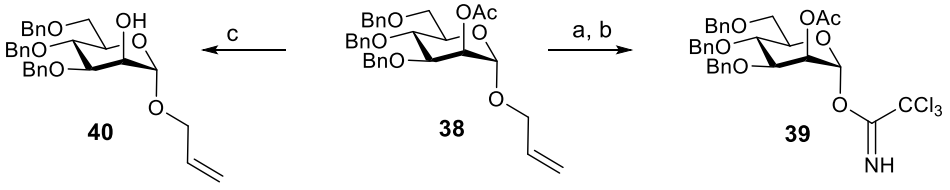

Scheme 3.3: Synthesis of Man-II building block. a) i. $[Ir(Cod)(PPh_2Me)_2]PF_6$, H_2, THF ii. $HgCl_2$, HgO, water, acetone, 69 %; b) Cl_3CCN, DBU, DCM, 0 °C, 89 %; c) NaOMe, MeOH, rt, 95 %.

The glycosyl donor **39** was activated using TMSOTf at -40 °C and used to glycosylate the acceptor **37** to give the dimannose **41** as pure α-anomer in 95 % yield. Subsequently, the resulting dimannose was globally deprotected to get the dimannose **43**. The hemiacetal at the reducing end was converted into an anomeric azide **44** by installation of a chloride with 2-chloro-1,3-dimethylinidazolinium chloride (DMC) and its following substitution with sodium azide (NaN_3) (Scheme 3.4). The preferential substitution of the anomeric hydroxyl group by the chloride is based on the p*Ka* value of hemiacetal group, which is lower than the pKa from the other hydroxyl groups and from water.

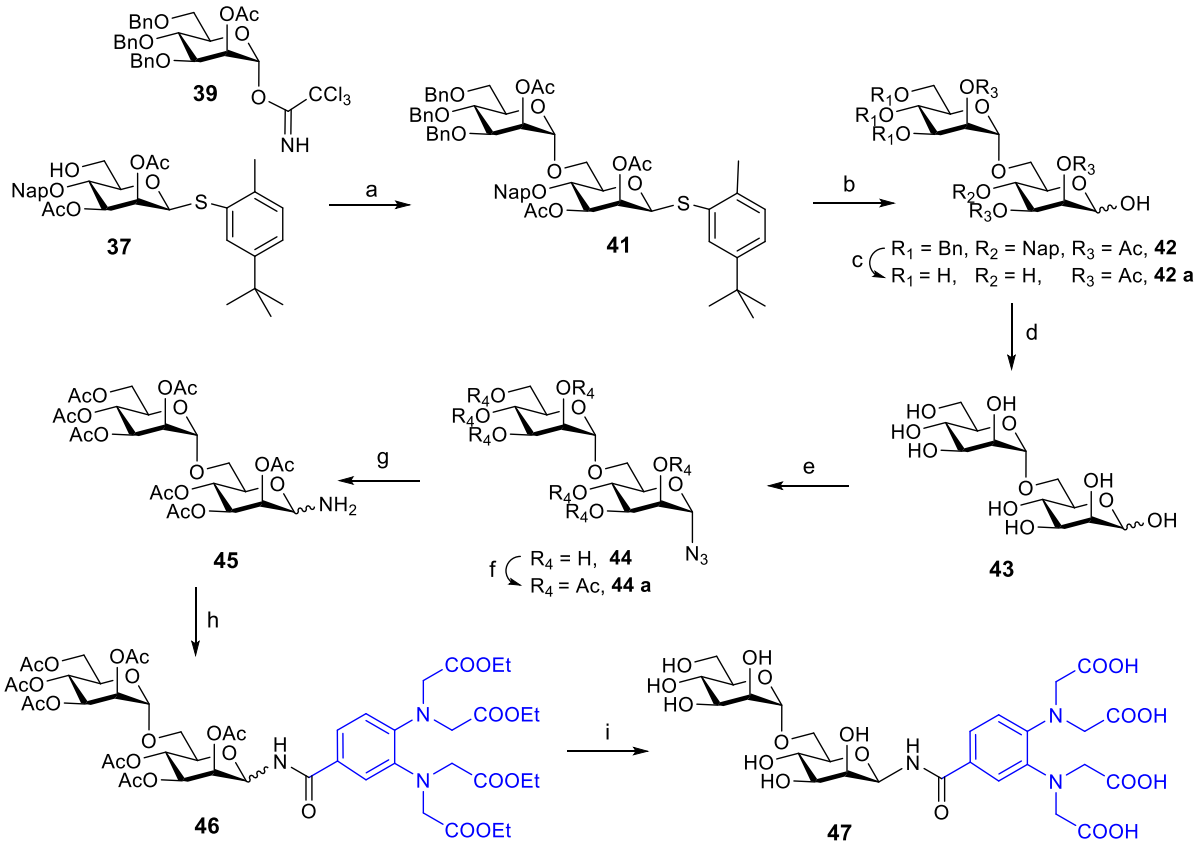

Scheme 3.4: Synthesis of chelating tagged Manα1→6Man. a) TMSOTf, anhy. DCM, -40 °C, 95 %; b) NBS, Acetone:H_2O (9:1), 30 min, rt, 70 %; c) Pd/C, anhy. MeOH, rt, 14 h, 95 %; d) NaOMe, MeOH, rt, 30 min, 95 %; e) DMC, NaN_3, DIPEA, D_2O, 0 °C, 81 %; f) Ac_2O, Pyridine, 0-25 °C, 60 %; g) Pd/C, H_2, EtOAc; h) **27**, HATU, DIPEA, DMF, rt, 55 %; i) 1M NaOH, MeOH, 80 %

The dimannosyl azide **44** was peracetylated using acetic anhydride and pyridine at low temperature to obtain **44a**, which was further treated with hydrogen and Pd/C in

ethylacetate reducing the azide to give the glycosyl amine **45**. The chelating linker **27** was activated using HATU and DIPEA and couple to the crude amine **45** to deliver the tagged dimannose (**46**) as an α/β mixture. This coupling was evaluated using different coupling reagents such as PyBop, but the yield was very low from 10-25 %, only by using HATU, the product was obtained in moderate yield of 55 %. The esters of **46** were saponified using 1M NaOH solution in methanol. The resulting tagged disaccharide **47** was purified using high performance liquid chromatography (HPLC) to give the final product **47** as pure β-anomer ready for NMR experiments in the presence of lanthanides (Figure 3.4).

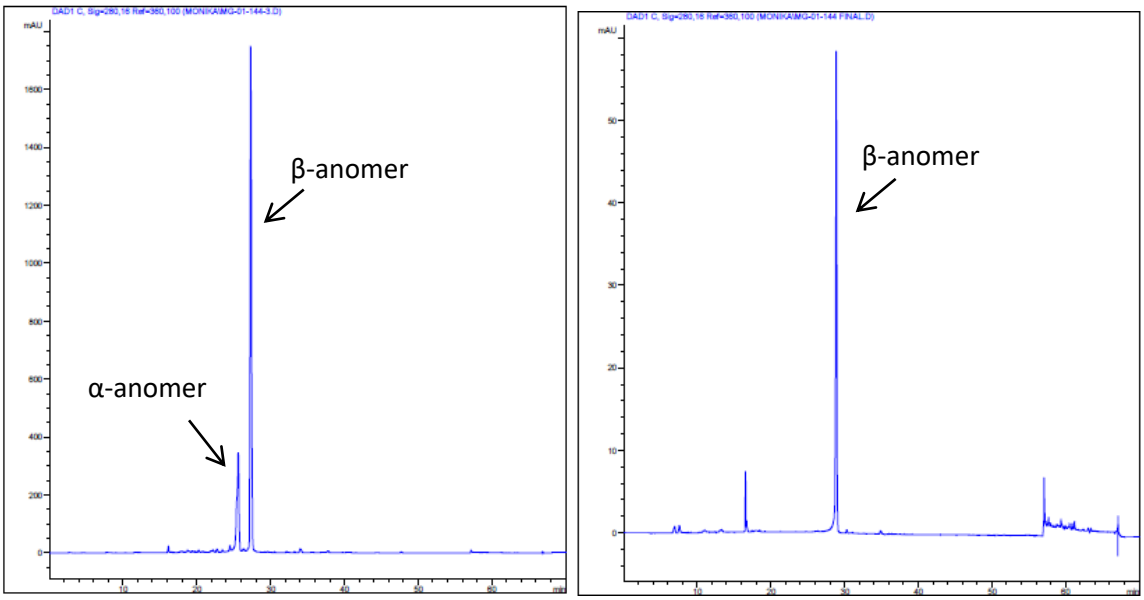

Figure 3.4: HPLC profile of crude **47** (left) and after purification. The purification was carried out using a Synergy 4 µ Hydro-RP 80A (250 x 10 mm) column, 3mL/min flow rate and a gradient from 0-30 % acetonitrile (0.1 % formic acid) in water.

3.3.3 Synthesis of the tagged Manα1→2Man disaccharide fragment

For the synthesis of tagged Manα1→2Man disaccharide fragment, the glycosyl acceptor **40** was glycosylated using trichloroacetimidate donor **39** using TMSOTf activation at -40 °C to give the dimannose **48**. The obtained allyl group of **48** was removed using the above described two-steps protocol with iridium and mercury salts to get the hemiacetal **49**, which was further deprotected by hydrogenolysis and treatment with base to deliver the dimannose **50** in good yield (Scheme 3.5). The unprotected dimannose **50** was converted into the anomeric azide using DMC and sodium azide. The hydroxyl groups

were acetylated using acetic anhydride and pyridine to give the glycosyl azide **51**. The azide of **51** was reduced to obtain the glycosyl amine **52** and was coupled with the chelating linker **27** using HATU as activator and DIPEA as base to get the tagged dimannose **53** as an α/β mixture in 65 % yield. The saponification of the esters of **53** was performed using 1M NaOH solution in methanol. The product was purified using high performance liquid chromatography (HPLC) to obtain **54** as pure β-anomer ready for NMR experiments using lanthanides (Figure 3.5).

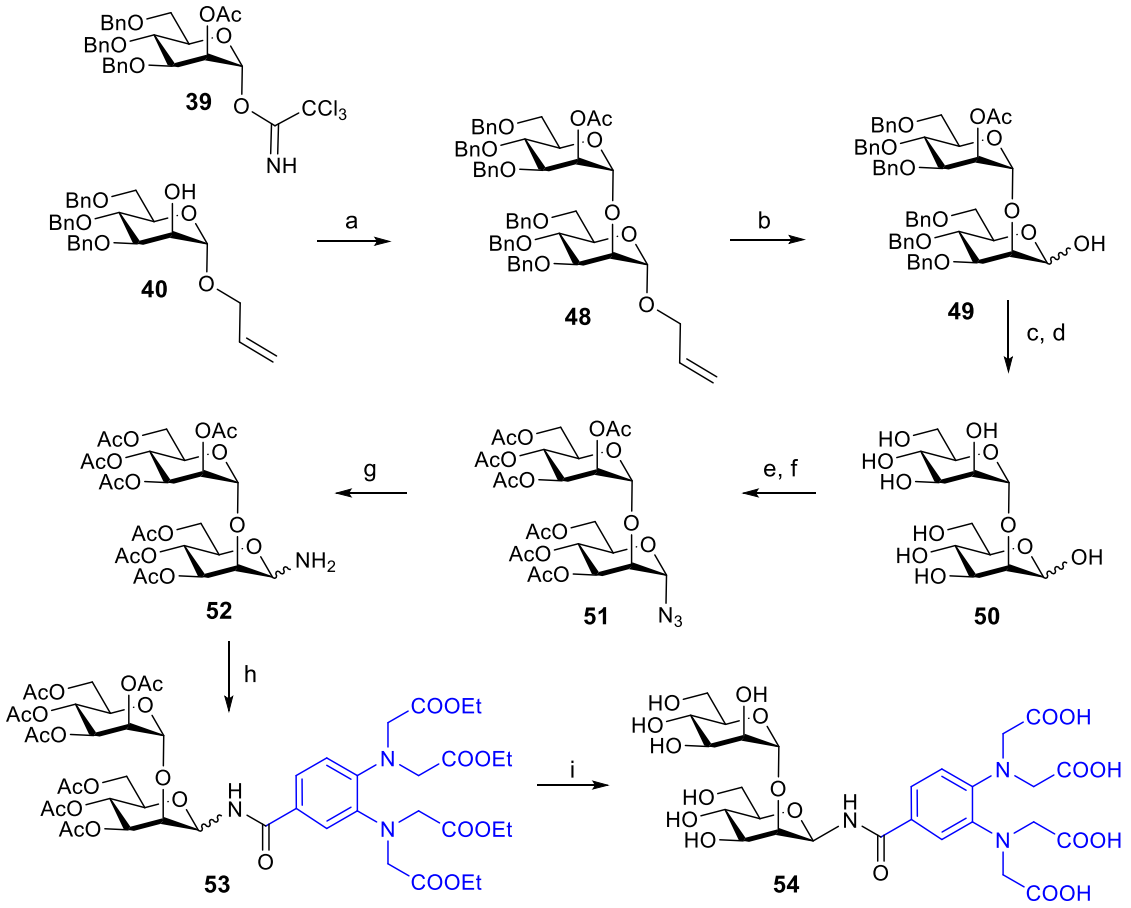

Scheme 3.5: Synthesis of chelating tagged Manα1→2Man. a) TMSOTf, anhy. DCM, -40 °C, 70 %; b) i. $[Ir(Cod)(PPh_2Me)_2]PF_6$, H_2, THF ii. I_2, water, 65 %; c) NaOMe, MeOH, rt, 30 min, 98 %; d) Pd/C, MeOH, H_2, 95 %; e) DMC, NaN_3, DIPEA, D_2O, 0 °C, 55 %; f) Ac_2O, Pyridine, 0-25 °C, 98 %; g) Pd/C, H_2, EtOAc; 50 %; h) **27**, HATU, DIPEA, DMF, rt, 65 %; i) 1M NaOH, MeOH, 80 %

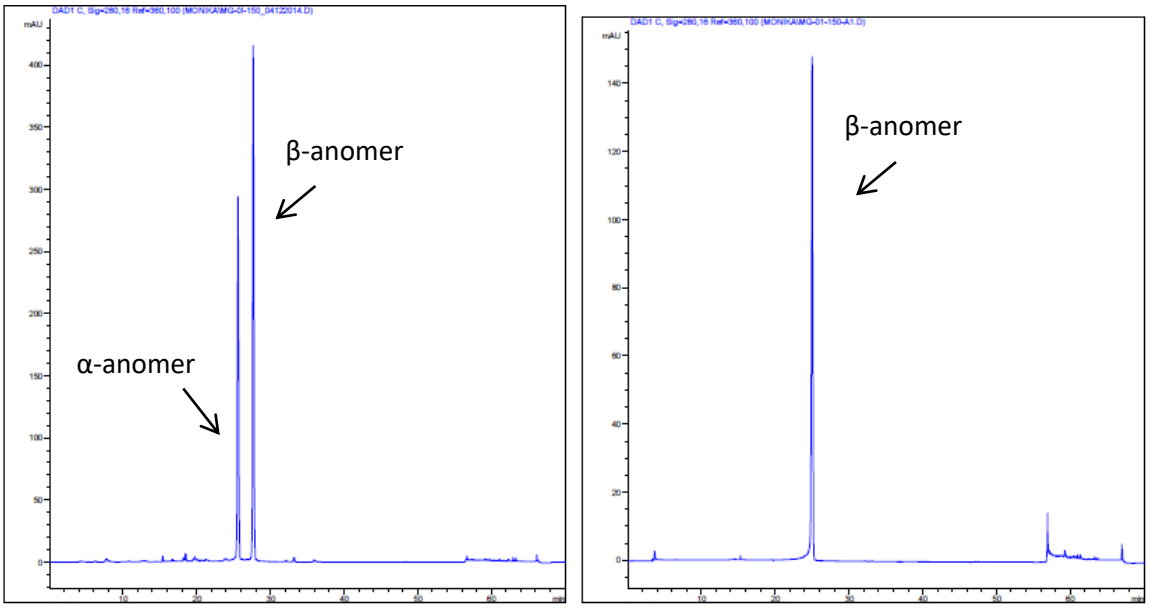

Figure 3.5: HPLC profile of crude **54** (left) and after purification. The purification was carried out using a Synergy 4 µ Hydro-RP 80A (250 x 10 mm) column, 3mL/min flow rate and a gradient from 0-30 % acetonitrile (0.1 % formic acid) in water.

3.3.4 Synthesis of the tagged Manα1→2Man α1→6Man trisaccharide fragment

The synthesis of the trimannose was started by conversion of the dimannose **49** into the trichloroacetimidate donor and the glycosylation of acceptor **40**. However, due to the absence of a participating group at the 2-*O* position, the trisaccharide was obtained only as an α/β mixture in ratio 1:1, which was not easy to separate. To obtain pure α-linkages in the trimannose and in good yield, a new synthesis plan was designed and started with the building blocks **56** and **64**, which were converted into the donor **62** and acceptor **67** respectively. Building blocks **56** and **64** were synthesized from mannose **55**, which was provided by Dr. Bo-Young Lee in sufficient quantity. The building block **56** was transformed into the mannoside **59** by protection of the 4-O and 6-*O* positions using NapBr, following removal of *iso*-propylidene group and a regioselective installation of naphthyl methyl ether on the 3-*O* groups of the resultant diol **58** (Scheme 3.6A). The 2-*O* position of the mannose **59** was protected as a levulinoyl ester (Lev) group to obtain mannose building block **60** in 93 % yield. The levulinoyl group is a participating group that will favor the formation of the desired α-product and can be selectively removed with hydrazine acetate in the presence of acetyl groups to give the acceptor **69**. The levulinoyl-protected mannoside **60** was converted into the trichloroacetmidate donor **62**

by the removal of the allyl ether with $PdCl_2$ and following reaction of the resultant hemiacetal **61** with trichloroacetonitrile in the presence of DBU (Scheme 3.6A). The glycosyl acceptor **67** was generated in excellent yield from the diol **64** by regioselective installation of naphthyl-methyl ether on the 3-*O* position, following the acetylation of the 2-O position of **65** and subsequently cleavage of silyl ether group with HF-pyridine (Scheme 3.6B). A glycosylation of the acceptor **67** with the trichloroacetamidate donor **62** using TMSOTf activation in dichloromethane at 0 ^{o}C provided the desired α-dimannoside **68**. The removal of the Lev group of the 2-*O* position delivered the dimannose acceptor **69** (Scheme 3.6C).

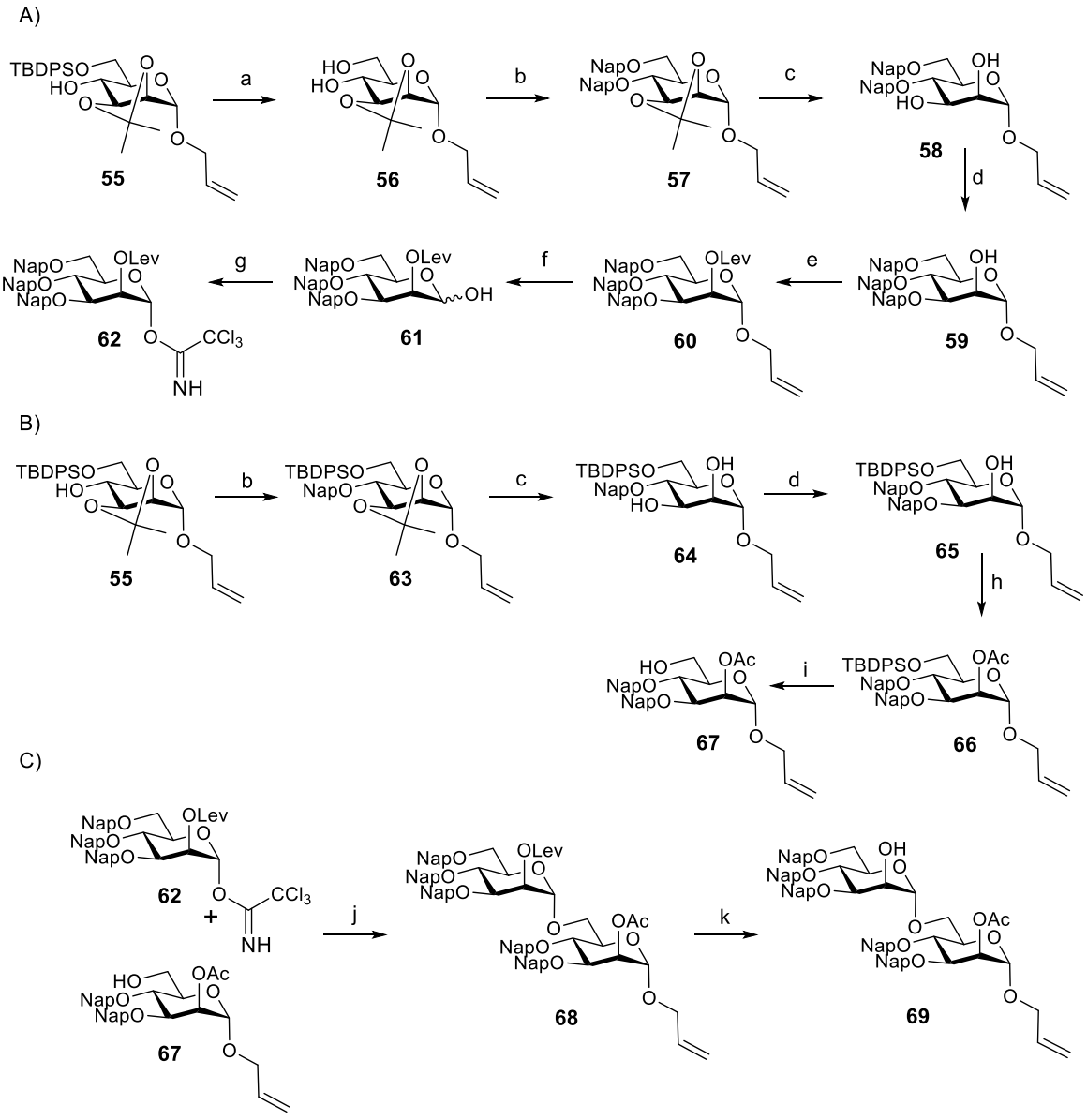

Scheme 3.6: Synthesis of disaccharide. a) TBAF,, THF, rt, 2 h, 83 %; b) NapBr, NaH, DMF, rt, 16 h, 85 %; c) CSA, MeOH, rt, 5h, 88 %; d) Bu_2SnO, toluene, reflux, 3h then NapBr, TBAI, DMF, 60 °C, 5 h, 75 % (2 steps); e) LevOH, DIC, DMAP, DCM, rt, 2h, 93 %; f) $PdCl_2$, MeOH, rt, 4h, 85 %; g) CCl_3CN, DBU, DCM, 0 °C, 90 % h) Ac_2O, Pyridine, DMAP, DCM, rt, 2h, 97 %; i) HF.Pyridine, THF, rt, 16 h, 91 %; j) TMSOTf, DCM, 0 °C, 1 h, 96 %; k) H_2NNH_2, AcOH, DCM, rt, 16 h, 93 %

Glycosylation of the acceptor **69** with the imidate donor **39** was performed using TMSOTf as activator at -40 °C to get the trimannose **70** in 95 % yield. This trimannose was global deprotected to get trimannose **72** (Scheme 3.7). To obtain the tagged trimannose **75**, the trimannose **72** was submitted under the same reactions used for the dimannoses **47** and **54**, inlcuding conversion of unprotected trimannose to anomeric azide, followed by the acetylation, reduction of azide and coupling with the linker **27**. Contrary to the case with the dimannoses, the coupling of the protected trimannose to the linker delivers the tagged product only in 5-10 % yield. Effort to perform this coupling using PyBOP as activator did not improve the outcome of the reaction. By using the unprotected trimannose with anomeric azide **25** directly for coupling to **27**, the yield was improved from 5 % to 45 %. Also in this case, the use of PyBOP as coupling reagent did not improve the yield. The anomeric mixture of trimannose **74** was separated using HPLC before the final deprotection to obtain **75** (Figure 3.6).

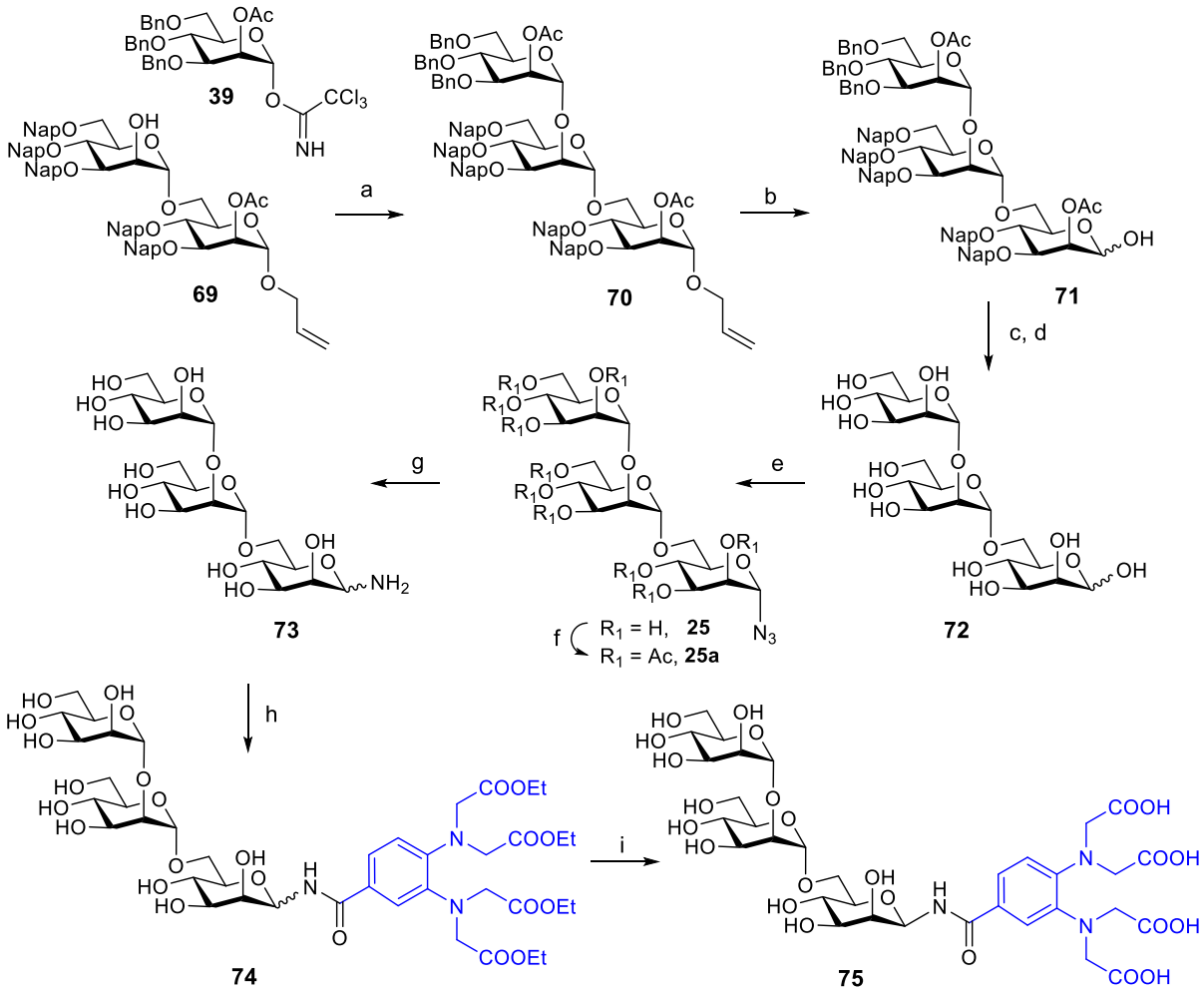

Scheme 3.7: Synthesis of chelating tagged Manα1→2Manα1→6Man. a) TMSOTf, anhy. DCM, -40 °C, 95 %; b) i. $[Ir(Cod)(PPh_2Me)_2]PF_6$, H_2, THF ii. NBS, water, 81 %; c) NaOMe, MeOH, rt, 30 min, 95 %; d) Pd/C, MeOH, H_2, rt, 14 h, 95 %; e) DMC, NaN_3, DIPEA, D_2O, 0 °C, 65 %; f) Ac2O, Pyridine, 0-45 °C, 70 %; g) Pd/C, H_2, EtOAc; 91 %; h) **27**, HATU, DIPEA, DMF, rt, 45 %; i) 1M NaOH, MeOH, 75 %

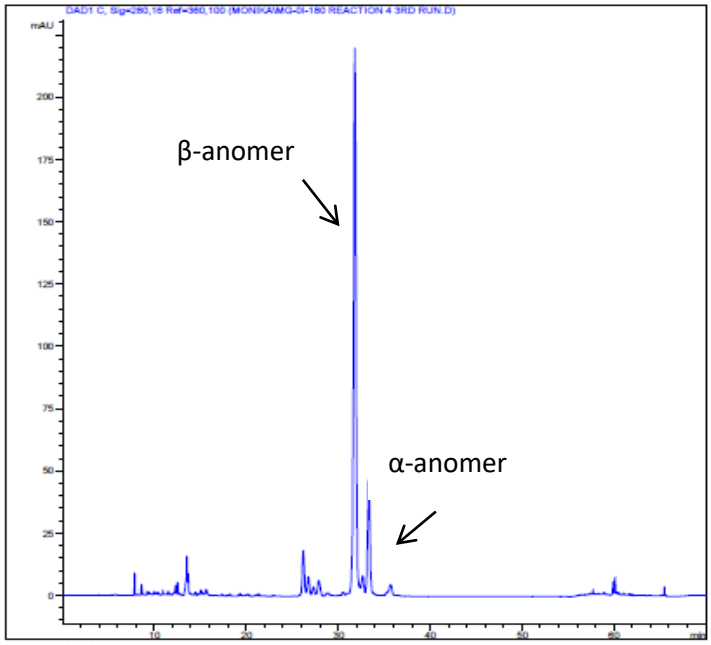

Figure 3.6: HPLC profile of crude **74**.

After synthesizing all the three fragments from the GPI core structure **47**, **54** and **75**, these compounds were dissolved in D_2O (0.5 mL) to a final concentration of 3 mM. The pH of the solution was increased to pH 8.0 and a D_2O solution of MCl_3 (3 mM; M = La^{3+}, Yb^{3+}, Dy^{3+}, Eu^{3+}) was added along with the 100 µM of trimethylsilylpropionic acid (TSP) as a standard. ^{1}H-NMR and ^{1}H-^{13}C HSQC NMR measurements of the solution were recorded.

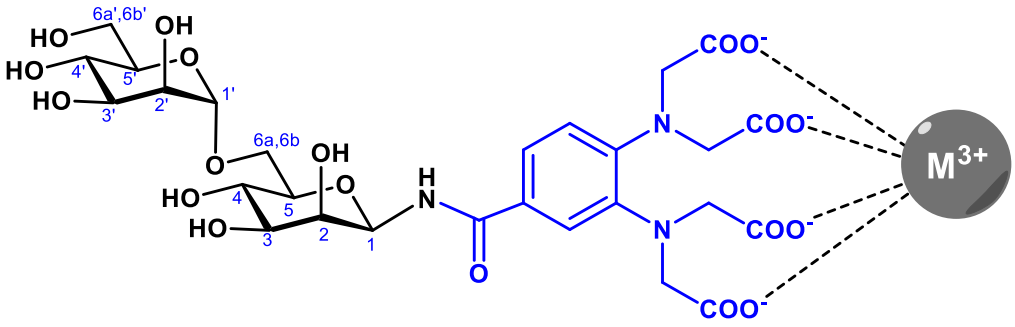

Figure 3.7: Representation of the paramagnetic Manα1→6Man with the metal ion in the NMR experiment.

The PCS values were calculated from the analyzed ^{1}H-^{13}C HSQC spectra as the difference between the ^{1}H and ^{13}C chemical shifts of the compound chelated with a paramagnetic ion (Eu^{3+} , Yb^{3+}, Dy^{3+}) and those observed with the diamagnetic ion (La^{3+}) as reference.

The spectra were acquired in the equal concentration of each metal ion and the choice of the metal ion was made on the basis of magnetic susceptibility component. Europium and ytterbium have small magnetic susceptibility component as compared to the dysprosium that leads to the small broadening of the signals. For the disaccharides **47** and **54** and the trisaccharide **75** the metal ions with the small magnetic susceptibility would give the largest chemical shift with small signal broadening. For larger oligosaccharides, the lanthanide ions with the larger magnetic susceptibility component are recommended to obtain long-distance information. This observation was confirmed when ^{1}H-NMR and ^{1}H-^{13}C HSQC NMR spectra of α1,6-dimannose **47** were acquired in the presence of dysprosium ions, the signals were completely disappeared in the spectrum due to the high magnetization of dysprosium (Figure 3.8).

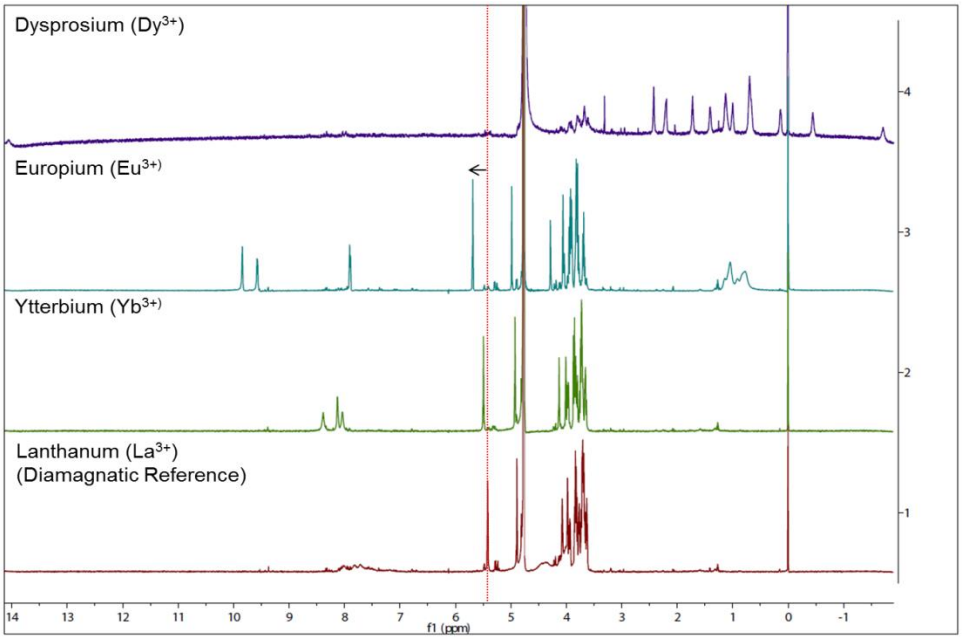

Figure 3.8: ^{1}H-NMR spectra of chelating unit tagged Manα1→6Man with the metal ion La^{3+}, Yb^{3+}, Dy^{3+}, Eu^{3+}.

The spectra were also acquired in the presence of La^{3+} as a diamagnetic reference and Yb^{3+}, Eu^{3+} as paramagnetic ions (Figure 3.9). As expected for extended structures, the observed PCS values were largest for the anomeric proton and carbon located at the reducing end of the glycan, closer to the linker, and smaller for the more distant atoms (Table 3.2).

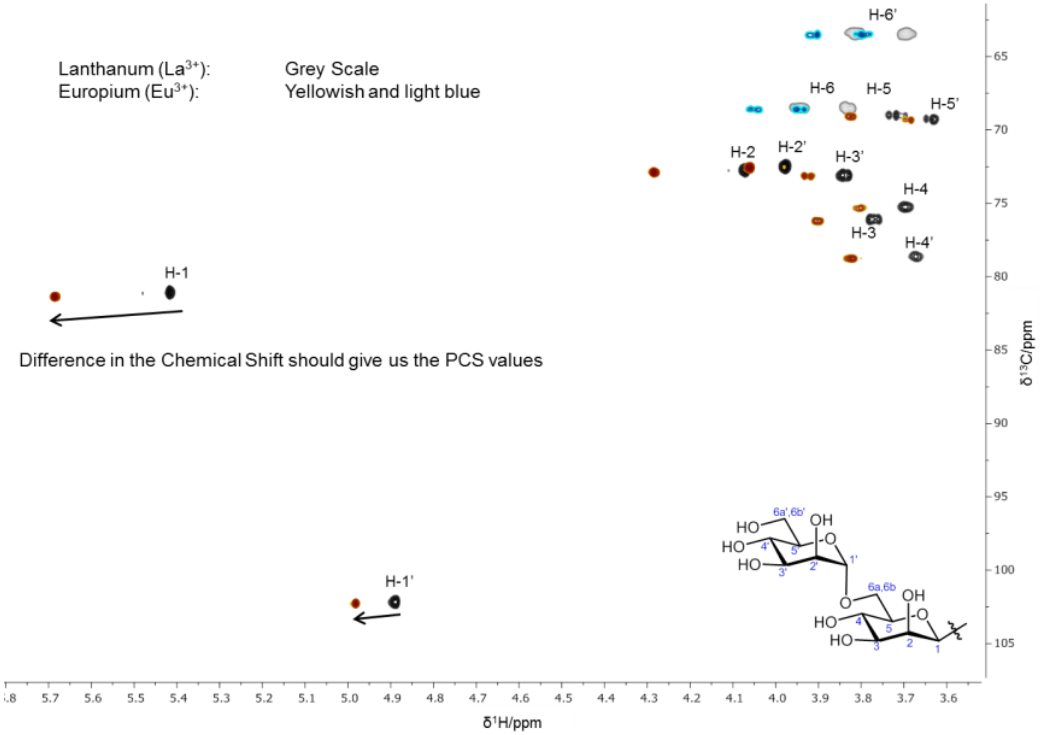

Figure 3.9: ^{1}H-^{13}C HSQC NMR spectra of the dimannose **47** (Manα1→6Man) with the metal ions La^{3+}, Eu^{3+}. The chemical shift change of the anomeric proton is indicated by the arrow.

Table 3.1 ^{1}H and ^{13}C chemical shifts of Manα1→6Man with La^{3+}, Eu^{3+}, Yb^{3+}.

H/C residues	La^{3+} (ppm)		Eu^{3+} (ppm)		Yb^{3+} (ppm)	
	δ^{1}H/ppm	δ^{13}C/ppm	δ^{1}H/ppm	δ^{13}C/ppm	δ^{1}H/ppm	δ^{13}C/ppm
1	5.416	81.07	5.686	81.38	5.493	81.23
2	4.073	72.73	4.286	72.89	4.127	72.76
3	3.770	76.08	3.903	76.18	3.803	76.08
4	3.707	69.04	3.825	69.07	3.733	68.96
5	3.640	69.28	3.691	69.30	3.655	69.28
6a	3.945	68.50	4.051	68.61	3.971	68.50
b	3.829	68.50	3.941	68.61	3.858	68.50
1‘	4.890	102.17	4.982	102.26	4.922	102.19
2‘	3.978	72.50	4.057	72.57	4.002	73.51
3‘	3.838	73.04	3.925	73.12	3.858	73.08
4‘	3.672	78.67	3.822	78.75	3.717	78.66
5‘	3.719	75.26	3.803	75.34	3.740	75.25
6a‘	3.809	63.42	3.911	63.51	3.835	63.45
b‘	3.692	63.42	3.799	63.51	3.718	63.45

Table 3.2 Calculated PCS values for Manα1→6Man.

H residue	Eu^{3+} (ppm) PCS values	Yb^{3+} (ppm) PCS values
1	0.270	0.077
2	0.213	0.054
3	0.113	0.033
4	0.118	0.026
5	0.051	0.026
6a	0.106	0.026
b	0.113	0.029
1‘	0.092	0.032
2‘	0.081	0.024
3‘	0.087	0.020
4‘	0.150	0.045
5‘	0.106	0.023
6a‘	0.102	0.026
b‘	0.107	0.026

In case of the α1→2-dimannose **47,** the PCS values observed for the H-6 protons of non-reducing mannose were higher than to the values for the anomeric center. This observation can be attributed to a close proximity of these atoms to the metal ion due to a bending of the mannose at the non-reducing end in direction to the linker (Table 3.3). The same trend was also observed, although in lower level, when the α1→2 linkage was distantly located from the metal ion in the trimannose **75** (Table 3.4).

Table 3.3 Calculated PCS values for Manα1→2Man.

H residue	Eu^{3+} (ppm) PCS values	Yb^{3+} (ppm) PCS values
1	0.280	0.088
2	0.232	0.038
3	0.136	0.029
4	0.119	0.022
5	0.157	0.045
6a	0.120	0.040
b	0.127	0.044
1‘	0.175	-0.026
2‘	0.064	-0.073
3‘	0.098	-0.115
4‘	0.067	-0.022
5‘	**0.304**	-0.057
6a‘	**0.391**	-0.070
b‘	**0.491**	0.019

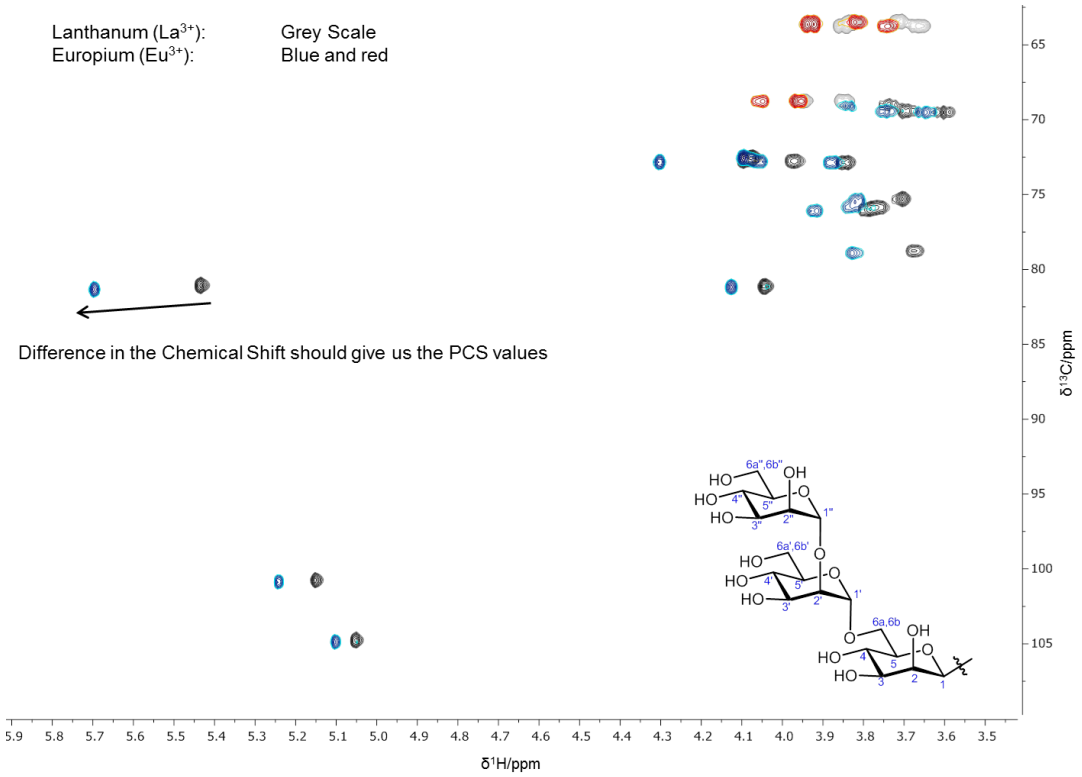

Figure 3.10: ^{1}H-^{13}C HSQC NMR spectra of chelating unit tagged Manα1→2Manα1→6Man with the metal ion La^{3+}, Eu^{3+}. The chemical shift change of the anomeric proton is indicated by the arrow.

Table 3.4 Calculated PCS values for Manα1→2Manα1→6Man.

H residue	Eu^{3+} (ppm) PCS values	H residue	Eu^{3+} (ppm) PCS values	H residue	Eu^{3+} (ppm) PCS values
1	0.263	1‘	0.092	1‘‘	0.051
2	0.209	2‘	0.081	2‘‘	0.020
3	0.139	3‘	0.088	3‘‘	0.031
4	0.158	4‘	0.049	4‘‘	0.108
5	0.100	5‘	0.046	5‘‘	0.042
6a	0.100	6a‘	0.092	6a‘‘	0.076
b	0.112	b‘	0.105	b“	0.077

3.3.5 Molecular Dynamics Study[I]

The pseudo contact shifts (PCSs) can be used to assess the conformational flexibility of the glycans. Figure 3.11 shows the chemical structures of the α1→2 and α1→6 linked mannose disaccharides with the lanthanide tags, and snapshots of the molecular geometry

[I] Molecular Dynamic Study was performed by Dr. Mark Santer and Dr. Marko Wehle at Max Planck Institute for colloids and Interfaces. All the Figures from 3.11 to 3.14 were generated and analyzed by Dr. Mark Santer and Dr. Marko Wehle.

taken from MD simulation. The molecular models were constructed using the GLYCAM06 force field,[147] with special amendments provided by Karl N. Kirschner[II] to represent the linker topology. Figure 3.11 shows two snapshots capturing the characteristics of the molecular geometries. In the α1→2 linkage the non-reducing mannose Man2 is in close proximity to the lanthanide complex which is also observed from the NMR experiments (Table 3.3). In the α1→6 case, Man2 is all the time sufficiently far away from the ion chelating moiety. The difference in interaction has consequences for the distribution of the phenyl torsion.

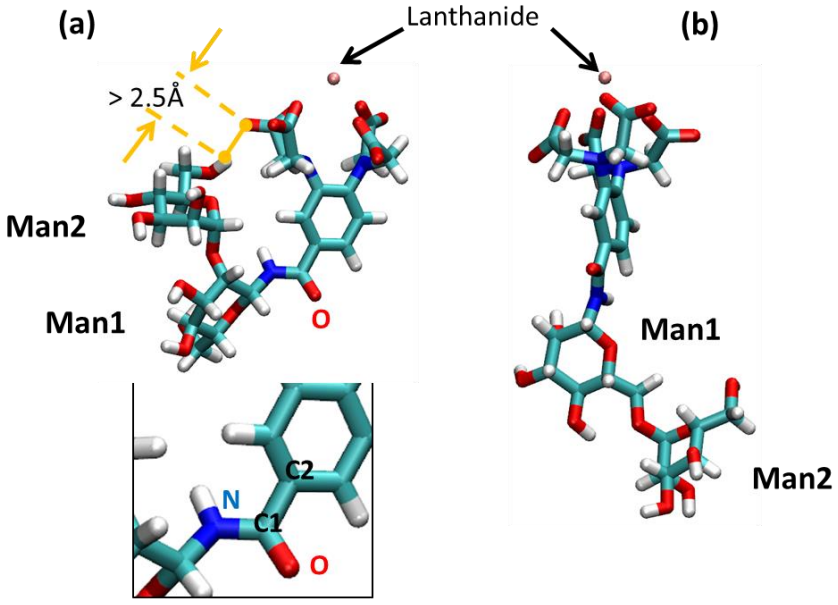

Figure 3.11: (a) Man α1→2Man, with linker attached as a β-anomer. (b) Same for Manα1→6Man. The enhancement of (a) shows atom names that are referred to in the text.

The obtained data show an overlay of the peptide bonds involving the nitrogen and oxygen for the two cases. The interaction of Man2 in the α1→2 case leads to a concentration on one orientation, whereas there is a balanced account of orientations in the α1→6 case (Figure 3.12).

[II] Parameterization of chelating linker for the MD study was performed by Dr. Karl N. Kirschner at Bonn-Rhein-Sieg University of Applied Sciences, Grantham-Allee 20, 54757 Sankt Augustin, Germany

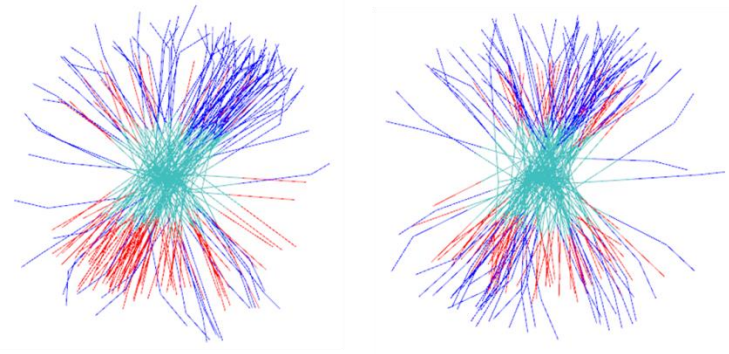

(a) Man α1→2Man (b) Man α1→6Man

Figure 3.12. Orientation of the C1-O, C1-N bonds of the quasi-peptide bond terminating at the phenyl torsion around C2-C1, shown in Figure 3.11. The direction of view is along C1-C2.

These interactions should be kept in mind while interpreting the PCS values for computing PCS, which shall make use of the metal centered point-dipole approximation. For this, it was assumed that the magnetic moment generated by the lanthanides can be approximated by a point dipole located at the center of the metal ion. We concentrated on comparing the PCS values of the reducing end Man1 only, as this maintains a fixed orientation w.r.t. to the ion-phenyl axis. The hydrogens in questions are more than 8 Å away from the ion center, beyond which the dipole approximation is said to hold. In addition the restriction to Man1 avoids the problem of defining a suitable frame of reference by averaging over the ion position.

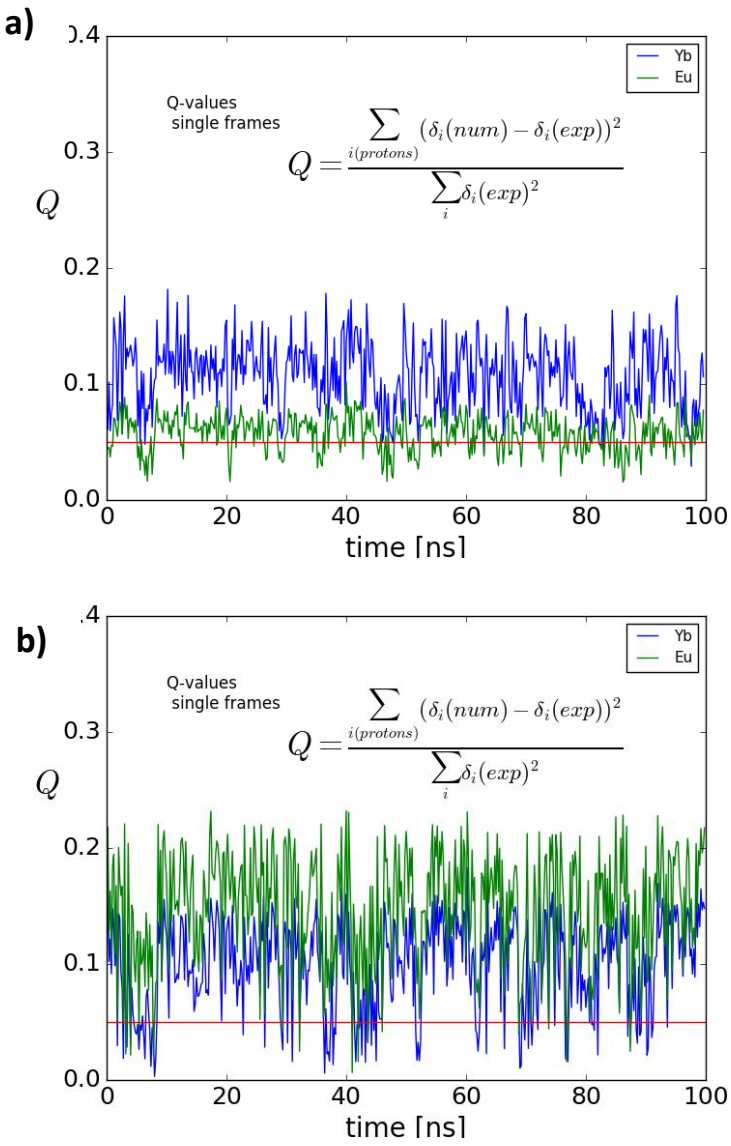

Figure 3.13. **a)** Q-values for the pseudo-contact shifts on Man1 of Man α1→2Man; **b)** Q-values for the pseudo-contact shifts on Man1 of Man α1→6Man; computed for single frames along an MD trajectory segment of 100ns duration at 303K, for the lanthanides Yb and Eu. The red line marks a Q-value of 0.05, which in general is considered indicative of a "good" agreement.

The Q-values of the back-calculated pseudo-contact shifts for both dimannoses are shown in Figure 3.13. it was noted that the behavior of Yb is rather similar in both cases, despite the qualitative difference in the conformational ensemble. A similar tendency was observed by Eu, which in the case of Man α1→2Man shows a narrow distribution around 0.05, a value in the literature that is generally considered a high quality fit.[108] The insensitive could have been expected, as it was already demonstrate with the experiments at reduced temperature that Yb should not be an ideal lanthanide for our purposes due to

its weak magnetic moment. It is therefore remarkable that it is for Yb that can produce the lowest Q-values on the selected single frames lower than 0.01 (see Figure 3.13b).

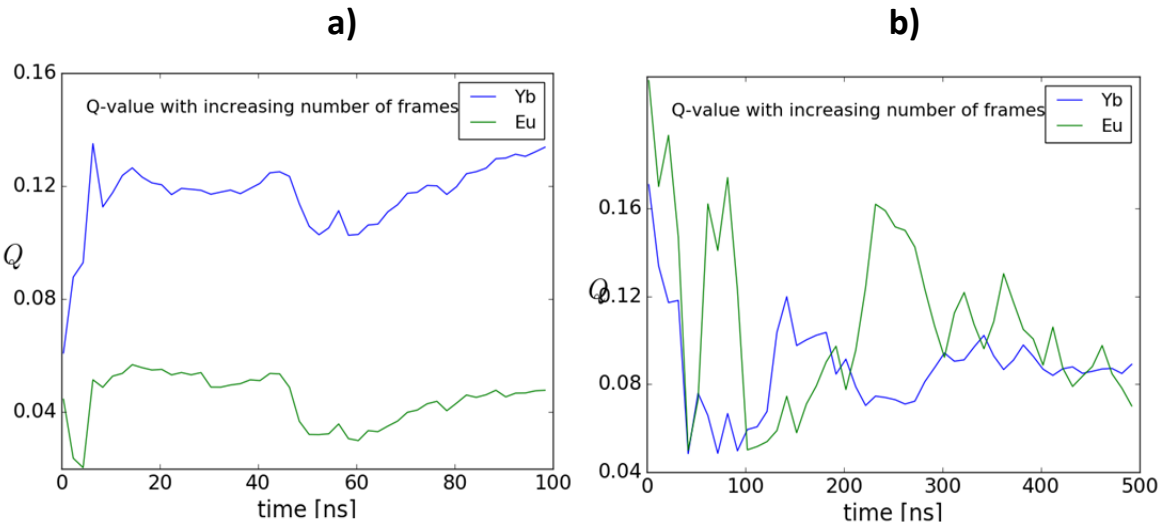

Figure 3.14. Evolution of the Q-value taking an increasing number of frames into account, for **a)** Man α1→2Man; **b)** Man α1→6Man. At 100ns, a total of 500 frames go into the fitting process.

The evolution of Q-values over an increasing number of frames was also considered. The difference between the "good" (Eu) and the "bad" (Yb) is again pronounced for Man α1→2Man, the Q-values appears to level off at a value similar to the single frame case in Figure 3.13a. Here we may formulate the hypothesis that with the α1→2 linkage, indeed the interaction of Man2 with the linker complex restricts the conformational space of the phenyl ring torsion as a true physical effect. As a consequence of this interaction both, the experimental as well as the molecular model would agree in the conformational ensemble, facilitating the determination of the magnetic susceptibility tensor. On the other hand, if in the α1→6 case the torsion distribution of the computational model is somewhat off the true distribution, we might see effects as in Figure 3.14b, where even after 500 frames the Q-value is still unsatisfactorily high (close to 0.1), and Yb and Eu apparently are "equally good".

3.4 Conclusion

To study the conformational behavior of GPI anchor, Paramagnetic NMR technique was employed along with the MD simulations. For paramagnetic ions (Lanthanides) assisted NMR spectroscopy the chelating unit tagged disaccharides Manα1→2Man and Manα1→6Man, and the trisaccharide Manα1→2Manα1→6Man, that are part of core structure of GPI anchor were successfully synthesized. ^{1}H and ^{1}H-^{13}C HSQC spectra of synthesized GPI fragments were acquired in the presence of diamagnetic reference (La^{3+}) and paramagnetic metal ions (Dy^{3+}, Yb^{3+}, Eu^{3+}) and analyzed. From the NMR experiments it was found out that dysprosium (Dy^{3+}) metal ion is not ideal for small saccharides because of high magnetization, which leads to the disappearance of the signals.

The PCS values were measured as the difference of ^{1}H and ^{13}C chemical shift values between the carbohydrate complex with paramagnetic metal ion and diamagnetic reference in all the three fragments and compared with the data obtained from the computational analysis. The results showed good agreement with the back calculated PCS (Q) values. This is reflected by europium (Eu) in the case of Man α1→2Man showing a narrow distribution around 0.05 and by ytterbium (Yb) that can produce the lowest Q-values on the selected single frames even lower than 0.01 suggesting that both the metal ions are equally good.

However, before the analysis can be carried out further for both disaccharides and trisaccharide, the suitability of the Q-value approach should be carefully reviewed which is currently ongoing, to remove any artifacts that have been mentioned before.

Chapter 4

Synthesis of GPIs for the Semi-synthesis of GPI-anchored proteins

4.1 Introduction to the GPI-anchored protein

Proteins and glycoproteins are attached to the cell membrane through transmembrane domains or by using lipids that are added as a posttranslational modification (PTM). The PTMs can be simple lipidation or a complex glypiation, the attachment of complex glycosylphosphatidylinositols (GPIs). Glypiation of proteins is one of the most complex type of modification as it involves the attachment of a molecule containing lipids, carbohydrates and phosphate groups.[43, 148] Proteins and glycoproteins that are attached to the lipid bilayer using GPIs are also called as GPI-anchored proteins (GPI-APs). GPI-APs play an important role in different processes including cellular communication,[33] signal transduction,[34] cell adhesion,[412] protein trafficking and prion disease pathogenesis.[57]

The anchoring to the membranes using a phosphatidylinositol was first reported in the mid-1970s based on the ability of a highly purified bacterial phosphatidylinositol-specific phospholipase C (PI-PLC) to release alkaline phosphatase and 5′-nucleotidase from mammalian plasma membranes. In 1980s, the first structure of a glycosylphosphatidylinositol (GPI) anchor was reported.[1] The complexity and diversity in the structure of GPIs (as described in chapter 1), together with the conserved nature and their ubiquity among eukaryotes are indications of additional function that may be accredited to these glycolipids.

Glypiation is a posttranslational modification that has not been studied in detail. GPI-APs are mostly obtained by expression methods in cell lines, which insert cell-specific GPI-structures and deliver heterogeneous GPI-APs mixture that makes it difficult to evaluate the effect of this modification to the protein function. Semisynthetic methods are emerging as an alternative to obtain GPI-APs with natural and well defined structures.[112]

These semisynthetic methods exploit the advances in chemical synthesis and recombinant protein engineering, which in combination with ligation reactions facilitate the access to well defined homogeneous proteins or glycoproteins.[149-151]

First attempt to synthesize GPI-anchored peptides and glycopeptides was made by Guo et al, performing the first total synthesis of GPI anchored peptide[152] and the chemical synthesis of the skeleton structure of sperm CD52, a GPI-anchored glycopeptide.[153] Later on, Bertozzi's and Becker's group achieved the semi-synthesis of various GPI anchored proteins analogs using expressed protein ligation.[154, 155] More recently, Seeberger and coworkers reported the synthesis of a GPI-anchored Prion protein containing a monolipidated GPI anchor using the same strategy.[112, 155]

In order to evaluate the biological significance and also to study the effect of GPI anchoring on the folding and activity of protein, our group at the Max Planck Institute of Colloids and Interfaces is developing strategies to synthesize structurally well-defined GPI-APs containing natural GPI-structures either from protozoan or mammalian proteins (e.g.-Thy-1, Prion protein, Merozoite Surface Protein 1 of *Plasmodium falciparum* and some cytokines like IL2, INFα2A). In order to reveal the importance of glypiation, two model GPIs (one from protozoan and other from mammalian cells) were selected to compare and standardize the different methods of ligation of the GPI to the proteins and peptides. This project is carried out interdisciplinary with the biochemist and biologist who is working on the recombinant expression and purification of desired protein, chemist synthesizing peptide thioesters and the required GPI glycolipids. For this purpose, two cysteine tagged model GPI anchors (**76** and **77;** Scheme 4.2 & 4.3) were synthesized for the native chemical ligation to access well-defined GPI-APs as part of this work.

4.2 Retrosynthesis of a Cysteine-containing GPI-anchor

For the synthesis of GPI-anchored proteins using native chemical ligation, a synthetic GPI containing a cysteine residue attached to the phosphoethanolamine unit is required. This cysteine moiety can undergo a reaction with a *C*-terminal thioester via a trans-thioesterification and rearrangement processes to give GPI anchored proteins. Different synthetic approaches can be applied for the synthesis of GPI-anchors containing cysteine

residue. The preferred strategy involves the coupling of cysteine to the phosphoethanolamine unit prior to the phosphorylation of the GPI anchor, which is performed at the last stage of the synthesis process. The amine and thiol functions of the cysteine can be protected using acid labile groups, which can be removed by acid treatment of the GPIs after the debenzylation of the glycan by hydrogenolysis. The core glycan part of GPI anchor can be obtained using a general synthetic approach established in our group, which involve the orthogonally protected building block **6, 7, 82** and **83**.[87]

After the assembly of the orthogonally protected pseudopentasaccharide (core glycan), this glycan will be further decorated by subsequent deprotections and two-step phosphorylations. Finally, a three-steps global deprotection will give access to GPI anchor with a cysteine residue ready for ligation with the peptide or the protein of interest.

By applying the general synthetic strategy, two GPI anchors will be synthesized, one is the protozoan GPI anchor **76** (referred as bilipidated and bisphosphorylated GPI) and the other one is a GPI having the minimal structure of mammalian GPIs **77**, which include an additional phosphoethanolamine 2-*O* position of Man-I residue (referred as monolipidated and triphosphorylated GPI).

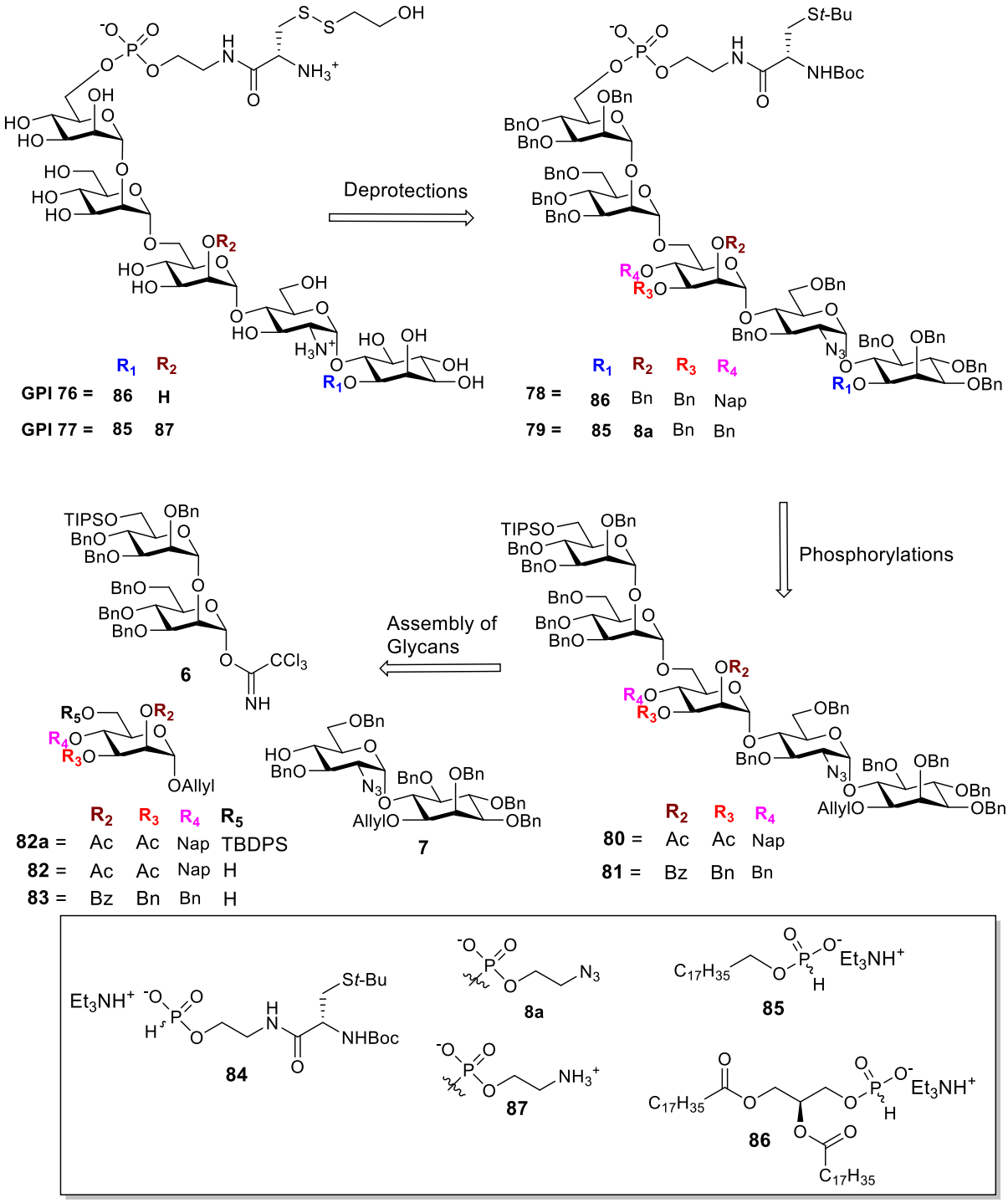

Figure 4.1: Retrosynthetic analysis of cysteine-containing GPIs for the semi-synthesis of GPI anchored proteins.

4.3 Assembly of glycan core of GPI-anchor

For the synthesis of both protozoan (**76**) and mammalian (**77**) GPIs, two different mannose building blocks were used to install the Man-I residue. For the synthesis of **76** a mannose containing an acetyl (Ac) group on 2-*O* and 3-*O* position (**82**) was used. For the synthesis of **77,** the building block was protected with a benzyl ester on 2-*O* and benzyl (Bn) on the 3-*O* position (**83**). The building block **83** was used for the synthesis of mammalian GPIs wherein benzyl ester can be removed selectively to install a phosphoethanolamine unit on 2-*O* position of Man-I residue (a distinguishing feature of mammalian GPIs), and building block **82** was used for other GPI. For the synthesis of mammalian GPI **77**, compound **94** was synthesized by Dr. Xinyu Liu. (Scheme 4.3) For the synthesis of protozoan GPI **76**, the Man-I building block **82** was glycosylated with the α-(1→2)-dimannose trichloroacetimidate donor (**6**) (Scheme 4.1). To get the better α-selectivity (75-80 % of pure α-product), the glycosylation reaction was performed at room temperature using TBSOTf as an activator and thiophene as an additive. Under these conditions the trimannoside **88** was obtained in 80 % yield.[87] Subsequently, the allyl group of the obtained trisaccharide was removed in a two-steps process involving an isomerization with activated iridium catalyst and a hydrolysis with mercury salts. The resulting hemiacetal was treated with trichloroacetonitrile and DBU to get trichloroacetimidate donor **90** in 80 % yield over two steps. To complete the GPI glycan core synthesis, the trichloroacetimidate **90** was activated with TMSOTf at -40 °C and used to glycosylate the pseudodisaccharide **7** giving the pseudopentasaccharide **80** in 80 % yield. Dr. Xinyu Liu also synthesized the core pentasaccharide using same strategy.[112] Finally, some protecting groups were exchanged and the allyl protecting group on the 1-*O* position of inositol residue was removed, under the conditions mentioned above, to deliver the pseudopentasaccharide ready for the late-stage phosphorylations.

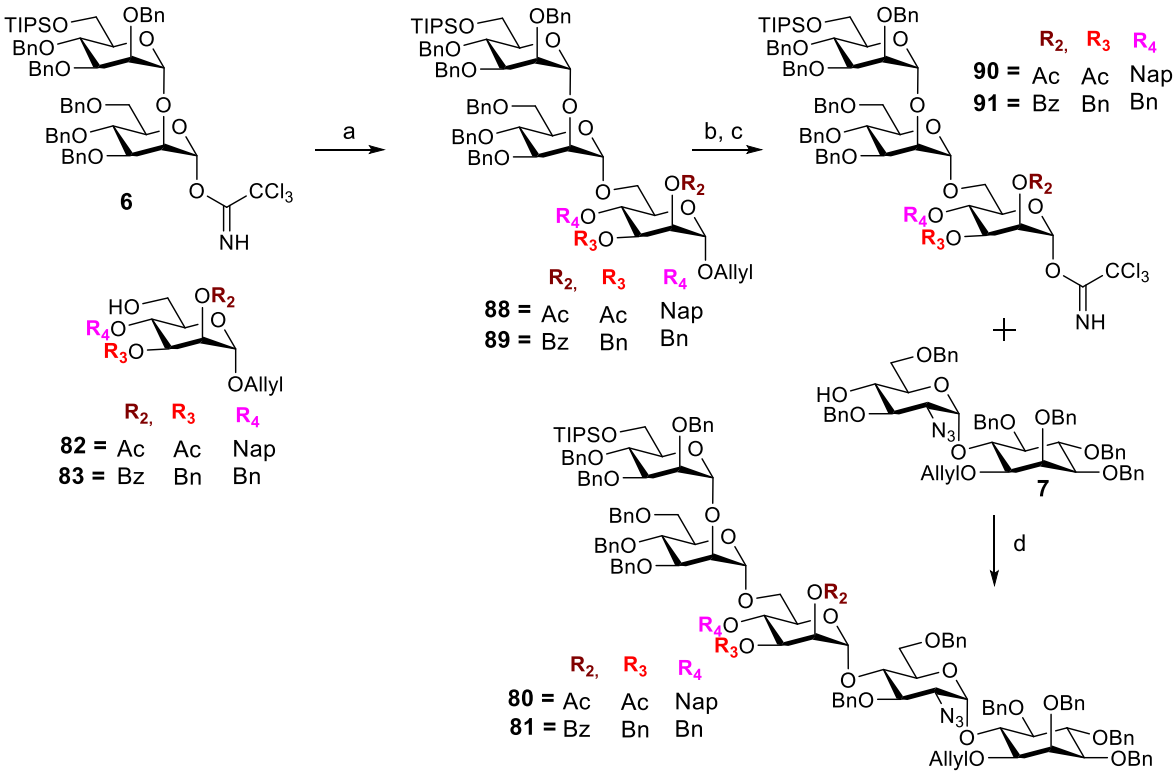

Scheme 4.1: Synthesis of core Pentasaccharide. a) TBSOTf, Thiophene: Toluene (2:1), 80 %(α), 20 %(β), **88**; b) i. $[Ir(Cod)(PPh_2Me)_2]PF_6$, H_2, THF ii. HgO, $HgCl_2$, Acetone, Water; c) Cl_3CCN, DBU, DCM, 0 °C, 80 %, **90**; d) TMSOTf, Toluene, -40 °C, 80 %, **80**

4.4 Synthesis of protozoan GPI anchor containing a Cysteine residue

The pseudopentasaccharide **80** was used for the synthesis of the protozoan GPI **76**. The acetyl groups present on 2-*O* and 3-*O* of Man-I were exchanged to benzyl ethers before the removal of the allyl group and subsequent phosphorylations. This transformation was necessary to avoid the use of basic conditions for the deacetylation at the end of the synthesis and the concomitant risk of saponification of the fatty acids of the lipid. The exchange of acetyl groups in **80** was perfomed by saponification using Zemplén conditions and a following benzylation using BnBr and NaH. Subsequently the removal of the allyl group from 1-*O* position of *myo*-inositol was performed to obtain **92** in 80 % yield (Scheme 4.2). The resulted alcohol **92** was phosphitylated with the H-phosphonate **86** using pivaloyl chloride in pyridine. After the completion of the reaction, an oxidation with iodine in wet pyridine delivered the phospholipidated compound **93**. Next, triethylammonium salt of **93** was exchange with Amberlite IR120 Na^+ form and the the

silyl group (TIPS) present on 6-*O* position of Man-III was removed under acidic conditions using $Sc(OTf)_3$. The resulted primary alcohol was phosphitylated with the cysteine containing phosphonate **84** and oxidized under the same conditions used for **93** to deliver the fully protected and lipidated GPI anchor **78**. Finally, GPI **76** was obtained in 35 % yield after a two-step global deprotection involving a hydrogenation with palladium on charcoal, and removal of N-Boc and S*t*-Bu protecting groups using $Hg(TFA)_2$ in trifluoroacetic acid (Scheme 4.2).

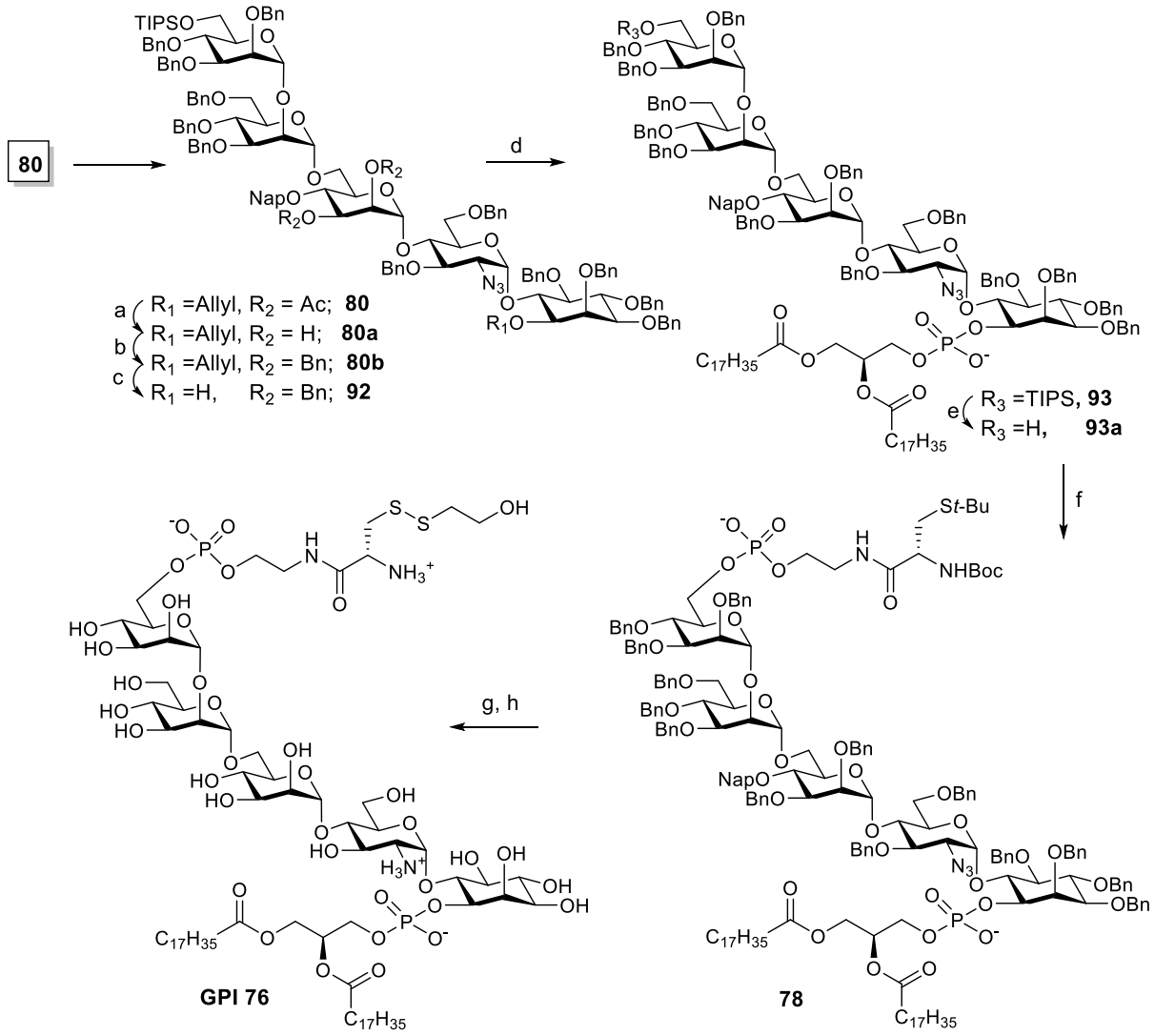

Scheme 4.2: Synthesis of GPI 76. a) NaOMe, NaOH, 1 h, 95 %; b) NaH, BnBr, 15 Crown-5, THF:DMF (1:1), 3 h, 40 °C, 86 %; c) i. $[Ir(Cod)(PPh_2Me)_2]PF_6$, H_2, THF ii. HgO, $HgCl_2$, Acetone, Water, 80 %; d) **86,** PivCl, Pyridine then, I_2, water, 55 %; e) amberlite Na+ resin exchange, $Sc(OTf)_3$, ACN, $CHCl_3$, 67 %; f) **84,** PivCl, Pyridine then, I_2, water, 70 %; g) THF:Methanol:water (3:3:1), Pd/C, H_2, 4 days, 70 %; h) TFA:Anisole (10:1), $Hg(TFA)_2$, 0 °C, 30 min then $CH_3COOH:H_2O$ (7:3), mercaptoethanol, 12 h, 35 %.

4.5 Synthesis of a mammalian GPI anchor containing a Cysteine residue

For the synthesis of mammalian GPI **77**, bisphosphorylated compound **94** was provided by Dr. Xinyu Liu, which was synthesized from pentasaccharide core **81**. The triethylammonium salt of **94** was exchanged with Amberlite IR120 Na^+ form before the the silyl group (TIPS) present on 6-*O* position of Man-III was removed under acidic conditions using $Sc(OTf)_3$. The resulted alcohol was phosphitylated with the cysteine containing phosphonate **84** and after completion of the reaction, an oxidation with iodine in wet pyridine delivered the fully protected and phospholipidated compound **79**. Finally, GPI **77** was obtained in 50 % yield after a two-step global deprotection involving a hydrogenation with palladium on charcoal, and removal of N-Boc and S*t*-Bu protecting groups using $Hg(TFA)_2$ in trifluoroacetic acid (Scheme 4.3).

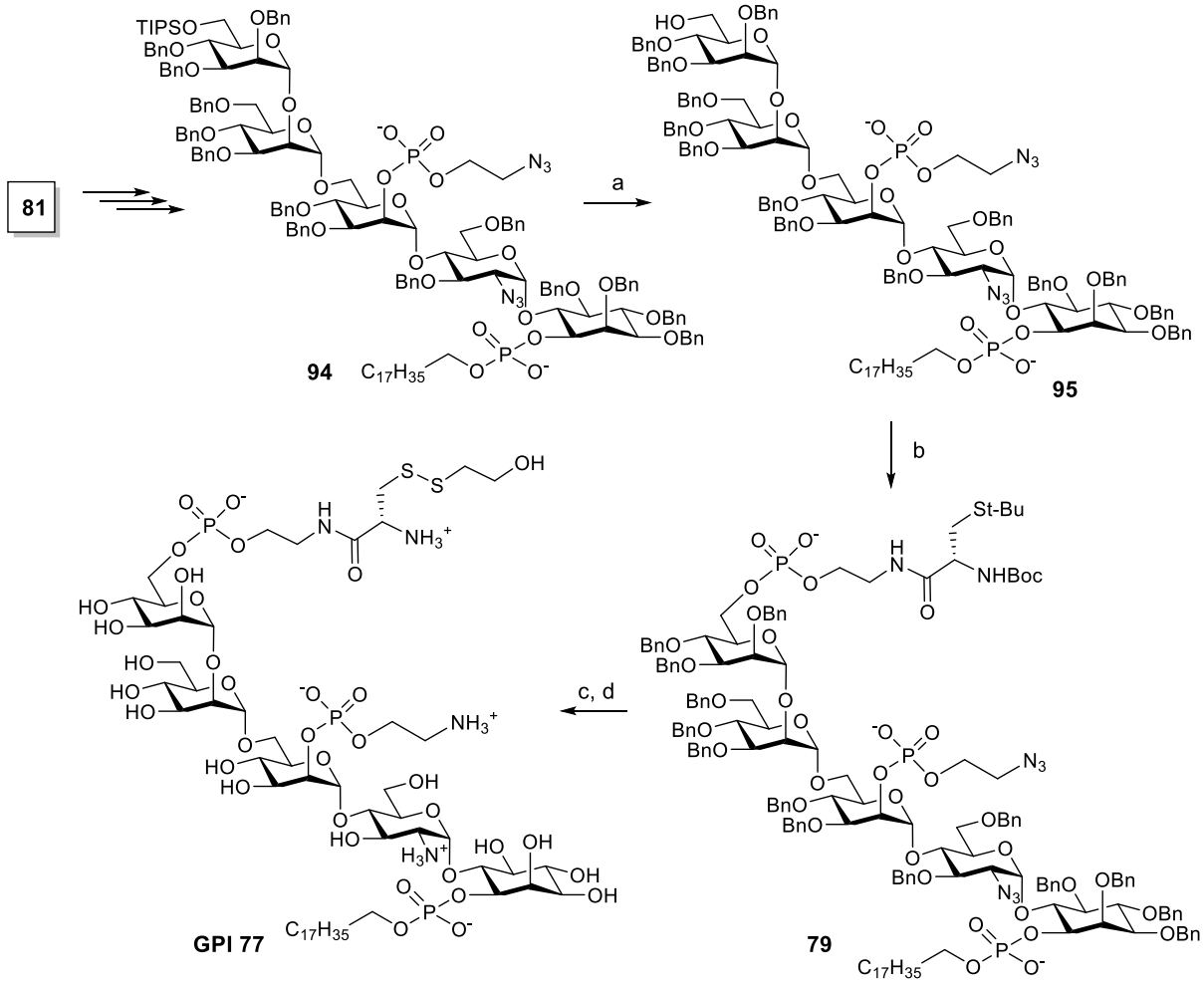

Scheme 4.3: Synthesis of GPI **77**. a Amberlite Na^+ resin exchange, $Sc(OTf)_3$, ACN, $CHCl_3$, 67 %; b) **84,** PivCl, Pyridine then, I_2, water, 70 %; c) THF:Methanol:water (3:3:1), Pd/C, H_2, 4 days, 70 %; d) TFA:Anisole (10:1), $Hg(TFA)_2$, 0 °C, 30 min then CH_3COOH:H_2O (7:3), mercaptoethanol, 12 h, 50 %.

4.6 Conclusion and perspective

Two GPIs corresponding to model protozoan GPI (**76)** and mammalian GPI (**77)** were successfully synthesized by applying the general synthetic strategy. The synthesis of cysteine containing GPI anchor was not straight forward and the sequence of glycosylation was also critical for the complete synthesis of GPIs. First challenge in the assembly of glycan core structure was the introduction of pure α(1→6)-linkage, which was improved to 80 % by using thiophene as an additive. Also the monitoring of the reaction was intriguing after phosphorylation because of the charges present in the molecules which interact with the silica on thin layer chromatographic (TLC) plate used for analysis. However, the main issue was the solubility of the deprotected compound, especially in the GPI containing bilipid chains, which is why the obtained yield was lower in case bilipidated GPI **76** than the monolipidated GPI **77.**

These structures (**76** and **77**) are currently being used for the development of semi-synthetic methods to obtain homogeneous GPI-anchored proteins. Now, my colleagues are comparing the different methods of ligation and standardizing the condition for the ligation the cysteine-containing GPIs to diverse proteins of interest including the GFP as a model protein and some naturally GPI-anchored parasitic proteins. Further, the biological studies of these anchored proteins might reveal the significance of glypiation in the structure and activity of these proteins as well as the role of GPI in the organization of the membrane and the participation of GPIs in the formation of lipid rafts.

Chapter 5

Experimental Section

5.1 General Materials and Methods

All purchased chemicals were of reagent grade and all anhydrous solvents were of high-purity grade and used as supplied except where noted otherwise. Reactions were performed in oven-dried glassware under an inert argon atmosphere unless noted otherwise. Reagent grade thiophene was dried over activated molecular sieves prior to use. Pyridine was distilled over CaH_2 prior to use. Sodium hydride suspension was washed with hexane and THF and stored in an anhydrous environment. Benzyl bromide was passed through activated basic aluminum oxide prior to use. Molecular sieves were powdered and activated by heating under high vacuum prior to use. Analytical thin layer chromatography (TLC) was performed on Merck silica gel 60 F_{254} plates (0.25mm). Compounds were visualized by UV irradiation or heating the plate after dipping in staining solution. The staining solutions were cerium sulfate-ammonium molybdate (CAM) solution, basic potassium permanganate solution, acidic ninhydrin-acetone solution, or a 3-methoxyphenol-sulfuric acid solution (Sugar Stain). Flash column chromatography was carried out using a forced flow of the indicated solvent on Sigma Aldrich silica gel high purity grade 60 Å (230-400 mesh particle size, for preparative column chromatography).

^{1}H, ^{13}C and ^{31}P-NMR as well as all 2D-spectra (^{1}H-^{1}H COSY, ^{1}H-^{1}H TOCSY, ^{1}H-^{13}C HSQC, ^{1}H-^{13}C HMBC) were recorded on a Varian 400 (400 MHz), a Varian 600 (600 MHz), a Bruker 400 (400 MHz) and a Bruker Ascend 400 (400 MHz) spectrometer in $CDCl_3$ (7.26 ppm ^{1}H, 77.1 ppm ^{13}C), D_2O (4.79 ppm ^{1}H), MeOD (4.87 ppm and 3.31 ppm ^{1}H, 49.00 ppm ^{13}C), Acetone-d_6 (2.05 ppm and 2.84 ppm ^{1}H, 206.26 ppm and 29.84 ppm ^{13}C) unless otherwise stated. The coupling constants (*J*) are reported in Hertz (Hz). Splitting patterns are indicated as s, singlet; d, doublet; t, triplet; q, quartet; br, broad singlet; dd, doublet of doublets; m, multiplet; dt, doublet of triplets; h, hextet for ^{1}H NMR data. Signals were assigned by means of ^{1}H-^{1}H COSY, ^{1}H-^{1}H TOCSY, ^{1}H-^{13}C HSQC, ^{1}H-^{13}C HMBC spectra and version thereof. ESI mass analyses were performed by the MS-service at the Institute for Chemistry and Biochemistry at the Free University of

Berlin using a modified MAT 711 spectrometer, the MS-service at the Institute for Chemistry at the University of Potsdam using an ESI-Q-TOF micro spectrometer, Waters Xevo G2-XS Q-TOF with an Acquity H-class UPLC and a Bruker Autoflex-speed MALDI-TOF spectrometer. Infrared (FTIR) spectra were recorded as thin films on a Perkin Elmer Spectrum 100 FTIR spectrophotometer. Optical rotations were measured with a Schmidt & Haensch UniPol L 1000 at a concentration (c) expressed in g/100 mL. HPLC supported purifications were conducted using Agilent 1100 and Agilent 1200 systems.

5.2 Experiment to Chapter 2

All mannose, glucose, glucosamine, galactose and inositol building blocks were synthesized and assembled according to the established protocol in our laboratory.[87]

5.2.1 Synthesis of the GPI 1 from *T. gondii*.

Allyl 3-*O*-benzyl-6-*O*-*tert*-butyldiphenylsilyl-2-*O*-levulinyl-α-D-mannopyranoside (3)

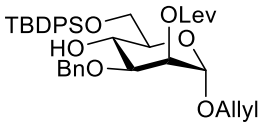

Orthogonally protected Mannose[87] (Man-I, **3a**) (1.9 g, 2.41 mmol) was dissolved in PBS buffer (1.0 M, 1 mL, pH 7.4) and dichloromethane (19 mL) to give a colorless solution. DDQ (0.82 g, 3.62 mmol) was added at 0 °C. After 5 h, the reaction mixture was diluted with DCM and washed with saturated $NaHCO_3$ (aq), dried over Na_2SO_4, filtered and concentrated. The crude product was purified by silica gel column chromatography to give mannoside **3** (1.56 g, 2.41 mmol, 92 % yield) as a colorless oil: R_f = 0.20 (EtOAc/Cyclohexane 1:2); ^{1}H NMR (400 MHz, $CDCl_3$) δ 7.71-7.69 (m, 4H), 7.42-7.26 (m, 11H), 5.86 (dddd, *J* = 16.6, 10.4, 6.1, 5.2 Hz, 1H, =CH-), 5.35 (dd, *J* = 3.2, 1.7 Hz, 1H, Man-2), 5.24 (dq, *J* = 17.2, 1.6 Hz, 1H, =CH_2), 5.17 (ddd, *J* = 10.4, 2.7, 1.3 Hz, 1H, =CH_2), 4.84 (d, *J* = 1.7 Hz, 1H, Man-1), 4.69 (d, *J* = 11.2 Hz, 1H, CH_2), 4.45 (d, *J* = 11.2 Hz, 1H, CH_2), 4.14 (ddt, *J* = 13.0, 5.6, 1.5 Hz, 1H, -OCH_2- of allyl), 3.99 – 3.88 (m, 4H, -OCH_2- of allyl, Man-4, Man-6), 3.80 (dd, *J* = 9.4, 3.2 Hz, 1H, Man-3), 3.69 (dt, *J* = 9.4, 4.0 Hz, 1H, Man-5), 2.77 – 2.53 (m, 4H, -CH_2CH_2-), 2.10 (s, 3H, Me), 1.05 (s, 9H, *t*-Bu); ^{13}C NMR (101 MHz, $CDCl_3$) δ 206.15, 172.00, 137.77, 135.70, 135.59, 133.50, 133.45,

133.26, 129.67, 129.66, 128.45, 128.14, 127.88, 127.65, 127.62, 117.67, 96.83, 77.64, 72.35, 71.52, 68.22, 67.93, 67.26, 63.87, 37.94, 29.77, 28.07, 26.80, 19.31; ESI-MS (*m*/*z*): $[M+Na]^+$ cald 669.2854, obsd 669.2858.

Allyl 3,6-di-*O*-benzyl-2-deoxy-2-trichloroacetamido-β-D-galactopyranosyl-(1→4)-3-*O*benzyl-6-*O*-(*tert*-butyldiphenylsilyl)-2-*O*-levulinyl-α-D-mannopyranoside (10)

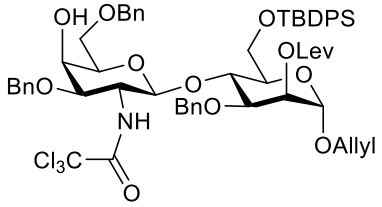

A mixture of galactosyl phosphate **4** (0.78 g, 0.928 mmol) and mannoside **3** (0.402 g, 0.621 mmol) were dissolved and co-evaporated three times with toluene and dried under high vacuum for 30 min. To a DCM solution (10 mL) of acceptor and donor at -40 °C, TMSOTf (135 μL, 0.746 mmol) was added. After 1 h, PBS buffer (1.0 M, pH 7.4, 1 mL) and DDQ (0.282 g, 1.24 mmol) were added, and the reaction mixture was kept at 20 °C for 2 h. Then, the reaction mixture was diluted with dichloromethane and washed with saturated $NaHCO_3$ (aq), dried over Na_2SO_4, filtered and concentrated. The crude product was purified by silica gel column chromatography to give disaccharide **10** (0.660 g, 0.582 mmol, 94 % yield) as a white foam: R_f = 0.33 (EtOAc/Hexane 1:2); ^{1}H NMR (600 MHz, $CDCl_3$) δ 7.74-7.71 (m, 4H), 7.41-7.20 (m, 21H), 6.33 (d, *J* = 7.6 Hz, 1H, NH), 5.87 (m, 1H, vinyl), 5.35 (dd, *J* = 1.9, 3.4 Hz, 1H, Man-2), 5.26 (dq, *J* = 17.1, 1.4 Hz, 1H, =CH2), 5.19 (dq, *J* = 10.4, 1.4 Hz, 1H, =CH2), 5.03 (d, *J* = 8.3 Hz, 1H, Gal-1), 4.84 (d, *J* = 1.9 Hz, 1H, Man-1), 4.67 (d, *J* = 11.6 Hz, 1H, -CH_2-), 4.65 (d, *J* = 11.5 Hz, 1H, -CH_2-), 4.63 (d, *J* = 11.6 Hz, 1H, -CH_2-), 4.50 (d, *J* = 11.5 Hz, 1H, -CH_2-), 4.45 (d, *J* = 12.0 Hz, 1H, -CH_2-), 4.40 (d, *J* = 12.0 Hz, 1H, -CH_2-), 4.18-4.15 (m, 2H, -OCH_2- of allyl & Man-4), 4.09 (br-d, *J* = 3.1 Hz, 1H, Gal-4), 3.99-3.94 (m, 3H, -OCH_2- of allyl, Man-3 & Man-6), 3.88 (dd, *J* = 3.1, 10.7 Hz, 1H, Gal-3), 3.83 (dd, *J* = 5.0, 11.3 Hz, 1H, Man-6), 3.74 (br-dd, *J* = 4.4, 10.0 Hz, 1H, Man-5), 3.68-3.63 (m, 2H, Gal-2 & Gal-6), 3.46 (dd, *J* = 5.3, 9.8 Hz, 1H, Gal-6), 3.42 (br-dd, *J* = 5.3, 6.0 Hz, 1H, Gal-5), 2.65-2.40 (m, 4H, -CH_2CH_2-), 2.04 (s, 3H, Me), 1.08 (s, 9H, *tert*-Bu); ^{13}C NMR (151 MHz, $CDCl_3$) δ 206.39, 171.99, 161.80, 138.62, 138.01, 137.33, 135.98, 135.63, 133.78, 133.49, 133.13, 129.86, 129.81, 128.60, 128.38, 128.20, 128.13, 127.90, 127.78, 127.73, 127.71, 127.65, 127.62, 127.22, 127.11, 117.87, 98.29, 96.39, 92.27, 76.18, 75.92, 73.56, 72.93, 72.47,

72.37, 71.60, 71.33, 69.18, 68.63, 67.98, 65.06, 63.21, 55.71, 37.93, 29.71, 28.04, 26.70, 19.33; ESI-MS (*m*/*z*): $[M+Na]^+$ cald 1154.3423, obsd 1154.3481

Allyl 2,3,4,6-tetra-*O*-benzyl-α-D-glucopyranosyl-(1→4)-3,6-di-*O*-benzyl-2-deoxy-2 trichloroacetamido-β-D-galactopyranosyl-3-*O*-benzyl-2-*O*-levulinyl-α-D mannopyranoside (11)

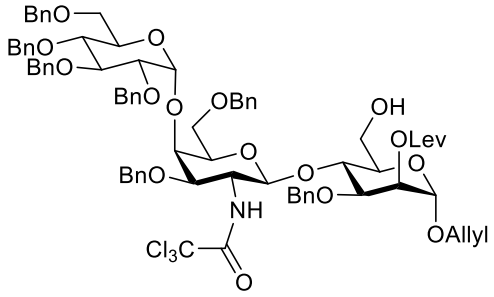

In first step, A mixture of glucosyl phosphate **5** (0.195 g, 0.265 mmol) and disaccharide **10** (0.250 g, 0.221 mmol) were dissolved and co-evaporated three times with toluene and dried under high vacuum for 1 h. To a solution of acceptor and donor in thiophene:toluene (2:1, 10 mL) at 0 °C, TBSOTf (68 μL, 0.373 mmol) was added. After 1 h, the reaction mixture was diluted with dichloromethane and washed with saturated $NaHCO_3$ (aq), dried over Na_2SO_4, filtered and concentrated. The crude product was purified by silica gel column chromatography to give trisaccharide as an α,β-mixture (8.5:1) (0.330 g, 0.199 mmol, 90 % yield) as a white foam: R_f = 0.35 (EtOAc/Hexane 1:3). The spectral data was in accordance with the reported data.[88]

In second step, To a THF solution (6 mL) of trisaccharide (0.300 g, 0.181 mmol), HF-pyridine complex (~70 % HF, 0.100 mL, 3.62 mmol) was added. After two days, the reaction mixture was quenched by adding saturated $NaHCO_3$ (aq) dropwise, until no more gas formation was observed. The reaction mixture was dissolved in DCM and washed one time with water and with brine solution. The combined organic layers were dried over Na_2SO_4, filtered and concentrated. The crude product was purified by silica gel column chromatography to give trisaccharide **11** (0.210 g, 0.148 mmol, 82 % yield) in pure α anomer as a white foam: R_f = 0.25 (EtOAc/Hexane 3:1); ^{1}H NMR (400 MHz, $CDCl_3$) δ 7.29 – 6.90 (m, 36H, NH & Ph), 5.74 (ddd, *J* = 22.3, 10.8, 5.7 Hz, 1H), 5.20 – 5.10 (m, 3H), 5.07 (d, *J* = 10.4 Hz, 1H), 4.96 (d, *J* = 3.3 Hz, 1H), 4.77 – 4.49 (m, 9H), 4.35 (d, *J* = 11.8 Hz, 1H), 4.31 (d, *J* = 12.2 Hz, 1H), 4.25 (d, *J* = 10.7 Hz, 1H), 4.11 –

3.91 (m, 10H), 3.88 (dd, *J* = 9.2, 3.4 Hz, 1H), 3.83 (dd, *J* = 12.9, 6.2 Hz, 1H), 3.80 – 3.70 (m, 3H), 3.66 – 3.57 (m, 2H), 3.48 – 3.45 (m, *2*H), 3.35 (dd, *J* = 9.4, 5.6 Hz, 1H), 3.24 (brd, *J* = 9.3 Hz, 1H), 2.87 (brd, *J* = 9.7 Hz, 1H), 2.44 – 2.30 (m, 4H), 1.92 (s, 3H); ^{13}C NMR (101 MHz, $CDCl_3$) δ 206.57, 171.99, 162.00, 138.84, 138.45, 138.41, 138.34, 138.11, 137.92, 137.88, 133.37, 128.49, 128.45, 128.42, 128.40, 128.32, 128.29, 128.26, 128.23, 128.17, 128.14, 128.01, 127.98, 127.92, 127.76, 127.69, 127.63, 127.60, 127.55, 127.44, 127.37, 127.25, 127.02, 117.84, 100.04, 98.95, 96.67, 92.64, 82.04, 80.13, 77.79, 76.32, 75.81, 75.35, 74.95, 73.82, 117 73.65, 73.54, 73.25, 73.07, 73.01, 71.74, 71.56, 71.22, 70.76, 69.28, 68.30, 67.57, 61.75, 56.37, 37.86, 29.66, 28.07; ESI-MS (*m*/*z*): $[M+Na]^+$ cald 1440.4622, obsd 1440.4645.

2,3,4-tri-*O*-benzyl-6-*O*-triisopropylsilyl-α-D-mannopyranosyl-(1→2)-3,4,6-tri-*O*benzyl-α-D-mannopyranosyl-(1→*6*)-3-*O*-benzyl-4-*O*-(2,3,4,6-tetra-*O*-benzyl-α-D-glucopyranosyl-(1→4)-3,6-di-*O*-benzyl-2-deoxy-2-acetamido-β-D-galactopyranosyl)-2-*O*-levulinyl-α-D-mannopyranoside (12)

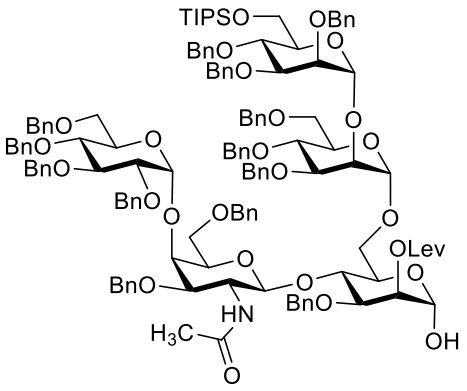

A dimannosyl trichloroacetimidate **6** (0.224 g, 0.197 mmol) and trisaccharide **11** (0.200 g, 0.141 mmol) were dissolved and co-evaporated three times with toluene. The residue was dissolved in a mixture of thiophene:toluene (2:1, 3 mL). Then, MS (4Å, 0.1 g) and TBSOTf (25 μL, 0.120 mmol) were added. After 1 h, triethylamine was added and the reaction mixture was filtered through a pad of Celite. The filtrate was evaporated to dryness to give a yellow oil that was purified by silica gel column chromatography to afford pentasaccharide (0.270 g, 0.141 mmol, 80 % yield): R_f = 0.33 (EtOAc/Hexane 1:3); ESI-MS (*m*/*z*): $[M+Na]^+$ cald 2458.9854, obsd 2458.9827.

In a 25 mL round-bottomed flask pentasaccharide (0.21 g, 0.086 mmol) was dissolved in acetic acid (3 mL) to give a colorless solution. To this solution, zinc (0.535 g, 8.18 mmol) was added at 55 °C in portions over 30 min. After 3 h at 55 °C, the reaction mixture was filtered through a pad of celite. The filtrate was concentrated and purified by silica gel column chromatography to give pentasaccharide (0.16 g, 0.068 mmol, 80 % yield): R_f = 0.41 (EtOAc/Hexane 2:3).

A solution of $[IrCOD(PPh_2Me)_2]PF_6$ (5 mg, 5.8 μmol) in THF (3 mL) was stirred under hydrogen at room temperature until the color turned from red to colorless to pale yellow. The hydrogen atmosphere was exchanged with Argon. This solution was then added to a flask containing solution of pentasaccharide (96 mg, 0.041 mmol) in THF. After stirring overnight, the solvent was removed and the residue was dissolved in a mixture of acetone (2.7 mL) and water (0.3 mL). Mercury (II) chloride (66.9 mg, 0.247 mmol) and mercury (II) oxide (2.0 mg, 9.2 μmol) were added. After 1 h, the reaction mixture was diluted with chloroform and washed with saturated $NaHCO_3$ (aq), dried over Na_2SO_4, filtered and concentrated to give the crude lactol **12**: R_f = 0.28 (EtOAc/Hexane 2:3).

2,3,4-Tri-*O*-benzyl-6-*O*-tri*iso*propylsilyl-α-D-mannopyranosyl-(1→2)-3,4,6-tri-*O*-benzyl-α-D-mannopyranosyl-(1→6)-3-*O*-benzyl-4-*O*-(2,3,4,6-tetra-*O*-benzyl-α-D-glucopyranosyl-(1→4)-3,6-di-*O*-benzyl-2-deoxy-2-acetamido-β-D-galactopyranosyl)-2-*O*-levulinyl-α-Dmannopyranosyl-(1→4)-2-azido-3,6-di-*O*-benzyl-2-deoxy-α-D-glucopyranosyl-(1→6)-1-*O*allyl-2,3,4,5-tetra-*O*-benzyl-D-*myo*-inositol (13)

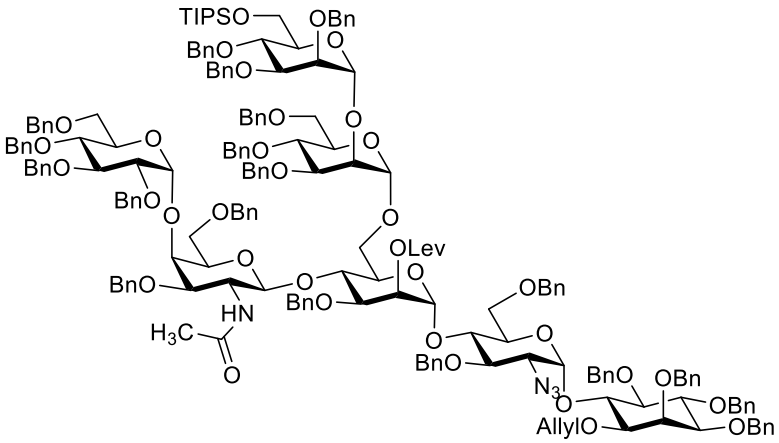

To a dichloromethane (3 mL) solution of the crude lactol (**12**), 2,2,2-trichloroacetonitrile (0.20 mL, 2.0 mmol) and DBU (2.6 μl, 0.017 mmol) were added. After 1 h, the solvent

was removed to give a brown oil that was purified by flash column chromatography to give glycosyl imidate (83 mg, 0.034 mmol, 83 % yield): R_f = 0.43 (EtOAc/Hexane 2:3).

A mixture of glycosyl imidate (83 mg, 0.034 mmol) and pseudodisaccharide **7** (32 mg, 0.034 mmol) were dissolved and co-evaporated three times with toluene and dried under high vacuum for 2 h. To a toluene solution (3 mL) of this mixture, molecular sieves (4Å, 50 mg) and TMSOTf (3 µL, 0.017 mmol) were added at -40 °C. After 1 h, triethylamine was added. The reaction mixture was filtered and concentrated to give a yellow oil that was purified by silica gel column chromatography to give pseudoheptasaccharide **13** (87 mg, 0.027 mmol, 80 % yield): R_f = 0.43 (EtOAc/Hexane 1:2); ESI-MS (*m*/*z*): $[M+2Na]^{2+}$ cald 1634.7427, obsd 1634.7484

2,3,4-Tri-*O*-benzyl-6-*O*-triisopropylsilyl-α-D-mannopyranosyl-(1→2)-3,4,6-tri-*O*-benzyl-α-D-mannopyranosyl-(1→6)-3-*O*-benzyl-4-*O*-(2,3,4,6-tetra-*O*-benzyl-α-D-glucopyranosyl-(1→4)-3,6-di-*O*-benzyl-2-deoxy-2-acetamido-β-D-galactopyranosyl)-2-*O*-levulinyl-α-D-mannopyranosyl-(1→4)-2-azido-3,6-di-*O*-benzyl-2-deoxy-α-D-glucopyranosyl-(1→6)-2,3,4,5-tetra-*O*- benzyl-D-*myo*-inositol (13a)

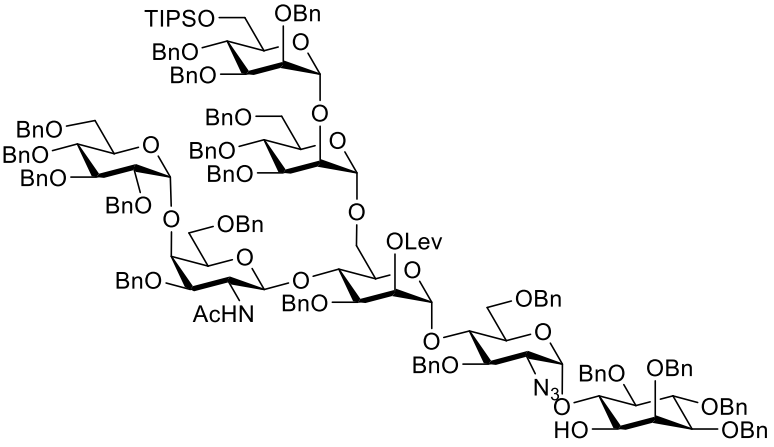

A solution of $[IrCOD(PPh_2Me)_2]PF_6$ (4.0 mg, 4.7 µmol) in THF (1 mL) was stirred under hydrogen until the color turned from red to colorless to pale yellow. The hydrogen atmosphere was exchanged with Argon. This solution was added to a THF (1 mL) solution of pseudoheptasaccharide **13** (80 mg, 0.025 mmol). After 16 h, the solvent was removed and the residue was dissolved in a mixture of acetone (2.7 mL) and water (0.3 mL). Mercury(II) chloride (40.4 mg, 0.149 mmol) and mercury(II) oxide (2.0 mg, 9.2 µmol) were added. After 1 h, saturated $NaHCO_3$ (aq) was added and the reaction mixture was extracted three times with dichloromethane. The combined organic layers were dried

over Na_2SO_4, filtered and concentrated. The crude product was purified by silica gel column chromatography to give pseudoheptasaccharide **13a** (75 mg, 0.024 mmol, 95 % yield) as colorless oil. R_f = 0.36 (EtOAc/Hexane 1:2). Spectral data was in agreement with the previous reported data.[88] ESI-MS (*m*/*z*): $[M+2Na]^{2+}$ cald 1614.7270, obsd 1614.7344; $[M+H]^+$ cald 3184.4829, obsd 3184.4836.

Triethylammonium (2,3,4-tri-*O*-benzyl-6-*O*-triisopropylsilyl-α-D-mannopyranosyl-(1→2)-3,4,6-tri-*O*-benzyl-α-D-mannopyranosyl-(1→6)-3-*O*-benzyl-4-*O*-(2,3,4,6-tetra-*O*-benzyl-α-D-glucopyranosyl-(1→4)-3,6-di-*O*-benzyl-2-deoxy-2-acetamido-β-D-galactopyranosyl)-2-*O*-levulinyl-α-D-mannopyranosyl-(1→4)-2-azido-3,6-di-*O*-benzyl-2-deoxy-α-D-glucopyranosyl-(1→6)-2,3,4,5-tetra-*O*-benzyl-1-*O*-(6-(benzylthio)hexylpho-sphonato)-D-*myo*-inositol (14)

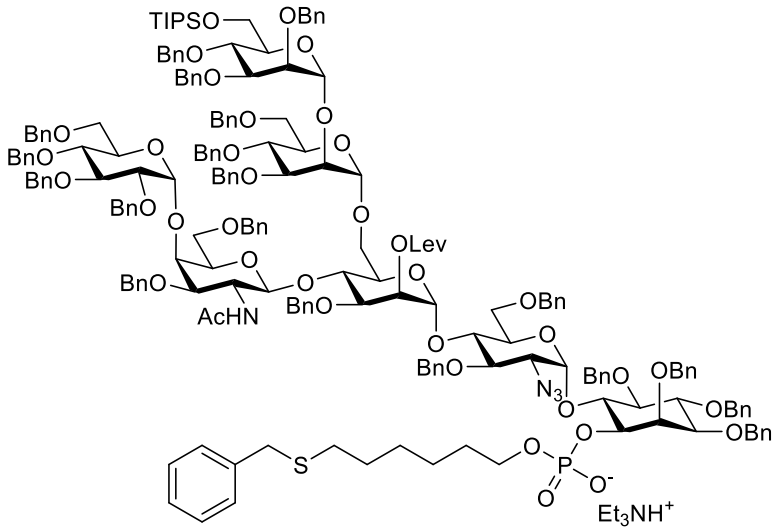

The alcohol **13a** (57 mg, 0.018 mmol) and H-phosphonate[146] **9** (51 mg, 0.179 mmol) were dissolved and dried by co-evaporation with dry pyridine (3 X 3 mL). The residue was dissolved in dry pyridine (2 mL) and PivCl (22 μL, 0.179 mmol) was added dropwise. The solution was stirred for 2 h at room temperature. Water (20 μL) and iodine (45 mg, 0.179 mmol) were added and the red solution of the reaction mixture was stirred for 1 h and reaction was quenched with sat. $Na_2S_2O_3$. The reaction mixture was diluted with chloroform (10 mL) and water content was dried using Na_2SO_4. Then, the reaction mixture was filtered and concentrated in *vacuo* and the residue was purified by using flash column chromatography on deactivated (with 1 % TEA in $CHCl_3$) silica gel by

using a gradient of MeOH in $CHCl_3$ from 0 % - >5 % MeOH. The phosphate **14** was obtained as yellow oil (54 mg, 0.016 mmol) in 87 % yield. R_f = 0.43 (MeOH/$CHCl_3$ = 1:20). Spectral data was in agreement with the previous reported data.[88]

Triethylammonium (2,3,4-tri-*O*-benzyl-α-D-mannopyranosyl-(1→2)-3,4,6-tri-*O*-benzyl-α-D-mannopyranosyl-(1→6)-3-*O*-benzyl-4-*O*-(2,3,4,6-tetra-*O*-benzyl-α-D-glucopyranosyl-(1→4)-3,6-di-*O*-benzyl-2-deoxy-2-acetamido-β-D-galactopyranosyl)-2-*O*-levulinyl-α-D-mannopyranosyl-(1→4)-2-azido-3,6-di-*O*-benzyl-2-deoxy-α-Dglucopyranosyl-(1→6)-2,3,4,5-tetra-*O*-benzyl-1-*O*-(6-(benzylthio)hexyl-phosphonato)-D-*myo*-inositol (14a)

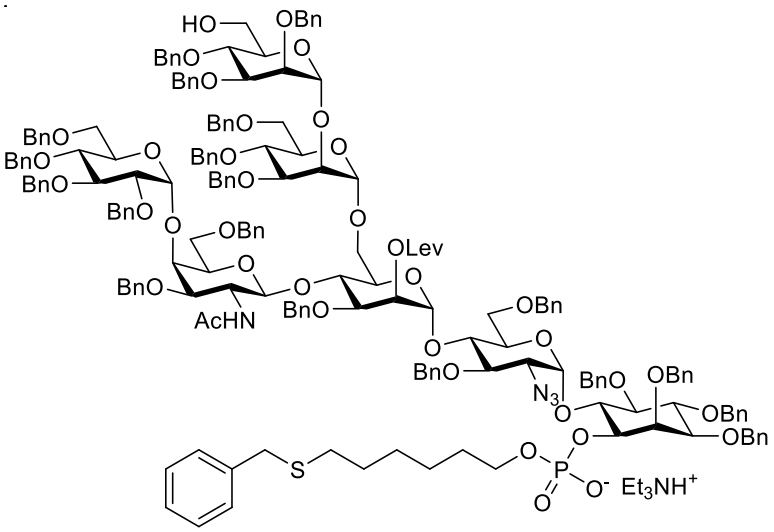

To a solution of phosphate **14** (54 mg, 0.016 mmol) in MeCN (2 mL), water (10 μL) and $Sc(OTf)_3$ (77 mg, 0.156 mmol) were added and this reaction mixture was heated up to 50 °C for 5 h. The reaction was quenched with pyridine (10μL) and the solvents were removed *in vacuo*. The residue was co-evaporated with toluene (3 x 2 mL) and purified through flash column chromatography on deactivated (with 1 % TEA in $CHCl_3$) silica gel (starting from $CHCl_3$/MeOH, 0 % - >5 % MeOH) to yield primary alcohol **14a** as a colorless oil (34 mg, 10.26 μmol, 65 %).

Triethylammonium 2-[(*N*-benzyloxycarbonyl)amino]ethyl H-phosphonate (8)

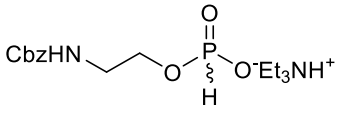

A mixture of benzyl (2-hydroxyethyl)carbamate (1.50 g, 7.68 mmol) and phosphonic acid (0.693 g, 8.45 mmol) were co-evaporated three times with pyridine. The mixture was dissolved in dry pyridine (30 mL) and PivCl (1.04 ml, 8.45 mmol) was added. After stirring overnight, the solvent was removed to give colorless oil that was purified by silica gel column chromatography to give a white solid (2 g, mixture of product and triethylammonium salts). The white residue was then dissolved in TEAB buffer, and extracted three times with 5% trifluoroethanol in chloroform. The combined organic layers were concentrated to give triethylammonium 2-[(N-benzyloxycarbonyl)amino]ethyl H-phosphonate **8** (1.66 g, 4.61 mmol, 60 % yield) as a colorless oil: R_f = 0.38 ($CHCl_3$/MeOH 3:1 with ~0.5 % NEt_3); ^{1}H NMR (600 MHz, $CDCl_3$) δ 12.45 (s, 1H, Et_3NH^+), 7.31 - 7.18 (m, 5H, Ph), 6.30 (br, 1H, NH), 6.26 (br, 1H, PH), 5.01 (s, 2H, -CH_2- of Cbz), 3.90 (m, 2H, -OCH_2-), 3.36 (dd, *J* = 9.5, 4.8 Hz, 2H, -NCH_2-), 2.92 (q, *J* = 7.2 Hz, 6H, -CH_2- of NEt_3), 1.20 (t, *J* = 7.2 Hz, 9H, Me of NEt_3); ^{13}C NMR (151 MHz, $CDCl_3$) δ 156.52 (carbonyl), 136.83, 128.39, 128.13, 127.92, 66.40 (-CH_2- of Cbz), 62.34 (-OCH_2-), 45.39 (-CH_2- of NEt_3), 42.34 (-NCH_2-), 8.44 (Me of NEt_3); ^{31}P NMR (242.9 MHz, $CDCl_3$) δ 5.66; ESI-MS (*m*/*z*): $[M-H]^-$ cald 258.0537, obsd 258.0538.

Bistriethylammonium(2,3,4-tri-*O*-benzyl-6-*O*-(2-(N-benzyloxycarbonyl)aminoethyl phosphonato)-α-D-mannopyranosyl-(1→2)-3,4,6-tri-*O*-benzyl-α-D-mannopyranosyl-(1→6)-3-*O*-benzyl-4-*O*-(2,3,4,6-tetra-*O*-benzyl-α-D-glucopyranosyl-(1→4)-3,6-di-*O*-benzyl-2-deoxy-2-acetamido-β-D-galactopyranosyl)-α-D-mannopyranosyl-(1→4)-2-azido-3,6-di-*O*-benzyl-2-deoxy-α-D-glucopyranosyl-(1→6)-2,3,4,5-tetra-*O*-benzyl-1-*O*-(6-(benzylthio)hexyl-phosphonato)-D-*myo*-inositol (15)

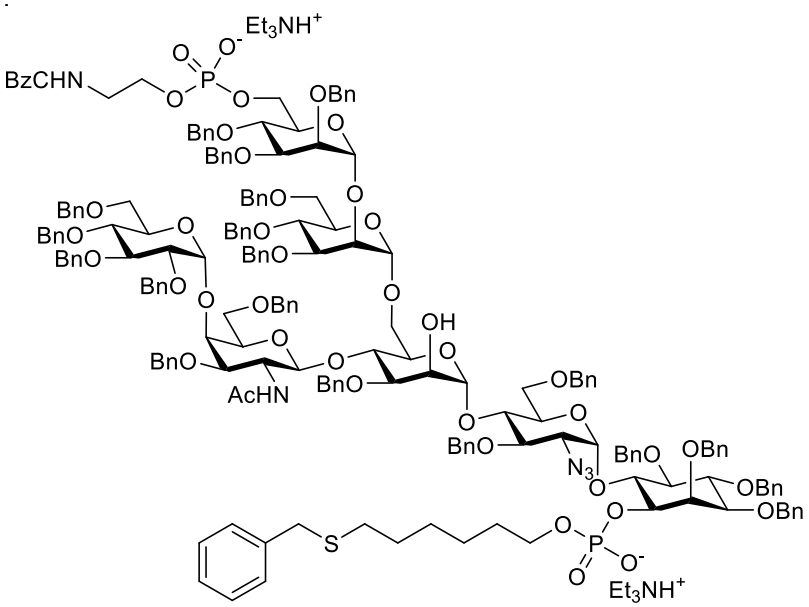

The alcohol **14a** (34 mg, 0.010 mmol) and H-phosphonate **8** (25.5 mg, 0.106 mmol) were dissolved and dried by co-evaporation with dry pyridine (3 x 3 mL). The residue was dissolved in dry pyridine (2 mL) and PivCl (13 µL, 0.106 mmol) was added. The solution was stirred for 2 h at room temperature. Water (15 µL) and iodine (27 mg, 0.106 mmol) were added and the red solution was stirred for 1 h and with sat. $Na_2S_2O_3$. The reaction mixture was diluted with chloroform (10 mL) and dried over Na_2SO_4. The reaction mixture was filtered and concentrated in *vacuo*. The crude residue (30 mg, 8.44 µmol) was dissolved in a mixture of dichloromethane 91 mL), pyridine (40 µL) and acetic acid (20 µL) before hydrazine (20 µL) was added. The reaction mixture was stirred for 14 h. The solvents were removed in *vacuo* and the product was purified by using flash column chromatography on deactivated (with 1 % TEA in $CHCl_3$) silica gel by using a gradient of MeOH in $CHCl_3$ from 0 % - >10 % MeOH. The bisphosphate **15** was obtained as yellow oil (15 mg, 4.34 µmol) in 51 % yield. MALDI-MS (*m*/*z*): $[M+NH_3]^+$ cald 3471.4454, obsd 3471.4911.

6-*O*-Aminoethylphosphonato-α-D-mannopyranosyl-(1→2)-α-D-mannopyranosyl-(1→6)-4-*O*-(α-D-glucopyranosyl-(1→4)-2-deoxy-2-acetamido-β-D-galactopyranosyl)-α D-mannopyranosyl-(1→4)-2-amino-2-deoxy-α-D-glucopyranosyl-(1→6)-1-*O*-(thiohexylphosphonato)-D-*myo*-inositol (GPI 1)

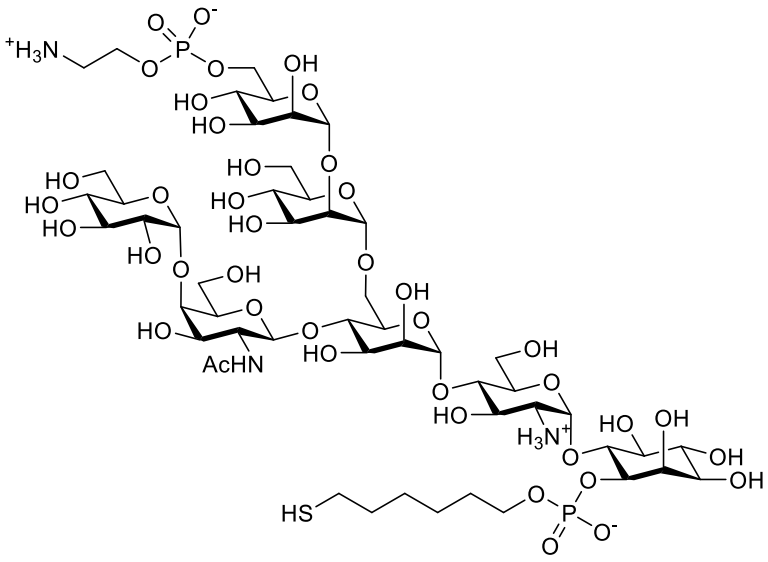

The bisphosphate **15** (10 mg, 2.89 µmol) was dissolved in dry THF (2 mL) and *tert*-butanol (2 drops). The solution was cooled down to -78 °C and approximately 10 mL ammonia was condensed in the flask. Afterwards small fresh cut pieces of sodium were added till a dark blue color was established. The reaction was stirred for 35 min at -78 °C. The reaction was quenched with MeOH (2 mL) and ammonia was blown off using a stream of nitrogen. The solution was adjusted to pH 7 with concentrated acetic acid. The water was removed by freeze drying and the residue was purified using a Sephadex® super fine G-25 (GE Healthcare) column (1 cm x 20 cm) to yield GPI **1** as disulfide, white solid (3 mg, 1.0 µmol, 35 %). ^{31}P NMR (162 MHz, D_2O) δ 0.40, 0.22; ESI-MS (*m*/*z*): $[2M-2H]^{2-}$ cald 1569.4697, obsd 1569.4454.

5.2.2 Synthesis of the cross-linker for the modification of MagPlex beads

3-(2,5-Dioxo-2,5-dihydro-pyrrol-1-yl)-propylammonium trifluoroacetate (16)

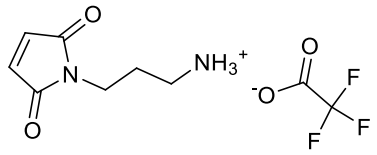

In a 250 mL round bottomed flask, N-(t-butoxycarbonyl)propanolamine (3.17 mL, 18.54 mmol) and diisopropyl azodicarboxylate (4.37 mL, 22.46 mmol) were added to a solution of maleimide (2.0 g, 20.6 mmol) and PPh_3 (5.3 g, 20.19 mmol) in THF (100 mL). The solution was stirred at room temperature for 48 h, concentrated and purified by

column chromatography using silica gel (4:1 to 2:1 hexanes/EtOAc) to yield a mixture of the N-Boc protected product and diisopropyl hydrazinedicarboxylate. Then, the reaction mixture was dissolved in a solution of CH_2Cl_2 (15 mL) and H_2O (1 mL), and trifluoroacetic acid (TFA, 3.5 mL) was added. The reaction was stirred for 5 h at room temperature and diluted with CH_2Cl_2 (50 mL) and H_2O (50 mL). The aqueous layer was washed with CH_2Cl_2 (3 x 50 mL) and the combined aqueous layer was concentrated to yield the desired product **16** as yellow oil (3 g, 94 %). IR: 3435, 2959, 2917, 2849, 1707, 1683 cm^{-1}. ^1H NMR (DMSO-d_6, 400 MHz): δ 1.85-1.65 (app m, 2H), 2.87-2.86 (m, 2H), 3.46 (t, 2H, J=6.8 Hz), 7.03 (s, 2H), 7.81 (br s, 3H). ^{13}C NMR (DMSO-d_6, 100 MHz): δ 26.5, 34.5, 36.7, 115.9 (q, 289.0 Hz), 134.6, 158.5 (q, J=36.0 Hz), 171.2. ESI-MS (*m*/*z*): $[M+H]^+$ cald 155.0821, obsd 155.0824.

5.2.3 Experiments for the Luminex-based Assay

5.2.3.1 General Materials

The Carboxy- group functionalized Magplex magnetic microspheres were obtained from the Luminex Corporation and were analyzed using a Bio-Plex 200 system from Bio-Rad. Phosphate buffered saline (PBS), Bovine Serum Albumin (BSA), Human Serum Albumin (HSA) Tween-20, Triton-X100 and Sodium azide (NaN_3) were purchased from Sigma-Aldrich. 1-Ethyl-3-[3-dimethylaminopropyl]carbodiimide hydrochloride (EDC-HCl), N-hydroxysulfosuccinimide (Sulfo-NHS) and Streptavidin-phycoerythrin(SAPE) were ordered from Thermo Fisher Scientific. Affinity pure Goat Anti-Human IgG(H+L), Biotin-SP conjugated Affinity Pure Goat Anti-Human IgG (H+L), R-Phycoerythrin conjugated Affinity Pure Goat Anti-Human IgG (Fc Fragment specific) from Jackson Immunoresearch Laboratories were ordered from Dianova.

The Serum samples used in this study were from Robert Koch Institute, Berlin, Germany.

5.2.3.2 Modification of MagPlex microsphere with Maleimide

In order to keep the amine groups of GPIs unmodified, a thiol group was installed at the *O*-1 position of *myo*-inositol instead of naturally occurring lipid moiety for the conjugation to the beads. To make the carboxy- group functionalized MagPlex magnetic microspheres suitable for the conjugation with the thiol-linker of GPIs, the surface of the microspheres was modified with maleimide groups. The maleimide (**16**) groups were

installed to the surface of carboxy-beads using the method described in the Luminex cookbook, A permanent magnet was used as a magnetic separator during the washing steps. The microspheres were handled in absence of light during all the steps of the procedure. 100 µL (approx. 1.25 x 10^6 Beads) of the carboxylated microspheres stock suspension were transferred to a microcentrifuge tube, were pellet down using the permanent magnet and the supernatant was removed. The microspheres were resuspended in 0.1 M 2-(N-morpholino)ethanesulfonic acid (MES) buffer pH-6.0, vortexed, sonicated for appr. 20 sec and pellet by using the magnet. After aspirating the supernatant, the microspheres were resuspended in 100 µL of maleimide (1mg/mL in 0.1 M MES, pH-6.0) followed by the addition of 50 µL of a 10 mg/mL EDC (freshly prepared in 0.1 M MES, pH-6.0) solution and mixed. The microspheres were incubated for 1-2 h under continuous mixing by rotation at room temperature. The reaction was quenched by adding 250 µL of 0.1M MES, pH-4.5 and mixing. The beads were pellet using the magnet and the supernatant was removed. The maleimide coupled microspheres were washed twice with 250 µL of 0.1 M MES, pH-4.5. Finally, the microspheres were resuspended in 250 µL of 0.1 M MES, pH-4.5 and stored in the refrigerator at 4 °C in the dark or used right away for the coupling to the thiol linked **GPI 1** and the trimannoside **23.**

5.2.3.3 Coupling of Thiol linked GPIs/Trimannoside to the maleimide-modified MagPlex beads

The 0.1 M MES buffer was removed from the maleimide-modified microspheres by using the magnetic separator. The 1.25 x 10^6 microspheres were washed with 0.1 M Sodium phosphate, 50 mM NaCl, pH-7.0 and resuspended in 100 µL of 0.1 M sodium phosphate buffer. 25 µg of the reduced thiol-containing molecule (either GPI **1** or trimannoside **23**) in 100 mM Tris, pH-7.4 was added to 1.25 x 10^6 beads and the final volume was adjusted to 250 µL with 100 mM Tris buffer pH-7.4. The reaction mixture was incubated at room temperature for 1 h in darkness. After 1h, the microspheres were pelleted and the supernatant was removed. Then, the unreacted maleimide groups on the beads were quenched by adding 100 µL of 50 mM L-cysteine hydrochloride in 100 mM Tris buffer pH-7.4. After 1h, the microspheres were removed from the supernatant using magnetic separator, washed twice with 100 µL of PBS containing 1 % BSA and stored in 250 µL of PBS-TBN buffer at 4 °C.

5.2.3.4 Coupling of Anti-Human IgG (Positive control) and Human serum albumin (HSA) to the MagPlex beads

The coupling of the carboxy-functionalized microspheres with either Anti-Human IgG, which was used as a positive control or Human Serum Albumin (HSA), which was used as a negative control in this study was performed using activation of the carboxylate with EDC-sulfo NHS and following reaction with the proteins. 1.5 x 10^6 Microspheres were transferred to the microcentrifuge tube, washed with 100 µL of water, resuspended in 80 µL of 100 mM monobasic sodium phosphate buffer pH-6.2, mixed by vortexing and sonication for 20 sec. Sulfo-NHS (10 µL of 50 mg/mL) and EDC (10 µL of 50 mg/mL) were added and the reaction mixture was incubated for 40 min at room temperature in darkness and gentle mixing. The microspheres were separated from the solution using the magnet, resuspended in 100 µL of 50 mM MES pH-5.0 buffer, and washed twice with the same buffer. The activated microspheres were resuspended in 100 µL of 50 mM MES buffer by vortex and sonication for 20 sec and 25 µg of the corresponding protein (HSA or IgG) were added to the microspheres slurry. The total volume was set up to 250 µL with 50 mM MES buffer and the reaction mixture was incubated for 3-4 h under mixing by rotation at room temperature. The microspheres were separated and washed three times using 250 µL of the PBS-TBN buffer and finally stored in 500 µL of the same buffer at 4 °C.

5.2.3.5 MagPlex Immunoassay

The immunoassays were performed in Greiner 96 well plates recommended by Luminex. 50 µL of stabilguard (stabilizer to maintain the stability of the proteins) and 50 µL of each microsphere suspension containing 50 beads/µL in PBS + 0.25 % Triton X100 + 300 mM NaCl) of containing the GPI **1** (020), Trimannoside **23** (042), Anti-Human IgG (033) and HSA (007) were added per well. After approx. 40 min incubation at room temperature or overnight at 4 °C, 50 µL of diluted sera (1:100 dilution in PBS + 0.25 % Triton X100 + 300 mM NaCl) were added to the appropriate well. Each sera was analyzed in duplicate. The plate was incubated for 1 h at room temperature by constant vortexing. After that, the beads were washed using magnetic plate washer. To detected the captured antibodies from the serum samples, 100 µL of directly coupled secondary antibody R-Phycoerythrin AffinityPure Goat Anti-Human IgG, Fcγ Fragment Specific (1.5 µg/mL working concentration in PBS + 0.25 % Triton X100 + 300 mM NaCl, code:

109-115-098) were added. After 50 min, the beads were washed using the magnetic plate washer (From TECAN), resuspended in 125 µL/well of PBS + 0.25 % Triton X100 + 300 mM NaCl and analyzed using the Bip-Plex 200 systems analyzer. The mean fluorescence intensity (MFI) values for each sample and for each microsphere in each well were determined using the Bio-Plex Manager 6.1 software. For further analysis, the MFI values were used after subtracting the blank MFI (control beads, no serum sample was added). Receiver operating characteristic (ROC) curves were used to show the performance of the assay.

5.3 Experiment to Chapter 3

5.3.1 Synthesis of protected Chelating Linker:

Tetraethyl-2,2',2'',2'''-(1,2-phenylenebis(azanetriyl))tetraacetate (30)

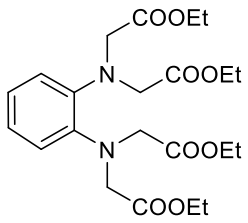

In a 250 mL round bottomed flask a solution of ethylbromoacetate (3.09 mL, 27.7 mmol) was added to a solution of ortho-phenylenediamine (0.500 g, 4.62 mmol) and diisopropylethylamine (4.85 mL, 27.7 mmol) in Acetonitrile (40 mL). The mixture was heated to 60 °C and stirred; the reaction progress was monitored by using mass spectrometry (ESI-MS). After 46 h, the solvent was evaporated under reduced pressure, the residue was dissolved in hexane (100 mL) and stirred vigorously while refluxing for 1 h. Then the solution was filtered, the solvent was evaporated under reduced pressure, phosphate buffer (0.1M, pH-2.0, 50 mL) was added, and the compound was extracted using dichloromethane, dried over Na_2SO_4, filtered and concentrated. The residue was purified by silica gel column chromatography (hexane/EtOAc = 8:2) to give the tetraester **30** (1.778g, 85 %). ^{1}H NMR (400 MHz, $CDCl_3$) δ 7.03 (dd, *J* = 5.9, 3.6 Hz, 1H), 6.93 (dd, *J* = 6.1, 3.5 Hz, 1H), 4.29 (s, 8H), 4.09 (q, *J* = 7.2 Hz, 8H), 1.18 (t, *J* = 7.1 Hz, 12H). ^{13}C NMR (101 MHz, $CDCl_3$) δ 171.1, 141.5, 123.2, 121.5, 60.6, 52.5, 14.2. ESI-MS (*m*/*z*): $[M+Na]^+$ cald 475.2051, obsd: 475.2.

Tetraethyl-2,2',2'',2'''-(4-bromo-1,2-phenylenebis(azanetriyl))tetraacetate (31)

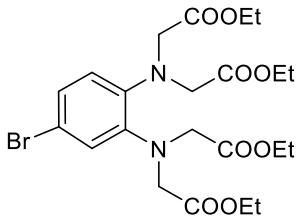

Oxone (2.405 g, 3.91 mmol) was added to a solution of tetraester **30** (1.77g, 3.91 mmol) and KBr (0.452 g, 3.79 mmol) in a dry methanol (15 mL), and the reaction mixture was stirred at room temperature for 24 h. The reaction mixture was filtered through a celite

pad and the solvent was removed under reduced pressure. The remaining was dissolved in DCM and filtered through pad containing a layer of 2.5 cm of silica gel over a layer of 1 cm of celite. The filtrate was concentrated to give the bromide **31** (1.5g, 75 %). ^{1}H NMR (400 MHz, $CDCl_3$) δ 7.13 (d, *J* = 2.2 Hz, 1H), 7.07 – 7.02 (m, 1H), 6.91 (d, *J* = 8.6 Hz, 1H), 4.27 (s, 4H), 4.25 (s, 4H), 4.16 – 4.06 (m, 8H), 1.24 – 1.15 (m, 12H). ^{13}C NMR (101 MHz, $CDCl_3$) δ 170.8, 170.7, 142.9, 140.6, 126.0, 124.8, 123.0, 115.9, 60.8, 52.4, 52.3, 14.3. ESI-MS (*m*/*z*): $[M+Na]^+$ cald 553.1156, obsd 553.0.

3,4-bis(bis(2-ethoxy-2-oxoethyl)amino)benzoic acid (27)

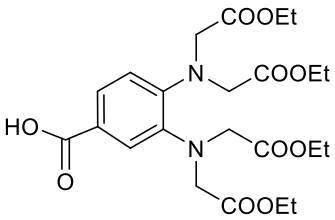

To a stirred solution of bromide **31** (0.350 g, 0.659 mmol) in DCM (10 mL), oven dried lithium formate (0.305g, 5.86 mmol) and $PdCl_2$(dppf) (0.048 g, 0.0659 mmol) were added in an argon atmosphere. After that argon gas was bubbled through the solution for 25 minutes. Acetic anhydride (0.373 mL, 3.95 mmol) and DIPEA (0.690 mL, 3.95 mmol) were added to the reaction mixture and the reaction was stirred at 120 °C in a sealed flask. The progress of the reaction was monitored using mass spectrometry and TLC. After 46 h, the reaction mixture was cooled down to room temperature, diluted with EtOAc (50 mL) and the organic layer was extracted with 2M HCl. The organic phase was dried over anhy. Na_2SO_4, filtered and concentrated. The residue was purified using silica gel column chromatography with 0.01 % of formic acid as a eluent to give the product **27** (0.169 g, 51 %). ^{1}H NMR (400 MHz, $CDCl_3$) δ 7.80 (d, *J* = 1.9 Hz, 1H), 7.74 – 7.67 (m, 1H), 7.03 (d, *J* = 8.5 Hz, 1H), 4.40 (s, 4H), 4.27 (s, 4H), 4.17 – 4.05 (m, 8H), 1.27 – 1.13 (m, 12H). ^{13}C NMR (101 MHz, $CDCl_3$) δ 171.5, 170.6, 170.5, 146.6, 140.5, 125.8, 124.0, 123.1, 120.4, 60.8, 60.7, 52.2, 52.1, 14.1. ESI-MS (*m*/*z*): $[M+Na]^+$ cald 519.1949, obsd 519.2.

5.3.2 Synthesis of tagged Disaccharide (Manα1→6Man):

2-Methyl-5-tert-butylphenyl 2,3,4,6-tetra-*O*-acetyl-1-thio-α-D-mannopyranoside (33)

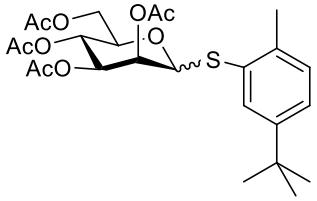

To a solution of peracetylated D-mannose **32** (10 g, 25.6 mmol) in DCM (50 mL), 2-methyl-5-*tert*butyl- thiophenol (5.84 mL, 31,8 mmol) and tin tetrachloride (2.099 mL, 17.93 mmol) were added sequentially with stirring. After 3 h, the reaction was quenched by the addition of 1 M NaOH, diluted with 100 mL of CH_2Cl_2 and extracted one time with 1 M NaOH and two times with water. The combined organic layer was dried over $MgSO_4$, filtered and concentrated. The obtained residue was purified by silica gel column chromatography (Hexane / EtOAc = 2:1) to give thioglycoside **33** (9.8 g, 75% yield) as a colorless syrup: R_f = 0.62 (hexane/EtOAc 1:1); ^{1}H NMR (400 MHz, $CDCl_3$) δ 7.52 (d, *J* = 2.1 Hz, 1H), 7.24 – 7.20 (m, 1H), 7.14 (s, 1H), 5.54 – 5.51 (m, 1H), 5.42 (d, *J* = 1.6 Hz, 1H), 5.36 (d, *J* = 6.7 Hz, 2H), 4.52 (dd, *J* = 4.8, 2.0 Hz, 1H), 4.34 (dd, *J* = 12.4, 5.0 Hz, 1H), 4.10 – 4.04 (m, 1H), 2.40 (s, 3H), 2.16 (s, 3H), 2.07 (s, 3H), 2.05 (s, 3H), 2.02 (s, 3H), 1.29 (s, 9H). ^{13}C NMR (101 MHz, $CDCl_3$) δ 170.7, 170.1, 170.0, 169.8, 150.1, 136.9, 131.8, 130.3, 129.8, 125.5, 86, 71.5, 70.0, 69.5, 66.3, 62.5, 34.3, 31.5, 31.4, 21.1, 20.9, 20.8, 20.4; ESI-MS (*m*/*z*): $[M+Na]^+$ cald 533.1821, obsd 533.2.

2-Methyl-5-tert-butylphenyl-1-thio-α-D-mannopyranoside (33a)

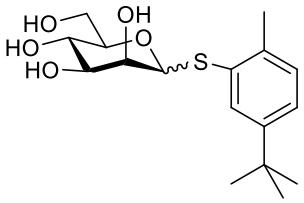

To a solution of peracetylated thioglycoside **33** (9.8 g, 19.27 mmol) was added freshly prepared sodium methoxide solution, the pH of the reaction mixture was kept over 9.0. After that reaction progress was monitored by TLC. After 30 min, the reaction mixture was neutralized with Amberlite IR120 resin (H^+-form), filtered and evaporated the solvent on rotavapour to obtain the pure product **33a** (6.5 g, 98 %). ^{1}H NMR (400 MHz, CD_3OD) δ 7.60 (d, *J* = 2.1 Hz, 1H), 7.22 (dd, *J* = 8.0, 2.1 Hz, 1H), 7.13 (d, *J* = 8.0 Hz, 1H), 5.33 (d, *J* = 1.5 Hz, 1H), 4.11 (dd, *J* = 2.8, 1.7 Hz, 1H), 4.07 – 3.98 (m, 1H), 3.76 (dt, *J* = 4.2, 2.8 Hz, 3H), 3.30 (dt, *J* = 3.3, 1.6 Hz, 1H), 2.38 (s, 3H), 1.28 (s, 9H). ^{13}C NMR (101 MHz, CD_3OD) δ 150.9, 138.0, 134.3, 131.4, 131.0, 126.0, 90.4, 75.7, 74.1,

73.2, 68.5, 62.5, 49.6, 49.4, 49.2, 49.0, 48.8, 48.6, 48.4, 35.3, 31.7, 31.7, 20.5. ESI-MS (*m*/*z*): $[M+Na]^+$ cald 365.1393, obsd 365.2.

2-Methyl-5-tert-butylphenyl-6-*O*-tert-butyldiphenylsilyl-1-thio-α-D-mannopyranoside (34)

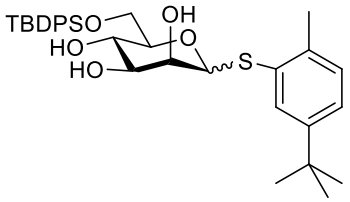

To a stirred solution of **33a** (5.426 g, 15.84 mmol) in DMF (50 mL), imidazole (1.888 g, 27.7 mmol) and TBDPSCl (4.90 mL, 19.01 mmol) were added subsequently. The reaction mixture was stirred at room temperature for 1 h and then heated to 50 °C. After 3 h, the solvent was evaporated under reduced pressure. The residue was dissolved in DCM (100 mL) and the resulting solution was washed with water and then dried over sodium sulfate, filtered and concentrated. The residue was purified through silica gel column chromatography (Hexane/EtOAc = 3:1) to afford thioglycoside **34** (7.88 g, 86 % yield) as a white foam. ^{1}H NMR (400 MHz, $CDCl_3$) δ 7.68 – 7.63 (m, 4H), 7.47 (d, *J* = 2.0 Hz, 1H), 7.44 – 7.33 (m, 6H), 7.17 (dd, *J* = 8.0, 2.0 Hz, 1H), 7.10 (d, *J* = 8.0 Hz, 1H), 5.45 (d, *J* = 0.9 Hz, 1H), 4.25 (dd, *J* = 3.2, 1.4 Hz, 1H), 4.24 – 4.16 (m, 1H), 4.05 (t, *J* = 9.2 Hz, 1H), 3.96 (d, *J* = 3.3 Hz, 1H), 3.93 (dd, *J* = 6.2, 4.1 Hz, 1H), 3.88 (dd, *J* = 10.5, 6.3 Hz, 1H), 2.34 (s, 1H), 1.20 (s, 9H), 1.06 (s, 9H). ^{13}C NMR (101 MHz, $CDCl_3$) δ 149.8, 136.5, 135.7, 135.6, 132.9, 132.6, 130.1, 130.1, 130.0, 129.4, 128.0, 128.0, 124.9, 87.8, 72.3, 72.2, 71.3, 71.2, 65.5, 34.5, 31.4, 27.0, 20.4, 19.3. LC-MS (*m*/*z*): $[M+Na]^+$ cald 603.2571, obsd 603.1.

2-Methyl-5-tert-butylphenyl-2,3-isopropylidene-6-*O*-tert-butyldiphenylsilyl-1-thio-α-D-mannopyranoside (35)

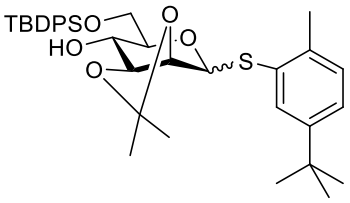

To a solution of triol **34** (6.423 g, 11.06 mmol) in 2,2-dimethoxypropane (50 mL),camphor sulphonic acid (CSA) (0.257 g, 1.106 mmol) was added. The reaction progress was monitored using TLC and the reaction mixture was neutralized by using 25 % ammonia solution after 2 h and the solvent was evaporated. The residue was dissolved

in EtOAc and washed successively with saturated $NaHCO_3$ (aq), water and brine. The organic phase was dried over $MgSO_4$, filtered and evaporated. The obtained residue was purified by silica gel column chromatography (hexane / EtOAc = 9:1) to give 2,3-*O*-*iso*-propylidene **35** (6.79 g, 95 % yield) as a white foam. ^{1}H NMR (400 MHz, $CDCl_3$) δ 7.65 – 7.59 (m, 4H), 7.46 (d, *J* = 2.0 Hz, 1H), 7.42 – 7.38 (m, 2H), 7.37 – 7.29 (m, 4H), 7.16 (dd, *J* = 8.0, 2.0 Hz, 1H), 7.10 (d, *J* = 8.0 Hz, 1H), 5.74 (s, 1H), 4.39 (dd, *J* = 5.6, 0.9 Hz, 1H), 4.26 – 4.19 (m, 1H), 4.10 – 3.96 (m, 2H), 3.89 (dd, *J* = 10.7, 3.7 Hz, 1H), 3.76 (dd, *J* = 10.7, 5.2 Hz, 1H), 2.34 (s, 3H), 1.56 (s, 3H), 1.40 (s, 3H), 1.18 (s, 9H), 1.03 (s, 9H). ^{13}C NMR (101 MHz, $CDCl_3$) δ 149.7, 136.6, 135.7, 135.6, 132.0, 130.1, 130.1, 130.0, 129.6, 128.0, 127.9, 124.9, 109.9, 83.5, 78.1, 76.5, 71.9, 69.8, 64.8, 34.5, 31.38, 28.3, 26.9, 26.6, 20.3, 19.3. LC-MS (*m*/*z*): $[M+Na]^+$ cald 643.2884, obsd 643.2.

2-Methyl-5-tert-butylphenyl-2,3-*O*-*iso*-propylidene-4-*O*-(2-naphthylmethyl)-6-*O*-tert-butyldiphenylsilyl-1-thio-α-D-mannopyranoside (35a)

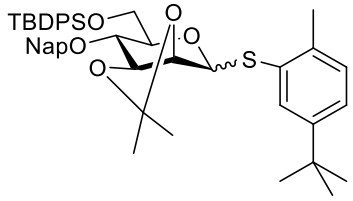

To a solution of *iso*-propylidene **35** (6. 7 g, 10.79 mmol) in DMF (70 mL) at 0 °C, NaH (518 mg, 12.95 mmol) was added followed by the addition of naphthyl bromide (NapBr) (3.34 g, 15.11mmol). The reaction mixture was warmed up to room temperature, after stirring for 2 h the reaction mixture was cooled down to 0 °C, quenched by the addition of H_2O dropwise and the solvent was evaporated using rotavapour. Then, the residue was extracted using ethylacetate two times. The combined organic layer was dried over anhy. Na_2SO_4, filtered and concentrated. The residue was purified using silica gel column chromatography to give thioglycoside **35a** (7.5 g, 75 %). ^{1}H NMR (400 MHz, $CDCl_3$) δ 7.87 – 7.74 (m, 4H), 7.63 (ddd, *J* = 8.1, 4.7, 1.0 Hz, 4H), 7.51 – 7.40 (m, 4H), 7.40 – 7.29 (m, 2H), 7.29 – 7.16 (m, 5H), 7.13 (d, *J* = 8.0 Hz, 1H), 5.85 (s, 1H), 5.15 (d, *J* = 11.3 Hz, 1H), 4.84 (d, *J* = 11.3 Hz, 1H), 4.56 – 4.41 (m, 2H), 4.20 – 4.00 (m, 3H), 3.78 (d, *J* = 10.8 Hz, 1H), 2.39 (s, 3H), 1.62 (s, 3H), 1.46 (s, 3H), 1.19 (s, 9H), 1.01 (s, 9H). ^{13}C NMR (101 MHz, $CDCl_3$) δ 149.7, 136.9, 136.0, 135.9, 135.6, 133.9, 133.4, 133.1, 133.1, 131.9, 130.2, 130.0, 129.6, 129.5, 128.2, 128.1, 127.8, 127.7, 127.6, 126.7, 126.2, 126.1, 125.9,

125.1, 109.7, 83.7, 79.0, 77.0, 75.7, 73.7, 71.2, 62.7, 34.5, 31.4, 28.2, 26.9, 26.9, 20.4, 19.5. LC-MS (*m*/*z*): $[M+H_2O]^+$ cald 778.3718, obsd 778.3.

2-Methyl-5-tert-butylphenyl-4-*O*-(2-naphthylmethyl)-6-*O*-tert-butyldiphenylsilyl-1-thio- α-D-mannopyranoside (36)

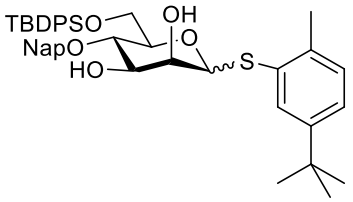

To a solution of *iso*-propylidene **35a** (5.7 g, 7.79 mmol) in chloroform (40 mL), acetic acid (80 %, 160 mL) was added. The solution was heated to 65 °C and the reaction progress was monitored with thin layer chromatography. After 5 h, the solvent was evaporated under reduced pressure and the residue was purified using silica gel column chromatography to obtain diol **36** (3.8 g, 70 %). ^{1}H NMR (400 MHz, $CDCl_3$) δ 7.86 – 7.76 (m, 3H), 7.73 (s, 1H), 7.70 – 7.64 (m, 4H), 7.49 (dd, *J* = 5.8, 3.6 Hz, 3H), 7.43 – 7.34 (m, 3H), 7.32 – 7.24 (m, 4H), 7.19 (d, *J* = 2.0 Hz, 1H), 7.12 (d, *J* = 8.0 Hz, 1H), 5.49 (d, *J* = 1.6 Hz, 1H), 4.96 (dd, *J* = 37.2, 11.4 Hz, 1H), 4.26 – 4.05 (m, 5H), 3.94 (d, *J* = 1.4 Hz, 1H), 2.34 (s, 3H), 1.22 (s, 9H), 1.08 (s, 9H). ^{13}C NMR (101 MHz, $CDCl_3$) δ 149.8, 136.6, 135.9, 135.8, 135.7, 133.6, 133.4, 133.2, 132.9, 130.1, 129.8, 129.7, 129.4, 128.6, 128.1, 127.8, 127.7, 126.8, 126.3, 126.1, 125.9, 124.9, 87.8, 75.9, 75.1, 73.6, 73.1, 72.4, 63.0, 34.5, 31.4, 27.1, 20.4, 19.6. LC-MS (*m*/*z*): $[M+Na]^+$ cald 743.3197, obsd 743.3.

2,3-di-*O*-acetyl-2-Methyl-5-tert-butylphenyl-4-*O*-(2-naphthylmethyl)-6-*O*-tert-butyldiphenylsilyl-1-thio-α-D-mannopyranoside (36a)

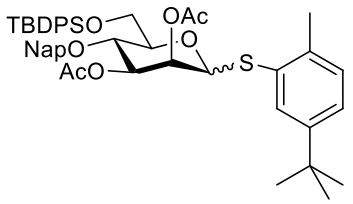

To a stirred solution of diol **36** (1.0 g, 1.47 mmol) in pyridine (3 mL), acetic anhydride (app. 1.5 mL) was added at 0 °C. The reaction mixture was stirred for 2 h. The solvent was evaporated on the rotavapour and the residue was purified using silica gel column chromatography to obtain compound **36a** (1.14 g, 96 %). ^{1}H NMR (400 MHz, $CDCl_3$) δ 7.88 – 7.75 (m, 3H), 7.68 (dd, *J* = 4.3, 3.7 Hz, 5H), 7.52 – 7.44 (m, 3H), 7.42 – 7.22 (m,

7H), 7.20 (dd, *J* = 8.0, 2.0 Hz, 1H), 7.13 (d, *J* = 8.0 Hz, 1H), 5.56 (dd, *J* = 3.0, 1.8 Hz, 1H), 5.47 (dd, *J* = 9.8, 3.2 Hz, 1H), 5.42 (d, *J* = 1.6 Hz, 1H), 4.90 (q, *J* = 11.5 Hz, 2H), 4.44 (t, *J* = 9.7 Hz, 1H), 4.28 (d, *J* = 9.5 Hz, 1H), 4.18 (dd, *J* = 11.5, 2.4 Hz, 1H), 3.95 – 3.86 (m, 1H), 2.38 (s, 3H), 2.15 (s, 3H), 1.99 (s, 3H), 1.21 (s, 9H), 1.12 (s, 9H). ^{13}C NMR (101 MHz, $CDCl_3$) δ 170.2, 170.1, 149.8, 137.1, 136.0, 135.8, 135.6, 133.9, 133.4, 133.1, 132.9, 132.6, 130.1, 130.1, 129.8, 129.8, 128.3, 128.0, 127.8, 127.8, 127.7, 126.3, 126.2, 126.1, 125.6, 125.2, 85.8, 75.3, 73.9, 73.1, 72.4, 72.3, 62.6, 34.5, 31.4, 27.0, 21.1, 21.1, 20.6, 19.7. LC-MS (*m*/*z*): $[M+Na]^+$ cald 827.3408, obsd 827.3.

2,3-di-*O*-acetyl-2-Methyl-5-tert-butylphenyl-4-*O*-(2-naphthylmethyl)-1-thio-α-D-mannopyranoside (37)

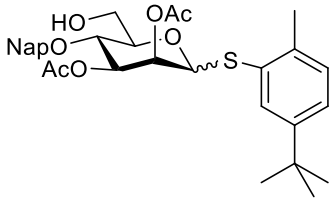

To a solution of silylether **36a** (1.1 g, 1.416 mmol) in THF (6 mL), a solution of HF-pyridine (800 μL) was added and the reaction mixture was stirred at room temperature. After 24 h, the reaction was quenched by using saturated sodium bicarbonate and extracted twice by using dichloromethane. The combined organic layer was dried over anh. Na_2SO_4, filtered and concentrated. The residue was purified using silica gel column chromatography to obtain primary alcohol **37** (0.756 g, 94 %). ^{1}H NMR (400 MHz, $CDCl_3$) δ 7.84 (dd, *J* = 6.8, 3.5 Hz, 3H), 7.78 (s, 1H), 7.50 (ddd, *J* = 5.3, 4.5, 1.6 Hz, 3H), 7.43 (dd, *J* = 8.4, 1.6 Hz, 1H), 7.24 (dd, *J* = 8.0, 2.0 Hz, 1H), 7.15 (d, *J* = 8.0 Hz, 1H), 5.55 (dd, *J* = 3.3, 1.6 Hz, 1H), 5.44 (dd, *J* = 9.8, 3.3 Hz, 1H), 5.36 (d, *J* = 1.4 Hz, 1H), 4.88 (d, *J* = 5.6 Hz, 2H), 4.33 (dd, *J* = 7.8, 4.9 Hz, 1H), 4.09 (t, *J* = 9.8 Hz, 1H), 3.93 – 3.78 (m, 2H), 2.41 (s, 3H), 2.14 (s, 3H), 1.97 (s, 3H), 1.29 (s, 9H). ^{13}C NMR (101 MHz, $CDCl_3$) δ 170.1, 170.0, 149.9, 137.4, 135.4, 133.4, 133.1, 131.8, 130.6, 130.3, 128.43, 128.0, 127.8, 126.6, 126.4, 126.2, 125.7, 125.6, 85.7, 77.5, 77.2, 76.8, 75.3, 73.2, 73.1, 72.2, 72.0, 61.9, 34.6, 31.4, 21.1, 21.0, 20.5; LC-MS (*m*/*z*): $[M+Na]^+$ cald 589.2230, obsd 584.2 and 589.2.

2-Methyl-5-tert-butylphenyl-2-*O*-acetyl-3,4,6-tri-*O*-benzyl-α-D-mannopyranosyl-(1→6)-2,3-di-*O*-acetyl-4-*O*-(2-naphthylmethyl)-1-thio-α-D-mannopyranoside (41)

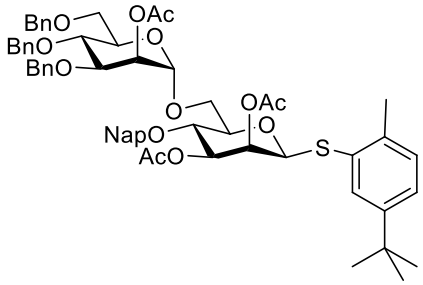

A mixture of glycosyl acceptor **37** (0.746g, 1.316 mmol) and glycosyl donor **39** (from Dr. Ivan, 1.090 g, 1.71 mmol) was dissolved and co-evaporated with dry toluene three times and dried under high vacuum for 2 h. The reaction mixture was dissolved in dry DCM (20 mL) under argon atmosphere, followed by the addition of activated powdered molecular sieves and cooled down the reaction mixture to -40 °C. Then 48 µL of TMSOTf was added to the reaction mixture under argon atmosphere and maintained the temperature at -40 °C, after 1h, the reaction was quinched by using triethylamine, filtered the molecular sieves and concentrated. The residue was purified using column chromatography to obtain disaccharide **41** (1.36 g, 98 %). ^{1}H NMR (400 MHz, $CDCl_3$) δ 7.82 – 7.76 (m, 1H), 7.75 – 7.67 (m, 3H), 7.52 (d, *J* = 2.0 Hz, 1H), 7.47 – 7.41 (m, 2H), 7.38 – 7.19 (m, 15H), 7.17 – 7.08 (m, 1H), 5.55 (dd, *J* = 3.2, 1.5 Hz, 2H), 5.46 (dd, *J* = 9.8, 3.3 Hz, 1H), 5.37 (d, *J* = 1.5 Hz, 1H), 4.99 (d, *J* = 1.6 Hz, 1H), 4.84 (dd, *J* = 18.4, 11.2 Hz, 2H), 4.71 (dd, *J* = 13.6, 11.6 Hz, 2H), 4.55 (dd, *J* = 18.6, 11.7 Hz, 2H), 4.45 (d, *J* = 10.7 Hz, 1H), 4.36 (dd, *J* = 18.4, 10.8 Hz, 2H), 4.08 (ddd, *J* = 11.9, 10.7, 2.3 Hz, 2H), 3.99 (dd, *J* = 9.4, 3.2 Hz, 1H), 3.90 (t, *J* = 9.5 Hz, 1H), 3.75 – 3.58 (m, 3H), 3.49 (dd, *J* = 10.8, 1.5 Hz, 1H), 2.40 (s, 3H), 2.17 (s, 3H), 2.15 (s, 3H), 2.01 (s, 3H), 1.29 (s, 9H). ^{13}C NMR (101 MHz, $CDCl_3$) δ 170.3, 170.2, 169.8, 149.8, 138.4, 138.1, 137.8, 137.2, 135.4, 133.2, 132.9, 131.9, 130.2, 130.1, 128.5, 128.3, 128.3, 128.2, 127.9, 127.9, 127.8, 127.8, 127.7, 127.6, 127.6, 126.2, 125.9, 125.8, 125.4, 125.2, 98.4, 77.6, 75.3, 74.9, 74.1, 73.3, 73.0, 72.5, 72.2, 72.0, 71.7, 71.4, 68.5, 68.1, 65.7, 34.5, 31.3, 21.1, 20.9, 20.4. LC-MS (*m*/*z*): $[M+Na]^+$ cald 1063.4273, obsd 1058.3 and 1063.3.

2-*O*-acetyl-3,4,6-tri-*O*-benzyl-α-D-mannopyranosyl-(1→6)-2,3-di-*O*-acetyl-4-*O*-(2-naphthylmethyl)-α-D-mannopyranoside (42)

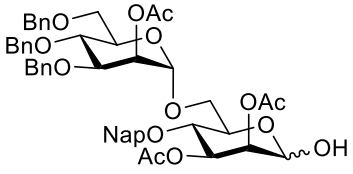

To a solution of **41** (0.250 g, 0.240 mmol) in a acetone-water (9:1) mixture was added NBS (0.214 g, 1.200 mmol). The reaction progress was monitored with TLC and after 30 min., the reaction mixture was evaporated on the rotavapour, dissolved in ethylacetate and washed twice with saturated $NaHCO_3$, water and brine solution. The organic layer was dried over anh. Na_2SO_4, filtered and concentrated. The residue was purified using silica gel column chromatography to obtain hemiacetal **42** (0.127 g, 60 %) as a mixture of alpha and beta anomers (α:β=9:1) ^{1}H NMR (400 MHz, $CDCl_3$) δ 7.85 – 7.64 (m, 4H), 7.49 – 7.40 (m, 2H), 7.37 – 7.21 (m, 14H), 7.18 – 7.09 (m, 2H), 5.53 – 5.44 (m, 2H), 5.27 (dd, *J* = 3.2, 1.7 Hz, 1H), 5.12 (s, 1H), 4.99 (s, 1H), 4.83 (dd, *J* = 16.4, 11.2 Hz, 3H), 4.70 (dd, *J* = 11.5, 7.8 Hz, 3H), 4.55 (dd, *J* = 20.1, 11.7 Hz, 2H), 4.43 (dd, *J* = 11.4, 5.8 Hz, 2H), 4.14 (d, *J* = 9.9 Hz, 1H), 4.00 (dd, *J* = 8.2, 2.8 Hz, 1H), 3.90 – 3.77 (m, 6H), 3.65 – 3.56 (m, 2H), 2.15 (s, 3H), 2.14 (s, 3H), 1.97 (s, 3H). ^{13}C NMR (101 MHz, $CDCl_3$) δ 170.6, 170.3, 170.0, 138.3, 137.9, 137.8, 135.5, 133.3, 133.0, 128.6 (2C), 128.5 (2C), 128.4 (2C), 128.3 (2C), 128.1 (2C), 128.0, 127.9, 127.9, 127.8, 127.8, 127.8, 126.3, 126.1, 126.0, 125.5, 98.5, 92.2, 77.7, 75.4, 74.8, 74.5, 73.4, 73.4, 71.8, 71.6, 71.1, 70.7, 69.1, 68.6, 67.2, 29.8, 29.7, 21.2, 21.1, 21.0. LC-MS (*m*/*z*): $[M+Na]^+$ cald 901.3406, obsd 901.2.

2-*O*-acetyl-α-D-mannopyranosyl-(1→6)-2,3-di-*O*-acetyl-α-D-mannopyranoside (43)

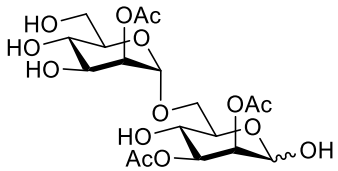

Palladium over carbon (13 mg, 0.1 equiv.) was added to a stirred solution of **42** (0.110 g, 0.125 mmol) in methanol (3 mL). Hydrogen gas was bubbled through the solution for 10 min. The reaction mixture was stirred overnight at room temperature under a hydrogen gas atmosphere. The palladium was filtered using celite pad and the residue was purified normal phase silica gel chromatography (EtOAc/MeOH=9.5/0.5) to obtain **42a** (0.055g, 94 %). ^{1}H NMR (400 MHz, CD_3OD) δ 5.21 (dd, *J* = 9.3, 3.4 Hz, 1H), 5.16 (ddd, *J* = 6.7, 3.4, 1.8 Hz, 2H), 5.09 (d, *J* = 1.7 Hz, 1H), 4.92 (d, *J* = 1.7 Hz, 1H), 4.05 – 3.92 (m, 4H), 3.89 – 3.84 (m, 1H), 3.80 – 3.72 (m, 2H), 3.70 – 3.65 (m, 2H), 2.14 (s, 3H), 2.12 (s, 3H), 2.06 (s, 3H). ^{13}C NMR (101 MHz, CD_3OD) δ 200.3 (2C), 200.3, 127.1, 121.2, 102.7, 101.8, 101.4, 101.0, 100.2, 98.9, 96.8, 95.1, 93.9, 90.7, 49.1, 49.0, 49.0. LC-MS (*m*/*z*): $[M+Na]^+$ cald 491.1371, obsd 491.0.

α-D-mannopyranosyl-(1→6)-α-D-mannopyranoside (43)

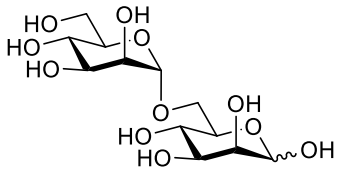

To a solution of **42a** (0.055 g, 0.117 mmol) was added freshly prepared sodium methoxide solution and checked the pH of the reaction mixture whether it is basic or not. After that reaction progress was monitored with TLC. After 30 min, reaction mixture was neutralized by using amberlite resin (H^+-form) and then filtered the solution to remove the resin and evaporated the solvent on rotavapour to get the pure product **43** (0.039 g, 97 %). ^{1}H NMR (400 MHz, CD_3OD) δ 5.01 (d, *J* = 1.4 Hz, 1H), 4.78 (d, *J* = 1.3 Hz, 1H), 3.88 (dd, *J* = 10.8, 5.4 Hz, 1H), 3.83 – 3.79 (m, 2H), 3.77 – 3.74 (m, 2H), 3.70 – 3.67 (m, 2H), 3.67 – 3.62 (m, 3H), 3.59 (d, *J* = 6.9 Hz, 2H). ^{13}C NMR (101 MHz, CD_3OD) δ 100.0, 94.5, 72.9, 71.4, 71.2, 71.1, 71.0, 70.6, 67.3, 67.2, 66.2, 61.4. LC-MS (*m*/*z*): $[M+Na]^+$ cald 365.1054, obsd 365.0.

Azido-α-D-mannopyranosyl-(1→6)-α-D-mannopyranoside (44)

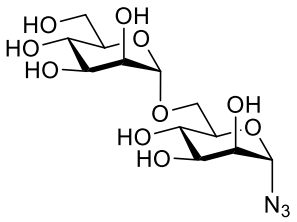

To a stirred solution of dimannose **43** (39 mg, 0.114 mmol) in D_2O (1.5 mL), DIPEA (0.200 mL, 1.139 mmol), sodium azide (74 mg, 1.139 mmol) and imidazolonium salt (46 mg, 0.342 mmol) were added at 0 °C. After 2 h, the solvent was evaporated and the residue was purified silica gel column chromatography using DCM: Methanol (9:1) as an eluent to obtain **44** (0.034g, 81 %). ^{1}H NMR (400 MHz, D_2O) δ 5.43 (s, 1H), 4.90 (s, 1H), 3.98 – 3.91 (m, 3H), 3.87 (d, *J* = 10.3 Hz, 3H), 3.81 (d, *J* = 3.3 Hz, 1H), 3.79 – 3.73 (m, 1H), 3.72 (d, *J* = 5.0 Hz, 3H), 3.66 (dd, *J* = 12.2, 7.3 Hz, 1H). ^{13}C NMR (101 MHz, D_2O) δ 99.3, 89.7, 72.7, 72.6, 70.4, 70.0, 69.8, 69.6, 66.6, 66.0, 65.4, 60.8. LC-MS (*m*/*z*): $[M+Na]^+$ cald 390.1119, obsd 390.2.

Azido-2,3,4,6-tetra-*O*-acetyl-α-D-mannopyranosyl-(1→6)-2,3,4-tri-*O*-acetyl-α-D-manno pyranoside (44a)

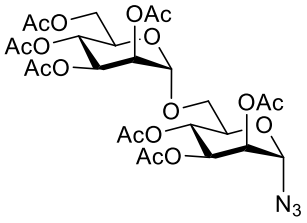

To a stirred solution of azide **44** (0.034g, 0.027 mmol) in 1 mL of pyridine, 500 µL of acetic anhydride was added at 0 °C. The reaction mixture was warmed up to room temperature and solvent was evaporated after 16 h. The crude product was purified by silica gel column chromatography using Hexane: Ethylacetate (3:2) as an eluent to obtain **44a** (60 %). ^{1}H NMR (400 MHz, $CDCl_3$) δ 5.37 (d, *J* = 1.7 Hz, 1H), 5.35 – 5.21 (m, 5H), 5.14 (t, *J* = 2.3 Hz, 1H), 4.85 (s, 1H), 4.25 (dd, *J* = 12.1, 5.3 Hz, 1H), 4.17 – 4.01 (m, 3H), 3.79 (dd, *J* = 11.3, 5.1 Hz, 1H), 3.63 (dd, *J* = 11.3, 2.6 Hz, 1H), 2.17 (s, 3H), 2.15 (s, 3H), 2.10 (s, 3H), 2.06 (s, 2H), 2.04 (s, 2H), 1.99 (s, 3H), 1.97 (s, 3H). ^{13}C NMR (101 MHz, $cdcl_3$) δ 170.62, 170.02, 169.97, 169.81, 169.78, 169.66, 169.65, 97.68, 87.31, 77.32, 77.00, 76.68, 71.31, 69.26, 69.00, 68.92, 68.59, 68.26, 66.48, 65.90, 65.85, 62.41, 20.87, 20.74, 20.70 (2C), 20.68, 20.64, 20.61. LC-MS (*m*/*z*): $[M+Na]^+$ cald 684.1859, obsd 684.19.

3,4-bis(bis(2-ethoxy-2-oxoethyl)amino)benzamido-2,3,4,6-tetra-*O*-acetyl-α-D-mannopyranosyl-(1→6)-2,3,4-tri-*O*-acetyl-β-D-mannopyranoside (46)

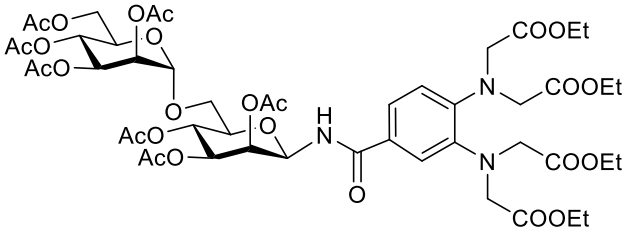

To the solution of azido dimannose **44a** (30 mg, 0.045 mmol) in ethylacetate (1 mL), Pd/C was added and reaction mixture was stirred at room temperature under hydrogen atmosphere. After 2 h, the palladium was filtered through a celite pad to obtain the desired amine. The crude amine **45** was added to a solution containing acid **27** (25 mg, 0.050 mmol), HATU (17 mg, 0.046 mmol) and DIPEA (40 µL, 0.228 mmol) in 1 mL of DMF. The reaction mixture was stirred at room temperature and the reaction progress was monitored with TLC. After 14 h, the volatiles were evaporated and the residue was purified by silica gel column chromatography using DCM:Methanol (9:1) to give the desired product **46** as an inseparable mixture of anomers. (20 mg, 0.018 mmol, 40 %). ^{1}H

NMR (400 MHz, $CDCl_3$) δ 7.60 (d, *J* = 2.0 Hz, 1H), 7.39 (ddd, *J* = 10.5, 8.2, 2.1 Hz, 1H), 7.11 (d, *J* = 9.2 Hz, 1H), 7.00 (d, *J* = 8.4 Hz, 1H), 5.74 (d, *J* = 9.2 Hz, 1H), 5.45 – 5.32 (m, 4H), 5.31 – 5.25 (m, 1H), 5.23 (d, *J* = 9.9 Hz, 1H), 5.17 (dd, *J* = 10.2, 3.2 Hz, 1H), 4.90 (d, *J* = 1.7 Hz, 1H), 4.86 (s, 0H), 4.35 (d, *J* = 6.3 Hz, 4H), 4.30 (d, *J* = 2.6 Hz, 2H), 4.26 (s, 3H), 4.21 (dd, *J* = 12.2, 5.6 Hz, 1H), 4.09 (qd, *J* = 7.0, 2.4 Hz, 11H), 3.73 (d, *J* = 3.5 Hz, 2H), 2.24 (s, 3H), 2.15 (s, 2H), 2.11 (s, 1H), 2.10 (s, 1H), 2.09 (s, 3H), 2.08 (s, 1H), 2.07 (s, 3H), 2.01 (s, 3H), 2.00 (s, 3H), 1.96 (s, 4H), 1.96 (s, 3H), 1.25 (s, 3H), 1.19 (td, *J* = 7.1, 2.4 Hz, 12H). ^{13}C NMR (101 MHz, $cdcl_3$) δ 170.72, 170.55, 170.45, 169.95, 169.60, 169.50, 166.03, 145.05, 141.07, 127.02, 122.08, 121.94, 120.47, 98.54, 74.93, 71.63, 70.17, 69.56, 69.01, 68.48, 66.49, 66.03, 65.22, 62.49, 60.74(2-C), 60.70(2-C), 52.25(2-C), 52.16(2-C), 20.78(4-C), 20.61(3-C), 14.12(4-C). LC-MS (*m*/*z*): $[M+Na]^+$ cald 1136.3904, obsd 1136.4.

3,4-bis(bis(2-carboxy-2-oxoethyl)amino)benzamido-α-D-mannopyranosyl-(1→6)-β-D-mannopyranoside

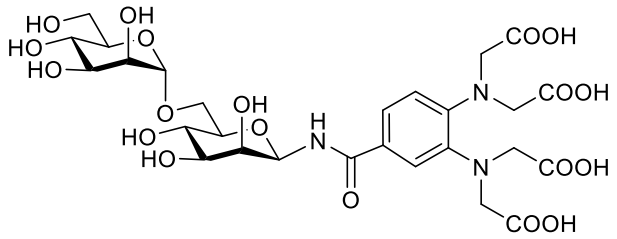

To a stirred solution of protected chelating linker tagged dimannose **46** (0.020 g, 0.018 mmol) in 1 ml of methanol, 100 µL of 1 M NaOH solution was added and kept the pH over 10. The reaction mixture was stirred at room temperature for 2 h and the reaction mixture was concentrated in *vacuo* and dried under high vacuum. The crude compound was purified by using HPLC to get pure β-anomer **47** (4 mg); Synergy 4 µ Hydro-RP 80A (250 x 10 mm), 3mL/min. ^1H NMR (400 MHz, Deuterium Oxide) δ 7.54 (s, 1H, Aromatic), 7.44 (d, *J* = 8.4 Hz, 1H, Aromatic), 7.13 (d, *J* = 8.4 Hz, 1H Aromatic), 5.37 (s, 1H, H-1), 4.85 (d, *J* = 1.5 Hz, 1H, H-1'), 4.41 (s, 4H, $-CH_2$), 4.31 (s, 4H, $-CH_2$), 4.03 (d, *J* = 2.2 Hz, 1H, H-2), 3.95 (dd, *J* = 3.3, 1.7 Hz, 1H, H-2'), 3.95 – 3.87 (m, 1H, H-6a), 3.85 – 3.72 (m, 3H, H-6b, 3', 5), 3.75 – 3.68 (m, 1H, H-3), 3.71 – 3.56 (m, 5H, H-4, 4', 5, 6a', 6b'). ^{13}C NMR (151 MHz, d_2o) δ 177.80(2-C), 177.73(2-C), 172.51 (Amide carbonyl), 147.67 (Ar), 142.67 (Ar), 128.90 (Ar), 125.41 (Ar), 123.35 (Ar), 122.86 (Ar),

102.21 (C1'), 80.98 (C1), 78.54 (C5'), 76.10 (C3), 75.24 (C4'), 73.09 (C3'), 72.81 (C2), 72.49 (C2'), 69.26 (C5), 68.99 (C4), 68.53 (C6), 63.41 (C6'), 54.84(2-C, -CH_2), 54.73(2-C, -CH_2). LC-MS (*m/z*): $[M-H]^-$ cald 706.1948, obsd 706.2.2.

5.3.3 Synthesis of tagged Disaccharide (Manα1→2Man):

Allyl-2-*O*-acetyl-3,4,6-tri-*O*-benzyl-α-D-mannopyranosyl-(1→2)-3,4,6-tri-*O*-benzyl-α-D-mannopyranoside (48)

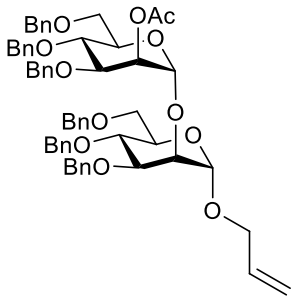

A glycosyl acceptor **40** (1.7 g, 3.47 mmol) and glycosyl donor **39** (2.428 g, 3.81 mmol) were dissolved and co-evaporated with dry toluene three times and dried under high vacuum for 2 h. The reaction mixture was dissolved in dry DCM (20 mL) under argon atmosphere, followed by the addition of activated powdered molecular sieves and cooled down the reaction mixture to -40 °C. Then, 63 µL of TMSOTf was added to the reaction mixture under argon atmosphere and maintained the temperature at -40 °C. The reaction was quenched by using triethylamine, filtered the molecular sieves and concentrated. The residue was purified using column chromatography to obtain disaccharide **48** (2.695 g, 81 %). ^{1}H NMR (400 MHz, $CDCl_3$) δ 7.43 – 6.92 (m, 30H), 5.87 – 5.72 (m, 1H), 5.53 (dd, *J* = 3.3, 1.8 Hz, 1H), 5.21 – 5.09 (m, 2H), 5.08 (d, *J* = 1.8 Hz, 1H), 4.91 (d, *J* = 1.8 Hz, 1H), 4.84 (dd, *J* = 10.8, 5.9 Hz, 2H), 4.65 (dd, *J* = 14.5, 3.2 Hz, 5H), 4.56 – 4.37 (m, 5H), 4.09 – 4.05 (m, 1H), 4.02 (t, *J* = 2.4 Hz, 1H), 3.99 – 3.90 (m, 3H), 3.87 – 3.79 (m, 3H), 3.76 (td, *J* = 8.0, 7.4, 3.4 Hz, 3H), 3.72 – 3.65 (m, 2H), 2.11 (s, 3H). ^{13}C NMR (101 MHz, $cdcl_3$) δ 170.15, 138.42, 138.39, 138.31, 138.10, 137.95, 133.70, 128.36, 128.32, 128.28, 128.25, 128.15, 128.04, 127.81, 127.77, 127.64, 127.62, 127.58, 127.53, 127.51, 127.49, 127.43, 127.41, 117.19, 99.54, 97.86, 79.67, 78.12, 75.17, 75.05, 74.71, 74.58, 74.28, 73.39, 73.25, 72.01, 71.90, 71.80, 71.75, 69.17, 68.92, 68.67, 67.82, 21.14. ESI-HRMS: m/z $[M+Na]^+$ cald 987.4290, obsd 987.4333.

2-*O*-acetyl-3,4,6-tri-*O*-benzyl-α-D-mannopyranosyl-(1→2)-3,4,6-tri-*O*-benzyl-α-D-mannopyranoside (49)

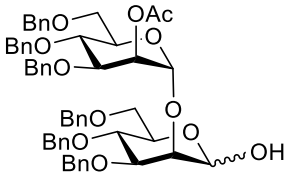

A solution of $[IrCOD(PPh_2Me)_2]PF_6$ (4.0 mg, 4.7 μmol) in THF (1 mL) was stirred under hydrogen gas until the color of the solution turned from red to colorless to pale yellow. The hydrogen atmosphere was exchanged with Argon. This activated solution of the catalyst was added to a solution of disaccharide **48** (0.680 g, 0.713 mmol) in THF (7 mL). After 16 h, water (1 mL) was added to the reaction mixture followed by the addition of Iodine (0.2 g, 0.777 mmol). After 1 h, saturated $NaHCO_3$ (aq) solution was added and the reaction mixture was extracted three times with dichloromethane. The combined organic layer was dried over Na_2SO_4, filtered and concentrated. The crude product was purified by silica gel column chromatography to give hemiacetal of disaccharide **49** (0.5 g, 0.541 mmol, 70% yield) as colorless oil. ^{1}H NMR (400 MHz, $CDCl_3$) (α:β mixture-1:0.2) δ 7.42 – 7.20 (m, 39H), 5.62 (d, *J* = 2.7 Hz, 1H), 5.29 (d, *J* = 1.9 Hz, 1H), 5.16 (d, *J* = 1.8 Hz, 1H), 4.91 (dd, *J* = 10.8, 4.6 Hz, 3H), 4.78 – 4.71 (m, 5H), 4.68 – 4.48 (m, 7H), 4.11 (d, *J* = 2.5 Hz, 1H), 4.08 – 3.88 (m, 4H), 3.86 – 3.79 (m, 2H), 3.78 – 3.68 (m, 3H), 2.18 (s, 3H). ^{13}C NMR (101 MHz, $CDCl_3$) δ 170.23, 138.40, 138.36, 138.30, 138.23, 138.18, 138.02, 128.45, 128.41, 128.39, 128.37, 128.26, 128.14, 127.95, 127.88, 127.80, 127.69, 127.46, 99.47, 93.43, 79.27, 78.14, 75.22, 75.12, 74.82, 74.76, 74.34, 73.42, 73.38, 72.06, 71.96, 71.82, 71.65, 69.55, 68.88, 68.70, 21.24. LC-MS (*m*/*z*): $[M+Na]^+$ cald 947.3944, obsd 947.4.

α-D-mannopyranosyl-(1→2)-α-D-mannopyranoside (50)

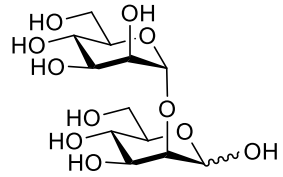

To a stirred solution of hemiacetal **49** (0.270 g, 0.292 mmol) in methanol (3 mL), palladium over carbon (30 mg, 0.1 equiv.) was added. The hydrogen gas was bubbled through the solution for 10 min. and the reaction mixture was stirred overnight at room

temperature under hydrogen gas atmosphere. The palladium was filtered using a celite pad and purified the residue using normal phase silica gel chromatography (EtOAc/MeOH=9/1) to obtain debenzylated disaccharide (0.110 g, 98 %). To a solution of debenzylated disaccharide (0.110 g, 0.286 mmol) in methanol (3mL), freshly prepared sodium methoxide solution was added and the pH of the reaction mixture was maintained over 9.0. The reaction progress was monitored with TLC. After 30 min, the reaction mixture was neutralized by using amberlite IR120 resin (H^+-form), filtered the solution to remove the resin and evaporated the solvent on rotavapour to get the pure product **50** (0.095 g, 97 %). ^{1}H NMR (400 MHz, Methanol-d_4) δ 5.20 (d, J = 1.8 Hz, 1H), 3.87 (dd, J = 3.3, 1.8 Hz, 1H), 3.80 – 3.75 (m, 1H), 3.73 – 3.66 (m, 3H), 3.65 – 3.54 (m, 6H), 3.49 (dd, J = 10.1, 8.6 Hz, 2H). ^{13}C NMR (101 MHz, cd_3od) δ 103.87, 94.19, 81.04, 74.75, 73.96, 72.30, 71.82, 71.79, 69.05, 68.56, 62.99, 62.83. LC-MS (*m*/*z*): $[M+Na]^+$ cald 390.1119, obsd 390.2.

Azido-2,3,4,6-tetra-*O*-acetyl-α-D-mannopyranosyl-(1→2)-3,4,6-tri-*O*-acetyl-β-D-mannopyranoside (51)

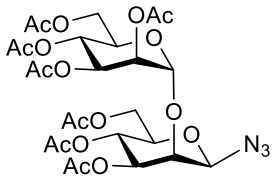

To a stirred solution of deprotected dimannose **50** (39 mg, 0.114 mmol) in D_2O (1.5 mL), DIPEA (0.200 mL, 1.139 mmol), sodium azide (74 mg, 1.139 mmol) and imidazolonium salt (46 mg, 0.342 mmol) were added at 0 °C. After 2 h, the reaction mixture was concentrated and purified by silica gel column chromatography using DCM: Methanol (9:1) as an eluent to obtain azido dimannose (0.034g, 81 %).

To a stirred solution of azide (0.034g, 0.027 mmol) in 1 mL of pyridine, 500 µL of acetic anhydride was added at 0 °C and let the reaction mixture warmed up to room temperature and later on heated up to 45 °C. After 16 h, the solvent was evaporated and the crude product was purified by silica gel column chromatography using Hexane: Ethylacetate (3:2) as an eluent to obtain **51**. ESI-HRMS (*m*/*z*): $[M+Na]^+$ cald 684.1859, obsd 684.1884.

3,4-bis(bis(2-carboxy-2-oxoethyl)amino)benzamido-α-D-mannopyranosyl-(1→2)-β-D-mannopyranoside (54)

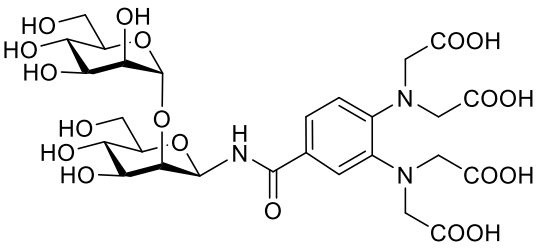

To the solution of azido dimannose (30 mg, 0.045 mmol) in ethylacetate (1 mL), Pd/C was added and the reaction mixture was stirred at room temperature under hydrogen gas atmosphere. After 2 h, the palladium was filtered through a celite pad to obtain the desired amine. The crude amine **52** was added to a solution containing acid **27** (25 mg, 0.050 mmol), HATU (17 mg, 0.046 mmol) and DIPEA (40 µL, 0.228 mmol) in 1 mL of DMF. The reaction progress was monitored with TLC. The volatiles were evaporated after 16 h and the residue was purified by silica gel column chromatography using DCM:Methanol (9:1) to give the desired product as an inseparable mixture of anomers. (20 mg, 0.018 mmol, 40 %). To a stirred solution of protected linker tagged dimannose (0.020 g, 0.018 mmol) in 1 ml of methanol, 100 µL of 1 M NaOH solution was added and pH of the reation mixture was maintained over 10.0. The reaction mixture was stirred at room temperature for 2 h, concentrated in *vacuo* and dried under high vacuum. The crude compound was purified by using HPLC to give β-anomer **54** (4 mg); Synergy 4 µ Hydro-RP 80A (250 x 10 mm), 3mL/min. ^{1}H NMR (600 MHz, Deuterium Oxide) δ 7.61 (s, 1H, Aromatic), 7.51 (d, *J* = 8.2 Hz, 1H, Aromatic), 7.19 (d, *J* = 8.1 Hz, 1H, Aromatic), 5.42 (s, 1H, H-1), 5.20 (s, 1H, H-1'), 4.56 – 4.28 (m, 8H, -CH_2), 4.22 (s, 1H, H-2), 4.18 – 4.16 (m, 1H, H-2'), 3.94 (t, *J* = 13.1 Hz, 3H, H-6a, 3, 3'), 3.77 (d, *J* = 5.2 Hz, 3H, H-6b, 5', 4'), 3.72 (t, *J* = 9.7 Hz, 1H, H-4), 3.57 (dd, *J* = 8.7, 6.5 Hz, 1H, H-5), 3.50 (d, *J* = 12.3 Hz, 1H, H-6a'), 3.31 (d, *J* = 12.2 Hz, 1H, H-6b'). ^{13}C NMR (151 MHz, d_2o) δ 177.83 (2-C), 177.77 (2-C), 172.08 (Amide carbonyl), 147.75 (Ar), 142.85 (Ar), 128.7 (Ar), 125.21 (Ar), 123.56 (Ar), 122.92 (Ar), 105.15 (C1'), 83.08 (C2), 81.06 (C5), 80.67 (C1), 76.14 (C4'), 75.86 (C3), 72.79 (C2'), 72.73 (C3'), 69.12 (C4), 68.69 (C5'), 63.51 (C6), 62.54 (C6'), 54.94 (2-C, -CH_2), 54.82 (2-C, -CH_2). ESI-MS (*m*/*z*): $[M-H]^-$ cald 706.1948, obsd 706.2.

5.3.4 Synthesis of tagged Trisaccharide (Manα1→2 Manα1→6Man):

Allyl 2,3-*O*-isopropylidene-4,6-di-*O*-(2-naphthyl)methyl-α-D-mannopyranoside (57)

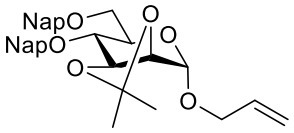

To a solution of diol **56** (1.77 g, 6.80 mmol) in DMF (70 mL), NaH (0.68 g, 17.0 mmol, 60% in mineral oil) and NapBr (3.76 g, 17.0 mmol) were added at 0 °C. After stirring the reaction mixture overnight at room temperature, the reaction was quenched with aq.NH_4Cl and extracted three times with EtOAc. The combined organic layer was washed with brine, dried over $MgSO_4$, filtered and concentrated. The crude product was purified by silica gel column chromatography to give mannoside **57** in 85% yield (3.12 g, 5.77 mmol) as a colorless oil; $[\alpha]_D^{20}$: 34.7 (c = 1.68, $CHCl_3$); ATR-FTIR (cm^{-1}): 3057, 2988, 2934, 2867, 1604, 1510, 1458, 1382, 1372, 1272, 1244, 1221, 1171, 1142, 1124, 1121, 1070, 1025, 993, 962, 931, 893, 857, 815, 752; ^{1}H NMR (400 MHz, $CDCl_3$) δ 7.82-7.73 (m, 5H), 7.67-7.62 (m, 3H), 7.48-7.40 (m, 5H), 7.30 (dd, *J* = 8.4, 1.3 Hz, 1H), 5.98-5.86 (m, 1H, -CH= of allyl), 5.34-5.18 (m, 2H, =CH_2 of allyl), 5.15 (s, 1H, Man-1), 5.01 & 4.70 (ABq, *J* = 11.6 Hz, 2H, -CH_2- of Nap), 4.81 & 4.69 (ABq, *J* = 12.3 Hz, 2H, -CH_2- of Nap), 4.39 (t, *J* = 6.5 Hz, Man-4), 4.29-4.23 (m, 1H, -CH_2- of allyl), 4.21 (d, *J* = 5.8 Hz, 1H, Man-2), 4.07-4.00 (m, 1H, -CH_2- of allyl), 3.88-3.80 (m, 2H, Man-3, Man-6), 3.76 (dd, *J* = 10.7, 5.1 Hz, 1H, Man-6), 3.67 (dd, *J* = 10.2, 7.0 Hz, 1H, Man-5), 1.53 (s, 3H, -CH_3 of isopropylidene), 1.40 (s, 3H, -CH_3 of isopropylidene); ^{13}C NMR (100 MHz, $CDCl_3$) δ 135.9, 135.7, 133.7 (-CH= of allyl), 133.4, 133.3, 133.1, 133.0, 128.2, 128.1, 127.99, 127.97, 127.8, 127.7, 126.8, 126.5, 126.2, 126.1, 125.91, 125.87, 125.86, 118.0 (=CH_2 of allyl), 109.5 (-C- of isopropylidene), 96.5 (C1, J_{CH} = 168.3 Hz), 79.1 (C4), 76.0 (C2), 75.8 (C5), 73.6 (-CH_2- of Nap), 73.0 (-CH_2- of Nap), 69.3 (C6), 68.5 (C3), 68.0 (-CH_2- of allyl), 28.1 (-CH_3 of isopropylidene), 26.5 (-CH_3 of isopropylidene); ESI-MS (*m*/*z*): $[M+Na]^+$ cald 563.2410, obsd 563.2411.

Allyl 4,6-di-*O*-(2-naphthyl)methyl-α-D-mannopyranoside (58)

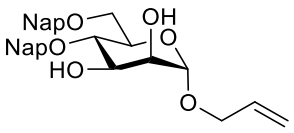

Camphor sulfonic acid (0.268 g, 1.15 mmol) was added to the solution of *iso*-propylidene **57** (3.12 g, 5.77 mmol) in CH_2Cl_2/MeOH (v/v = 1:1, 30 mL). The reaction mixture was stirred overnight at room temperature, neutralized with Et_3N, and concentrated to dryness under reduced pressure. The residue was purified by silica gel column chromatography to give diol **58** in 88% yield (2.53 g, 5.05 mmol) as a white solid; $[\alpha]_D^{20}$: 71.2 (c = 3.45, $CHCl_3$); ATR-FTIR (cm^{-1}): 3422, 3057, 3019, 2918, 2869, 1510, 1460, 1367, 1272, 1216, 1172, 1125, 1087, 1056, 992, 928, 892, 856, 812, 751; ^{1}H NMR (400 MHz, $CDCl_3$)) δ 7.82-7.75 (m, 5H), 7.67-7.60 (m, 2H), 7.55-7.40 (m, 6H), 7.24 (dd, *J* = 8.4, 1.5 Hz, 1H), 5.94-5.81 (m, 1H, -CH= of allyl), 5.31-5.16 (m, 2H, =CH_2 of allyl), 4.93 (d, *J* = 1.4 Hz, 1H, Man-1), 4.88 & 4.68 (ABq, *J* = 11.4 Hz, 2H, -CH_2- of Nap), 4.86 & 4.67 (ABq, *J* = 12.0 Hz, 2H, -CH_2- of Nap), 4.22-4.15 (m, 1H, -CH_2- of allyl), 4.03-3.92 (m, 3H, -CH_2- of allyl, Man-2, Man-5), 3.89-3.75 (m, 4H, Man-3, Man-4, Man-6); ^{13}C NMR (100 MHz, $CDCl_3$) δ 135.7, 135.5, 133.7 (-CH= of allyl), 133.32, 133.29, 133.2, 133.1, 128.40, 128.38, 128.04, 128.03, 127.9, 127.8, 127.1, 126.8, 126.3, 126.20, 126.19, 126.09, 126.05, 125.8, 117.7 (=CH_2 of allyl), 98.8 (C1, J_{CH} = 165.8 Hz), 75.9 (C4), 74.9 (-CH_2- of Nap), 73.8 (-CH_2- of Nap), 72.1 (C5), 71.3 (C2), 70.9 (C3), 68.8 (C6), 68.2 (-CH_2- of allyl); ESI-MS (*m*/*z*): $[M+Na]^+$ cald 523.2097, obsd 523.2098.

Allyl 3,4,6-tri-*O*-(2-naphthyl)methyl-α-D-mannopyranoside (59)

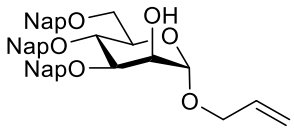

To a solution of allyl mannoside **58** (4.33 g, 8.65 mmol) in toluene (100 mL) was added Bu_2SnO (2.58 g, 10.38 mmol). The resulting solution was refluxed for 3 h and then concentrated in vacuo. The residue was dissolved in DMF (60 mL) and then 2-naphthylmethyl bromide (2.30 g, 10.38 mmol) and Bu_4NI (3.20 g, 8.65 mmol) were added. After stirred at 60 ^{o}C for 5 h, the solution was cooled, diluted with ethyl acetate, washed with $Na_2S_2O_3$ (5% in water), saturated NaCl solution, and water, dried over $MgSO_4$, filtered and concentrated. The residue was purified by flash column chromatography on silica gel to afford alcohol **59** (5.06 g, 7.90 mmol, 91 %) as a colorless syrup.; $[\alpha]_D^{20}$: 32.3 (c = 0.73, $CHCl_3$); ATR-FTIR (cm^{-1}): 3459, 3059, 3015, 2923, 2866, 1604, 1510, 1461, 1367, 1272, 1216, 1172, 1125, 1056, 1020, 951, 893, 856, 814, 761; ^{1}H NMR (400 MHz, $CDCl_3$) δ 7.84-7.71 (m, 9H), 7.58-7.39 (m, 11H), 7.14 (dd, *J* = 8.4, 1.5 Hz, 1H), 5.95-5.83 (m, 1H, -CH= of allyl), 5.27 (ddd, *J* = 17.2, 3.1, 1.5

Hz, 1H, =CH_2 of allyl), 5.18 (ddd, *J* = 10.4, 2.4, 1.4 Hz, 1H, =CH_2 of allyl), 5.01 (d, *J* = 1.6 Hz, 1H, Man-1), 4.98 (d, *J* = 11.2 Hz, 1H, -CH_2- of Nap), 4.93-4.82 (m, 3H, -CH_2- of Nap), 4.67 (d, *J* = 12.5 Hz, 1H, -CH_2- of Nap), 4.64 (d, *J* = 11.1 Hz, 1H, -CH_2- of Nap), 4.21 (ddt, *J* = 12.9, 5.1, 1.4 Hz, 1H, -CH_2- of allyl), 4.16-4.12 (m, 1H, Man-2), 4.05-3.95 (m, 3H, -CH_2- of allyl, Man-4, Man-5), 3.89-3.82 (m, 2H, Man-3, Man-6), 3.80-3.74 (m, 1H, Man-6); ^{13}C NMR (100 MHz, $CDCl_3$) δ 135.9, 135.8, 135.5, 133.9 (-CH= of allyl), 133.41, 133.39, 133.3, 133.18, 133.15, 133.0, 128.5, 128.3, 128.10, 128.07, 128.0, 127.8, 127.7, 126.8, 126.7, 126.5, 126.3, 126.2, 126.14, 126.13, 126.0, 125.94, 125.92, 125.90, 125.88, 117.7 (=CH_2 of allyl), 98.6 (C1, J_{CH} = 171.6 Hz), 80.5 (C4), 75.3 (-CH_2- of Nap), 74.6 (C5), 73.7 (-CH_2- of Nap), 72.2 (-CH_2- of Nap), 71.4 (C3), 69.1 (C6), 68.6 (C2), 68.2 (-CH_2- of allyl); ESI-MS (*m*/*z*): $[M+Na]^+$ cald 663.2723, obsd 663.2729.

Allyl 2-*O*-levulinyl-3,4,6-tri-*O*-(2-naphthyl)methyl-α-D-mannopyranoside (60)

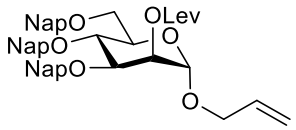

To a stirred solution of alcohol **59** (5.06 g, 7.90 mmol) and DMAP (0.193 g, 1.579 mmol) in CH_2Cl_2 (80 mL) at room temperature, LevOH (0.961 mL, 9.48 mmol) and DIC (1.476 mL, 9.48 mmol) were added. The reaction mixture was stirred overnight at room temperatureand after completion of the reaction, the product was extracted using CH_2Cl_2, washed with brine, dried over anh. Na_2SO_4, filtered and concentrated in *vacuo*. The residue was purified by flash column chromatography on silica gel to afford mannoside **60** (5.42 g, 7.34 mmol, 93%) as a colorless syrup.; $[\alpha]_D^{20}$: 0.98 (c = 0.93, $CHCl_3$); ATR-FTIR (cm^{-1}): 3058, 3018, 2924, 2865, 1741, 1720, 1637, 1603, 1510, 1461, 1408, 1364, 1252, 1216, 1156, 1137, 1126, 1085, 1059, 1019, 989, 928, 894, 856, 816, 711; ^{1}H NMR (400 MHz, $CDCl_3$) δ 7.81-7.68 (m, 9H), 7.58-7.54 (m, 2H), 7.50-7.38 (m, 9H), 7.16 (dd, *J* = 8.4, 1.6 Hz, 1H), 5.94-5.82 (m, 1H, -CH= of allyl), 5.46 (dd, *J* = 3.3, 1.9 Hz, 1H, Man-2), 5.26 (dq, *J* = 17.2, 1.6 Hz, 1H, =CH_2 of allyl), 5.18 (ddd, *J* = 10.4, 2.8, 1.3 Hz, 1H, =CH_2 of allyl), 5.02 & 4.65 (ABq, *J* = 11.1 Hz, 2H, -CH_2- of Nap), 4.92 (d, *J* = 1.8 Hz, 1H, Man-1), 4.87 & 4.69 (ABq, *J* = 11.0 Hz, 2H, -CH_2- of Nap), 4.85 & 4.66 (ABq, *J* = 12.2 Hz, 2H, -CH_2- of Nap), 4.18 (ddt, *J* = 12.9, 5.2, 1.5 Hz, 1H, -CH_2- of allyl), 4.10 (dd, *J* = 9.2, 3.4 Hz, 1H, Man-3), 4.01 (ddt, *J* = 12.3, 6.1, 1.3 Hz, 1H, -CH_2- of allyl), 3.96 (t, *J* = 9.3 Hz, 1H, Man-4), 3.90-3.85 (m, 2H, Man-5, Man-6), 3.78 (q, *J* = 3.5 Hz, 1H, Man-6), 2.76-2.64 (m, 4H, -CH_2-CH_2- of Lev), 2.12 (s, 3H, -CH_3 of Lev); ^{13}C NMR

(100 MHz, $CDCl_3$) δ 206.4 (C=O of Lev), 172.2 (-O=C-O- of Lev), 135.8, 135.7, 135.6, 133.5 (-CH= of allyl), 133.33, 133.27, 133.2, 133.1, 133,0, 132.9, 128.3, 128.2, 128.02, 127.95, 127.9, 127.8, 127.71, 127.65, 126.9, 126.8, 126.4, 126.21, 126.20, 126.1, 126.04, 125.97, 125.95, 125.91, 125.88, 125.8, 117.9 (=CH_2 of allyl), 97.0 (C1), 78.3 (C3), 75.3 (-CH_2- of Nap), 74.4 (C4), 73.6 (-CH_2- of PMB), 71.7 (-CH_2- of Nap), 71.5 (C5), 69.0 (C2), 68.8 (C6), 68.3 (-CH_2- of allyl), 38.1 (-CH_2- of Lev), 29.8 (-CH_3 of Lev), 28.3 (-CH_2- of Lev); ESI-MS (*m*/*z*): $[M+Na]^+$ cald 761.3090, obsd 761.3074.

2-*O*-levulinyl-3,4,6-tri-*O*-(2-naphthyl)methyl-α-D-mannopyranosyl trichloroacetimidate (45)

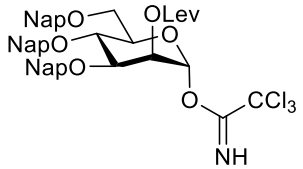

To the hemiacetal compound **61** (2.02 g, 2.89 mmol) in CH_2Cl_2, CCl_3CN (0.580 mL, 5.78 mmol) and DBU (0.044 mL, 0.289 mmol) were added. The reaction mixture was stirred at 0 °C for 2 h and the solvent was removed in *vacuo*. The residue was purified by flash column chromatography on silica gel to afford mannosyl donor **62** (2.11 g, 2.50 mmol, 87 %) as a colorless syrup; ^{1}H NMR (400 MHz, $CDCl_3$) δ 8.69 (s, 1H, =NH), 7.85-7.70 (m, 9H), 7.63-7.57 (m, 2H), 7.54-7.42 (m, 9H), 7.21 (dd, *J* = 8.4, 1.6 Hz, 1H), 6.34 (d, *J* = 1.9 Hz, 1H, Man-1), 5.56 (t, *J* = 2.4 Hz, 1H, Man-2), 5.06 & 4.71 (ABq, *J* = 10.9 Hz, 2H, -CH_2- of Nap), 4.92 & 4.76 (ABq, *J* = 11.4 Hz, 2H, -CH_2- of Nap), 4.86 & 4.65 (ABq, *J* = 12.2 Hz, 2H, -CH_2- of Nap), 4.17-4.10 (m, 2H, Man-3, Man-5), 4.06-4.01 (m, 1H, Man-4), 3.92 (dd, *J* = 11.1, 3.7 Hz, 1H, Man-6), 3.79 (dd, *J* = 11.1, 1.8 Hz, 1H, Man-6), 2.81-2.71 (m, 4H, -CH_2-CH_2- of Lev), 2.12 (s, 3H, -CH_3 of Lev); ^{13}C NMR (100 MHz, $CDCl_3$) δ 206.3 (C=O of Lev), 172.0 (-O=C-O- of Lev), 160.0 (-C=NH), 135.63, 135.56, 135.1, 133.31, 133.27, 133.2, 133.1, 133,0, 128.4, 128.3, 128.2, 128.04, 128.02, 127.99, 127.82, 127.79, 127.7, 127.4, 126.81, 126.80, 126.4, 126.24, 126.21, 126.10, 126.08, 126.01, 125.97, 95.4 (C1, J_{CH} = 179.0 Hz), 90.8 (-CCl_3), 77.2 (C3), 75.6 (-CH_2- of Nap), 74.4 (C4), 73.70 (C5), 73.66 (-CH_2- of PMB), 72.1 (-CH_2- of Nap), 68.4 (C6), 67.7 (C2), 38.0 (-CH_2- of Lev), 29.9 (-CH_3 of Lev), 28.3 (-CH_2- of Lev); ESI-MS (*m*/*z*): $[M+Na]^+$ cald 864.1874, obsd 864.1862.

Allyl 3,4-di-*O*-(2-naphthyl)methyl-6-*O*-*tert*-butyldiphenylsilyl-α-D-mannopyranosiede (65)

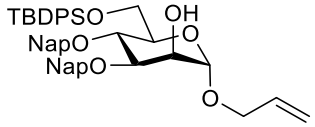

Diol mannoside **64** (4.16 g, 6.95 mmol) and dibutyltin oxide (1.73 g, 6.95 mmol) in 70 mL of toluene were refluxed in a Dean-Stark apparatus for 3 h. After that the reaction mixture was evaporated to remove toluene and dried under high vacuum for 1 h. The reaction mixture was dissolved in DMF (50 mL), 2-naphthylmethyl bromide (2.00 g, 9.03 mmol) and Bu_4NI (2.57 g, 6.95 mmol) were added to the above reaction mixture and stirred at 60 ^oC for 5 h. The reaction mixture was cooled down, diluted with ethyl acetate, washed with aq.NH_4Cl. the organic layer was dried $MgSO_4$, filtered and concentrated. The crude product was purified by flash chromatography to give protected compound **65** in 97 % yield (3.87 g, 5.24 mmol) as a colorless oil; $[\alpha]_D^{20}$: 6.82 (c = 0.87, $CHCl_3$); ATR-FTIR (cm^{-1}): 3462, 3055, 3016, 2931, 2859, 1510, 1473, 1463, 1429, 1391, 1363, 1263, 1217, 1105, 1053, 998, 934, 893, 856, 813, 774, 701; ^1H NMR (400 MHz, $CDCl_3$) δ 7.87-7.68 (m, 11H), 7.64 (s, 1H), 7.54-7.31 (m, 11H), 7.29 (dd, *J* = 8.4, 1.5 Hz, 1H), 5.97-5.84 (m, 1H, -CH= of allyl), 5.31-5.17 (m, 2H, $=CH_2$ of allyl), 5.06 & 4.78 (ABq, *J* = 11.1 Hz, 2H, -CH_2- of Nap), 5.00 (d, *J* = 1.1 Hz, 1H, Man-1), 4.94 & 4.88 (ABq, *J* = 11.6 Hz, 2H, -CH_2- of Nap), 4.25-4.15 (m, 2H, -CH_2- of allyl, Man-2), 4.09-3.94 (m, 5H, Man-3, Man-6, Man-4, -CH_2- of allyl), 3.82 (dt, *J* = 9.6, 3.2 Hz, 1H, Man-5), 2.52 (d, *J* = 2.6 Hz, 1H, OH), 1.09 (s, 9H, *t*-Butyl of TBDPS); ^{13}C NMR (100 MHz, $CDCl_3$) δ 136.0, 135.9, 135.7, 135.5, 133.84 (-CH= of allyl), 133.81, 133.40, 133.37, 133.2, 133.1, 129.7, 128.5, 128.2, 128.1, 127.82, 127.79, 127.78, 127.7, 126.8, 126.6, 126.3, 126.2, 126.11, 126.06, 125.97, 125.95, 117.8 ($=CH_2$ of allyl), 98.2 (C1, J_{CH} = 169.07 Hz), 80.5 (C3), 75.4 (-CH_2- of Nap), 74.5 (C4), 72.6 (C5), 72.3 (-CH_2- of Nap), 68.7 (C2), 67.8 (-CH_2- of allyl), 63.3 (C6), 26.9 (CH_3- of *t*-Butyl), 19.4 (-C- of *t*-Butyl); ESI-MS (*m*/*z*): $[M+Na]^+$ cald 761.3274, obsd 761.3279.

Allyl 2-*O*-acetyl-3,4-di-*O*-(2-naphthyl)methyl-6-*O*-*tert*-butyldiphenylsilyl-α-D-mannopyranosiede (66)

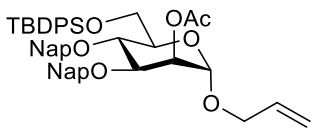

To the alcohol **65** (3.8 g, 5.14 mmol) in CH_2Cl_2 (50 mL), Ac_2O (0.97 mL, 10.3 mmol), DMAP (0.13 g, 1.03 mmol) and pyridine (1.66 mL, 20.6 mmol) were added at 0 °C. The

reaction mixture was stirred at room temperature for 2 h. The reaction was quenched with aq.HCl and extrated with CH_2Cl_2. The combined organic layer was washed with aq.HCl, aq.$NaHCO_3$ and then brine. The organic layer was dried over $MgSO_4$, filtered and concentrated in *vacuo*. The crude product was purified by flash column chromatography using silica gel to give protected compound **66** in 97 % yield (3.89 g, 4.98 mmol) as a colorless oil; $[\alpha]_D^{20}$: -10.4 (c = 1.25, $CHCl_3$); ATR-FTIR (cm^{-1}): 3019, 2933, 2861, 1745, 1511, 1474, 1429, 1372, 1240, 1216, 1140, 1105, 1059, 1017, 998, 934, 896, 857, 822, 734, 703; ^{1}H NMR (400 MHz, $CDCl_3$) δ 7.86-7.69 (m, 11H), 7.65 (s, 1H), 7.53-7.29 (m, 12H), 5.88 (dddd, *J* = 16.9, 10.4, 6.2, 5.2 Hz, 1H, -CH= of allyl), 5.49 (dd, *J* = 2.6, 2.1 Hz, 1H, Man-2), 5.26 (dq, *J* = 17.2, 1.6 Hz, 1H, =CH_2 of allyl), 5.19 (ddd, *J* = 10.4, 2.7, 1.3 Hz, 1H, =CH_2 of allyl), 5.12 & 4.81 (ABq, *J* = 11.1 Hz, 2H, -CH_2- of Nap), 4.93 (d, *J* = 1.7 Hz, 1H, Man-1), 4.93 & 4.75 (ABq, *J* = 11.5 Hz, 2H, -CH_2- of Nap), 4.19-4.14 (m, 2H, -CH_2- of allyl, Man-3), 4.13 (t, *J* = 9.5 Hz, 1H, Man-4), 4.07 (dd, *J* = 11.2, 4.0 Hz, 1H, Man-6), 4.02-3.93 (m, 2H, -CH_2- of allyl, Man-6), 3.81-3.74 (m, 1H, Man-5), 2.19 (s, 3H, -CH_3 of Ac), 1.10 (s, 9H, *t*-Butyl of TBDPS); ^{13}C NMR (100 MHz, $CDCl_3$) δ 170.7 (-O=C-O- of Ac), 136.13, 136.08, 135.7, 135.6, 134.0, 133.7 (-CH= of allyl), 133.42, 133.41, 133.3, 133.13, 133.07, 129.7, 128.3, 128.2, 128.10, 128.08, 127.80, 127.79, 127.7, 127.0, 126.5, 126.3, 126.12, 126.10, 126.04, 125.99, 125.9, 117.9 (=CH_2 of allyl), 96.8 (C1, J_{CH} = 171.0 Hz), 78.4 (C3), 75.5 (-CH_2- of Nap), 74.4 (C4), 72.9 (C5), 72.0 (-CH_2- of Nap), 69.2 (C2), 68.0 (-CH_2- of allyl), 63.0 (C6), 26.9 (CH_3- of *t*-Butyl), 21.3 (-CH_2- of Ac), 19.5 (-C- of *t*-Butyl); ESI-MS (*m*/*z*): $[M+Na]^+$ cald 803.3380, obsd 803.3410.

Allyl 2-*O*-acetyl-3,4-di-*O*-(2-naphthyl)methyl-α-D-mannopyranosiede (67)

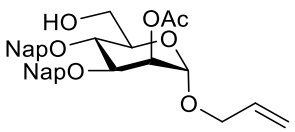

To a THF solution of fully protected compound **66** (1.6 g, 2.05 mmol), HF-pyridine complex (~70% HF) was added. The reaction mixture was stirred overnight at room temperature. The reaction was quenched using saturated $NaHCO_3$ until no more gas formation was observed. The reaction mixture was extracted three times with dichloromethane. The combined organic layer was dried over Na_2SO_4, filtered and concentrated. The crude product was purified by silica gel column chromatography to give acceptor **67** in 91 % yield (1.01 g, 1.86 mmol) as a colorless oil; $[\alpha]_D^{20}$: -21.0 (c =

0.81, $CHCl_3$); ATR-FTIR (cm^{-1}): 3485, 3058, 3016, 2925, 2857, 1746, 1604, 1510, 1459, 1370, 1234, 1126, 1076, 1036, 979, 929, 894, 856, 817, 761; ^{1}H NMR (400 MHz, $CDCl_3$) δ 7.87-7.67 (m, 8H), 7.52-7.37 (m, 6H), 5.95-5.81 (m, 1H, -CH= of allyl), 5.49 (dd, *J* = 3.3, 1.8 Hz, 1H, Man-2), 5.28 (dq, *J* = 17.2, 1.5 Hz, 1H, =CH_2 of allyl), 5.21 (dq, *J* = 10.4, 1.3 Hz, 1H, =CH_2 of allyl), 5.13 & 4.84 (ABq, *J* = 11.1 Hz, 2H, -CH_2- of Nap), 4.92 & 4.73 (ABq, *J* = 11.4 Hz, 2H, -CH_2- of Nap), 4.89 (d, *J* = 1.7 Hz, 1H, Man-1), 4.21-4.15 (m, 1H, -CH_2- of allyl), 4.14 (dd, *J* = 9.3, 3.2 Hz, 1H, Man-3), 3.99 (ddt, *J* = 12.9, 6.2, 1.2 Hz, 1H, -CH_2- of allyl), 3.93 (t, *J* = 9.6 Hz, 1H, Man-4), 3.90 (dd, *J* = 11.6, 2.9 Hz, 1H, Man-6), 3.86 (dd, *J* = 11.8, 4.1 Hz, 1H, Man-6), 3.82-3.76 (m, 1H, Man-5), 2.19 (s, 3H, -CH_3 of Ac); ^{13}C NMR (100 MHz, $CDCl_3$) δ 170.5 (-O=C-O- of Ac), 135.8, 135.5, 133.39 (-CH= of allyl), 133.37, 133.10, 133.09, 128.30, 128.29, 128.1, 128.0, 127.80, 127.77, 126.9, 126.7, 126.2, 126.1, 126.01, 125.99, 118.1 (=CH_2 of allyl), 97.1 (C1), 78.2 (C3), 75.5 (-CH_2- of Nap), 74.4 (C4), 72.0 (C5), 71.9 (-CH_2- of Nap), 68.9 (C2), 68.4 (-CH_2- of allyl), 62.3 (C6), 21.3 (-CH_2- of Ac); ESI-MS (*m*/*z*): $[M+Na]^+$ cald 565.2202, obsd 565.2217.

Allyl 2-*O*-levulinyl-3,4,6-tri-*O*-(2-naphthyl)methyl-α-D-mannopyranosyl-(1→6)-2-*O*-acetyl-3,4-di-*O*-(2-naphthyl)methyl-α-D-mannopyranoside (68)

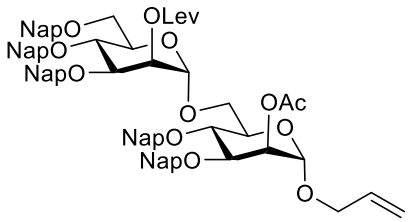

A glycosyl donor **62** (1.41 g, 1.66 mmol) and acceptor **67** (0.75 g, 1.38 mmol) were dissolved and co-evaporated with toluene using three times. The mixture was dissolved in CH_2Cl_2 (13 mL) at room temperature and cooled down to 0 °C. TMSOTf (0.050 mL, 0.277 mmol) was added to the stirred mixture at 0 °C. After stirring for 1 h at 0 °C, the reaction was quenched with Et_3N and then the solvent was removed in *vacuo*. The crude product was purified by flash chromatography to give disaccharide **68** in 96 % yield (1.63 g, 1.33 mmol) as a colorless oil; $[\alpha]_D^{20}$: 25.3 (c = 2.22, $CHCl_3$); ATR-FTIR (cm^{-1}): 3018, 2926, 1742, 1604, 1510, 1461, 1369, 1237, 1216, 1140, 1126, 1085, 982, 928, 894, 857, 818, 711; ^{1}H NMR (400 MHz, $CDCl_3$) δ 7.82-7.66 (m, 12H), 7.64-7.55 (m, 5H), 7.51-7.34 (m, 15H), 7.28-7.20 (m, 2H), 7.06 (dd, *J* = 8.4, 1.5 Hz, 1H), 5.88-5.76 (m, 1H, -CH= of allyl), 5.57 (dd, *J* = 3.2, 2.1 Hz, 1H, ManII-2), 5.47 (dd, *J* = 3.1, 1.8 Hz, 1H,

ManI-2), 5.27-5.20 (m, 1H, =CH_2 of allyl), 5.17-5.12 (m, 1H, =CH_2 of allyl), 5.04 (d, *J* = 1.5 Hz, 1H, ManII-1), 5.02-4.97 (m, 2H, -CH_2- of Nap), 4.89 & 4.68 (ABq, *J* = 11.2 Hz, 2H, -CH_2- of Nap), 4.85 (d, *J* = 1.6 Hz, 1H, ManI-1), 4.84 & 4.63 (ABq, *J* = 11.6 Hz, 2H, -CH_2- of Nap), 4.75 & 4.48 (ABq, *J* = 12.3 Hz, 2H, -CH_2- of Nap), 4.59 (d, *J* = 11.0 Hz, 1H, -CH_2- of Nap), 4.56 (d, *J* = 10.8 Hz, 1H, -CH_2- of Nap), 4.11 (dd, *J* = 8.9, 3.3 Hz, 1H, ManI-3), 4.11-4.05 (m, 1H, -CH_2- of allyl), 4.04 (dd, *J* = 9.5, 3.4 Hz, 1H, ManII-3), 3.97 (dd, *J* = 11.8, 4.5 Hz, 1H, ManII-6), 3.96-3.86 (m, 3H, -CH_2- of allyl, ManII-4, ManI-4), 3.85-3.75 (m, 3H, ManII-5, ManI-5, ManII-6), 3.69 (dd, *J* = 10.8, 4.0 Hz, 1H, ManI-6), 3.58 (dd, *J* = 10.8, 1.7 Hz, 1H, ManI-6), 2.78-2.66 (m, 4H, -CH_2-CH_2- of Lev), 2.17 (s, 3H, -CH_3 of Ac), 2.10 (s, 3H, -CH_3 of Lev); ^{13}C NMR (100 MHz, $CDCl_3$) δ 206.5 (C=O of Lev), 172.1 (-O=C-O- of Lev), 170.7 (O=C-O- of AcO), 136.0, 135.9, 135.7, 135.42, 135.35, 133.38, 133.35 (-CH= of allyl), 133.34, 133.31, 133.27, 133.2, 133.14, 133.05, 133.0, 132.9, 128.34, 128.29, 128.2, 128.12, 128.10, 128.01, 127.98, 127.96, 127.95, 127.81, 127.78, 127.75, 127.7, 127.2, 127.1, 126.7, 126.4, 126.3, 126.20, 126.15, 126.12, 126.05, 125.98, 125.96, 125.9, 125.84, 125.81, 125.6, 118.2 (=CH_2 of allyl), 98.1 (ManII-C1, J_{CH} = 172.1 Hz), 96.8 (ManI-C1, J_{CH} = 171.1 Hz), 78.5 (ManI-C3), 77.7 (ManII-C3), 75.21 (-CH_2- of Nap), 75.17 (-CH_2- of Nap), 74.3 (ManI-C4), 74.2 (ManII-C4), 73.5 (-CH_2- of Nap), 72.0 (-CH_2- of Nap), 71.5 (ManII-C5), 71.4 (-CH_2- of Nap), 71.1 (ManI-C5), 68.8 (ManI-C2), 68.7(ManI-C6), 68.6 (ManII-C2), 68.2 (-CH_2- of allyl), 66.1 (ManII-C6), 38.1 (-CH_2- of Lev), 29.9 (-CH_3 of Lev), 28.3 (-CH_2- of Lev), 21.3 (-CH_3 of Ac); ESI-MS (*m*/*z*): $[M+Na]^+$ cald 1245.4976, obsd 1245.4996.

Allyl 3,4,6-tri-*O*-(2-naphthyl)methyl-α-D-mannopyranosyl-(1→6)-2-*O*-acetyl-3,4-di-*O*-(2-naphthyl)methyl-α-D-mannopyranoside (69)

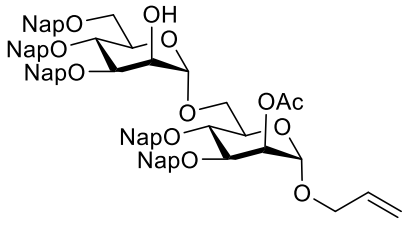

To a solution of dimannoside **68** (1.61g, 1.32 mmol) in CH_2Cl_2, hydrazine acetate (0.182 g, 1.97 mmol) was added. The reaction mixture was stirred overnight at room temperature. The reaction mixture was diluted with DCM and washed twice with saturated aq. $NaHCO_3$ and brine. The organic layer was dried over $MgSO_4$, filtered and concentrated in *vacuo*. The residue was purified by flash chromatography to give

acceptor **69** in 93 % yield (1.37 g, 1.22 mmol) as a colorless oil; $[\alpha]_D^{20}$: 44.4 (c = 0.95, $CHCl_3$); ATR-FTIR (cm^{-1}): 3058, 3016, 2926, 1746, 1604, 1510, 1461, 1370, 1237, 1216, 1171, 1126, 1059, 980, 930, 893, 857, 815, 710; ^{1}H NMR (400 MHz, $CDCl_3$) δ 7.86-7.61 (m, 17H), 7.56-7.32 (m, 16H), 7.29 (dd, *J* = 8.4, 1.6 Hz, 1H), 7.11 (dd, *J* = 8.4, 1.7 Hz, 1H), 5.87 (dddd, *J* = 16.7, 10.4, 6.3, 5.2 Hz, 1H, -CH= of allyl), 5.52 (dd, *J* = 3.3, 1.9 Hz, 1H, ManI-2), 5.28 (dq, *J* = 17.3, 1.5 Hz, 1H, =CH_2 of allyl), 5.21-5.17 (m, 2H, =CH_2 of allyl, ManII-1), 5.07 & 4.68 (ABq, *J* = 11.4 Hz, 2H, -CH_2- of Nap), 5.00 & 4.61 (ABq, *J* = 11.2 Hz, 2H, -CH_2- of Nap), 4.93 & 4.72 (ABq, *J* = 11.2 Hz, 2H, -CH_2- of Nap), 4.92 & 4.83 (ABq, *J* = 11.8 Hz, 2H, -CH_2- of Nap), 4.90 (d, *J* = 1.9 Hz, 1H, ManI-1), 4.76 & 4.52 (ABq, *J* = 12.4 Hz, 2H, -CH_2- of Nap), 4.27 (t, *J* = 2.1 Hz, 1H, ManII-2), 4.18-4.11 (m, 2H, -CH_2- of allyl, ManI-3), 4.06 (dd, *J* = 11.4, 3.8 Hz, 1H, ManII-6), 4.03-3.90 (m, 5H, -CH_2- of allyl, ManII-3, ManII-4, ManII-5, ManI-4), 3.89-3.81 (m, 2H, ManI-5, ManII-6), 3.70 (dd, *J* = 10.8, 4.0 Hz, 1H, ManI-6), 3.62 (dd, *J* = 10.7, 2.0 Hz, 1H, ManI-6), 2.16 (s, 3H, -CH_3 of AcO); ^{13}C NMR (100 MHz, $CDCl_3$) δ 170.5 (O=C-O- of AcO), 135.93, 135.89, 135.6, 135.4, 135.2, 133.4, 133.33, 133.30 (-CH= of allyl), 133.27, 133.25, 133.2, 133.12, 133.08, 133.04, 132.95, 132.9, 128.5, 128.3, 128.2, 128.12, 128.06, 127.98, 127.96, 127.78, 127.76, 127.73, 127.67, 127.2, 126.9, 126.8, 126.32, 126.29, 126.2, 126.13, 126.11, 126.08, 126.04, 125.98, 125.90, 125.85, 125.8, 125.6, 118.2 (=CH_2 of allyl), 99.6 (ManII-C1, J_{CH} = 171.2 Hz), 96.8 (ManI-C1, J_{CH} = 170.5 Hz), 79.7 (ManII-C3), 78.5 (ManI-C3), 75.1 (-CH_2- of Nap), 74.4 (ManI-C4), 74.3 (ManII-C4), 73.5 (-CH_2- of Nap), 72.0 (-CH_2- of Nap), 71.8 (-CH_2- of Nap), 71.2 (ManI-C5, ManII-C5), 68.9 (ManI-C2), 68.7 (ManI-C6), 68.3 (ManII-C2), 68.2 (-CH_2- of allyl), 66.1 (ManII-C6), 21.2 (-CH_3 of AcO); ESI-MS (*m*/*z*): $[M+Na]^+$ cald 1147.4608, obsd 1147.4586.

Allyl-2-*O*-acetyl-3,4,6-tri-*O*-benzyl-α-D-mannopyranosyl-(1→2)-3,4,6-tri-*O*-(2-naphthyl)methyl-α-D-mannopyranosyl-(1→6)-2-*O*-acetyl-3,4-di-*O*-(2-naphthyl)methyl-α-D-mannopyranoside (70)

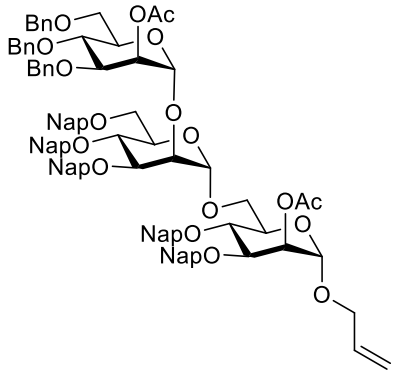

A glycosyl acceptor **69** (0.300 g, 0.269 mmol) and glycosyl donor **39** (0.257 g, 0.404 mmol) were dissolved and co-evaporated with dry toluene three times and dried under high vacuum for 2 h. The reaction mixture was dissolved in dry DCM (20 mL) under argon atmosphere, followed by the addition of activated powdered molecular sieves and cooled down the reaction mixture to -40 °C. Then 24 µL of TMSOTf was added to the reaction mixture under argon atmosphere and maintained the temperature at -40 °C. After 2 h, the reaction mixture was quenched by using triethylamine, filtered the molecular sieves and concentrated. The residue was purified using column chromatography to obtain **70** (0.420 g, 97 %). ^{1}H NMR (400 MHz, $CDCl_3$) δ 7.85 – 7.07 (m, 50H), 5.81 (ddt, *J* = 16.3, 11.0, 6.0 Hz, 1H), 5.61 (s, 1H), 5.48 (s, 1H), 5.28 – 5.11 (m, 3H), 5.05 (s, 1H), 5.00 (dd, *J* = 11.2, 6.3 Hz, 2H), 4.90 – 4.75 (m, 5H), 4.64 (p, *J* = 12.1 Hz, 6H), 4.51 – 4.40 (m, 3H), 4.35 (d, *J* = 10.9 Hz, 1H), 4.24 (s, 1H), 4.14 – 3.77 (m, 13H), 3.70 – 3.54 (m, 4H), 2.12 (s, 3H), 2.09 (s, 3H). ^{13}C NMR (101 MHz, $cdcl_3$) δ 170.42, 170.28, 138.46, 138.13, 137.88, 135.87, 135.84, 135.82, 135.48, 135.22, 133.22, 133.21, 133.18, 133.15, 133.10, 132.98, 132.84, 132.81, 132.78, 132.76, 128.27, 128.25, 128.23, 128.19, 128.05, 128.04, 127.94, 127.87, 127.85, 127.80, 127.74, 127.63, 127.60, 127.56, 127.54, 127.51, 127.49, 127.07, 126.34, 126.24, 126.14, 126.01, 125.98, 125.93, 125.91, 125.80, 125.75, 125.69, 125.66, 125.62, 125.42, 118.16, 99.48, 98.94, 96.63, 79.30, 78.48, 78.08, 77.21, 75.07, 74.90, 74.41, 74.33, 74.18, 74.11, 73.32, 73.20, 71.89, 71.84, 71.67, 70.83, 68.94, 68.77, 68.68, 67.99, 66.16, 21.15, 21.10. ESI-MS (*m*/*z*): $[M+Na]^+$ cald 1621.6645, obsd 1621.6.

2-*O*-acetyl-3,4,6-tri-*O*-benzyl-α-D-mannopyranosyl-(1→2)-3,4,6-tri-*O*-(2-naphthyl)methyl-α-D-mannopyranosyl-(1→6)-2-*O*-acetyl-3,4-di-*O*-(2-naphthyl)methyl-α-D-mannopyranoside (71)

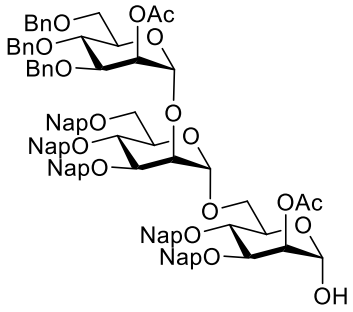

A solution of $[IrCOD(PPh_2Me)_2]PF_6$ (4.0 mg, 4.7 μmol) in THF (1 mL) was stirred under hydrogen gas atmosphere until the color of the solution turned from red to colorless to pale yellow. The hydrogen atmosphere was exchanged with argon. This solution was added to a solution of trisaccharide **70** (0.420 g, 0.263 mmol) in THF (3 mL) and the reaction mixture was stirred for 16 h. Water (1 mL) was added to the reaction mixture followed by the addition of NBS (0.070 g, 0.394 mmol). After 1 h, saturated $NaHCO_3$ (aq) was added and the reaction mixture was extracted three times with dichloromethane. The combined organic layer was dried over Na_2SO_4, filtered and concentrated. The crude product was purified by silica gel column chromatography to give hemiacetal of trisaccharide **71** (0.390 g, 0.250 mmol, 95 % yield) as colorless oil. ^{1}H NMR (400 MHz, $CDCl_3$) δ 7.67 (ddd, *J* = 27.0, 14.1, 6.2 Hz, 15H), 7.53 – 7.08 (m, 35H), 5.52 (s, 1H), 5.32 (s, 1H), 5.11 (s, 1H), 4.98 (d, *J* = 11.6 Hz, 2H), 4.81 (q, *J* = 9.4, 7.3 Hz, 5H), 4.59 (dt, *J* = 33.3, 11.4 Hz, 7H), 4.48 – 4.37 (m, 3H), 4.18 – 4.05 (m, 4H), 4.02 – 3.91 (m, 4H), 3.82 (t, *J* = 9.2 Hz, 3H), 3.70 (dd, *J* = 10.5, 6.6 Hz, 3H), 3.59 (dd, *J* = 14.9, 9.0 Hz, 3H), 2.09 (s, 3H), 2.06 (s, 3H). ^{13}C NMR (101 MHz, $CDCl_3$) δ 170.28, 170.16, 137.87, 137.73, 135.70, 135.43, 135.39, 135.20, 133.06, 132.97, 132.93, 132.80, 132.72, 132.65, 128.22, 128.21, 128.18, 128.15, 128.11, 128.08, 128.06, 128.03, 127.97, 127.95, 127.91, 127.87, 127.80, 127.75, 127.69, 127.58, 127.49, 127.46, 127.44, 127.38, 126.81, 126.36, 126.19, 126.07, 125.89, 125.86, 125.83, 125.77, 125.72, 125.67, 125.60, 125.57, 125.54, 125.42, 98.51, 92.05, 77.87, 75.15, 74.67, 74.62, 74.48, 74.43, 74.23, 73.78, 73.22, 73.07, 71.76, 71.73, 71.67, 71.61, 71.56, 71.50, 70.13, 69.15, 69.07, 68.71, 68.60, 67.17, 20.97, 20.94. ESI-MS (*m*/*z*): $[M+Na]^+$ cald 1581.6332, obsd 1581.6.

α-D-mannopyranosyl-(1→2)-α-D-mannopyranosyl-(1→6)-α-D-mannopyranoside (72)

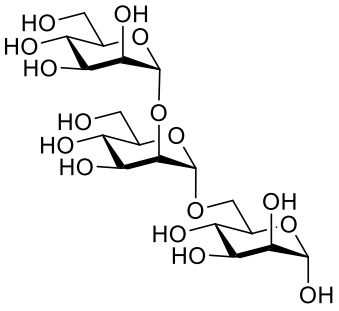

To a stirred solution of hemiacetal **71** (0.270 g, 0.292 mmol) in methanol (3 mL), palladium over carbon (30 mg, 0.1 equiv.) was added. The hydrogen gas was bubbled through the solution for 10 min. and the reaction mixture stirred overnight at room temperature under hydrogen gas atmosphere. The palladium was filtered using a celite pad and the residue was purified using normal phase silica gel chromatography (EtOAc/MeOH=9:1) to obtain debenzylated trisaccharide (0.110 g, 98 %). To a solution of this trisaccharide (0.110 g, 0.286 mmol) in methanol (3mL), freshly prepared sodium methoxide solution was added and pH of the reaction mixture was maintained over 9.0. The reaction progress was monitored with TLC. After 30 min, reaction mixture was neutralized by using amberlite resin (H^+-form) and then filtered the solution to remove the resin and evaporated the solvent on rotavapour to get the pure product **72** (0.095 g, 97 %). ^{1}H NMR (600 MHz, Deuterium Oxide) δ 5.17 (d, *J* = 1.7 Hz, 1H), 5.05 (t, *J* = 1.8 Hz, 1H), 4.78 – 4.75 (m, 1H), 4.09 (dd, *J* = 3.4, 1.8 Hz, 1H), 4.03 (d, *J* = 3.6 Hz, 1H), 3.97 (ddd, *J* = 10.4, 5.8, 2.6 Hz, 3H), 3.93 – 3.84 (m, 4H), 3.82 – 3.69 (m, 8H), 3.65 (s, 1H). ^{13}C NMR (151 MHz, d_2o) δ 102.24, 100.94, 97.88, 78.58, 73.16, 72.66, 70.66, 70.61, 70.23, 70.14, 69.87, 69.79, 66.84, 66.78, 66.44, 65.67, 61.03, 60.84. ESI-MS (*m*/*z*): $[M+Na]^+$ cald 527.1583, obsd 527.1.

Azido-α-D-mannopyranosyl-(1→2)-α-D-mannopyranosyl-(1→6)-α-D-mannopyranoside (25)

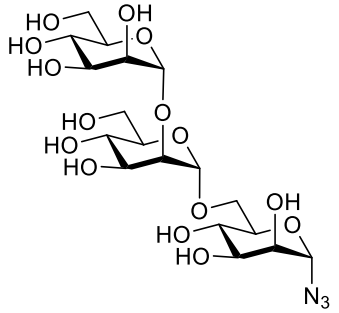

To a stirred solution of trimannose **72** (39 mg, 0.114 mmol) in D_2O (1.5 mL), DIPEA (0.200 mL, 1.139 mmol), sodium azide (74 mg, 1.139 mmol), imidazolonium salt (46 mg, 0.342 mmol) were added at 0 °C. After 1.5 h, the reaction mixture was concentrated and purified by silica gel column chromatography using DCM:Methanol (9:1) as an eluent to obtain azide **25** (0.034 g, 81 %). ^{1}H NMR (600 MHz, Methanol-d_4) δ 5.34 (d, *J* = 1.6 Hz, 1H), 5.14 (s, 1H), 4.98 (d, *J* = 1.7 Hz, 1H), 3.98 (d, *J* = 2.3 Hz, 1H), 3.95 – 3.90 (m, 2H), 3.88 – 3.82 (m, 4H), 3.72 (tdd, *J* = 18.4, 10.1, 3.3 Hz, 8H), 3.66 – 3.58 (m, 3H). ^{13}C NMR (151 MHz, cd_3od) δ 104.11, 100.01, 91.92, 80.49, 75.63, 74.88, 74.50, 72.41, 72.14, 72.01, 71.90, 71.69, 69.02, 68.73, 67.97, 67.36, 63.01, 62.95. ESI-MS (*m*/*z*): $[M+Na]^+$ cald 552.1647, obsd 552.2.

Azido-2, 3, 4, 6-tetra-*O*-acetyl-α-D-mannopyranosyl-(1→2)-3, 4, 6-tri-*O*-acetyl-α-D-mannopyranosyl-(1→6)-2, 3, 4-tri-*O*-acetyl-α-D-mannopyranoside (25a)

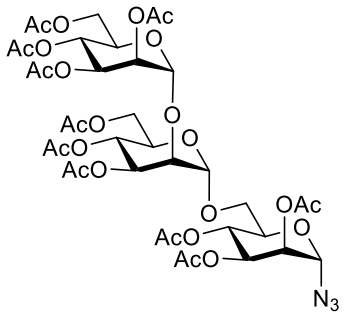

To a stirred solution of azide **25** (0.034 g, 0.027 mmol) in 1 mL of pyridine, 500 µL of acetic anhydride was added at 0 °C. The reaction mixture was stirred at room temperature and heated up to 45 °C. After 16 h, the solvent was evaporated and the crude product was purified by silica gel column chromatography using Hexane: Ethylacetate (3:2) as an eluent to obtain **25a**.^{1}H NMR (400 MHz, Chloroform-*d*) δ 5.45 – 5.20 (m, 9H), 5.15 (t, *J* = 2.4 Hz, 1H), 4.97 (d, *J* = 1.9 Hz, 1H), 4.90 (d, *J* = 1.9 Hz, 1H), 4.28 – 4.07 (m, 7H), 3.99 (ddd, *J* = 9.8, 4.3, 2.5 Hz, 1H), 3.88 – 3.77 (m, 1H), 3.62 (dd, *J* = 11.1, 2.7 Hz, 1H), 2.17 (s, 3H), 2.15 (s, 3H), 2.14 (s, 3H), 2.09 (s, 3H), 2.07 (s, 3H), 2.06 (s, 3H), 2.04 (s, 3H), 2.04 (s, 3H), 2.01 (s, 3H), 1.99 (s, 3H). ^{13}C NMR (101 MHz, $cdcl_3$) δ 170.84, 170.48, 170.22, 169.87, 169.85, 169.74, 169.69, 169.60, 169.48, 169.45, 99.21, 98.28, 87.33, 76.83, 71.15, 70.16, 69.73, 69.06, 68.97, 68.65, 68.29, 68.22, 66.65, 66.32, 65.91, 65.77, 62.41, 62.11, 20.86, 20.69, 20.66, 20.64, 20.60. ESI-MS (*m*/*z*): $[M+Na]^+$ cald 972.2704, obsd 972.3.

3,4-bis(bis(2-ethoxy-2-oxoethyl)amino)benzamido-α-D-mannopyranosyl-(1→2)-α-D-mannopyranosyl-(1→6)-β-D-mannopyranoside (74)

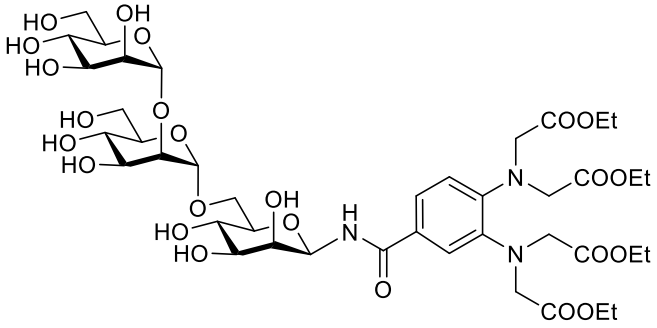

To the solution of azido-trimannose **25** (30 mg, 0.045 mmol) in ethylacetate (1 mL), Pd/C was added and the reaction mixture was stirred at room temperature under hydrogen gas atmosphere. After 2 h, the palladium was filtered through a celite pad to obtain the desired amine. The crude amine **73** was added to a solution containing acid **27** (25 mg, 0.050 mmol), HATU (17 mg, 0.046 mmol) and DIPEA (40 µL, 0.228 mmol) in 1 mL of DMF. The reaction progress was monitored with TLC. The volatiles were evaporated after 16 h and the residue was purified by silica gel column chromatography using DCM:Methanol (9:1) to give the desired product as an inseparable mixture of anomers. (20 mg, 0.018 mmol, 40 %). But before going to the next step, the anomers were separated by using HPLC to give β-anomer **74** (3 mg); Synergy 4 µ Hydro-RP 80A (250 x 10 mm), 3mL/min. ^{1}H NMR (600 MHz, Methanol-d_4) β-anomer: δ 7.61 (d, *J* = 2.1 Hz, 1H), 7.47 (dd, *J* = 8.4, 2.1 Hz, 1H), 7.06 (d, *J* = 8.5 Hz, 1H), 5.35 (d, *J* = 1.0 Hz, 1H), 5.14 (d, *J* = 1.4 Hz, 1H), 4.98 (d, *J* = 1.5 Hz, 1H), 4.39 (s, 4H), 4.30 (s, 4H), 4.11 – 4.06 (m, 8H), 3.96 (dd, *J* = 3.2, 1.8 Hz, 1H), 3.93 – 3.90 (m, 2H), 3.88 – 3.86 (m, 1H), 3.84 (dd, *J* = 9.0, 3.3 Hz, 1H), 3.77 (dt, *J* = 11.8, 1.9 Hz, 3H), 3.72 – 3.67 (m, 3H), 3.65 – 3.61 (m, 1H), 3.60 – 3.54 (m, 4H), 3.51 (t, *J* = 9.7 Hz, 1H), 3.44 (ddd, *J* = 9.8, 4.6, 1.7 Hz, 1H), 1.20 – 1.15 (m, 12H). ^{13}C NMR (101 MHz, MeOD) δ 172.32, 172.28, 168.92, 146.64, 142.30, 128.36, 123.35, 122.52, 121.61, 104.19, 99.97, 80.58, 79.94, 78.73, 75.68, 74.98, 74.50, 72.41, 72.33, 72.10, 71.88, 68.99, 67.92, 63.32, 62.99, 61.81, 61.78, 53.34, 53.20, 14.53, 14.50. ESI-MS (*m*/*z*): $[M+Na]^+$ cald 1004.3694, obsd 1004.3676.

3,4-bis(bis(2-carboxy-2-oxoethyl)amino)benzamido-α-D-mannopyranosyl-(1→2)-α-D-mannopyranosyl-(1→6)-β-D-mannopyranoside (75)

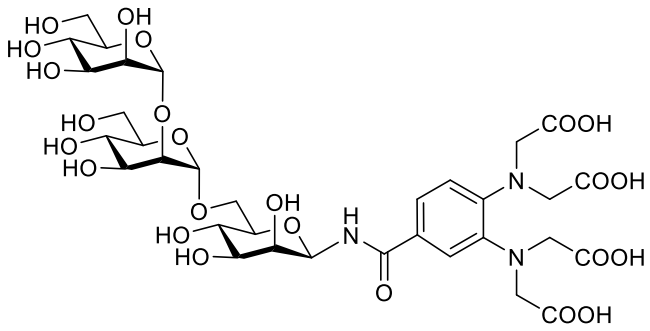

To a stirred solution of protected linker tagged trimannose **74** (0.020 g, 0.018 mmol) in 1 ml of methanol, 100 µL of 1 M NaOH solution was added and pH of the reaction mixture was maintained over 10.0. The reaction mixture was stirred at room temperature for 2 h, the reaction mixture was concentrated in *vacuo* and dried under high vacuum. Afterwards, the compound was purified using G-25 column to give **75** as a pure β-anomer for NMR study.

5.4 Experiment to Chapter 4

5.4.1 Synthesis of Man-I

Allyl-2, 3-di-*O*-acetyl-4-*O*-(2-naphthylmethyl)-6-*O*-*tert*butyldiphenylsilyl-α-D-mannopyranoside (82a)

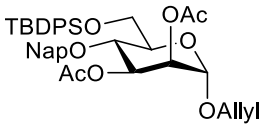

To a stirred solution of diol **64** (4.1 g, 6.85 mmol) in pyridine (10 mL) at 0 °C, acetic anhydride (6.5 mL) was added. The reaction mixture was warmed up to room temperature and let it stirred for 10 h. After that the reaction mixture was diluted using DCM and washed with saturated solution of $NaHCO_3$, the product was extracted three times using DCM. The combined organic layer was washed with brine, dried over Na_2SO_4, filtered and concentrated under reduced pressure. The crude product was purified using silica gel chromatography to yield the desired product **82a** (4.3 g, 6.85 mmol, 94 %) ^{1}H NMR (400 MHz, $CDCl_3$) δ 7.88 – 7.57 (m, 8H), 7.52 – 7.27 (m, 9H), 5.87 (d, *J* = 5.1 Hz, 1H), 5.46 (dd, *J* = 9.9, 3.3 Hz, 1H), 5.32 – 5.14 (m, 3H), 4.91 – 4.73 (m, 3H), 4.24 – 4.10 (m, 2H), 4.08 – 3.90 (m, 3H), 3.82 (ddd, *J* = 9.9, 3.6, 1.6 Hz, 1H), 2.14 (s, 3H), 1.97 (s, 3H), 1.12 (s, 9H). ^{13}C NMR (101 MHz, $CDCl_3$) δ 170.18, 169.94,

135.96, 135.60, 135.50, 133.79, 133.37, 133.20, 132.94, 132.90, 129.66, 129.64, 128.12, 127.86, 127.69, 127.64, 127.52, 126.13, 126.09, 125.89, 125.55, 117.90, 96.21, 75.02, 73.07, 72.53, 71.86, 70.46, 67.96, 62.60, 26.78, 21.00, 20.94, 19.43.

Allyl-2, 3-di-*O*-acetyl-4-*O*-(2-naphthylmethyl)-α-D-mannopyranoside (82)

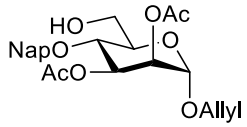

In a 50 ml centrifuge tube, to the stirred solution of silyl ether **82a** (2 g, 2.93 mmol) in THF (5 mL), 1.8 mL of HF-Pyridine was added and the reaction mixture was stirred at room temperature for 12-16 hours. The reaction mixture was quenched by adding sat. $NaHCO_3$ solution drop wise. The resulting mixture was extracted three times (25 mL) with DCM and the combined organic layer was dried over Na_2SO_4, filtered and concentrated under reduced pressure. The crude residue was purified using silica column chromatography to yield the desired product **82** (1.2 g, 2.93 mmol, 94 %). ^{1}H NMR (400 MHz, $CDCl_3$) δ 7.87 – 7.79 (m, 3H), 7.74 (s, 1H), 7.48 (dd, *J* = 6.6, 2.9 Hz, 2H), 7.40 (dd, *J* = 8.5, 1.6 Hz, 1H), 5.88 (td, *J* = 10.8, 5.2 Hz, 1H), 5.43 (dd, *J* = 9.8, 3.4 Hz, 1H), 5.33 – 5.26 (m, 2H), 5.21 (dd, *J* = 10.5, 1.5 Hz, 1H), 4.90 – 4.81 (m, 3H), 4.22 – 4.13 (m, 1H), 4.06 – 3.95 (m, 2H), 3.85 (ddd, *J* = 13.5, 7.3, 3.4 Hz, 3H), 2.13 (s, 3H), 1.94 (s, 3H). ^{13}C NMR (101 MHz, $CDCl_3$) δ 170.00, 169.83, 135.35, 133.19, 133.14, 132.94, 128.22, 127.85, 127.77, 127.66, 126.34, 126.19, 125.99, 125.55, 118.40, 118.07, 96.63, 77.31, 76.99, 76.67, 75.02, 72.86, 72.21, 71.79, 71.70, 70.19, 68.69, 68.35, 67.31, 61.72, 20.90. ESI-HRMS (*m*/*z*): $[M+Na]^+$ cald 467.1676, obsd 467.1677.

5.4.2 Synthesis of bilipidated biphosphorylated GPI

Allyl-2,3,4-tri-*O*-benzyl-6-*O*-tri*iso*propylsilyl-α-D-mannopyranosyl-(1→2)-3,4,6-tri-*O*-benyl-α-D-mannopyranosyl-(1→6)-2,3-di-*O*-acetyl-4-*O*-(2-naphthyl)methyl-α-D-mannopyranoside (88)

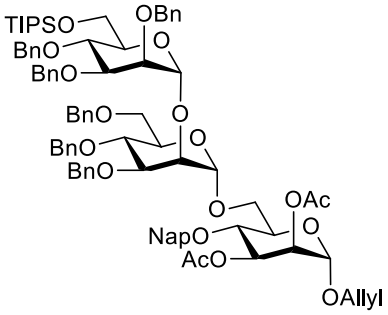

A glycosyl acceptor **82** (0.250 g, 0.562 mmol) and glycosyl donor **6** (0.732 g, 0.619 mmol) were dissolved and co-evaporated with dry toluene three times and dried under high vacuum for 2 h. The reaction mixture was dissolved in dry thiophene:toluene (2:1) under argon atmosphere, followed by the addition of activated powdered molecular sieves. Then, 25 μL of TBSOTf was added to the reaction mixture under argon atmosphere. After 2 h, the reaction was quenched by using triethylamine, filtered the molecular sieves and concentrated. The residue was purified using column chromatography to obtain trisaccharide **88** (0.420 g, 51 %, only α-anomer, rest is β-anomer) ^{1}H NMR (400 MHz, $CDCl_3$) δ 7.72 – 7.57 (m, 4H), 7.40 – 7.33 (m, 2H), 7.27 – 7.04 (m, 31H), 5.85 – 5.74 (m, 1H), 5.36 (dd, *J* = 9.5, 3.5 Hz, 1H), 5.25 – 5.17 (m, 5H), 5.09 (dq, *J* = 10.3, 1.3 Hz, 1H), 4.85 – 4.68 (m, 5H), 4.62 (d, *J* = 11.7 Hz, 1H), 4.57 – 4.34 (m, 9H), 4.29 (d, *J* = 12.2 Hz, 1H), 4.15 (t, *J* = 2.3 Hz, 1H), 4.07 (ddt, *J* = 12.9, 5.1, 1.5 Hz, 1H), 3.94 – 3.81 (m, 7H), 3.76 (t, *J* = 9.5 Hz, 1H), 3.71 – 3.67 (m, 3H), 3.63 (ddd, *J* = 9.6, 4.1, 2.2 Hz, 1H), 3.60 – 3.49 (m, 3H), 3.43 (d, *J* = 11.1 Hz, 1H), 2.01 (s, 3H), 1.85 (s, 3H), 0.96 (d, *J* = 4.3 Hz, 18H). ^{13}C NMR (101 MHz, $CDCl_3$) δ 169.98, 169.75, 138.78, 138.69, 138.47, 138.42, 137.96, 135.39, 133.18, 133.09, 132.84, 128.45, 128.35, 128.30, 128.27, 128.21, 128.19, 128.11, 128.06, 128.03, 127.98, 127.95, 127.92, 127.84, 127.73, 127.69, 127.65, 127.62, 127.48, 127.41, 127.36, 127.33, 127.31, 126.10, 125.84, 125.67, 125.12, 118.38, 99.09, 98.48, 96.14, 80.15, 79.67, 75.17, 75.06, 74.85, 74.68, 74.66, 74.64, 73.94, 73.43, 73.11, 72.25, 72.14, 72.10, 71.95, 71.93, 71.84, 70.54, 70.21, 69.04, 68.06, 66.09, 63.17, 53.42, 20.91, 20.90, 18.04, 18.00, 11.97.

2,3,4-tri-*O*-benzyl-6-*O*-tri*iso*propylsilyl-α-D-mannopyranosyl-(1→2)-3,4,6-tri-*O*-benyl-α-D-mannopyranosyl-(1→6)-2,3-di-*O*-acetyl-4-*O*-(2-naphthyl)methyl-α-D-mannopyranosyl trichloroacetamidate (90)

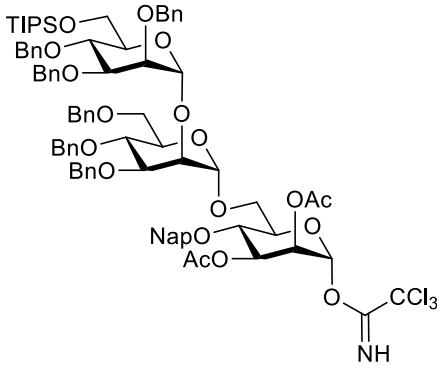

A solution of $[IrCOD(PPh_2Me)_2]PF_6$ (10.0 mg) in THF (1 mL) was stirred under hydrogen atmosphere until the color of the solution turned from red to colorless to pale yellow. The hydrogen atmosphere was exchanged with Argon. This solution was added to a solution of trisaccharide **88** (0.300 g, 0.205 mmol) in THF (7 mL). After 16 h, the solvent was removed in *vacuo* and the residue was dissolved in a mixture of acetone (2.7 mL) and water (0.3 mL). Mercury (II) chloride (278 mg, 1.023 mmol) and mercury(II) oxide (4.5 mg, 0.020 mmol) were added. After 1 h, saturated $NaHCO_3$ (aq) was added and the reaction mixture was extracted three times with dichloromethane. The combined organic layer was dried over Na_2SO_4, filtered and concentrated. The crude product was purified by silica gel column chromatography to give trisaccharide hemiacetal (260 mg, 0.205 mmol, 89 % yield) as colorless oil.

To a stirred solution of hemiacetal (240 mg, 0.168 mmol) in a dry DCM (5 mL), 2,2,2-trichloroacetonitrile (169 µL, 1.683 mmol) and DBU (5 µL, 0.034 mmol) were added at 0 °C. The reaction mixture was stirred and warmed up to room temperature. After 2 h, volatiles were evaporated and the crude reaction mixture was purified using silica gel column chromatography to get the imidate **90** (220 mg, 0.168 mmol, 83 %)

2,3,4-Tri-*O*-benzyl-6-*O*-triisopropylsilyl-α-D-mannopyranosyl-(1→2)-3,4,6-tri-*O*-benzyl-α-D-mannopyranosyl-(1→6)-4-*O*-(2-naphthyl)methyl-α-D-mannopyranosyl-(1→4)-2-azido-3,6-di-*O*-benzyl-2-deoxy-α-D-glucopyranosyl-(1→6)-1-*O*-allyl-2,3,4,5-tetra-*O*-benzyl-D-*myo*-inositol (80a)

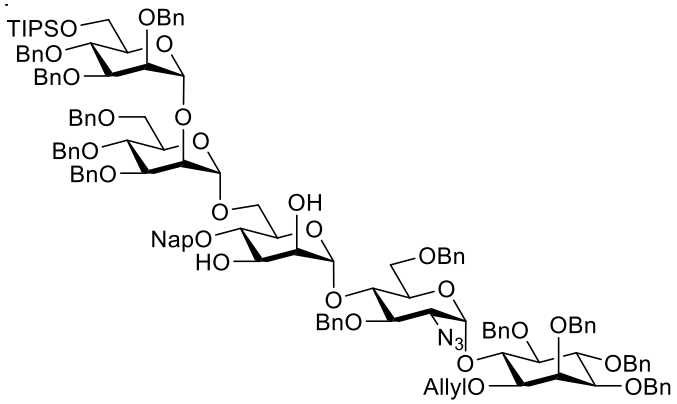

A mixture of glycosyl acceptor **7** (0.110 g, 0.116 mmol) and glycosyl donor **90** (0.220 g, 0.139 mmol) was dissolved and co-evaporated with dry toluene three times and dried under high vacuum for 2 h. The dried reaction mixture was dissolved in dry toluene (5 mL) under argon atmosphere followed by the addition of activated powdered molecular sieves. Then, 15 μL of TMSOTf was added to the reaction mixture under argon atmosphere at -40 °C, after 1.30 h, the reaction was quenched by using triethylamine, filtered the molecular sieves and concentrated. The residue was purified using column chromatography to obtain **80** (0.230 g, 84 %, only α-anomer). The compound was characterized using mass spectrometry. MALDI-MS (*m*/*z*): $[M+Na-N_2]^+$ cald 2349.0761, obsd 2349.074.

In the next step, pentasaccharide **80** was dissolved in Methanol:DCM (7:3) followed by the addition of freshly prepared sodium methoxide. The reaction mixture was stirred at room temperature and maintained the pH above 8.0. The reaction was quenched using Amberlite H^+ resin. The reaction mixture was filtered and purified using silica gel column chromatography to obtain **80a** (0.147 g, 0.065 mmol, 66 %).^{1}H NMR (400 MHz, $CDCl_3$) δ 7.77 – 7.57 (m, 4H), 7.40 – 6.99 (m, 63H), 5.86 (ddt, *J* = 17.2, 10.6, 5.5 Hz, 1H), 5.67 (d, *J* = 3.7 Hz, 1H), 5.21 (dd, *J* = 17.3, 1.6 Hz, 2H), 5.14 – 5.08 (m, 2H), 4.98 – 4.90 (m, 3H), 4.83 (dd, *J* = 10.7, 7.7 Hz, 2H), 4.77 (s, 2H), 4.73 – 4.52 (m, 10H), 4.47 (s, 2H), 4.40 – 4.29 (m, 6H), 4.26 (d, *J* = 1.6 Hz, 2H), 4.19 (d, *J* = 9.6 Hz, 1H), 4.12 (s, 1H), 4.01 (d, *J* = 5.9 Hz, 1H), 3.96 – 3.88 (m, 5H), 3.83 – 3.60 (m, 10H), 3.58 – 3.48 (m, 4H), 3.42 – 3.36 (m, 1H), 3.35 – 3.27 (m, 4H), 3.26 – 3.19 (m, 3H), 3.15 (dd, *J* = 10.2, 3.7 Hz, 1H), 3.04 (dd, *J* = 11.3, 3.3 Hz, 1H), 0.97 (h, *J* = 1.7 Hz, 21H). ^{13}C NMR (101 MHz, $CDCl_3$) δ 139.02, 138.82, 138.76, 138.63, 138.56, 138.47, 138.43, 138.38, 138.24, 138.20, 138.09, 137.75, 136.28, 134.21, 133.30, 132.85, 128.61, 128.55, 128.43, 128.41, 128.36, 128.31, 128.27, 128.24, 128.18, 128.12, 128.04, 128.03, 127.97, 127.95, 127.90,

127.88, 127.77, 127.73, 127.71, 127.67, 127.65, 127.56, 127.52, 127.42, 127.38, 127.30, 127.28, 127.22, 126.84, 126.08, 125.76, 125.55, 125.40, 117.13, 100.98, 99.12, 98.17, 97.43, 81.90, 81.84, 81.42, 80.83, 80.72, 80.11, 79.68, 75.86, 75.43, 75.07, 75.04, 74.86, 74.64, 74.49, 74.38, 74.29, 74.06, 73.66, 73.21, 73.13, 72.84, 72.75, 72.08, 72.04, 71.95, 71.83, 71.63, 71.35, 70.82, 69.50, 68.97, 68.35, 65.75, 63.45, 62.83, 18.10, 18.06, 12.04. MALDI-MS (*m*/*z*): $[M+Na-N_2]^+$ cald 2265.0550, obsd 2265.168.

2,3,4-Tri-*O*-benzyl-6-*O*-triisopropylsilyl-α-D-mannopyranosyl-(1→2)-3,4,6-tri-*O*-benzyl-α-D-mannopyranosyl-(1→6)-2,3-di-*O*-benzyl-4-*O*-(2-naphthyl)methyl-α-D-mannopyranosyl-(1→4)-2-azido-3,6-di-*O*-benzyl-2-deoxy-α-D-glucopyranosyl-(1→6)-1-*O*-allyl-2,3,4,5-tetra-*O*-benzyl-D-*myo*-inositol (80b)

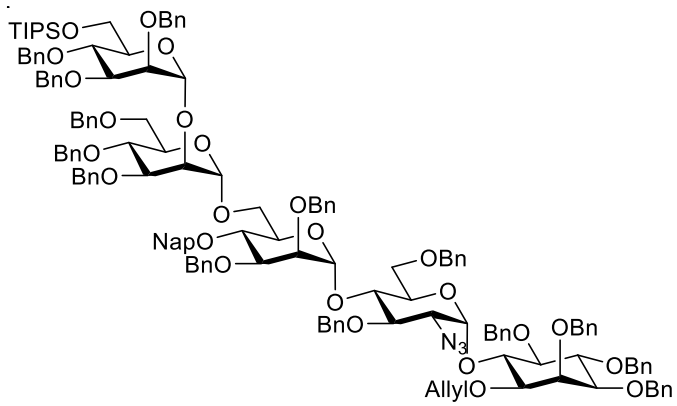

To a solution of **80a** (0.140 g, 0.062 mmol) in THF (2 mL) at 0 °C, NaH (6 mg, 0.247 mmol) and 15-crown-5 (0.014 g, 0.062 mmol) were added. The reaction mixture was stirred for 30 min and benzyl bromide (BnBr) (0.022 ml, 0.185 mmol) and DMF (2 mL) were added to the reaction mixture. The reaction mixture was stirred at room temperature for 2 h. The reaction mixture was cooled down to 0 °C, quenched by the addition of H_2O dropwise and the solvent was evaporated using rotavapour. The residue was extracted using ethylacetate and water. The organic layer was dried over anhydrous sodium sulfate, filtered and concentrated. The residue was purified using silica gel column chromatography to obtain compound **80b** (0.130 g, 86 %). ^{1}H NMR (400 MHz, $CDCl_3$) δ 7.75 – 7.53 (m, 4H), 7.38 – 6.95 (m, 73H), 5.84 (ddd, *J* = 11.9, 10.4, 5.2 Hz, 1H), 5.69 (d, *J* = 3.7 Hz, 1H), 5.24 – 5.02 (m, 5H), 4.94 – 4.76 (m, 6H), 4.71 – 4.51 (m, 11H), 4.45 – 4.21 (m, 13H), 4.19 – 4.09 (m, 2H), 4.07 – 3.98 (m, 5H), 3.98 – 3.89 (m, 3H), 3.85 – 3.70 (m, 7H), 3.63 – 3.47 (m, 6H), 3.39 – 3.21 (m, 7H), 3.17 (dt, *J* = 9.8, 4.2 Hz, 2H), 0.96 (q, *J* = 3.3, 2.3 Hz, 21H). ^{13}C NMR (101 MHz, $CDCl_3$) δ 139.08, 138.81, 138.70, 138.54, 138.47, 138.43, 138.34, 138.23, 138.18, 137.92, 137.84, 136.53, 134.16, 133.27,

132.72, 128.54, 128.48, 128.42, 128.39, 128.32, 128.27, 128.20, 128.16, 128.13, 128.10, 128.00, 127.98, 127.95, 127.86, 127.80, 127.75, 127.71, 127.68, 127.64, 127.61, 127.50, 127.47, 127.33, 127.24, 127.16, 127.13, 127.09, 127.05, 126.95, 126.80, 125.91, 125.56, 125.41, 125.32, 117.07, 100.41, 99.14, 98.30, 97.45, 81.85, 81.40, 80.83, 80.12, 80.02, 79.60, 76.14, 75.79, 75.42, 75.23, 74.99, 74.92, 74.83, 74.52, 74.30, 73.99, 73.72, 73.64, 73.18, 73.06, 72.77, 72.59, 72.48, 72.11, 72.01, 71.93, 71.83, 71.76, 71.44, 70.75, 69.57, 68.96, 68.51, 66.24, 65.35, 63.22, 62.76, 18.05, 18.01, 11.99. MALDI-MS (*m*/*z*): $[M+Na-N_2]^+$ cald 2445.1489, obsd 2445.080.

2,3,4-Tri-*O*-benzyl-6-*O*-triisopropylsilyl-α-D-mannopyranosyl-(1→2)-3,4,6-tri-*O*-benzyl-α-D-mannopyranosyl-(1→6)-2,3-di-*O*-benzyl-4-*O*-(2-naphthyl)methyl-α-D-mannopyranosyl-(1→4)-2-azido-3,6-di-*O*-benzyl-2-deoxy-α-D-glucopyranosyl-(1→6)-2,3,4,5-tetra-*O*-benzyl-D-*myo*-inositol (92)

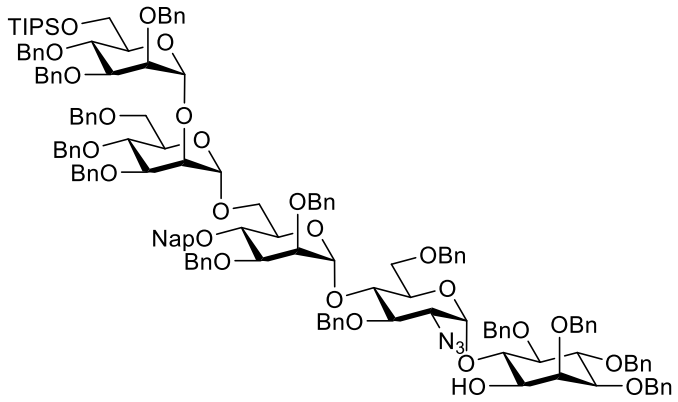

A solution of $[IrCOD(PPh_2Me)_2]PF_6$ (15.0 mg) in THF (1 mL) was stirred under hydrogen until the color turned from red to colorless to pale yellow. The hydrogen atmosphere was exchanged with Argon. This solution was added to a solution of pseudopentasaccharide **80b** (0.130 g, 0.053 mmol) in THF (2 mL). After 16 h, the solvent was removed and the residue was dissolved in a mixture of acetone (2.7 mL) and water (0.3 mL). Mercury (II) chloride (72 mg, 0.265 mmol) and mercury (II) oxide (2.5 mg, 10.60 µmol) were added. After 1 h, saturated $NaHCO_3$ (aq) was added and the reaction mixture was extracted three times with dichloromethane. The combined organic layers were dried over Na_2SO_4, filtered and concentrated. The crude product was purified by silica gel column chromatography to give pseudopentasaccharide **92** (100 mg, 0.041 mmol, 78 % yield) as colorless oil. ^{1}H NMR (400 MHz, $CDCl_3$) δ 7.76 – 7.66 (m, 1H), 7.64 – 7.55 (m, 3H), 7.40 – 6.94 (m, 73H), 5.44 (d, *J* = 3.6 Hz, 1H), 5.22 (d, *J* = 2.2 Hz, 1H), 5.14 (s, 1H), 5.04 – 4.79 (m, 6H), 4.63 (dddd, *J* = 30.7, 17.7, 11.5, 6.7 Hz, 10H),

4.43 – 4.19 (m, 13H), 4.12 (dd, *J* = 12.2, 3.1 Hz, 3H), 3.92 (tq, *J* = 6.4, 3.0 Hz, 5H), 3.87 – 3.70 (m, 7H), 3.64 – 3.53 (m, 8H), 3.40 (dd, *J* = 9.9, 2.3 Hz, 1H), 3.35 – 3.21 (m, 7H), 2.91 (d, *J* = 7.4 Hz, 1H), 0.95 (d, *J* = 4.0 Hz, 21H). ^{13}C NMR (101 MHz, cdcl$_3$) δ 139.04, 138.74, 138.64, 138.48, 138.46, 138.45, 138.41, 138.39, 138.36, 138.24, 138.08, 138.04, 137.95, 137.64, 136.36, 133.27, 132.77, 129.47, 128.46, 128.44, 128.42, 128.34, 128.30, 128.22, 128.16, 128.13, 128.10, 128.08, 127.98, 127.93, 127.87, 127.82, 127.80, 127.78, 127.76, 127.71, 127.69, 127.66, 127.63, 127.54, 127.50, 127.45, 127.40, 127.36, 127.34, 127.28, 127.22, 127.19, 126.86, 125.93, 125.61, 125.49, 125.45, 100.10, 99.17, 98.31, 97.56, 81.74, 81.31, 80.91, 80.52, 80.24, 79.65, 75.97, 75.78, 75.33, 75.00, 74.97, 74.91, 74.84, 74.56, 74.39, 74.24, 73.73, 73.30, 73.22, 73.09, 73.04, 72.55, 72.20, 72.10, 72.02, 71.88, 71.46, 70.40, 68.98, 68.68, 67.75, 66.28, 64.00, 62.87, 18.07, 18.03, 12.00. MALDI-MS (*m*/*z*): [M+K-N$_2$]$^+$ cald 2421.0951, obsd 2421.419.

Triethylammonium 1,2-di-*O*-stearoyl-*sn*-glycero-3-H-phosphonate (86)

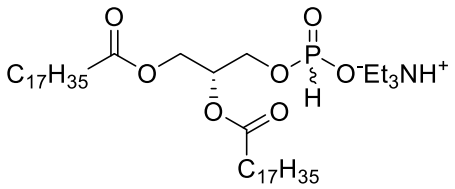

A mixture of 1,2-distearoyl-sn-glycerol (200 mg, 0.320 mmol) and phosphonic acid (26.2 mg, 0.320 mmol) were dissolved and co-evaporated three times with pyridine. The resulting mixture was dissolved in anhydrous pyridine (10 mL) and pivaloyl chloride (38.6 mg, 0.320 mmol) was added dropwise. The reaction mixture was stirred under nitrogen atmosphere at room temperature for two days. The volatiles were removed under reduced pressure and the resulting solid was purified by silica gel column chromatography to give H-phosphonate **86** (175 mg, 0.254 mmol, 79% yield) as a white solid. All spectra are in good agreement with literature.[29, 77] ^{31}P NMR (121 MHz, CDCl$_3$:MeOD = 10:1) d 4.87; MALDI-MS (*m*/*z*): [M+2Na]$^+$ cald 733.5119, obsd 733.5130.

2,3,4-Tri-*O*-benzyl-α-D-mannopyranosyl-(1→2)-3,4,6-tri-*O*-benzyl-α-D-mannopyranosyl-(1→6)-2,3-di-*O*-benzyl-4-*O*-(2-naphthyl)methyl-α-D-mannopyranosyl-(1→4)-2-azido-3,6-di-*O*-benzyl-2-deoxy-α-D-glucopyranosyl-

(1→6)-1-*O*-(1,2-dimyristoyl-sn-glyceryl-phosphonato)-2,3,4,5-tetra-*O*-benzyl-D-*myo*-inositol (93a)

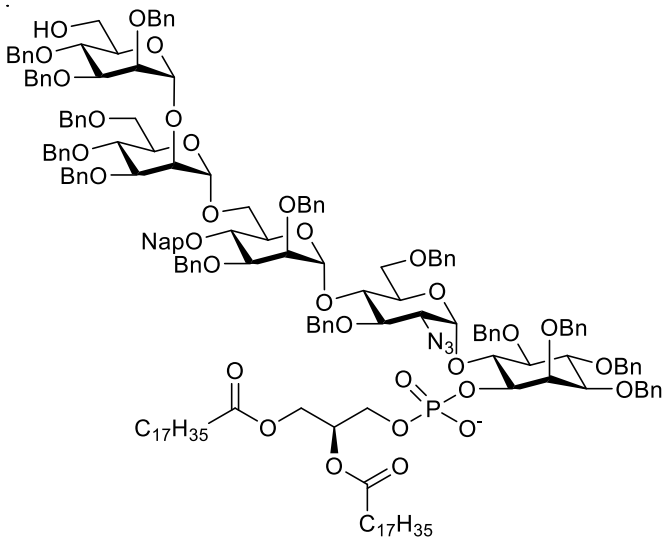

The pentasaccharide **92** (98 mg, 0.041 mmol) and H-phosphonate **86** (161 mg, 0.203 mmol) were dissolved and co-evaporated with anhydrous pyridine (3 x 3 mL) and dried under high vacuum overnight. The reaction mixture was dissolved in anhydrous pyridine (2 mL) at room temperature and pivaloyl chloride (20 µL, 0.163 mmol) was added. The resulting reaction mixture was stirred at room temperature for 3 h. Iodine (36.3 mg, 0.143 mmol) in a mixture of pyridine/water (19:1, 0.2 mL) was added to oxidize P (III) to P (V). The reaction mixture was further stirred for 2 h at room temperature to the complete the oxidation. The reaction mixture was diluted with $CHCl_3$ and washed with aqueous $Na_2S_2O_3$ solution to remove the excess iodine. The aqueous layer was further washed with $CHCl_3$ and the combined organic layer was dried over Na_2SO_4, filtered and concentrated under reduced pressure to give the crude residue, which was subjected to flash column with Et_3N-deactivated silica gel to give **93** (70 mg, 55 %) as a syrup. R_f = 0.25 ($CHCl_3$/MeOH = 20: 1).

In the second step, the pentasaccharide **93** (70 mg, 0.023 mmol) was passed through a column of Amberlite IR120 ion exchange resin (Na^+ form) using $CHCl_3$/MeOH (1:1) as eluent. The eluate was collected and concentrated to dryness. The obtained residue was then dissolved in CH_3CN (2.5 mL) with a trace of H_2O (100 µL). $Sc(OTf)_3$ (55.6 mg, 0.113 mmol) was added to the reaction mixture and the resulting mixture was heated to 45 ºC and stirred overnight. The reaction mixture was cooled down to room temperature

and few drops of pyridine was added to quench any excess $Sc(OTf)_3$. The reaction mixture was evaporated to dryness and subjected to flash column chromatography with Et_3N-deactivated silica gel to afford **93a** (45 mg, 67.7 %) as a syrup. R_f = 0.24 ($CHCl_3$/MeOH = 20 : 1); ^{1}H NMR (400 MHz, $CDCl_3$:MeOD=10:1) δ 7.77 – 7.69 (m, 1H), 7.62 (td, *J* = 10.6, 8.5, 5.3 Hz, 3H), 7.35 (ddd, *J* = 13.0, 6.1, 4.1 Hz, 4H), 7.27 – 6.99 (m, 69H), 5.81 (s, 1H), 5.17 (d, *J* = 9.2 Hz, 2H), 5.03 – 4.65 (m, 12H), 4.60 – 4.49 (m, 5H), 4.44 – 3.94 (m, 25H), 3.87 – 3.56 (m, 13H), 3.55 – 3.41 (m, 4H), 3.31 (d, *J* = 11.2 Hz, 3H), 2.84 (qd, *J* = 7.3, 4.2 Hz, 4H), 2.16 (dq, *J* = 8.0, 4.7 Hz, 4H), 1.52 – 1.37 (m, 4H), 1.21 – 1.09 (m, 56H), 0.81 (t, *J* = 6.7 Hz, 6H). ^{13}C NMR (101 MHz, $CDCl_3$:MeOD=10:1) δ 173.50, 173.10, 139.73, 138.64, 138.49, 138.43, 138.35, 138.03, 137.95, 136.52, 133.30, 132.80, 128.55, 128.47, 128.41, 128.34, 128.29, 128.22, 128.18, 128.07, 128.01, 127.96, 127.90, 127.84, 127.77, 127.69, 127.65, 127.49, 127.38, 127.24, 127.11, 126.87, 125.98, 125.65, 100.90, 99.53, 99.35, 96.59, 81.73, 80.98, 79.77, 79.30, 75.00, 74.85, 74.55, 74.19, 73.76, 73.15, 72.78, 72.30, 72.17, 72.05, 71.90, 71.69, 70.53, 69.54, 68.99, 68.73, 66.05, 63.73, 62.97, 62.79, 62.17, 50.85, 45.40, 34.31, 34.11, 31.96, 29.83, 29.76, 29.71, 29.58, 29.41, 29.20, 24.87, 22.73, 18.10, 14.17, 12.03, 8.44. ^{31}P NMR (162 MHz, $CDCl_3$:MeOD =10:1) δ -1.63. ESI-HRMS (*m*/*z*): $[M+Na+NH_4]^{2+}$ calcd 1491.2763; obsd, 1491.2341; $[M-H]^-$ cald 2939.5188, obsd, 2939.3640.

(6 *O*-(2-(*N*-(*tert*-butoxycarbonyl)-S-(*tert*-butyl)-L-cysteinyl)aminoethyl phosphonato)-2,3,4-Tri-*O*-benzyl-α-D-mannopyranosyl-(1→2)-3,4,6-tri-*O*-benzyl-α-D-mannopyranosyl-(1→6)-2,3-di-*O*-benzyl-4-*O*-(2-naphthyl)methyl-α-D-mannopyranosyl-(1→4)-2-azido-3,6-di-*O*-benzyl-2-deoxy-α-D-glucopyranosyl-(1→6)-1-*O*-(1,2-dimyristoyl-sn-glyceryl-phosphonato)-2,3,4,5-tetra-*O*-benzyl-D-*myo*-inositol (78)

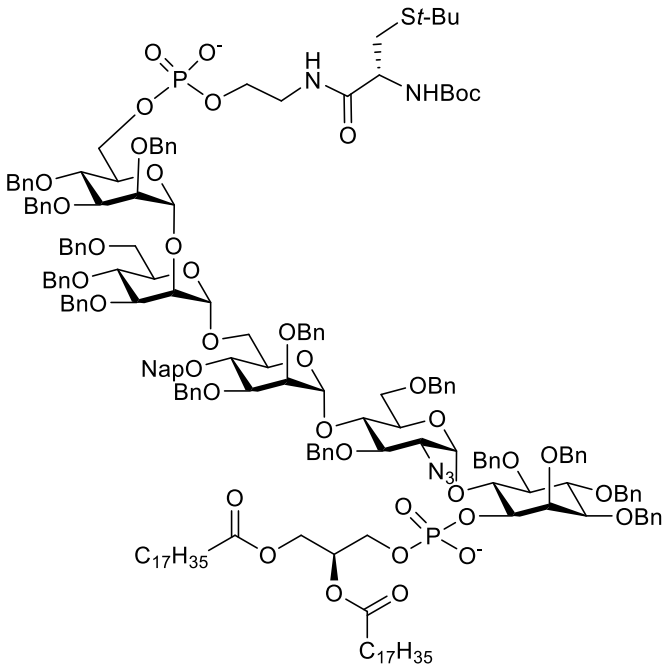

The bilipidated pseudopentasaccharide **93a** (40 mg, 0.014 mmol) and H-phosphonate **84** (39 mg, 0.102 mmol) were dissolved and co-evaporated with anhydrous pyridine (3 x 3 mL) and dried under high vacuum overnight. The reaction mixture was dissolved in anhydrous pyridine (2 mL) at room temperature and pivaloyl chloride (13 µL, 0.102 mmol) was added. The resulting reaction mixture was stirred at room temperature for 5 h. The progress of the reaction was monitored by using TLC analysis. Iodine (26 mg, 0.102 mmol) in a mixture of pyridine/water (19:1, 0.2 mL) was added to oxidize P (III) to P (V). The reaction mixture was further stirred for 2 h at room temperature to complete the oxidation, diluted with $CHCl_3$, washed with aqueous $Na_2S_2O_3$ solution to remove the excess iodine. The aqueous layer was further washed with $CHCl_3$ and the combined organic layer was dried over Na_2SO_4, filtered and concentrated under reduced pressure to give the crude residue, which was subjected to flash column with Et_3N-deactivated silica gel to give **78** (32 mg, 70 %) as a syrup. R_f = 0.35 ($CHCl_3$/MeOH = 10: 1); ^{1}H NMR (700 MHz, $CDCl_3$:MeOD=10:1) δ 7.73 (d, *J* = 7.8 Hz, 1H), 7.66 – 7.57 (m, 3H), 7.47 – 6.76 (m, 73H), 5.92 – 5.80 (m, 1H), 5.43 (d, *J* = 8.0 Hz, 1H), 5.23 – 5.13 (m, 1H), 4.99 (dd, *J* = 43.0, 10.7 Hz, 3H), 4.87 – 4.78 (m, 4H), 4.74 – 4.50 (m, 10H), 4.45 – 4.30 (m, 14H), 4.28 – 4.21 (m, 5H), 4.18 – 4.08 (m, 2H), 4.03 (dtd, *J* = 15.1, 10.3, 9.2, 6.4 Hz, 6H), 3.98 – 3.91 (m, 3H), 3.89 – 3.74 (m, 4H), 3.74 – 3.63 (m, 6H), 3.61 – 3.41 (m, 8H), 3.28 – 3.13 (m, 4H), 3.07 (d, *J* = 7.1 Hz, 1H), 2.81 (d, *J* = 5.4 Hz, 2H), 2.17 (qd, *J* = 8.3, 7.9, 4.8 Hz, 4H), 1.49 – 1.45 (m, 4H), 1.34 (s, 9H), 1.17 (d, *J* = 13.0 Hz, 65H), 0.81 (t, *J* = 7.0 Hz, 6H). ^{13}C NMR (151 MHz, $CDCl_3$:MeOD=10:1) δ 173.32, 172.95, 170.17, 155.15,

139.78, 138.84, 138.70, 138.63, 138.46, 138.36, 138.12, 137.99, 136.56, 133.27, 132.72, 128.50, 128.35, 128.31, 128.26, 128.20, 128.11, 128.04, 127.97, 127.88, 127.79, 127.74, 127.69, 127.63, 127.56, 127.47, 127.40, 127.31, 127.18, 127.08, 126.89, 125.91, 125.54, 125.39, 125.23, 100.81, 99.53, 99.04, 96.27, 81.82, 81.71, 80.98, 79.98, 79.86, 79.30, 76.34, 76.10, 75.93, 75.62, 74.83, 74.61, 74.49, 74.23, 73.84, 73.74, 73.10, 72.87, 72.30, 72.25, 72.17, 71.99, 71.83, 71.66, 70.57, 69.33, 68.96, 68.84, 66.30, 64.04, 63.78, 63.62, 63.10, 62.80, 54.13, 42.33, 41.28, 34.27, 34.06, 31.89, 31.66, 30.91, 29.68, 29.63, 29.50, 29.33, 29.13, 28.33, 24.88, 24.84, 22.65, 14.08. ^{31}P NMR (162 MHz, $CDCl_3$:MeOD = 10:1) δ 1.73, -1.61. ESI-HRMS (*m*/*z*): $[M+2K]^{2+}$ cald 1701.2959, obsd, 1701.2985; $[M-2H]^{2-}$ cald 1661.3255, obsd 1661.3218.

(6-(*N*-(S-S-mercaptoethanol-L-Cysteinyl)aminoethanol-phosphonato)-α-D-mannopyranosyl-(1→2)-α-D-mannopyranosyl-(1→6)-α-D-mannopyranosyl-(1→4)-2-amino-2-deoxy-α-D-glucopyranosyl-(1→6)-1-*O*-(1,2-dimyristoyl-sn-glycerol-phosphate)-D-*myo*-inositol (GPI 76)

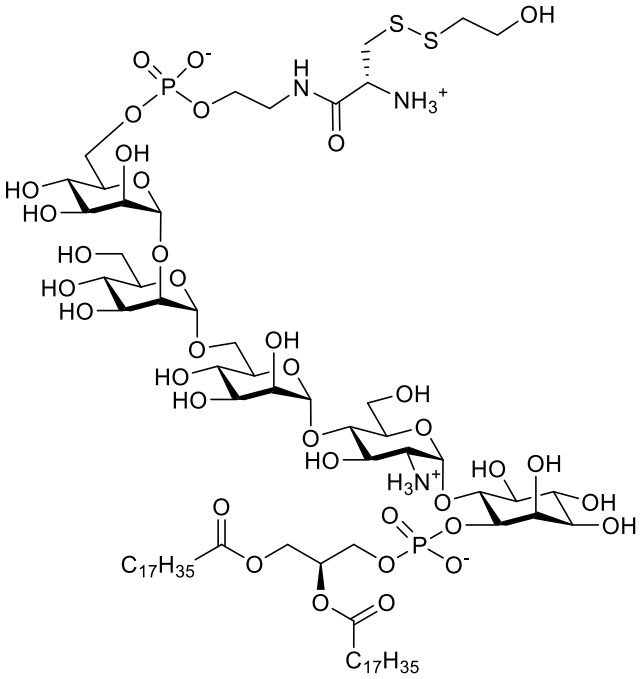

The bisphosphorylated pseudopentasaccharide **78** (10.0 mg, 0.003 mmol) was dissolved in mixture of THF/MeOH/H_2O (2:1:1, 5 mL) with formic acid (4 % v/v, 200 μL) at room temperature and Pd/C (256 mg, 0.24 mmol, 10% Pd content) was added. Hydrogen gas was bubbled through the solution for 15 min and the reaction mixture was stirred under an atmosphere of hydrogen gas for additional 16 h. The palladium was removed by

filtration through a pad of celite and the solvents were removed under reduced pressure to give 30 mg of the crude product. The debenzylated crude intermediate compound was confirmed by mass spectrometry. The crude material (4 mg) was then dissolved at 0 °C in a mixture of trifluoroacetic acid and anisole (11 ml, 10:1 v/v) and stirred for 5 min. Then $Hg(TFA)_2$ (9.1 mg, 21 μmol) was added to the reaction mixture and stirred for an additional 30 min. the volatiles were removed under high vacuum at 0 °C. The resulting solid residue was dissolved in an AcOH/water mixture (15 mL, 7:3 v/v) and mercaptoethanol (400 μL, 5.7 mmol) was added at room temperature. The mixture was stirred at the same temperature for 10 h. The solution was dried on a rotary evaporator, to give a pale yellow residue. The amphiphilic nature of GPI **76** (1.3 mg, 35 %) hampered the further purification process and the efforts to characterize it by NMR.

5.4.3 Synthesis of monolipidated triphosphorylated GPI

2,3,4-Tri-*O*-benzyl-6-*O*-triisopropylsilyl-α-D-mannopyranosyl-(1→2)-3,4,6-tri-*O*-benzyl-α-D-mannopyranosyl-(1→6)-3, 4-di-*O*-benzyl-2-*O*-(ethanolazido phosphate)-α-D-mannopyranosyl-(1→4)-2-azido-3,6-di-*O*-benzyl-2-deoxy-α-D-glucopyranosyl-(1→6)- 2,3,4,5-tetra-*O*-benzyl-1-*O*-octadecyl-phosphonato)-D-*myo*-inositol (94)

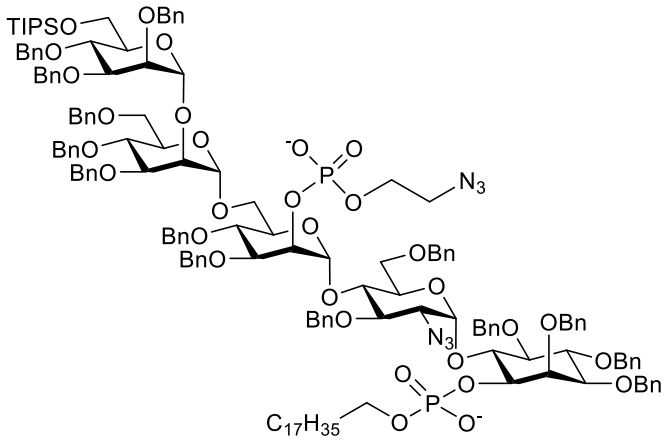

R_f = 0.35 ($CHCl_3$/MeOH = 10: 1); ^{1}H NMR (300 MHz, $CDCl_3$:MeOD=10:1) δ 7.41 – 7.09 (m, 70H), 5.63 (bs), 5.49 (bs), 5.16 (s, 1H), 4.93 – 4.23 (m, 32H), 4.05 – 3.32 (m, 25H), 3.13 (m, 2H), 2.97 (d, 3H), 2.74 (q, 4H), 1.54 (bs, 2H), 1.20 (bs, 2H), 1.03 (m, 46H), 0.81 (t, 6H). ^{31}P NMR (121 MHz, $CDCl_3$:MeOD=10:1) δ -0.07, -0.37. MALDI-HRMS (*m*/*z*); $[M+2H+Na]^+$ cald 2774.3082, obsd 2774.300.

2,3,4-Tri-*O*-benzyl-α-D-mannopyranosyl-(1→2)-3,4,6-tri-*O*-benzyl-α-D-mannopyranosyl-(1→6)-3, 4-di-*O*-benzyl-2-*O*-(ethanolazido phosphate)-α-D-

mannopyranosyl-(1→4)-2-azido-3,6-di-*O*-benzyl-2-deoxy-α-D-glucopyranosyl-(1→6)- 2,3,4,5-tetra-*O*-benzyl-1-*O*-octadecyl-phosphonato)-D-*myo*-inositol (95)

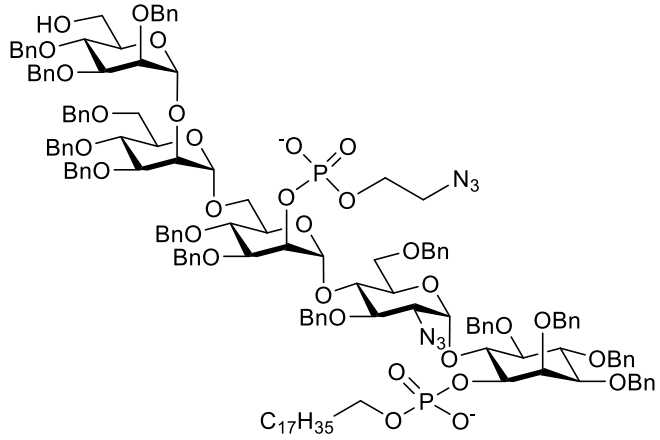

The bisphosphorylated pseudopentasaccharide **94** (55 mg, 14.7 mmol) was passed through a column of Amberlite IR120 ion exchange resin (Na^+ form) using $CHCl_3$/MeOH (1:1) as eluent. The eluate was collected and concentrated to dryness. The obtained residue was then dissolved in CH_3CN (2.5 mL) with a trace of H_2O (1.5 mL). $Sc(OTf)_3$ (28.9 mg, 58.8 mmol) was added to the reaction mixture and heated up to 45 ºC and stirred overnight. The reaction mixture was cooled down to the room temperature and few drops of pyridine were added to quench any excess $Sc(OTf)_3$ and the reaction mixture was evaporated to dryness and subjected to flash column chromatography with Et_3N-deactivated silica gel to afford **95** (40 mg, 77 %) as a syrup. R_f = 0.30 ($CHCl_3$/MeOH = 10 : 1); ^{1}H NMR (300 MHz, $CDCl_3$:MeOD=10:1) δ 7.51 – 7.02 (m, 70H), 5.71 (bs), 5.44 (bs), 5.12 (s, 1H), 4.95 – 4.29 (m, 32H), 4.18 – 3.17 (m, 25H), 3.13 (m, 2H), 3.07 (m, 2H), 2.90 (q, 4H), 2.16 (m, 1H),1.97 (m, 1H), 1.56 (bs, 2H), 1.30-1.16 (m, 26H), 0.81 (m, 3H). ^{13}C NMR (75 MHz, $CDCl_3$:MeOD=10:1) δ 140.78, 140.02, 139.95, 139.86, 139.76, 139.72, 139.63, 139.49, 139.42, 139.21, 131.25, 131.04, 129.85, 129.52, 129.41, 129.27, 129.23, 129.18, 128.98, 128.89, 128.77, 128.56, 128.49, 100.99, 100.59, 98.08, 83.13, 82.12, 81.04, 80.64, 79.87, 77.98, 77.23, 77.01, 76.44, 76.26, 76.17, 75.87, 74.65, 74.37, 74.06, 73.62, 73.38, 73.26, 73.07, 71.65, 70.31, 67.83, 67.48, 65.52, 64.25, 62.65, 53.83, 52.53, 47.31, 33.25, 32.19, 31.02, 30.84, 30.67, 30.59, 30.47, 28.47, 27.21, 27.04, 23.98, 15.16, 9.63; ^{31}P NMR (121 MHz, $CDCl_3$:MeOD=10:1) δ -0.06, -0.43. MALDI-HRMS (*m*/*z*); $[M+3Na]^+$ cald 2662.1386, obsd 2662.139.

6-*O*-(2-(*N*-(*tert*-butoxycarbonyl)-S-(*tert*-butyl)-L-cysteinyl)aminoethyl phosphonato)-2,3,4-Tri-*O*-benzyl-α-D-mannopyranosyl-(1→2)-3,4,6-tri-*O*-benzyl-α-

D-mannopyranosyl-(1→6)-3, 4-di-*O*-benzyl-2-*O*-(ethanolazido phosphate)-α-D-mannopyranosyl-(1→4)-2-azido-3,6-di-*O*-benzyl-2-deoxy-α-D-glucopyranosyl-(1→6)- 2,3,4,5-tetra-*O*-benzyl-1-*O*-octadecyl-phosphonato)-D-*myo*-inositol (79)

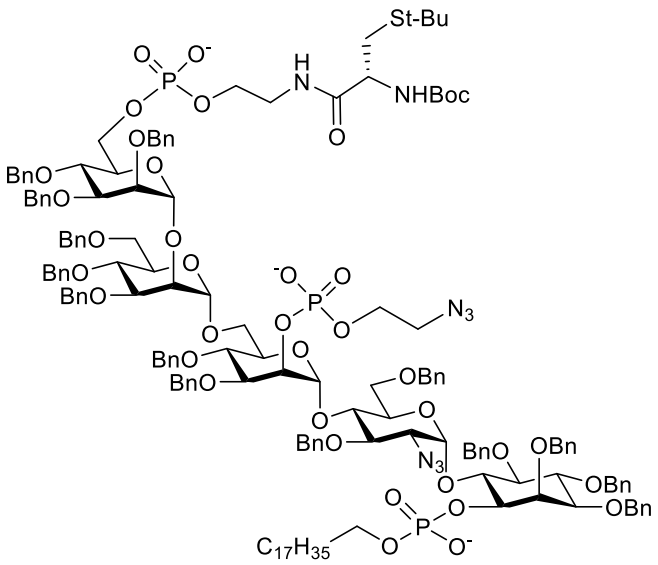

The bisphosphorylated pseudopentasaccharide **95** (40 mg) and H-phosphonate **84** (113 mg, 0.143 mmol) were dissolved and co-evaporated with anhydrous pyridine (3 x 3 mL) and dried under high vacuum overnight. The reaction mixture was dissolved in anhydrous pyridine (2 mL) at room temperature and pivaloyl chloride (35.2 mL, 0.284 mmol) was added. The resulting reaction mixture was stirred at room temperature for 5 h. The progress of the reaction was monitored by using TLC. Iodine (36.3 mg, 0.143 mmol) in a mixture of pyridine/water (19:1, 0.2 mL) was added to oxidize P (III) to P (V). The reaction mixture was further stirred for 2 h at room temperature to complete the oxidation, diluted with $CHCl_3$ and washed with aqueous $Na_2S_2O_3$ solution to remove the excess iodine. The aqueous layer was further washed with $CHCl_3$ and the combined organic layer was dried over Na_2SO_4, filtered and concentrated under reduced pressure to give the crude residue, which was subjected to flash column with Et_3N-deactivated silica gel to give **79** (55 mg, 72 %) as a syrup. R_f = 0.26 ($CHCl_3$/MeOH = 10: 1). ^{31}P NMR (242.9 MHz, $CDCl_3$: MeOD=1:1) δ -1.65, -2.08, -2.53; MALDI-HRMS (*m*/*z*); $[M+3H+Na]^+$ cald 3000.3075, obsd 3000.299.

6-(*N*-(*S*-*S*-mercaptoethanol-L-cysteinyl)aminoethyl phosphonato)-2,3,4-Tri-*O*-benzyl-α-D-mannopyranosyl-(1→2)-3,4,6-tri-*O*-benzyl-α-D-mannopyranosyl-(1→6)-3, 4-di-*O*-benzyl-2-*O*-(ethanolamino phosphate)-α-D-mannopyranosyl-(1→4)-2-

azido-3,6-di-*O*-benzyl-2-deoxy-α-D-glucopyranosyl-(1→6)- 2,3,4,5-tetra-*O*-benzyl-1-*O*-octadecyl-phosphonato)-D-*myo*-inositol (GPI 77)

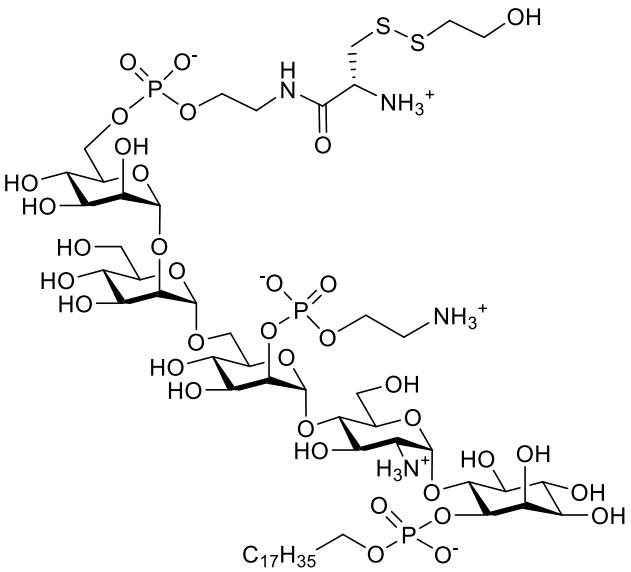

The triphosphorylated pseudopentasaccharide **79** (20.0 mg, 0.006 mmol) was dissolved in mixture of THF/MeOH/H_2O (2:1:1, 5 mL) with formic acid (4 % v/v, 200 μL) at room temperature and Pd/C (256 mg, 0.24 mmol, 10% Pd content) was added. Hydrogen gas was bubbled through the solution for 15 min and the reaction mixture was stirred under an atmosphere of hydrogen gas for additional 16 h. The palladium was removed by filtration through a pad of celite and the solvents were removed under reduced pressure to give 5 mg of crude product. The debenzylated intermediate was confirmed by mass spectrometry. The crude material (5 mg) was then dissolved at 0 °C in a mixture of trifluoroacetic acid and anisole (11 ml, 10:1 v/v) and stirred for 5 min. Then $Hg(TFA)_2$ (9.1 mg, 21 μmol) was added to the reaction mixture and stirred for an additional 30 min. All volatile compounds were then removed under high vacuum at 0 °C. The resulting solid residue was dissolved in an AcOH/water mixture (15 mL, 7:3 v/v) and mercaptoethanol (400 μL, 5.7 mmol) was added at room temperature. The reaction mixture was stirred for 10 h. After filtration of the solid residues over a pad of Celite, the solution was dried on a rotary evaporator to give a pale yellow residue. The amphiphilic nature of GPI **77** (2.4 mg, 50 %) hampered the further purification process and the efforts to characterize it by NMR. MALDI-HRMS (*m*/*z*); $[M+OH]^-$ cald 1601.5665, obsd 1601.5883.

Appendix 1

A. Synthesis of Glycan for affinity Chromatography

Carbohydrates are ubiquitous and play an important role in various inter- and intra-cellular processes. Over the last decade, the interactions between the carbohydrates and the proteins that recognize them have been described in many biological events such as cell adhesion,[156] signal transduction,[157] host pathogen recognition[158] and inflammation.[158] In many examples these carbohydrate-protein interactions are recognized as a key mode of interactions between microbial pathogens and animal cells.[156, 159]

Carbohydrates and proteins are targeted in the development of therapeutics. For this reason, it is highly important to investigate the structure and specificity of carbohydrate-binding proteins. One of the method that have found a broad application in this field is the isolation and purification of proteins by affinity chromatographic technique.[160] In this method, the carbohydrate of interest is conjugated to a solid support and is used as a ligand for proteins. Agarose beads are the most commonly used solid support used for the immobilization of the carbohydrate ligands containing a thiol or amino group. (Figure A.1)

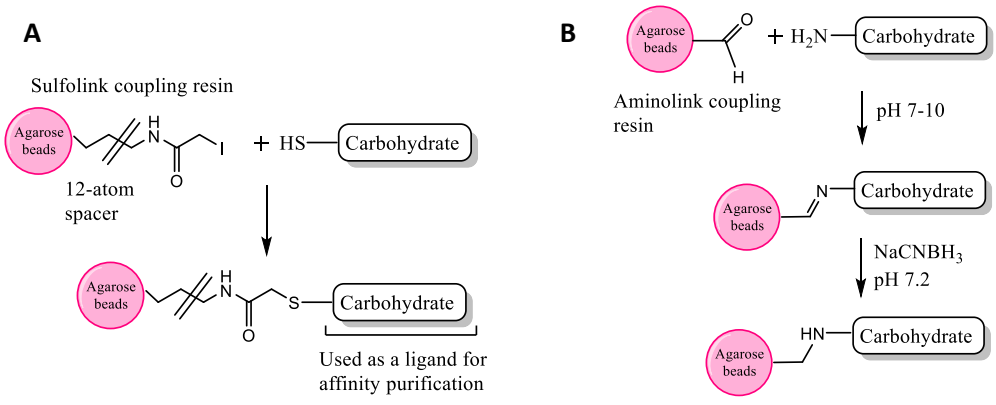

Figure A.1: Immobilization chemistry: **A**. Sulfhydryl groups react with iodoacetyl groups to form covalent bonds. **B.** Aldehyde activated beads which can be covalently attached to the primary amines.

A.1 Synthesis of a Trimannoside (Man*α*1-2-Man*α*1-6-Man) for the affinity purification of proteins

For the synthesis of phosphorylated trimannose **109** for glycan arrays and affinity purification of proteins, the required building blocks **40** and **101** were synthesized according to reported protocols.[87] For the assembly of trimannose using [2+1]-glycosylation strategy, a thiol linker will be first installed on the anomeric position of **101**. Then α (1→2)-dimannose donor can be used to glycosylate with acceptor of **103**.

First, the trichloroacetamidate donor **101** was used to glycosylate the thiol linker using TMSOTf to give **102** as pure α-product in 72 % yield. (Scheme A.1) Afterwards, the silyl protecting group (TIPS) was removed from 6-*O* position of **102** with scandium triflate to furnish the acceptor **103** in 75 % yield. The donor **105** was synthesized by glycosylation of the acceptor **40** with the donor **101** in four steps involving: a glycosylation using TMSOTf to form dimannose, removing allyl ether by isomerization and following hydrolysis of the intermediate enol ether. Finally, the imidate group was installed at the anomeric center of the dimannose and directly used in a [2+1]-glycosylation with acceptor **103**.

The glycosylation to obtain the α-trisaccharide **106** was carried out using thiophene and DCM in 2:1 ratio with TBSOTf as an activator. The product was isolated in 70 % yield. Removal of TIPS from 6-*O* position of the Man III residue from **106** using scandium triflate released the alcohol **107**, which was phosphitylated with H-phosphonate **8** and oxidized by using iodine in wet pyridine to obtain **108** in 85 % yield. Reductive global deprotection using birch conditions gave the crude trisaccharide **109,** which was purified by size exclusion chromatography giving pure compound **109** as a mixture of the free thiol and disulfide form.

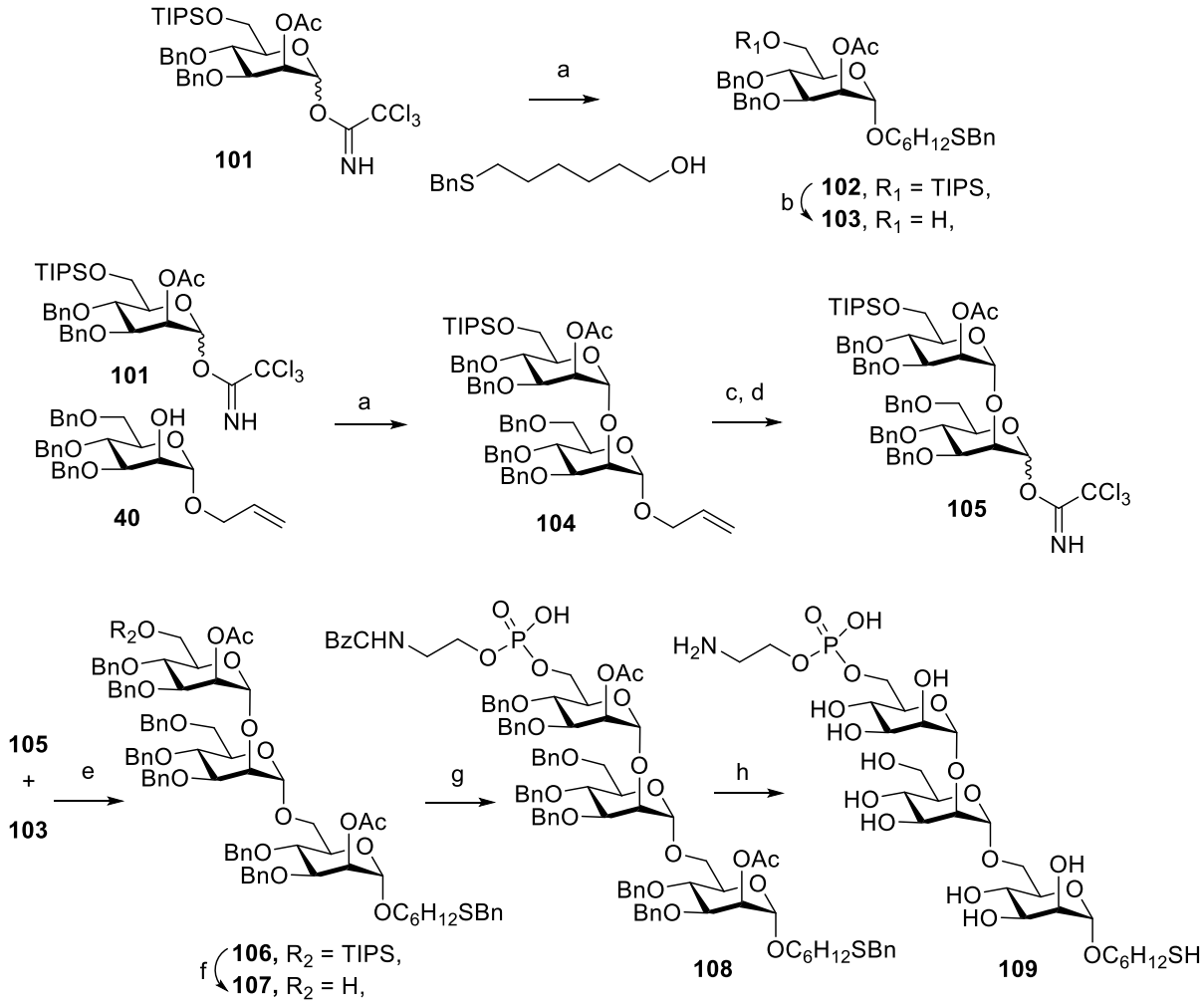

Scheme A.1: Synthesis of trimannoside phosphate: a) TMSOTf, DCM, 0 °C, 72 %; b) $Sc(OTf)_3$,ACN:DCM (2:1), H_2O, 75 %; c) i) H_2, $[Ir(COD)(PMePh_2)_2]PF_6$, THF; ii) HgO, $HgCl_2$, acetone, water, 5:1; d) CCl_3CN, DBU, DCM; e) TBSOTf, Thiophene: DCM (2:1), 0 °C, 70 %; f) $Sc(OTf)_3$,ACN:DCM (2:1), H_2O, 70 %; g) i) **8**, PivCl, pyr; ii) I_2, H_2O, pyr, 0 °C, 85 %; h) $NH_{3(l)}$, Na, MeOH, -78°C, 35 %

In order to perform affinity purification of proteins binding to **109**, the trisaccharide was covalently immobilized on agarose beads. To immobilize the compound, The thiol group of **109** was reacted with agarose beads containing a iodoacetyl group using50 mM Tris buffer at pH 8.5 (Figure A.1). Along with compound **109**, other carbohydrate structures of interest were also immobilized on the agarose beads. This project is carried out in collaboration with other colleagues of the department at the MPIKG, who are currently working on the affinity purification of the proteins and analyzing them using mass spectrometry. The results of these isolations and binding experiments will be reported separately.

A.2 Experimental Section

For general materials and methods, please refer to the experimental section 5.1, chapter 5.

1-*O*-(6-thiobenzyl) hexyl-2-*O*-acetyl-3,4-*O*-benzyl-6-*O*-tri*iso*propylsilyl-α-D-mannopyranoside (102)

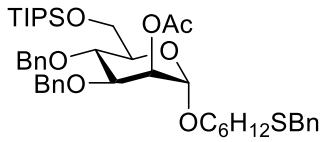

The trichloroacetamidate donor **101** (0.800 g, 1.138 mmol) and acceptor **110** (0.766 g, 3.41 mmol) were dissolved and coevaporated with dry toluene three times and dried under high vacuum for 1 h. After that the reaction mixture was dissolved in dry DCM under an atmosphere of argon followed by the addition of molecular sieves and let the reaction stirred for 10 min at 0 °C. Then, TMS-OTf (41 µL, 0.228 mmol) was added to the reaction mixture. After 1.30 h, the reaction was quenched by using trimethylamine, filtered and concentrated. The residue was purified using silica gel column chromatography to obtain **102** (625 mg, 72 %).^{1}H NMR (400 MHz, $CDCl_3$) δ 7.26 – 7.08 (m, 15H), 5.20 (dd, *J* = 3.3, 1.8 Hz, 1H), 4.79 (d, *J* = 10.7 Hz, 1H), 4.64 – 4.58 (m, 2H), 4.53 (d, *J* = 10.7 Hz, 1H), 4.45 (d, *J* = 11.1 Hz, 1H), 3.95 – 3.74 (m, 4H), 3.59 (d, *J* = 2.4 Hz, 2H), 3.52 (qd, *J* = 6.7, 3.7 Hz, 2H), 3.22 (dt, *J* = 9.7, 6.6 Hz, 1H), 2.29 (dd, *J* = 9.3, 5.4 Hz, 2H), 2.00 (s, 3H), 1.42 (dt, *J* = 14.5, 7.7 Hz, 4H), 1.25 – 1.16 (m, 4H), 0.97 (d, *J* = 4.6 Hz, 21H). ^{13}C NMR (101 MHz, $CDCl_3$) δ 170.56, 138.56, 138.52, 138.04, 128.78, 128.42, 128.40, 128.35, 128.34, 128.05, 128.02, 127.66, 127.65, 126.83, 97.28, 78.24, 75.29, 74.18, 72.78, 71.79, 69.00, 67.37, 62.70, 36.19, 31.20, 29.23, 29.04, 28.63, 25.75, 21.05, 17.99, 17.92, 11.99. ESI-MS (*m*/*z*): $[M+Na]^+$ cald 787.4034, obsd 787.4054.

1-*O*-(6-thiobenzyl)hexyl-2-*O*-acetyl-3,4-*O*-benzyl-α-D-mannopyranoside (103)

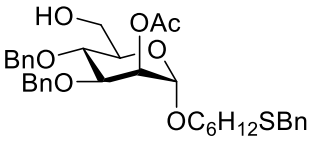

To a solution of **102** (0.600 mg, 0.784 mmol) in MeCN (10 mL) and DCM (5 mL), water (100 µL) and $Sc(OTf)_3$ (1.158 mg, 2.353 mmol) were added and the reaction mixture was heated up to 50 °C for 3 h. The reaction was quenched with pyridine (100 µL) and the

solvents were removed *in vacuo*. The residue was co evaporated with toluene (3 x 2 mL) and purified through silica gel column chromatography to obtain **103** (360 mg, 75 %). ^{1}H NMR (400 MHz, $CDCl_3$) δ 7.48 – 6.88 (m, 15H), 5.34 (dd, *J* = 3.4, 1.8 Hz, 1H), 4.90 (d, *J* = 10.9 Hz, 1H), 4.77 – 4.65 (m, 2H), 4.61 (d, *J* = 10.8 Hz, 1H), 4.53 (d, *J* = 11.2 Hz, 1H), 3.97 (dd, *J* = 9.3, 3.3 Hz, 1H), 3.79 (qd, *J* = 11.9, 5.4 Hz, 3H), 3.71 – 3.57 (m, 4H), 3.34 (dt, *J* = 9.6, 6.5 Hz, 1H), 2.39 (t, *J* = 7.3 Hz, 2H), 2.13 (s, 3H), 1.53 (q, *J* = 7.4 Hz, 4H), 1.39 – 1.23 (m, 4H). ^{13}C NMR (101 MHz, $CDCl_3$) δ 170.56, 138.56, 138.52, 138.04, 128.78, 128.42, 128.40, 128.35, 128.34, 128.05, 128.02, 127.66, 127.65, 126.83, 97.93, 78.10, 75.30, 74.25, 71.77, 71.67, 68.80, 67.83, 62.14, 36.22, 31.26, 29.33, 28.62, 25.97, 21.27. ESI-MS (*m*/*z*): $[M+Na]^+$ cald 631.2700, obsd 631.2714.

_n_-Allyl 2-_O_-acetyl-3,4-di-_O_-benzyl-6-_O_-tri_iso_propylsilyl-α-D-mannopyranosyl-(1→2)-3,4,6-tri-_O_-benzyl-α-D-mannopyranoside (104)

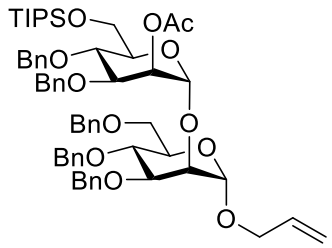

The mannosyl trichloroacetimidate **101** (1.65 g, 2.35 mmol) and allyl mannoside **40** (1.05 g, 2.13 mmol) were dissolved and coevaporated with toluene (10 mL x 3) and dried under high vacuum for 2 h. The reactants were dissolved in DCM (25 mL) and cooled down to 0 °C. Then, TMSOTf (45 μL, 0.24 mmol) was added to the reaction mixture and stirred at 0 °C for 30 min. The reaction mixture was quenched with Et_3N. The solvents were evaporated and the crude product was purified by silica gel column chromatography to give dimannose **104** (1.87 g, 85% yield) as a colorless oil. R_f = 0.33(EtOAc/cyclohexane 1:9); ^{1}H NMR (400 MHz, $CDCl_3$) δ 7.23-7.04 (m, 25 H), 5.74 (m, 1H), 5.38 (dd, *J* = 3.0, 1.9 Hz, 1H), 5.11 (ddd, *J* = 17.2, 3.2, 1.6 Hz, 1H), 5.04-5.01 (m, 2H), 4.78-4.72 (m, 3H), 4.60-4.50 (m, 5H), 4.43 (d, *J* = 11.0 Hz, 1H), 4.41 (d, *J* = 11.0 Hz, 1H), 4.31 (d, *J* = 11.0 Hz, 1H), 4.02 (ddt, *J* = 12.9, 5.1, 1.5 Hz, 1H), 3.98 (t, *J* = 2.3 Hz, 1H), 3.90-3.73 (m, 7H), 3.66-3.56 (m, 4H), 1.95 (s, 3H), 0.97 (s, 18 H), 0.96 (s, 3H); ^{13}C NMR (101 MHz, $CDCl_3$) δ 170.16, 138.89, 138.64, 138.57, 138.46, 138.32, 133.91, 128.45, 128.40, 128.25, 128.15, 127.99, 127.67, 127.62, 127.51, 117.27, 99.00, 98.25, 80.23, 78.21, 75.28, 74.76, 74.20, 73.63, 73.43, 73.28, 72.14, 72.08, 72.04, 69.42,

68.99, 67.91, 62.85, 21.06, 18.15, 18.09, 12.20; MALDI-HRMS (*m*/*z*): $[M+Na]^+$ cald 1053.5155, obsd 1053.5130.

2-*O*-Acetyl-3,4-di-*O*-benzyl-6-*O*-triisopropylsilyl-α-D-mannopyranosyl-(1→2)-3,4,6-tri- *O*-benzyl-α-D-mannopyranosyl trichloroacetimidate (105)

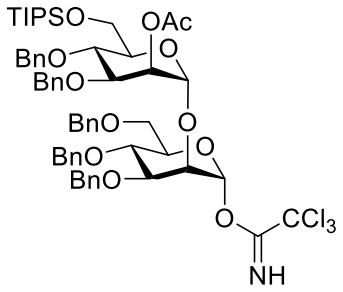

The dimannose **104** (74 mg, 0.072 mmol) was dissolved in MeOH (2 mL) and DCM (0.5 mL). $PdCl_2$ (4 mg, 0.023 mmol) was added to this solution. The reaction mixture was stirred for 5 h. The reaction mixture was diluted with ethyl acetate (20 mL) and washed with sat. sodium bicarbonate solution (3x 20 mL). The organic layer was dried over Na_2SO_4, filtered and evaporated to dryness. The residue was dissolved in DCM (1 mL) and 2,2,2-trichloroacetonitrile (72 μL, 0.718 mmol) and DBU (1.1 μL, 7.2 μmol) were added at 0 °C. The reaction mixture was stirred for 1 h at 0°C and solvents were evaporated to yield brown oil. The crude compound was purified using flash column chromatography on deactivated silica gel (with 0.5 % TEA) to give imidate **105** (48 mg, 0.042 mmol, 59 % yield over two steps) as yellow oil: R_f = 0.28 (hexane/ethyl acetate 10:1); [α]D20: + 29.4 (c = 0.80 $CHCl_3$); ^{1}H NMR (400 MHz, $CDCl_3$) δ 8.53 (s, 1H, NH), 7.39 – 7.13 (m, 25H), 6.29 (d, J = 1.9 Hz, 1H), 5.51 – 5.49 (m, 1H, =CH), 4.90 (d, J = 3.3 Hz, 1H), 4.87 (d, J = 3.3 Hz, 1H), 4.72 – 4.59 (m, 6H), 4.50 (d, J = 12.1 Hz, 1H), 4.44 (d, J = 11.1 Hz, 1H), 4.12 (t, J = 2.4 Hz, 1H), 4.09 – 3.86 (m, 8H), 3.83 – 3.77 (m, 2H), 3.73 – 3.68 (m, 1H), 2.11 (s, 3H, Me of Ac), 1.17 – 1.02 (m, 21H, TIPS).; ^{13}C NMR (101 MHz, $CDCl_3$) δ 170.32, 160.27, 138.93, 138.54, 138.36, 138.30, 138.10, 128.57, 128.50, 128.47, 128.42, 128.41, 128.31, 128.24, 128.07, 128.01, 127.91, 127.87, 127.72, 127.67, 127.63, 127.54, 99.31, 97.07, 91.11, 78.99, 78.16, 75.51, 75.35, 75.01, 74.10, 74.04, 73.69, 73.45, 72.46, 72.44, 72.16, 69.08, 68.90, 62.55, 45.99, 21.12, 18.19, 18.12, 12.25; ESI-MS (*m*/*z*): $[M+Na]^+$ cald 1158.3927, obsd 1158.3992.

1-*O*-(6-thiobenzyl)hexyl-2-*O*-acetyl-3,4-*O*-benzyl-6-*O*-tri*iso*propylsilyl-α-D-mannopyranosyl-(1→2)-3,4,6-tri-*O*-benzyl α-D-mannopyranosyl-(1→6)-2-*O*-acetyl-3,4-*O*-benzyl-α-D-mannopyranoside (106)

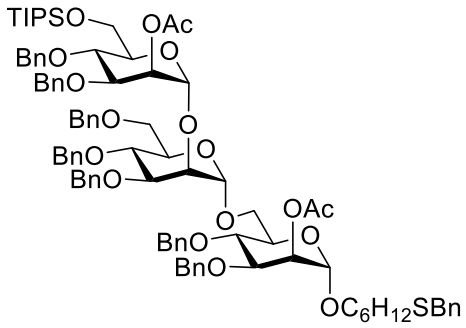

A mixture of trichloroacetamidate donor **105** (0.466 g, 0.411 mmol) and acceptor **103** (0.250 g, 0.411 mmol) was dissolved and coevaporated with dry toluene three times and dried under high vacuum for 1 h. After that the reaction mixture was dissolved in dry thiophene:DCM (2:1) mixture under an atmosphere of argon followed by the addition of molecular sieves. The reaction mixture was stirred for 10 min at 0 °C. Then, TBS-OTf (20 µL, 0.082 mmol) was added to the reaction mixture. After 1 h, the reaction mixture was quenched with trimethylamine, filtered and concentrated. The residue was purified using silica gel column chromatography to obtain **106** (300 mg, 46 %, only α). ^{1}H NMR (400 MHz, $CDCl_3$) δ 7.38 – 6.88 (m, 40H), 5.46 – 5.20 (m, 2H), 5.06 (s, 1H), 4.86 – 4.73 (m, 4H), 4.69 – 4.47 (m, 7H), 4.46 – 4.29 (m, 5H), 4.08 (s, 1H), 3.99 – 3.81 (m, 7H), 3.77 (t, *J* = 9.4 Hz, 1H), 3.69 – 3.59 (m, 6H), 3.54 – 3.42 (m, 4H), 3.30 – 3.20 (m, 1H), 2.32 (t, *J* = 7.3 Hz, 2H), 2.02 (s, 3H), 2.00 (s, 3H), 1.52 – 1.40 (m, 4H), 1.28 – 1.16 (m, 4H), 1.00 (d, *J* = 4.6 Hz, 21H). ^{13}C NMR (101 MHz, $CDCl_3$) δ 170.37, 170.21, 138.75, 138.56, 138.49, 138.39, 138.31, 138.10, 138.00, 137.76, 128.79, 128.51, 128.41, 128.37, 128.27, 128.22, 128.16, 127.88, 127.84, 127.76, 127.67, 127.60, 127.56, 127.51, 127.46, 127.33, 126.85, 98.88, 97.57, 79.55, 78.57, 77.92, 77.20, 75.20, 75.01, 74.89, 74.32, 73.95, 73.78, 73.34, 73.15, 73.10, 71.83, 71.69, 71.50, 70.52, 68.94, 68.86, 68.61, 67.70, 66.10, 62.54, 36.21, 31.21, 29.19, 29.03, 28.63, 25.81, 21.10, 21.02, 18.04, 17.96, 12.00. ESI-MS (*m*/*z*): $[M+Na]^+$ cald 1603.7544, obsd 1603.7558.

1-*O*-(6-thiobenzyl)hexyl-2-*O*-acetyl-3,4-*O*-benzyl-α-D-mannopyranosyl-(1→2)-3,4,6-tri-*O*-benzyl α-D-mannopyranosyl-(1→6)-2-*O*-acetyl-3,4-*O*-benzyl-α-D-mannopyranoside (107)

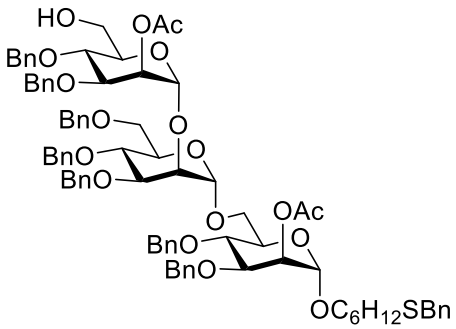

To a solution of trimannose **106** (0.300 mg, 0.190 mmol) in MeCN (5 mL) and DCM (3 mL), water (50 μL) and $Sc(OTf)_3$ (0.280 mg, 0.569 mmol) were added and the solution was heated up to 50 °C for 6 h. The reaction was quenched with pyridine (50 μL) and the solvents were removed *in vacuo*. The residue was co evaporated with toluene (3x 2 mL) and purified through silica gel column chromatography to obtain **107** (190 mg, 70 %). ^{1}H NMR (400 MHz, $CDCl_3$) δ 7.37 – 7.06 (m, 40H), 5.49 (t, *J* = 2.4 Hz, 1H), 5.37 – 5.31 (m, 1H), 5.00 (s, 2H), 4.90 – 4.79 (m, 3H), 4.75 – 4.56 (m, 7H), 4.52 – 4.35 (m, 5H), 4.04 (d, *J* = 2.2 Hz, 1H), 3.99 – 3.80 (m, 6H), 3.79 – 3.47 (m, 12H), 3.32 (dd, *J* = 9.5, 6.5 Hz, 1H), 2.38 (t, *J* = 7.3 Hz, 2H), 2.10 (s, 3H), 2.09 (s, 3H), 1.51 (dt, *J* = 13.9, 7.0 Hz, 4H), 1.37 – 1.28 (m, 4H). ESI-MS (*m*/*z*): $[M+Na]^+$ cald 1447.6210, obsd 1447.6229.

Triethylammonium-1-*O*-(6-thiobenzyl)hexyl-2-*O*-acetyl-3,4-*O*-benzyl-6-*O*-(2-*N*-benzyloxycarbonyl)aminoethyl-phosphonato-α-D-mannopyranosyl-(1→2)-3,4,6-tri-*O*-benzyl α-D-mannopyranosyl-(1→6)-2-*O*-acetyl-3,4-*O*-benzyl-α-D-mannopyranoside (108)

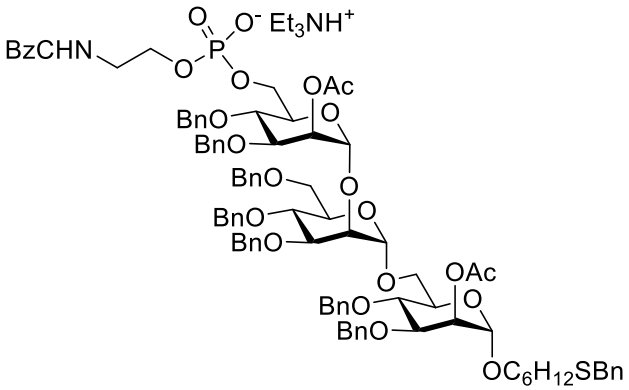

The alcohol **107** (0.125 g, 0.088 mmol) and H-phosphonate **8** (0.105 g, 0.438 mmol) were dissolved and co evaporated with dry pyridine (2 mL). The residue was dissolved in dry pyridine (2 mL) and PivCl (33 μL, 0.263 mmol) was added dropwise. The solution was stirred for 2 h at room temperature. Water (15 μL) and iodine (80 mg, 0.316 mmol) were added. The red solution was stirred for 1 h and quenched with sat. $Na_2S_2O_3$. The

reaction mixture was diluted with chloroform (10 mL) and dried over Na_2SO_4. The reaction mixture was filtered and concentrated in *vacuo*. The crude residue was purified through flash column chromatography on deactivated (1 % Et_3N in $CHCl_3$) silica gel using a gradient of MeOH in $CHCl_3$ from 0 %-<2 % MeOH to yield phosphate **108** as yellow oil (125 mg, 85 %). ^{1}H NMR (600 MHz, $CDCl_3$) δ 7.37 – 7.07 (m, 45H), 6.65 (t, *J* = 5.0 Hz, 1H), 5.50 (t, *J* = 2.1 Hz, 1H), 5.37 (dd, *J* = 3.4, 1.8 Hz, 1H), 5.09 – 5.00 (m, 3H), 4.94 (d, *J* = 2.0 Hz, 1H), 4.90 – 4.80 (m, 4H), 4.79 – 4.67 (m, 3H), 4.64 – 4.53 (m, 4H), 4.52 – 4.42 (m, 3H), 4.37 (dd, *J* = 11.7, 5.4 Hz, 2H), 4.27 (dt, *J* = 11.6, 3.8 Hz, 1H), 4.18 – 4.11 (m, 1H), 4.09 (t, *J* = 2.3 Hz, 1H), 4.02 – 3.86 (m, 7H), 3.82 (t, *J* = 9.6 Hz, 1H), 3.79 – 3.74 (m, 2H), 3.74 – 3.69 (m, 1H), 3.68 (s, 2H), 3.61 (dt, *J* = 9.8, 6.3 Hz, 2H), 3.56 (dd, *J* = 11.2, 4.7 Hz, 1H), 3.52 – 3.48 (m, 1H), 3.40 – 3.32 (m, 3H), 2.39 (t, *J* = 7.4 Hz, 2H), 2.11 (s, 3H), 2.07 (s, 3H), 1.57 – 1.48 (m, 4H), 1.37 – 1.23 (m, 4H). ^{13}C NMR (151 MHz, $cdcl_3$) δ 170.41, 170.02, 156.56, 138.87, 138.61, 138.56, 138.47, 138.17, 138.11, 137.89, 136.97, 128.80, 128.42, 128.39, 128.35, 128.26, 128.22, 128.18, 128.15, 128.13, 127.96, 127.89, 127.82, 127.71, 127.68, 127.59, 127.49, 127.43, 127.39, 127.35, 127.29, 126.84, 99.45, 98.84, 97.62, 79.31, 78.60, 77.91, 74.94, 74.88, 74.55, 74.40, 74.03, 73.93, 73.10, 71.81, 71.76, 71.71, 71.65, 71.60, 70.64, 69.01, 68.88, 68.69, 67.77, 66.26, 66.21, 64.33, 64.28, 64.24, 42.53, 36.27, 31.33, 29.26, 29.10, 28.66, 25.81, 21.12, 21.06. ^{31}P NMR (243 MHz, $cdcl_3$) δ 1.29. ESI-MS (*m*/*z*): $[M+H_3O+Et_3NH]^+$ cald 1783.8048, obsd 1783.8053.

1-*O*-(6-thiol)hexyl-6-*O*-aminoethyl-phosphonato-α-D-mannopyranosyl-(1→2)-α-D-mannopyranosyl-(1→6)-α-D-mannopyranoside

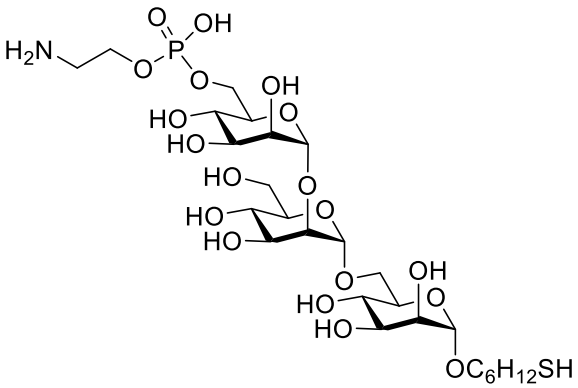

The phosphate **108** (50 mg, 0.030 mmol) was dissolved in dry THF (2 mL) and *tert*-butanol (2 drops). This solution was added to approximately 10 mL ammonia which was condensed at -78 °C and maintained the temperature during the reaction. Afterwards

small fresh cut pieces of sodium were added till a dark blue color was established. The reaction mixture was stirred for 35 min at -78 °C. The reaction was quenched with MeOH (2 mL) and ammonia was blown off using a stream of nitrogen. The solution was adjusted to pH 7 with concentrated acetic acid. The water was removed by freeze drying and the residue was purified using a Sephadex® super fine G-25 (GE Healthcare) column (1 cmx20 cm) to yield mixture of free thiol and disulphide **(109)** as white solid (19 mg, 35 %). ^{1}H NMR (400 MHz, Deuterium Oxide) δ 4.97 (s, 1.5H), 4.89 (s, 1.5H), 4.70 (s, 1.5H), 4.03 – 3.93 (m, 8H), 3.85 – 3.71 (m, 10H), 3.67 – 3.53 (m, 12H), 3.42 (dt, *J* = 10.9, 6.5 Hz, 2H), 3.14 (t, *J* = 4.9 Hz, 3H), 2.64 (t, *J* = 7.2 Hz, 1H), 2.41 (t, *J* = 7.1 Hz, 2H), 1.49 (q, *J* = 6.8 Hz, 6H), 1.32 – 1.12 (m, 6H). ^{13}C NMR (101 MHz, d_2o) δ 102.31, 99.76, 97.91, 78.90, 72.65, 71.97, 71.89, 71.07, 70.71, 70.14, 69.97, 69.80, 67.87, 66.81, 66.66, 66.18, 66.07, 64.70, 61.80, 60.81, 40.02, 32.82, 28.29, 27.07, 24.78, 23.61. ^{31}P NMR (162 MHz, d_2o) δ 0.25. ESI-MS (*m*/*z*): $[M+Na]^+$ cald 766.2328, obsd 766.2351.

B. Synthesis of *N*,*N*' diacetyllactosamine (LacDiNAc) for the analysis of *N*-glycome of Nematodes

Over the last years, glycan arrays have revolutionized the way to study carbohydrate-protein interactions. Also, modern analytical and biological approaches have transformed the available experimental tools to study the structure and function of glycans but still the glycome of many model organisms is poorly understood.[161] One of these model organisms e. g. nematodes are known to have immunomodulatory properties[162] and are relevant in terms of therapeutic targets.[163] It was shown that the glycans play an important role in host-parasite interaction, so it is important to study the glycome of these model organisms.

The nematodes express a wide variety of fucosylated glycans, including *N*-linked oligosaccharides with complex core modifications, which represents a target for lectins and potential therapeutics.[163, 164] Many enzymes have been characterized responsible for the biosynthesis of complex core modifications of nematode glycome.[161]

In addition to *N*-glycans, these nematodes have number of glycans which carry *N*,*N*' diacetyllactosamine (LacDiNAc) modified by fucose or phosphorylcholine.[161] So to identify more transferases involved in the biosynthesis of these glycans, LacDiNAc is synthesized as a positive or negative control for the enzyme assays.

B.1 Synthesis of LacDiNAc

The synthesis of LacDiNAc (GalNAc β1→4 GlcNAc) **121** was achieved by glycosylation of acceptor **119** with donor **115**, followed by global deprotection. Both donor **115** and acceptor **119** were synthesized from commercially available galactose and *N*-acetyl glucosamine respectively.

The synthesis of donor **115** started with the introduction of amine moiety in galactose. D-Galactose was peracetylated using acetic anhydride and pyridine. Then, the anomeric acetate was substituted with the bromine using HBr (33 % in acetic acid) and the resulting product was reduced with Zn/$CuSO_4$ to obtain tri-*O*-acetyl-galactal (**110**) in 65 % yield over three steps (Scheme B.1). Azido phenylselenylation of the enol ether **110** using diphenyldiselenide, iodobenzenediacetate and NaN_3 afforded 2-azido-2-deoxy-α-selenogalactoside **111** in 60 % yield. The acetyl groups of **111** were removed using

freshly prepared NaOMe, followed by a reaction with benzaldehyde dimethyl acetal and CSA to form 4,6-*O*-benzylidene **112** in 91 % yield. The free 3-*O* position of **112** was benzylated using NaH and BnBr. The benzylidene acetal was selective opened toward the 6-*O* position to get 4-*O* position free, which was orthogonally protected with 2-naphthylmethyl bromide and NaH (Nap) to obtain **114** in 60 % yield over two steps. The azido group of the galactose **114** was reduced with Zinc and the resulting amine was converted into a trichloroacetimide using 2,2,2-trichloroacetyl chloride to get the orthogonally protected building block **115**. This is an important building block for the synthesis of the *T. gondii* GPI. The galactose **115** was used for the synthesis of the building block **4**.

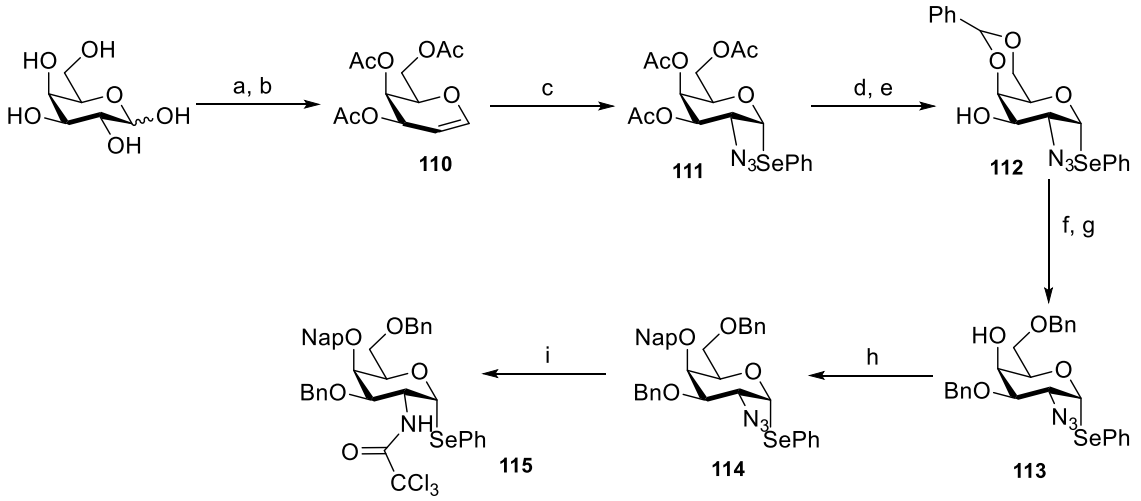

Scheme B.1: Conditions: a) Acetic anhydride, Pyridine, 0-25 °C, 14 h; b) HBr (33 %), DCE, 0-25 °C, 2 h, then $CuSO_4$, sodium acetate, zinc, acetic acid, H_2O, rt, 65 % (over 2 steps); c) Diphenyldiselenide, NaN_3, iodobenzenediacetate, DCM, rt, 48 h, 60 %; d) Sodium methoxide, MeOH, rt, 30 min, 95 %; e) Benzaldehyde dimethyl acetal, camphorsulphonic acid, ACN, rt, 2 h, 91 %; f) NaH, BnBr, DMF, 0-25 °C, 2h, 73 %; g) Trifluoroacetic anhydride (TFAA), triethylsilane (TES), Trifluoroacetic acid (TFA), 0-25 °C, 5 h, 88 %; h) NaH, 2-(bromomethyl)naphthalene, DMF, 0-25 °C, 2h, 60 %; i) Zinc, Acetic acid, 2 h, then pyridine, 2,2,2-trichloroacetyl chloride, 0-25 °C, 14 h, 87 %.

For the synthesis of acceptor **119**, the anomeric position of *N*-acetylglucosamine was allylated using allyl alcohol and $BF_3.OEt_2$, followed by the reaction with benzaldehyde dimethyl acetal to form 4,6-*O*-benzylidene compound **117**. The 3-*O* position of benzylidene was protected with benzyl ether using NaH and BnBr to obtain **118** in 55 % yield over two steps. The benzylidene acetal of **118** was selective opened toward the 6-*O* position to get 4-*O* position free acceptor **119** in 79 % yield. The glycosyl acceptor **119** was glycosylated with the donor **115**; the seleno group of donor was activated using N-

hydroxysuccinimide (NIS) and TMS-OTf and used to glycosylate the acceptor **119** to obtain protected disaccharide **120**, which is deprotected by hydrogenation using palladium over carbon to get crude **121**. Finally, crude compound was purified using size exclusion chromatography to get pure compound **121** in 63 % yield.

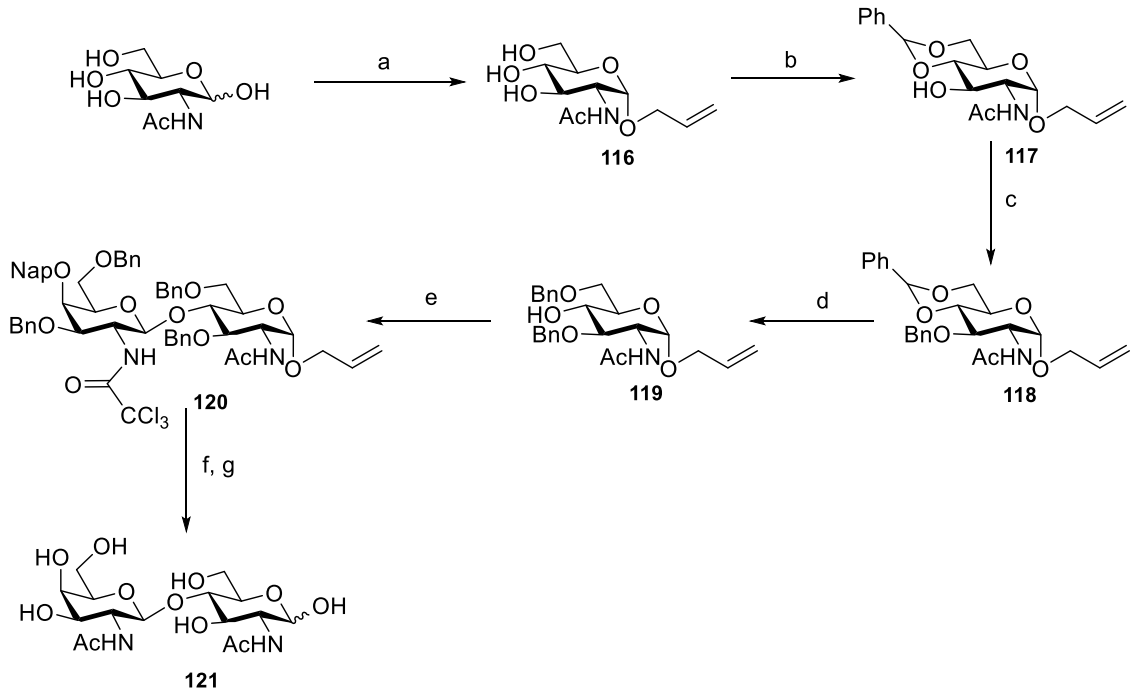

Scheme B.2: Conditions: a) $BF_3.OEt_2$, Allyl alcohol, rt, 14 h, 85 %; b) Benzaldehyde dimethyl acetal, camphorsulfonic acid, ACN, rt, 2 h, 80 %; c) NaH, BnBr, DMF, 0-25 °C, 2h, 55 %; d) Trifluoroacetic anhydride (TFAA), triethylsilane (TES), Trifluoroacetic acid (TFA), 0-25 °C, 2 h, 79 %; e) **115**, NIS, TMS-OTf, 0 °C, 2h, 65 %; f) $PdCl_2$, sodium acetate, Acetic acid, H_2O, rt, 3-4 h, 71 %; g) Pd-C, H_2, $CHCl_3$: MeOH (4:1), formic acid, 72 h, 63 %.

B.2 Experimental Section

For general material and methods, please refer to the experimental section 5.1, chapter 5.

3,4,6-tri-*O*-acetyl-2-deoxy-D-galactal (110)

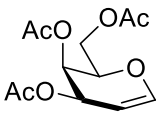

To a stirred solution of galactose (40 g, 222 mmol) in pyridine (250 mL), acetic anhydride (150 mL) was added at 0 °C to give peracetylated galactose (83 g, 95 %). Without any purification, to a solution of peracetylated galactose (11.3 g, 28.9 mmol) in

DCE (110 ml), hydrobromic acid (47 mL of 33 %, 289 mmol) was added at 0 °C. After 2 h, the volatiles were evaporated from the reaction mixture. The residue was dissolved in acetic acid (50 ml) and water (50 mL). The $CuSO_4$ (1.85 g, 11.58 mmol), Sodium acetate (28.5 g, 347 mmol) were added to the reaction mixture. Then, zinc (22.71 g, 347 mmol) was added to the reaction mixture in the portions at 0 °C. The reaction mixture was stirred overnight at room temperature. The reaction mixture was filtered through a celite pad and the filterate was extracted using DCM. The combined organic layer was washed with $NaHCO_3$ and brine solution. The organic layer was dried over anh. Na_2SO_4, filtered and concentrated. The crude product was purified using silica gel column chromatography to give **110** (5 g, 65 % yield) over two steps in quantitative yield. Spectral data was in agreement with the previous reported data.[165]

Phenyl-2-azido-3,4,6-*O*-acetyl-2-deoxy-1-seleno-α-D-galactopyranoside (111)

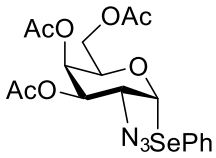

To a stirred solution of galactal **110** (2.9 g, 10.65 mmol) in DCM, diphenyldiselenide (5.82 g, 18.64 mmol), sodium azide (NaN_3) (3.46 g, 53.30 mmol) and iodobenzenediacetate (7.55 g, 23.43 mmol) were added under argon atmosphere. The reaction mixture was stirred at room temperature until the TLC shows the completion of the reaction. The reaction mixture was stirred for 3 days, diluted with DCM and washed using saturated solution of $NaHCO_3$ and brine. The organic layer was dried over Na_2SO_4, filtered and concentrated. The crude product was purified using silica gel column chromatography to give galactoside **111** (3 g, 60 % yield) as a white solid. Spectral data was in agreement with the previous reported data.[165]

Phenyl-2-azido-4,6-*O*-benzylidene-2-deoxy-1-seleno-α-D-galactopyranoside (112)

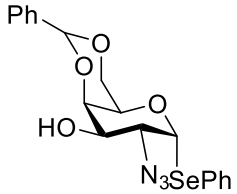

To a stirred solution of galactoside **111** (1.5 g 2.5 mmol), in methanol, freshly prepared sodium methoxide was added. The pH of reaction mixture was maintained over 9.0 and

neutralized using Amberlite IR120 resin (H^+-form). The reaction mixture was filtered through sintered funnel to give free galactose (1.1 g, 95 % yield).

To a stirred solution of free galactose (1.1 g, 2.37 mmol) in acetonitrile (15 mL), benzaldehyde dimethyl acetal (0.712 mL, 4.75 mmol) and camphorsulphonic acid (0.045 g, 0.237 mmol) were added at room temperature under argon atmosphere. The reaction mixture was stirred for 2 h and quenched with triethylamine. The volatiles were removed using rotavapour and the residue was dissolved in the DCM and washed with Sat. $NaHCO_3$ and brine. The organic layer was dried using Na_2SO_4, filtered and concentrated. The crude product was purified using silica gel column chromatography to give **112** (1.2 g, 91 % yield). Spectral data was in agreement with the previous reported data.[165]

Phenyl-2-azido-3,6-di-*O*-benzyl-2-deoxy-1-seleno-α-D-galactopyranoside (113)

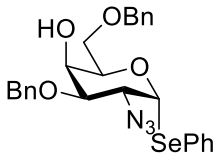

To a stirred solution of benzylidene **112** (1.2 g, 2.14 mmol) in anhy. Dimethylformamide (10 mL), sodium hydride (0.08 g, 3.21 mmol) was added under argon atmosphere at 0 °C. After 30 min, benzyl bromide (0.3 mL, 2.57 mmol) was added drop wise and let the reaction mixture stirred at room temperature for 2 h. The reaction mixture was quenched using methanol and volatiles were removed using rotavapour. The residue was dissolved in DCM and the reaction mixture was neutralized with 1N HCl (aq.) and extracted three times with DCM. The combined organic layer was dried over Na_2SO_4, filtered and concentrated. The crude product was purified using silica gel column chromatography (1 g, 73 % yield) as a white solid. Spectral data was in agreement with the previous reported data.[165]

To a stirred solution of galactoside (0.956 g, 1.83 mmol) in DCM (10 mL), trifluoroacetic anhydride (1 mL, 7.32 mmol) and triethylsilane (2 mL, 12.81 mmol) were added at 0 °C followed by the addition of trifluoroacetic acid (1 mL, 12.81 mmol) drop wise. The reaction mixture was stirred for 5 h at 0 °C. The reaction was quenched with Et_3N and the reaction mixture was filtered. The filtrate was concentrated to give a yellow oil that was purified by silica gel column chromatography to give galactoside **113** (0.845 g, 88 % yield) as a colorless oil[87]. R_f = 0.33 (Hexanes/EtOAc = 3 : 1); 1H NMR (400

MHz, $CDCl_3$) δ 7.53-7.51 (m, 2H), 7.34-7.10 (m, 13H), 5.85 (d, *J* = 5.4 Hz, 1H, H1), 4.66 (d, *J* = 11.6 Hz, 1H, -CH_2-), 4.63 (d, *J* = 11.6 Hz, 1H, -CH_2-), 4.45 (d, *J* = 11.8 Hz, 1H, -CH_2-), 4.41 (d, *J* = 11.8 Hz, 1H, -CH_2-), 4.32 (br-t, *J* = 5.5 Hz, 1H, H5), 4.16 (dd, *J* = 5.4, 10.2 Hz, 1H, H2), 4.08 (br, H4), 3.66 (dd, *J* = 5.4, 10.2 Hz, 1H, H6), 3.61-3.56 (m, 2H, H3 & H6); 13C NMR (75 MHz, $CDCl_3$) δ 137.76, 136.99, 134.77, 129.06, 128.69, 128.43, 128.30, 128.12, 128.04, 127.92, 127.78, 127.69, 85.22 (C1), 78.85 (C3), 73.57 (-CH_2-), 71.99 (-CH_2-), 71.23 (C5), 69.30 (C6), 66.39 (C4), 60.25 (C2).

Phenyl-2-azido-3,6-di-*O*-benzyl-2-deoxy-4-*O*-(2-naphthylmethyl)-1-seleno-α-D-galactopyranoside (114)

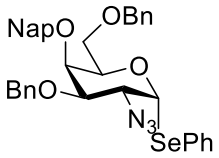

To a stirred solution of galactoside **113** (0.845 g, 1.61 mmol) in DMF (10 mL), 2-(bromomethyl)naphthalene (0.534 g, 2.42 mmol) was added to give a colorless solution. After 30 min, sodium hydride (0.077 g, 3.22 mmol) was added at 0 °C. The reaction mixture was stirred for 2 h and quenched by using methanol. The reaction mixture was neutralized with 1N HCl (aq) and extracted three times with dichloromethane. The combined organic layer was dried over Na_2SO_4, filtered and concentrated. The crude product was purified by silica gel column chromatography to give galatoside **114** (0.635 g, 60 % yield) as a white solid[87]: R_f = 0.25 (Hexanes/EtOAc = 9 : 1); ^{1}H NMR (400 MHz, $CDCl_3$) δ 7.70-7.64 (m, 3H), 7.56 (br, 1H), 7.50-7.49 (m, 2H), 7.37-7.07 (m, 16H), 5.85 (d, *J* = 5.3 Hz, 1H, H1), 4.94 (d, *J* = 11.6 Hz, 1H, -CH_2-), 4.64 (s, 2H), 4.61 (d, *J* = 11.6 Hz, 1H), 4.33-4.30 (m, 2H, H2 & H5), 4.29 (d, *J* = 11.7 Hz, 1H, -CH_2-), 4.24 (d, *J* = 11.7 Hz, 1H, -CH_2-), 3.99 (br, H4), 3.64 (d, *J* = 2.6, 10.6 Hz, 1H, H3), 3.53 (dd, *J* = 7.2, 9.3 Hz, 1H, H6), 3.37 (dd, *J* = 5.9, 9.3 Hz, 1H, H6); ^{13}C NMR (75 MHz, $CDCl_3$) δ 137.80, 137.43, 135.65, 134.77, 133.20, 133.03, 129.06, 128.63, 128.45, 128.38, 128.14, 128.07, 127.94, 127.88, 127.85, 127.82, 127.73, 126.80, 126.18, 126.13, 125.98, 85.55 (C1), 80.33 (C3), 74.95 (-CH_2-), 73.44 (-CH_2-), 72.97 (C4), 72.49 (-CH_2-), 71.97 (C5), 68.35 (C6), 61.11 (C2).

Phenyl-3,6-di-*O*-benzyl-2-deoxy-4-*O*-(2-naphthylmethyl)-1-seleno-2-trichloracetamido-α-D-galactopyranoside (115)

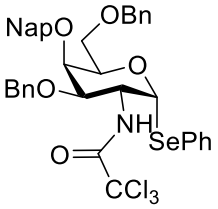

To a stirred solution of galatoside **114** (0.620 g, 0.93 mmol) in DCM (5 ml), acetic acid (5 mL) was added followed by the addition of zinc (1.2 g, 18.66 mmol) in portions. The reaction mixture was stirred for 2 h and filtered through a pad of celite, neutralize using sat. $NaHCO_3$ and extracted three times with dichloromethane. The combined organic layer was dried over Na_2SO_4, filtered and concentrated to give a white solid. To this residue (0.590 g, 0.92 mmol) in dichloromethane (10 mL), pyridine (1 mL) and 2,2,2-trichloroacetyl chloride (0.207 mL, 1.84 mmol) were added at 0 °C. The reaction mixture was stirred for 3 h and the solvent was evaporated in *vacuo* and the residue was recrystallized from MeOH to give galactoside **115** (0.630 g, 87 % yield) as a white solid[87]. R_f = 0.38 (Hexanes/EtOAc = 4 : 1); ^{1}H NMR (400 MHz, $CDCl_3$) δ 7.72-7.68 (m, 3H), 7.63 (br, 1H), 7.39-7.38 (m, 3H), 7.45-7.44 (m, 2H), 7.40-7.37 (m, 3H), 7.30-7.10 (m, 13H), 6.73 (d, *J* = 7.1 Hz, 1H, NH), 6.03 (d, *J* = 4.8 Hz, 1H, H1), 4.99 (d, *J* = 11.6 Hz, 1H, -CH_2-), 4.70 (m, 1H, H2), 4.69 (d, *J* = 11.6 Hz, 1H, -CH_2-), 4.62 (d, *J* = 12.0 Hz, 1H, -CH_2-), 4.41 (d, *J* = 12.0 Hz, 1H, -CH_2-), 4.38 (d, *J* = 11.6 Hz, 1H, -CH_2-), 4.32 (d, *J* = 11.6 Hz, 1H, -CH_2-), 4.28 (br-t, *J* = 6.6 Hz, H5), 4.11 (br, H4), 3.66 (dd, *J* = 7.5, 9.2 Hz, 1H, H6), 3.54-3.50 (m, H3 & H6); ^{13}C NMR (75 MHz, $CDCl_3$) δ 161.57 (amide), 137.74, 137.06, 135.52, 134.36, 133.18, 133.04, 129.26, 128.81, 128.80, 128.49, 128.48, 128.26, 128.19, 128.04, 127.96, 127.92, 127.91, 127.90, 127.88, 127.86, 127.84, 127.71, 126.84, 126.23, 126.10, 125.95, 92.44 (CCl_3), 88.69 (C1), 77.99 (C3), 74.74 (-CH_2-), 73.58 (-CH_2-), 72.81 (C5), 71.64 C4), 71.33 (-CH_2-), 68.30 (C6), 52.20 (C2); ESI-MS (*m*/*z*): $[M+Na]^+$ cald 806.0722, obsd 806.0733.

Allyl-2-acetamido-2-deoxy-α-D-glucopyranoside (116)

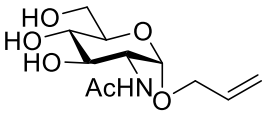

To a stirred solution of *N*-acetyl glucosamine (0.650 g, 2.94 mmol) in allyl alcohol (10 mL), $BF_3.OEt_2$ (1.5 mL, 5.88 mmol) was added at room temperature under argon atmosphere. The reaction mixture was stirred for 14 h and quenched by using Et_3N. The

volatiles were evaporated in *vacuo* and the product was crystallized using methanol and hexane to give **116** (0.655 g, 85 %) as a white solid. Spectral data was in agreement with the previous reported data.[166]

Allyl-2-acetamido-4,6-*O*-benzylidene-2-deoxy-α-D-glucopyranoside (117)

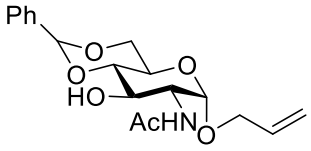

To a stirred solution of **116** (0.768 g, 2.94 mmol) in acetonitrile (15 mL), benzaldehyde dimethyl acetal (1.1 mL, 7.35 mmol) and camphorsulphonic acid (0.205 g, 0.88 mmol) were added at room temperature under argon atmosphere. The reaction mixture was stirred for 2 h and quenched by using triethylamine. The volatiles were removed using rotavapour and the residue was dissolved in the DCM and washed with Sat. $NaHCO_3$ and brine. The organic layer was dried using Na_2SO_4, filtered and concentrated. The crude product was purified using silica gel column chromatography to give **117** (0.820 g, 80 % yield). Spectral data was in agreement with the previous reported data.[166]

Allyl-2-acetamido-3-*O*-benzyl-4,6-*O*-benzylidene-2-deoxy-α-D-glucopyranoside (118)

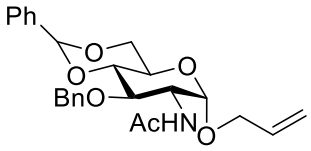

To a stirred solution of benzylidene **117** (1.0 g, 2.92 mmol) in anh. dimethylformamide (15 mL), sodium hydride (0.08 g, 3.21 mmol) was added under argon atmosphere at 0 °C. After 30 min, benzyl bromide (0.38 mL, 3.21 mmol) was added drop wise and the reaction mixture was stirred at room temperature. After 2 h, the reaction mixture was quenched using methanol and volatiles were removed using rotavapour. The residue was dissolved in DCM and the reaction mixture was neutralized with 1N HCl (aqueous) and extracted three times with DCM. The combined organic layer was dried over Na_2SO_4, filtered and concentrated. The crude product was purified using silica gel column chromatography to give **118** (0.715 g, 55 % yield) as a white solid. Spectral data was in agreement with the previous reported data.[166]

Allyl-2-acetamido-3,6-di-*O*-benzyl-2-deoxy-α-D-glucopyranoside (119)

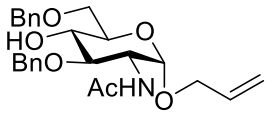

To a stirred solution of glucoside **118** (0.08 g, 0.19 mmol) in DCM (3 mL), trifluoroacetic anhydride (0.08 mL, 0.57 mmol) and triethylsilane (0.15 mL, 0.94 mmol) were added at 0 °C followed by the addition of trifluoroacetic acid (0.07 mL, 0.94 mmol) drop wise. After 5 h at 0 °C, the reaction was quenched using Et_3N and the reaction mixture was filtered. The filtrate was concentrated to give a yellow oil that was purified by silica gel column chromatography to give galactoside **119** (0.066 g, 79 % yield) as a colorless oil. Spectral data was in agreement with the previous reported data.[166] ^{1}H NMR (400 MHz, $CDCl_3$) δ 7.33 (s, 10H), 5.87 (m, 1H), 5.49 (d, *J* = 9.2 Hz, 1H), 5.22 (dd, *J* = 22.4, 13.7 Hz, 2H), 4.83 (d, *J* = 3.4 Hz, 1H), 4.77 (d, *J* = 11.7 Hz, 1H), 4.69 (d, *J* = 11.8 Hz, 1H), 4.58 (q, *J* = 12.0 Hz, 2H), 4.25 (td, *J* = 10.2, 3.4 Hz, 1H), 4.16 (dd, *J* = 12.9, 4.8 Hz, 1H), 3.95 (dd, *J* = 12.9, 6.1 Hz, 1H), 3.75 (dd, *J* = 19.1, 6.4 Hz, 4H), 1.89 (s, 3H). ^{13}C NMR (101 MHz, $CDCl_3$) δ 170.00, 138.60, 137.91, 133.69, 128.61(2), 128.51(2), 128.12(2), 127.91, 127.83, 127.72(2), 117.77, 96.94, 79.93, 73.93, 73.72, 72.14, 70.42, 70.21, 68.25, 51.91, 23.51.

Allyl-3,6-di-*O*-benzyl-2-deoxy-4-*O*-(2-naphthylmethyl)-2-trichloracetamido-α-D-galactopyranoside-β(1→4)-2-acetamido-3,6-di-*O*-benzyl-2-deoxy-α-D-glucopyranoside (120)

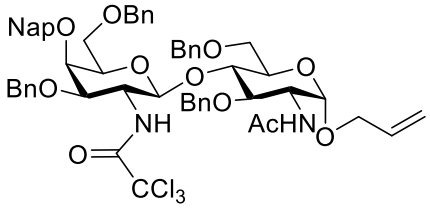

The glycosyl donor **119** (0.066 g, 0.149 mmol) and **115** (0.141 g, 0.179 mmol) were dissolved and coevaporated using toluene three times and dried under high vacuum overnight. Next morning, to a stirred mixture of acceptor and donor in DCM at 0 °C, N-hydroxysuccinimide (NIS) was added. After 20 min, TMS-OTf was added at 0 °C to a reaction mixture. The reaction mixture was stirred for 1 h and the reaction was quenched using saturated solution of $NaHCO_3$ and extracted twice using DCM. The organic layer was dried over Na_2SO_4, filtered and concentrated. The crude product was purified by silica gel chromatography to give disaccharide **120** (0.105 g, 65 % yield). $[\alpha]_D^{20}$ = +89.42 (c = 0.15, $CHCl_3$); ATR-FTIR (cm^{-1}): 3287.27, 3066.62, 2927.93, 1777.86, 1710.48,

1654.24, 1526.98, 1455.75, 1362.97, 1292.19, 1173.90, 1103.45, 1060.38, 821.06, 739.07, 699.21. ^{1}H NMR (400 MHz, $CDCl_3$) δ 7.76 (d, *J* = 7.8 Hz, 1H), 7.71 – 7.57 (m, 3H), 7.12 (dd, *J* = 5.6, 3.6 Hz, 23H), 6.64 (d, *J* = 8.1 Hz, 1H), 5.82 (m, 1H), 5.36 (d, *J* = 9.0 Hz, 1H), 5.23 (d, *J* = 1.5 Hz, 1H), 5.20 – 5.12 (m, 1H), 5.00 (d, *J* = 11.5 Hz, 1H), 4.91 (d, *J* = 11.7 Hz, 1H), 4.86 (d, *J* = 3.7 Hz, 1H), 4.73 – 4.59 (m, 4H), 4.55 (d, *J* = 11.8 Hz, 1H), 4.48 (s, 1H), 4.45 (d, *J* = 2.0 Hz, 1H), 4.35 (d, *J* = 11.7 Hz, 1H), 4.26 (d, *J* = 11.7 Hz, 1H), 4.21 (ddd, *J* = 10.7, 9.1, 3.7 Hz, 1H), 4.17 – 4.09 (m, 2H), 4.09 – 3.99 (m, 3H), 3.93 (dd, *J* = 13.0, 6.2 Hz, 1H), 3.82 (dd, *J* = 11.1, 2.6 Hz, 1H), 3.69 – 3.63 (m, 2H), 3.61 – 3.54 (m, 2H), 3.51 – 3.47 (m, 1H), 3.43 (dd, *J* = 12.4, 5.6 Hz, 2H), 1.87 (s, 3H).^{13}C NMR (101 MHz, $CDCl_3$) δ 177.17, 169.78, 161.75, 139.12, 138.14, 137.77, 137.45, 135.99, 133.58, 133.08, 132.83, 128.54, 128.41, 128.36, 128.07, 128.06, 127.98, 127.93, 127.89, 127.82, 127.77, 127.59, 127.10, 126.25, 125.99, 125.91, 125.72, 117.66, 98.48, 96.54, 74.92, 74.57, 73.70, 73.45, 73.06, 72.92, 71.73, 71.67, 70.50, 68.23, 67.83, 55.78, 51.98, 23.36. ESI-MS (*m*/*z*): $[M+Na]^+$ cald 1089.3233 , obsd 1089.3208.

2-acetamido-2-deoxy-α-D-galactopyranoside-β(1→4)-2-acetamido-2-deoxy-α-D-glucopyranoside (121)

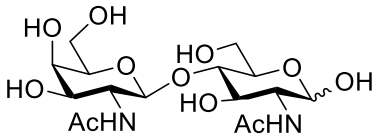

The protected disaccharide **120** (65 mg, 0.061 mmol) and sodium acetate (5 mg, 0.061 mmol) were dissolved in a mixture of acetic acid (1 mL) and MeOH (3 mL). The $PdCl_2$ (10 mg, 0.061 mmol) was added to the reaction mixture and stirred for 5 h. The reaction mixture was filtered through a pad of celite® and concentrated in *vacuo*. Then, the reaction mixture was poured into saturated solution of $NaHCO_3$ and the aqueous layer was extracted with ethyl acetate. The organic layer was dried over Na_2SO_4, filtered and concentrated. The residue was purified by flash column chromatography to afford alcohol in 71 % yield. To the deallylated compound in mixture of MeOH and $CHCl_3$ (4:1) with 50 μL of formic acid, Pd-C (50 mg) was added and the reaction mixture was stirred under hydrogen gas atmosphere for 2 days. The reaction mixture was filtered through a pad of celite® and concentrated in *vacuo*. The residue was purified using G15 sephadex column with 5 % Ethanol in dd H_2O to give α:β mixture of disaccharide **121** as a white fluffy powder (10 mg, 64 % yield). ATR-FTIR (cm^{-1}): 3332.41, 2944.46,

2834.21, 1644.79, 1557.72, 1377.99, 1024.81. ^{1}H NMR (600 MHz, D_2O) δ 5.21 (d, *J* = 3.2 Hz, 1H), 4.72 (d, *J* = 8.0 Hz, 1H), 4.54 (dd, *J* = 8.4, 5.8 Hz, 2H), 3.97 – 3.94 (m, 4H), 3.93 – 3.88 (m, 4H), 3.86 (d, *J* = 2.0 Hz, 1H), 3.84 – 3.81 (m, 2H), 3.81 – 3.63 (m, 15H), 3.56 – 3.51 (m, 2H), 2.08 (d, *J* = 1.1 Hz, 5H), 2.05 (s, 5H). ^{13}C NMR (151 MHz, D_2O) δ 177.35, 177.04, 104.33, 97.44, 93.02, 82.14, 81.67, 77.93, 77.19, 75.18, 73.29, 72.57, 71.93, 70.21, 63.54, 62.77, 62.65, 58.57, 56.14, 55.18, 24.78, 24.47. ESI-MS (*m*/*z*): $[M+Na]^+$ cald 447.1585, obsd 447.1750.

References

1. Varki, A.; Cummings, R. D.; Esko, J. D.; Freeze, H. H.; Stanley, P.; Bertozzi, C. R.; Hart, G. W.; Etzler, M. E.; Editors, *Essentials of Glycobiology; Second Edition*. Cold Spring Harbor Laboratory Press2009; p 784 pp.
2. Alberts B, J. A., Lewis J, et al., *Molecular Biology of the Cell. 4th edition. New York: Garland Science* **2002**.
3. Stanley P, S. H., Taniguchi N. , *Essentials of Glycobiology. 2nd edition. Cold Spring Harbor (NY): Cold Spring Harbor Laboratory Press;* **2009**.
4. Brockhausen I, S. H., Stanley P., *Essentials of Glycobiology. 2nd edition. Cold Spring Harbor (NY): Cold Spring Harbor Laboratory Press;* **2009**.
5. Iozzo, R. V.; Schaefer, L., *Matrix Biol.* **2015,** *42*, 11-55.
6. Lingwood, C. A., *Cold Spring Harbor Perspectives in Biology* **2011,** *3*.
7. Ferguson MAJ, K. T., Hart GW. , *Essentials of Glycobiology. 2nd edition. Cold Spring Harbor (NY): Cold Spring Harbor Laboratory Press;* **2009**.
8. Kinoshita, T.; Fujita, M.; Maeda, Y., *J. Biochem.* **2008,** *144*, 287-294.
9. Geoff Daniels, I. B., The RH blood group system. In *Essential Guide to Blood Groups*, John Wiley & Sons2013; pp 35-48.
10. Clark, G. F., *Biochem. Biophys. Res. Commun.* **2014,** *450*, 1195-1203.
11. Kimble, B.; Nieto, G. R.; Perez, D. R., *Virology Journal* **2010,** *7*, 365.
12. Ferguson, M. A., *J. Cell Sci.* **1999,** *112 (Pt 17)*, 2799-809.
13. Ilg, T.; Etges, R.; Overath, P.; McConville, M. J.; Thomas-Oates, J.; Thomas, J.; Homans, S. W.; Ferguson, M. A., *Journal of Biological Chemistry* **1992,** *267*, 6834-6840.
14. McConville, M. J.; Schnur, L. F.; Jaffe, C.; Schneider, P., *Biochem. J* **1995,** *310*, 807-818.
15. Ferguson, M. A. J.; Homans, S. W.; Dwek, R. A.; Rademacher, T. W., *Science* **1988,** *239*, 753-759.
16. Murakata, C.; Ogawa, T., *Tetrahedron Lett.* **1990,** *31*, 2439-2442.
17. Murakata, C.; Ogawa, T., *Tetrahedron Lett.* **1991,** *32*, 671-674.
18. Murakata, C.; Ogawa, T., *Tetrahedron Lett.* **1991,** *32*, 101-104.
19. Murakata, C.; Ogawa, T., *Carbohydr. Res.* **1992,** *235*, 95-114.
20. Murakata, C.; Ogawa, T., *Carbohydr. Res.* **1992,** *234*, 75-91.
21. Baeschlin, D. K.; Chaperon, A. R.; Charbonneau, V.; Green, L. G.; Ley, S. V.; Lücking, U.; Walther, E., *Angew. Chem. Int. Ed.* **1998,** *37*, 3423-3428.
22. Baeschlin, D. K.; Chaperon, A. R.; Green, L. G.; Hahn, M. G.; Ince, S. J.; Ley, S. V., *Chemistry – A European Journal* **2000,** *6*, 172-186.
23. Udodong, U. E.; Madsen, R.; Roberts, C.; Fraser-Reid, B., *J. Am. Chem. Soc.* **1993,** *115*, 7886-7887.
24. Campbell, A. S.; Fraser-Reid, B., *J. Am. Chem. Soc.* **1995,** *117*, 10387-10388.
25. Tailler, D.; Ferrières, V.; Pekari, K.; Schmidt, R. R., *Tetrahedron Lett.* **1999,** *40*, 679-682.
26. Pekari, K.; Schmidt, R. R., *The Journal of Organic Chemistry* **2003,** *68*, 1295-1308.
27. Lu, J.; Jayaprakash, K. N.; Schlueter, U.; Fraser-Reid, B., *J. Am. Chem. Soc.* **2004,** *126*, 7540-7547.
28. Lu, J.; Jayaprakash, K. N.; Fraser-Reid, B., *Tetrahedron Lett.* **2004,** *45*, 879-882.
29. Liu, X.; Kwon, Y.-U.; Seeberger, P. H., *J. Am. Chem. Soc.* **2005,** *127*, 5004-5005.

30. Schofield, L.; Hewitt, M. C.; Evans, K.; Siomos, M.-A.; Seeberger, P. H., *Nature* **2002,** *418*, 785-789.
31. Seeberger, P. H.; Soucy, R. L.; Kwon, Y.-U.; Snyder, D. A.; Kanemitsu, T., *Chem. Commun.* **2004**, 1706-1707.
32. Götze, S.; Azzouz, N.; Tsai, Y.-H.; Groß, U.; Reinhardt, A.; Anish, C.; Seeberger, P. H.; Varón Silva, D., *Angew. Chem. Int. Ed.* **2014,** *53*, 13701-13705.
33. Low, M. G.; Saltiel, A. R., *Science* **1988,** *239*, 268-75.
34. Robinson, P. J., *Adv Exp Med Biol* **1997,** *419*, 365-70.
35. Kinoshita, T.; Inoue, N.; Takeda, J., Defective Glycosyl Phosphatidylinositol Anchor Synthesis and Paroxysmal Nocturnal Hemoglobinuria. In *Advances in Immunology*, Frank, J. D., Ed. Academic Press1995; Vol. Volume 60, pp 57-103.
36. Wichroski, M. J.; Ward, G. E., *Eukaryotic Cell* **2003,** *2*, 1132-1136.
37. Kinoshita, T., *Proceedings of the Japan Academy, Series B* **2014,** *90*, 130-143.
38. Takeda, J.; Miyata, T.; Kawagoe, K.; Iida, Y.; Endo, Y.; Fujita, T.; Takahashi, M.; Kitani, T.; Kinoshita, T., *Cell 73*, 703-711.
39. Nakamura, N.; Inoue, N.; Watanabe, R.; Takahashi, M.; Takeda, J.; Stevens, V. L.; Kinoshita, T., *Journal of Biological Chemistry* **1997,** *272*, 15834-15840.
40. Vidugiriene, J.; Menon, A. K., *The Journal of Cell Biology* **1993,** *121*, 987-996.
41. Doerrler, W. T.; Ye, J.; Falck, J. R.; Lehrman, M. A., *Journal of Biological Chemistry* **1996,** *271*, 27031-27038.
42. Murakami, Y.; Siripanyapinyo, U.; Hong, Y.; Kang, J. Y.; Ishihara, S.; Nakakuma, H.; Maeda, Y.; Kinoshita, T., *Molecular Biology of the Cell* **2003,** *14*, 4285-4295.
43. Fujita, M.; Kinoshita, T., *FEBS Lett.* **2010,** *584*, 1670-1677.
44. Maeda, Y.; Tashima, Y.; Houjou, T.; Fujita, M.; Yoko-o, T.; Jigami, Y.; Taguchi, R.; Kinoshita, T., *Molecular Biology of the Cell* **2007,** *18*, 1497-1506.
45. Ferguson, M. A. J.; Mehlert, A.; Richardson, J. M., *J. Mol. Biol.* **1998,** *277*, 379-392.
46. Gerold, P.; Striepen, B.; Reitter, B.; Geyer, H.; Geyer, R.; Reinwald, E.; Risse, H. J.; Schwarz, R. T., *J. Mol. Biol.* **1996,** *261*, 181-194.
47. Previato, J. O.; Jones, C.; Xavier, M. T.; Wait, R.; Travassos, L. R.; Parodi, A. J.; Mendoncapreviato, L., *J. Biol. Chem.* **1995,** *270*, 7241-7250.
48. Fontaine, T.; Magnin, T.; Melhert, A.; Lamont, D.; Latge, J. P.; Ferguson, M. A. J., *Glycobiology* **2003,** *13*, 169-177.
49. Schneider, P.; Ferguson, M. A. J.; Mcconville, M. J.; Mehlert, A.; Homans, S. W.; Bordier, C., *J. Biol. Chem.* **1990,** *265*, 16955-16964.
50. Gowda, D. C.; Naik, R. S.; Branch, O. H.; Woods, A. S.; Vijaykumar, M.; Perkins, D. J.; Nahlen, B. L.; Lal, A. A.; Cotter, R. J.; Costello, C. E.; Ockenhouse, C. F.; Davidson, E. A., *J. Exp. Med.* **2000,** *192*, 1563-1575.
51. Gerold, P.; Schofield, L.; Blackman, M. J.; Holder, A. A.; Schwarz, R. T., *Mol. Biochem. Parasitol.* **1996,** *75*, 131-143.
52. Gerold, P.; Dieckmannschuppert, A.; Schwarz, R. T., *J. Biol. Chem.* **1994,** *269*, 2597-2606.
53. Striepen, B.; Zinecker, C. F.; Damm, J. B. L.; Melgers, P. A. T.; Gerwig, G. J.; Koolen, M.; Vliegenthart, J. F. G.; Dubremetz, J. F.; Schwarz, R. T., *J Mol Biol* **1997,** *266*, 797-813.
54. Fankhauser, C.; Homans, S. W.; Thomasoates, J. E.; Mcconville, M. J.; Desponds, C.; Conzelmann, A.; Ferguson, M. A. J., *J. Biol. Chem.* **1993,** *268*, 26365-26374.
55. Oxley, D.; Bacic, A., *Proc. Natl. Acad. Sci. USA* **1999,** *96*, 14246-14251.
56. Homans, S. W.; Ferguson, M. A.; Dwek, R. A.; Rademacher, T. W.; Anand, R.; Williams, A. F., *Nature* **1988,** *333*, 269-72.

57. Stahl, N.; Baldwin, M. A.; Hecker, R.; Pan, K. M.; Burlingame, A. L.; Prusiner, S. B., *Biochemistry* **1992,** *31*, 5043-5053.
58. Mukasa, R.; Umeda, M.; Endo, T.; Kobata, A.; Inoue, K., *Arch. Biochem. Biophys.* **1995,** *318*, 182-190.
59. Brewis, I. A.; Ferguson, M. A. J.; Mehlert, A.; Turner, A. J.; Hooper, N. M., *J. Biol. Chem.* **1995,** *270*, 22946-22956.
60. Mehlert, A.; Varon, L.; Silman, I.; Homans, S. W.; Ferguson, M. A. J., *Biochem. J.* **1993,** *296*, 473-479.
61. Deeg, M. A.; Humphrey, D. R.; Yang, S. H.; Ferguson, T. R.; Reinhold, V. N.; Rosenberry, T. L., *J. Biol. Chem.* **1992,** *267*, 18573-18580.
62. Treumann, A.; Lifely, M. R.; Schneider, P.; Ferguson, M. A. J., *J. Biol. Chem.* **1995,** *270*, 6088-6099.
63. Rudd, P. M.; Morgan, B. P.; Wormald, M. R.; Harvey, D. J.; vandenBerg, C. W.; Davis, S. J.; Ferguson, M. A. J.; Dwek, R. A., *J. Biol. Chem.* **1997,** *272*, 7229-7244.
64. Fukushima, K.; Ikehara, Y.; Kanai, M.; Kochibe, N.; Kuroki, M.; Yamashita, K., *J. Biol. Chem.* **2003,** *278*, 36296-36303.
65. Debierre-Grockiego, F.; Schwarz, R. T., *Glycobiology* **2010,** *20*, 801-811.
66. Low, M. G., *Biochem. J.* **1987,** *244*, 1-13.
67. Low, M. G., *The FASEB Journal* **1989,** *3*, 1600-8.
68. Barboni, E.; Rivero, B. P.; George, A. J.; Martin, S. R.; Renoup, D. V.; Hounsell, E. F.; Barber, P. C.; Morris, R. J., *Journal of Cell Science* **1995,** *108*, 487-497.
69. Homans, S. W.; Edge, C. J.; Ferguson, M. A.; Dwek, R. A.; Rademacher, T. W., *Biochemistry* **1989,** *28*, 2881-7.
70. Jones, D. R.; Varela-Nieto, I., *The International Journal of Biochemistry & Cell Biology* **1998,** *30*, 313-326.
71. Rajendran, L.; Simons, K., *J. Cell Sci.* **2005,** *118*, 1099-102.
72. Munro, S., *Cell* **2003,** *115*, 377-88.
73. Simons, K.; Toomre, D., *Nat Rev Mol Cell Biol* **2000,** *1*, 31-9.
74. Sharma, P.; Varma, R.; Sarasij, R. C.; Ira; Gousset, K.; Krishnamoorthy, G.; Rao, M.; Mayor, S., *Cell* **2004,** *116*, 577-589.
75. Medof, M. E.; Nagarajan, S.; Tykocinski, M. L., *The FASEB Journal* **1996,** *10*, 574-86.
76. Paulick, M. G.; Bertozzi, C. R., *Biochemistry* **2008,** *47*, 6991-7000.
77. Kwon, Y.-U.; Liu, X.; Seeberger, P. H., *Chem. Commun.* **2005**, 2280-2282.
78. Yashunsky, D. V.; Borodkin, V. S.; Ferguson, M. A. J.; Nikolaev, A. V., *Angew. Chem. Int. Ed.* **2006,** *45*, 468-474.
79. Swarts, B. M.; Guo, Z., *J. Am. Chem. Soc.* **2010,** *132*, 6648-6650.
80. Swarts, B. M.; Guo, Z. W., *Chemical Science* **2011,** *2*, 2342-2352.
81. Lee, B. Y.; Seeberger, P. H.; Varon Silva, D., *Chem. Commun.* **2016,** *52*, 1586-1589.
82. Lahmann, M.; Garegg, P. J.; Konradsson, P.; Oscarson, S., *Can. J. Chem.* **2002,** *80*, 1105-1111.
83. Lindberg, J.; Öhberg, L.; Garegg, P. J.; Konradsson, P., *Tetrahedron* **2002,** *58*, 1387-1398.
84. Reichardt, N.-C.; Martín-Lomas, M., *Angew. Chem. Int. Ed.* **2003,** *42*, 4674-4677.
85. Mayer, T. G.; Kratzer, B.; Schmidt, R. R., *Angewandte Chemie International Edition in English* **1994,** *33*, 2177-2181.
86. Mayer, T. G.; Schmidt, R. R., *Eur. J. Org. Chem.* **1999,** *1999*, 1153-1165.
87. Tsai, Y. H.; Gotze, S.; Vilotijevic, I.; Grube, M.; Silva, D. V.; Seeberger, P. H., *Chemical Science* **2013,** *4*, 468-481.

88. Tsai, Y. H.; Gotze, S.; Azzouz, N.; Hahm, H. S.; Seeberger, P. H.; Varon Silva, D., *Angew. Chem. Int. Ed. Engl.* **2011,** *50*, 9961-4.
89. Schofield, L.; McConville, M. J.; Hansen, D.; Campbell, A. S.; Fraser-Reid, B.; Grusby, M. J.; Tachado, S. D., *Science* **1999,** *283*, 225.
90. Debierre-Grockiego, F.; Azzouz, N.; Schmidt, J.; Dubremetz, J. F.; Geyer, H.; Geyer, R.; Weingart, R.; Schmidt, R. R.; Schwarz, R. T., *J. Biol. Chem.* **2003,** *278*, 32987-93.
91. Debierre-Grockiego, F.; Schwarz, R. T., *Glycobiology* **2010,** *20*, 801-811.
92. Bruce Grindley, T., Structure and Conformation of Carbohydrates. In *Glycoscience: Chemistry and Chemical Biology I–III*, Fraser-Reid, B. O.; Tatsuta, K.; Thiem, J., Eds. Springer Berlin Heidelberg: Berlin, Heidelberg, 2001; pp 3-51.
93. Jeffrey, G., *Acta Crystallographica Section B* **1990,** *46*, 89-103.
94. Rundlöf, T.; Venable, R. M.; Pastor, R. W.; Kowalewski, J.; Widmalm, G., *J. Am. Chem. Soc.* **1999,** *121*, 11847-11854.
95. Yang, M.; Angles d'Ortoli, T.; Sawen, E.; Jana, M.; Widmalm, G.; MacKerell, A. D., *PCCP* **2016,** *18*, 18776-18794.
96. Pendrill, R.; Engstrom, O.; Volpato, A.; Zerbetto, M.; Polimeno, A.; Widmalm, G., *PCCP* **2016,** *18*, 3086-3096.
97. Engstrom, O.; Munoz, A.; Illescas, B. M.; Martin, N.; Ribeiro-Viana, R.; Rojo, J.; Widmalm, G., *Organic & Biomolecular Chemistry* **2015,** *13*, 8750-8755.
98. Blasco, P.; Patel, D. S.; Engström, O.; Im, W.; Widmalm, G., *Biochemistry* **2017**.
99. Foley, B. L.; Tessier, M. B.; Woods, R. J., *Wiley interdisciplinary reviews. Computational molecular science* **2012,** *2*, 652-697.
100. Fadda, E.; Woods, R. J., *Drug Discovery Today* **2010,** *15*, 596-609.
101. Guvench, O.; Mallajosyula, S. S.; Raman, E. P.; Hatcher, E.; Vanommeslaeghe, K.; Foster, T. J.; Jamison, F. W.; MacKerell, A. D., *Journal of Chemical Theory and Computation* **2011,** *7*, 3162-3180.
102. Wehle, M.; Vilotijevic, I.; Lipowsky, R.; Seeberger, P. H.; Silva, D. V.; Santer, M., *J. Am. Chem. Soc.* **2012,** *134*, 18964-72.
103. Oh, J.; Kim, Y.; Won, Y., *Bull. Korean Chem. Soc.* **1995,** *16*, 1153-1162.
104. Hirotsu, K.; Shimada, A., *Bull. Chem. Soc. Jpn.* **1974,** *47*, 1872-1879.
105. Martin-Pastor, M.; Canales, A.; Corzana, F.; Asensio, J. L.; Jimenez-Barbero, J., *J. Am. Chem. Soc.* **2005,** *127*, 3589-95.
106. Chevalier, F.; Lopez-Prados, J.; Perez, S.; Martín-Lomas, M.; Nieto, P. M., *Eur. J. Org. Chem.* **2005,** *2005*, 3489-3498.
107. Yamamoto, S.; Yamaguchi, T.; Erdelyi, M.; Griesinger, C.; Kato, K., *Chemistry* **2011,** *17*, 9280-2.
108. Zhang, Y.; Yamamoto, S.; Yamaguchi, T.; Kato, K., *Molecules* **2012,** *17*, 6658-71.
109. Erdelyi, M.; d'Auvergne, E.; Navarro-Vazquez, A.; Leonov, A.; Griesinger, C., *Chemistry* **2011,** *17*, 9368-76.
110. Canales, A.; Mallagaray, A.; Perez-Castells, J.; Boos, I.; Unverzagt, C.; Andre, S.; Gabius, H. J.; Canada, F. J.; Jimenez-Barbero, J., *Angew. Chem. Int. Ed. Engl.* **2013,** *52*, 13789-93.
111. Liu, X.; Kwon, Y.-U.; Seeberger, P. H., *Journal of American chemical Society* **2005,** *127*.
112. Becker, C. F. W.; Liu, X.; Olschewski, D.; Castelli, R.; Seidel, R.; Seeberger, P. H., *Angew. Chem. Int. Ed.* **2008,** *47*, 8215-8219.
113. Götze, S.; Reinhardt, A.; Geissner, A.; Azzouz, N.; Tsai, Y.-H.; Kurucz, R.; Varón Silva, D.; Seeberger, P. H., *Glycobiology* **2015,** *25*, 984-991.

114. Tamborrini, M.; Liu, X.; Mugasa, J. P.; Kwon, Y.-U.; Kamena, F.; Seeberger, P. H.; Pluschke, G., *Biorg. Med. Chem.* **2010,** *18*, 3747-3752.
115. Kamena, F.; Tamborrini, M.; Liu, X.; Kwon, Y.-U.; Thompson, F.; Pluschke, G.; Seeberger, P. H., *Nat Chem Biol* **2008,** *4*, 238-240.
116. Hewitt, M. C.; Snyder, D. A.; Seeberger, P. H., *J. Am. Chem. Soc.* **2002,** *124*, 13434-13436.
117. Hunter, C. A.; Sibley, L. D., *Nat Rev Micro* **2012,** *10*, 766-778.
118. Debierre-Grockiego, F., *Trends in Parasitology* **2010,** *26*, 404-411.
119. Singh, G.; Sehgal, R., *Asian Journal of Transfusion Science* **2010,** *4*, 73-77.
120. Wormser, G. P.; Tolan, J. R. W., *Clinical Infectious Diseases* **2006,** *42*, 1062-1063.
121. Azzouz, N.; Shams-Eldin, H.; Niehus, S.; Debierre-Grockiego, F.; Bieker, U.; Schmidt, J.; Mercier, C.; Delauw, M.-F.; Dubremetz, J.-F.; Smith, T. K.; Schwarz, R. T., *The International Journal of Biochemistry & Cell Biology* **2006,** *38*, 1914-1925.
122. Sharma, S. D.; Mullenax, J.; Araujo, F. G.; Erlich, H. A.; Remington, J. S., *The Journal of Immunology* **1983,** *131*, 977-983.
123. Striepen, B.; Zinecker, C. F.; Damm, J. B. L.; Melgers, P. A. T.; Gerwig, G. J.; Koolen, M.; Vliegenthart, J. F. G.; Dubremetz, J.-F.; Schwarz, R. T., *J. Mol. Biol.* **1997,** *266*, 797-813.
124. Liu, Q.; Wang, Z.-D.; Huang, S.-Y.; Zhu, X.-Q., *Parasites & Vectors* **2015,** *8*, 292.
125. OLIVER LIESENFELD, 2 CYNTHIA PRESS,1; JUDITH L. ISAAC-RENTON, K. H., 5 AND JACK S. REMINGTON1,2; JOSE G. MONTOYA, 2,3 *; RAJ GILL.
126. Fujii, Y.; Kaneko, S.; Nzou, S. M.; Mwau, M.; Njenga, S. M.; Tanigawa, C.; Kimotho, J.; Mwangi, A. W.; Kiche, I.; Matsumoto, S.; Niki, M.; Osada-Oka, M.; Ichinose, Y.; Inoue, M.; Itoh, M.; Tachibana, H.; Ishii, K.; Tsuboi, T.; Yoshida, L. M.; Mondal, D.; Haque, R.; Hamano, S.; Changoma, M.; Hoshi, T.; Kamo, K.-i.; Karama, M.; Miura, M.; Hirayama, K., *PLOS Neglected Tropical Diseases* **2014,** *8*, e3040.
127. Nzou, S. M.; Fujii, Y.; Miura, M.; Mwau, M.; Mwangi, A. W.; Itoh, M.; Salam, M. A.; Hamano, S.; Hirayama, K.; Kaneko, S., *Parasitology International* **2016,** *65*, 121-127.
128. Karanikola, S. N.; Krücken, J.; Ramünke, S.; de Waal, T.; Höglund, J.; Charlier, J.; Weber, C.; Müller, E.; Kowalczyk, S. J.; Kaba, J.; von Samson-Himmelstjerna, G.; Demeler, J., *Parasites & Vectors* **2015,** *8*, 335.
129. al., B. e.
130. Lehle, L.; Tanner, W., *New Compr. Biochem.* **1995,** *29*, 475-509.
131. Johnson, M. A.; Jaseja, M.; Zou, W.; Jennings, H. J.; Copié, V.; Pinto, B. M.; Pincus, S. H., *Journal of Biological Chemistry* **2003,** *278*, 24740-24752.
132. Poveda, A.; Jimenez-Barbero, J., *Chem. Soc. Rev.* **1998,** *27*, 133-144.
133. Buda, S.; Nawój, M.; Mlynarski, J., *Annual Reports on NMR Spectroscopy* **2016,** *89*, 185-223.
134. Shorthouse, D.; Hedger, G.; Koldsø, H.; Sansom, M. S. P., *Biochimie* **2016,** *120*, 105-109.
135. Meynier, C.; Feracci, M.; Espeli, M.; Chaspoul, F.; Gallice, P.; Schiff, C.; Guerlesquin, F.; Roche, P., *Biophys. J.* **2009,** *97*, 3168-3177.
136. Lemieux, R. U.; Kullnig, R. K.; Bernstein, H. J.; Schneider, W. G., *J. Am. Chem. Soc.* **1958,** *80*, 6098-6105.
137. Hu, X.; Carmichael, I.; Serianni, A. S., *The Journal of Organic Chemistry* **2010,** *75*, 4899-4910.
138. Yamaguchi, Y.; Yamaguchi, T.; Kato, K., Structural Analysis of Oligosaccharides and Glycoconjugates Using NMR. In *Glycobiology of the Nervous System*, Yu, R. K.; Schengrund, C.-L., Eds. Springer New York: New York, NY, 2014; pp 165-183.

139. Ying, Z.; Takumi, Y.; Koichi, K., *Chem. Lett.* **2013,** *42*, 1455-1462.
140. Canales, Á.; Mallagaray, Á.; Berbís, M. Á.; Navarro-Vázquez, A.; Domínguez, G.; Cañada, F. J.; André, S.; Gabius, H.-J.; Pérez-Castells, J.; Jiménez-Barbero, J., *J. Am. Chem. Soc.* **2014,** *136*, 8011-8017.
141. Takumi, Y.; Yukiko, K.; Yeun-Mun, C.; Sayoko, Y.; Koichi, K., *Chem. Lett.* **2013,** *42*, 544-546.
142. Toukach, F. V.; Ananikov, V. P., *Chem. Soc. Rev.* **2013,** *42*, 8376-8415.
143. Yamamoto, S.; Zhang, Y.; Yamaguchi, T.; Kameda, T.; Kato, K., *Chem. Commun.* **2012,** *48*, 4752-4754.
144. Mallagaray, A.; Canales, A.; Dominguez, G.; Jimenez-Barbero, J.; Perez-Castells, J., *Chem. Commun.* **2011,** *47*, 7179-7181.
145. Kato, K.; Yamaguchi, T., *Glycoconjugate J.* **2015,** *32*, 505-513.
146. Kwon, Y. U.; Soucy, R. L.; Snyder, D. A.; Seeberger, P. H., *Chemistry* **2005,** *11*, 2493-504.
147. Kirschner, K. N.; Yongye, A. B.; Tschampel, S. M.; González-Outeiriño, J.; Daniels, C. R.; Foley, B. L.; Woods, R. J., *J. Comput. Chem.* **2008,** *29*, 622-655.
148. Magee, T.; Seabra, M. C., *Current Opinion in Cell Biology* **2005,** *17*, 190-196.
149. Muir, T. W., *Annu. Rev. Biochem* **2003,** *72*, 249-89.
150. Muralidharan, V.; Muir, T. W., *Nat Meth* **2006,** *3*, 429-438.
151. Kent, P. E. D. a. S. B. H.
152. Xue, J.; Shao, N.; Guo, Z., *The Journal of Organic Chemistry* **2003,** *68*, 4020-4029.
153. Shao, N.; Xue, J.; Guo, Z., *Angew. Chem. Int. Ed.* **2004,** *43*, 1569-1573.
154. Paulick, M. G.; Wise, A. R.; Forstner, M. B.; Groves, J. T.; Bertozzi, C. R., *J. Am. Chem. Soc.* **2007,** *129*, 11543-11550.
155. Olschewski, D.; Seidel, R.; Miesbauer, M.; Rambold, A. S.; Oesterhelt, D.; Winklhofer, K. F.; Tatzelt, J.; Engelhard, M.; Becker, C. F. W., *Chemistry & Biology* **2007,** *14*, 994-1006.
156. Brandley, B. K.; Schnaar, R. L., *Journal of Leukocyte Biology* **1986,** *40*, 97-111.
157. Sairam, M. R., *The FASEB Journal* **1989,** *3*, 1915-26.
158. Karlsson, K.-A., Pathogen-Host Protein-Carbohydrate Interactions as the Basis of Important Infections. In *The Molecular Immunology of Complex Carbohydrates —2*, Wu, A. M., Ed. Springer US: Boston, MA, 2001; pp 431-443.
159. Kato, K.; Ishiwa, A., *Tropical Medicine and Health* **2015,** *43*, 41-52.
160. Azzouz, N.; Kamena, F.; Seeberger, P. H., *Omics-a Journal of Integrative Biology* **2010,** *14*, 445-454.
161. Yan, S.; Serna, S.; Reichardt, N.-C.; Paschinger, K.; Wilson, I. B. H., *Journal of Biological Chemistry* **2013,** *288*, 21015-21028.
162. Tundup, S.; Srivastava, L.; Harn, J. D. A., *Ann. N.Y. Acad. Sci.* **2012,** *1253*, E1-E13.
163. Paschinger, K.; Wilson, I. B. H., *Glycobiology* **2015,** *25*, 585-590.
164. Wilson, I. B. H.; Paschinger, K., *Analytical and bioanalytical chemistry* **2016,** *408*, 461-471.
165. Ayadi, S. C. a. E., *Can.J.Chem.* **1995,** *73*, 343-350.
166. Feng, F.; Okuyama, K.; Niikura, K.; Ohta, T.; Sadamoto, R.; Monde, K.; Noguchi, T.; Nishimura, S.-I., *Organic & Biomolecular Chemistry* **2004,** *2*, 1617-1623.